Sterol Regulatory Element Binding Proteins; Central Metabolic Regulators of Natural Killer Cells

A dissertation submitted to Trinity College Dublin in candidature for the degree of Doctor of Philosophy

School of Biochemistry and Immunology
Trinity College, Dublin

2020

By Katie O'Brien

Under the supervision of Dr David Finlay

Declaration

I declare that this thesis has not been submitted as an exercise for a degree at this or any other university and it is entirely my own work unless otherwise stated.

I agree to deposit this thesis in the University's open access institutional repository or allow the library to do so on my behalf, subject to Irish Copyright Legislation and Trinity College Library conditions of use and acknowledgement.

Katie O'Brien

For my mom

Publications

Srebp-controlled glucose metabolism is essential for NK cell functional responses.

Assmann N, **O'Brien KL**, Donnelly RP, Dyck L, Zaiatz-Bittencourt V, Loftus RM, Heinrich P, Oefner PJ, Lynch L, Gardiner CM, Dettmer K, Finlay DK.

(Nature Immunology,2017)

Amino acid-dependent cMyc expression is essential for NK cell metabolic and functional responses in mice.

Loftus RM, Assmann N, Kedia-Mehta N, **O'Brien KL**, Garcia A, Gillespie C, Hukelmann JL, Oefner PJ, Lamond AI, Gardiner CM, Dettmer K, Cantrell DA, Sinclair LV, Finlay DK.

(Nature Communications, 2018)

Immunometabolism and natural killer cell responses.

O'Brien KL, Finlay DK.

(Nature Reviews Immunology,2019)

Summary

Natural killer (NK) cells are cytotoxic, innate lymphocytes with important functions in the immune response against pathogen-infected and transformed cells. Due to their anti-cancer abilities, NK cells are important for the success of many modern immunotherapeutic strategies, and ways to harness the cytotoxic potential of NK cells for the development of new treatments are constantly being explored. However, NK cells are reported to be dysfunctional in numerous physiological settings, including in obesity and cancer. In order to strategize ways to improve NK cell responses, there is a need to understand the mechanistic underpinnings of what causes these defects.

The growing field of immunometabolism has highlighted the importance of cellular metabolism in the control of immune cell functions. The metabolic changes that occur in NK cells following cytokine activation have been extensively investigated and it is accepted that metabolism of cytokine-activated NK cells is essential for their function. It has also been demonstrated that inhibition of central regulators of NK cell metabolism - such as cMYC or mTORC1, causes dramatic functional consequences. As mTORC1 signalling was shown to be critical for NK cell responses, it was hypothesised that Sterol Regulatory Element Binding Protein (SREBP) transcription factors , which are commonly activated downstream of mTORC1 in other cell types, may be important in NK cells.

SREBP transcription factors are considered to be 'master regulators' of *de novo* lipid-synthesis genes. The present study set out to determine whether SREBP transcription factors were active in cytokine-stimulated NK cells and whether they played a role in controlling NK cell metabolism or function. Indeed, the data reveal that SREBP transcription factors are expressed and are transcriptionally active in IL2/IL12-stimulated NK cells. To explore the role for SREBP transcription factors in NK cells, SREBP activity was inhibited through pharmacological or genetic approaches. Cytokine-induced cell growth and proliferation were found to require

SREBP activity. This was surprising as other members of our group have shown that direct inhibition of *de novo* lipid synthesis does not impact upon NK cell growth and proliferation. This argued that the function of SREBP transcription factors in NK cells was independent of their classical role as promoters of lipogenesis. Indeed, metabolic analysis of NK cells lacking SREBP activity revealed that SREBP was required for cytokine-induced increases in both glycolysis and OxPhos. Furthermore, it was identified that SREBP activity was required for optimal NK cell effector responses both *in vitro* and *in vivo*.

A link between SREBP activity and cellular metabolism is not immediately clear. However, parallel work by other researchers in our group identified that cytokine-activated NK cells metabolise glucose through a novel metabolic configuration known as the citrate-malate-shuttle (CMS) . Interestingly, two key components of the CMS – ACLY and SLC25A1 – are SREBP target genes. However, it was considered that the dramatic impact on NK cell metabolism and function when SREBP activity was inhibited, may not be solely due to inhibition of the CMS machinery. This idea was further explored and metabolomic analysis revealed a role for SREBP in the control of a peripheral metabolic pathway – *de novo* polyamine synthesis. The role of polyamine synthesis had not been investigated in NK cells to date. However, data herein reveal that polyamine biosynthesis is necessary for optimal NK cell metabolism and function. It was further revealed that this may be partially due to the link between polyamine synthesis and hypusination of eIF5A. Hypusination is a unique post-translational modification which requires the polyamine, spermidine, as a substrate. This work identifies that hypusination of eIF5A is essential for cytokine-induced increases in NK cell OxPhos. Furthermore, when hypusination is inhibited, NK cell effector responses are dampened. The intricacies of the mechanism linking SREBP activity to the control of *de novo* polyamine synthesis will require future investigation but preliminary experiments show that SREBP activity influences expression of cMYC in cytokine-stimulated NK cells. It is well established that cMYC can control transcript levels of the enzymes involved in the polyamine synthesis pathway. Considered together,

the data suggest that SREBP activity is necessary for polyamine synthesis and hypusination, through promotion of cMYC activity. Therefore, this study has identified SREBP transcription factors as central regulators of cytokine induced metabolic and functional responses in NK cells. Cholesterol and various oxysterol species, which inhibit SREBP activity, are often elevated in settings where NK cells are known to be defective, such as the tumour microenvironment . Therefore, these findings may have important implications for our understanding of NK responses in various disease states. Moving forward, this knowledge may help in developing improved NK cell-based immunotherapies.

Acknowledgements

Firstly I would like to thank Dr David Finlay for being a fantastic supervisor throughout this project. I could not have hoped for a more ambitious, motivating, and understanding PI. Thank-you so much Dave, for all the opportunities you have given me, the advice, the support and the guidance. You have gone above and beyond. It has been a pleasure to work in your lab and I cannot thank you enough for the opportunity.

Next, is a thank-you to all wonderful past and present members of the Finlay and Gardiner labs, for all you have taught me and for being the loveliest group of lab-mates I could have asked for. It has been amazing to see the Finlay lab grow over the last four years. To all the past members - Simon, Ray, Roisin, Nadine, Vanessa and Nidhi – thank you all for being so welcoming when Jess and I started. To all the newer members - Aisling, Diana, Elisabeth, Chloe, Leonard, Mona and Simon - it has been great getting to know you all and I'm sure you will all achieve amazing things here. Special thanks to Aisling for being so helpful around the lab. I would also like to thank Clair Gardiner for always providing us with NK cell expertise and for all your helpful input during lab meetings. To Alhanouf, Karen and Elena – you are the nicest and most helpful group to be around and I'm glad that we got to work so closely together.

When I signed up to undertake this PhD I was unaware that it would come with the added bonus of getting to meet so many amazing people. I am immensely grateful to all the wonderful friends I have made along the way - I would need an extra chapter in this thesis to detail you all. The following are just a few special mentions:

Roisin - I have so much to thank you for that it is difficult to know where to start - no written acknowledgement could possibly do justice to how lucky I feel to have had you around during this process. From my first day you were the most

welcoming and enthusiastic teacher, showing me everything from the superstitious ways of genotyping, to the best places to get matchas and eat tasty lunch - you were never too busy to help and always had time for fun! Over the past four years you have become one of my closest friends. Thank you for always being there for me. I am so grateful.

Nidhi – you've been there the whole time! I am so happy we went to Texas together and got to know each other so well .You are a great friend and such a hard-working scientist. I am excited to hear all the great things you get up to during your postdoc! Jess - we've come a long way since our shy first few days in the lab when we stuck together like glue and couldn't figure out how to lyse a RBC pellet between the two of us! I've missed having you around since you've moved to NIH, but it is so good seeing you so happy and doing so well over there. Karen – it has been so much fun having you around! Equally enthusiastic while singing ABBA with me late at night in tissue-culture or while having in-depth conversations about arginine metabolism, I've loved having your company both in and out of the lab. Elena, I think you are the most thoughtful and helpful person I have ever met. Thank you for always sharing your knowledge...and for teaching me not to be scared of the liquid nitrogen!

To all the old and new inhabitants of the 5th floor reading rooms - I'm sure you'll appreciate me saying: "You're all my favourites ! '' Very special thanks to Gavin and Peter for helping me proof-read some of this thesis - I hugely appreciate it. James (or should I say Dr O'Leary) and Sarah - it is impossible not to be smiling when you're around. Thank you for bringing so much positivity and energy to the reading room and for always being hungry enough to come for treats! James, your words of 'encouragement' were always 'appreciated' and brightened up many of my days. Aisling Anderson – we did it! From start to finish! You have always been so thoughtful and I've really appreciated having you around for some cheerful distractions, especially over the last few weeks! Lydia and Livia – you are both such good fun and I've loved getting to know you – thanks for letting me in on 'your lab

trip' to Innsbruck! Diana – I could talk to you about science for hours! Thank you for always showing interest in my project and for being there to bounce ideas off. Thanks to Darren, Natalie, Emma, Ji, Niki, Aoife, Louise, Ryan, Paul, Dan, Antoine, Clara, Dieter, Anna, Daire, Ellie, Sahar, Laura, Sadia, Salma, Ola, Isabel and everyone else who has made the fifth floor such a friendly place to work.

I would also like to thank all the staff in TBSI. Particularly Barry for his flow cytometry help, Ciaran, Viola and Rustam for their work in the CMU and Liam and Noel - for finding a way to fix almost anything.

I would also like to acknowledge all my RHC family. I don't think any hockey team understands the importance of feeding NK cells on a Saturday morning as much as you guys do! Thanks for all your encouragement and support while I was writing up (despite me not showing up to any trainings). I'm looking forward to getting back on the pitch!

Last, but not least, thank you to my wonderful parents – Wes and Trish. Thank you for always believing in me. Thank you for your encouragement. Thank you for your support, thank you for your love and thank you for your patience. I know I definitely don't say it enough but I am so lucky to have you.

Abbreviations

25HC	25-Hydroxycholesterol
27HC	27-Hydroxycholesterol
2DG	2-Deoxyglucose
4-OH TMX	4-hydroxytamoxifen
Acat2	Acetyl-CoA Acetyltransferase
ACC	Acetyl-CoA Carboxylase
ADCC	Antibody-Dependent Cell-Mediated Cytotoxicity
AMS	Aspartate-Malate-Shuttle
APC	Antigen Presenting Cell
APS	Ammonium Persulphate
ATF6	Activating Transcription Factor 6
ATTC	American Type Culture Collection
ATP	Adenosine Triphosphate
BMDM	Bone Marrow Derived Macrophage
BPTES	bis-2-(5-phenylacetamido-1,3,4-thiadiazol-2-yl)ethyl sulphide
C75	4-methylene-2-octyl-5-oxotetrahydrofuran-3-carboxylic acid
CAR	Chimeric Antigen Receptor
CH25H	Cholesterol-25-hydroxylase
CLP	Common Lymphoid Progenitor
CMS	Citrate-Malate-Shuttle
CSC	Cancer Stem Cells
CTL	Cytotoxic T Lymphocyte
DC	Dendritic Cell
DENSPM	Siethylnorspermine
DEPC	Diethylpyrocarbonate
DFMO	2-difluoromethylornithine
DHPS	Deoxyhypusine Synthase
DMEM	Dulbecco's Modified Eagle Medium
DOHH	Deoxyhypusine hydroxylase
DON	6-diazo-5-oxo-L-norleucine
DTT	1,4-Dithiothrotol
ECAR	Extracellular Acidification Rate
eIF5A	Eukaryotic initiation factor 5A
$eIF5A^{H}$	Hypusinated eIF5A
$eIF5A^{DH}$	Deoxyhypusinated eIF5A
ER	Endoplasmic Reticulum
ETC	Electron Transport Chain
$FADH_2$	Flavin Adenine Dinucleotide
FASL	Fas ligand
FASN	Fatty Acid Synthase
FCCP	Fluoro-Carbonyl Cyanide Phenylhdrazone
FCS	Foetal Calf Serum
G6P	Glucose-6-Phosphate
GC7	N1-guanyl-1,7-diamineheptane
Hmgcs1	3-Hydroxy-3-methylglutaryl-CoA Synthase 1
IFN	Interferon
ILC	Innate lymphoid cell

ITAM	Immunoreceptor Tyrosine-Based Activation Motif
KIR	Killer-Cell Immunoglobulin-Like Receptor
KO	Knock-Out
LDH-A	Lactate Dehydrogenase A
LXR	Liver X Receptor
mAb	Monoclonal Antibody
MACS	Magnetic-Activated Cell Sorting
MCMV	Murine Cytomegalovirus
mER	Modified Estrogen Receptor
MHC	Major Histocompatibility Complex
MIC	MHC Class 1 Chain-Related
MTOC	Microtubule Organising Centre
mTORC1	Mammalian Target of Rapamycin Complex 1
NAD	Nucleotide Adenine Dinucleotide
NCR	Natural Cytotoxicity Receptor
NK	Natural Killer
OAA	Oxaloacetate
OCR	Oxygen Consumption Rate
ODC	Ornithine decarboxylase
OxPhos	Oxidative Phosphorylation
PA	Polyamine
PBMC	Peripheral Blood Mononuclear Cells
PCR	Polymerase Chain Reaction
PPAR	Peroxisome proliferator-activated receptors
PPP	Pentose Phosphate Pathway
qRT	Quantitative Real Time
R5P	Ribulose-5-phosphate
RFX7	Regulatory factor X 7
RT	Room Temperature
S1P	Site-1-Protease
S2P	Site-2-Protease
S.C.	Sub-cutaneous
SCAP	SREBP Cleavage Activating Protein
SCD1	Stearoyl-CoA Desaturase 1
SMS	Spermine synthase
SPF	Specific-Pathogen-Free
SRE	Sterol Regulatory Element
SREBP	Sterol Regulatory Element Binding Protein
SRM	Spermidine synthase
SSAT	Spermidine/spermine N-1 acetyl transferase
TCA	Tricarboxylic Acid
TCR	T Cell Receptor
TEMED	Tetramethylethylenediamine
TME	Tumour Micro-environment
TMRM	Tetramethylrhodamine, methyl ester
TNF	Tumour Necrosis Factor
TOFA	5-tetradecyloxy-2-furoic acid
TRAIL	TNF-related apoptosis-inducing ligand

Table of contents

Table of Figures

Chapter 1

Chapter 2

Chapter 3

Chapter 4

Chapter 5

1 Introduction

1.1 Natural killer cells

Natural killer (NK) cells are granular lymphocytes belonging to the group 1 innate lymphoid cell (ILC) family (Spits et al. 2013). A unique, pan-NK cell marker is yet to be defined and as such, NK cells are commonly characterised either based on the absence of CD3 and expression of CD56 in humans or based on the absence of CD3 and expression of NKp46 in mice (Walzer, Jaeger, et al. 2007; Bezman et al. 2012; Walzer, Blery, et al. 2007). However, it has become apparent that NK cells may share these surface markers with ILC1 cells. Therefore, many studies to date do not differentiate between the two subsets (Vivier et al. 2018).

Although they recognise their target cells differently, NK cells are functionally similar to CD8+ cytotoxic T lymphocytes (CTLs) (Sun and Lanier 2011). NK cells have potent cytotoxic and cytokine-producing abilities and can eliminate transformed or pathogen-infected host cells. However, unlike CTLs, NK cells have the ability to exert their functions rapidly, as part of the innate immune response. For instance, NK cell cytotoxicity has been shown to occur *in vitro* within 28 minutes of NK-target cell binding (Eriksson et al. 1999). NK cells can also contribute to the adaptive immune response, shaping immune outcomes through the secretion of soluble mediators such as interferon gamma (IFNγ) and responding to T cell-derived IL2, enabling NK cells to persist and carry out their effector functions alongside T and B lymphocytes to resolve immune challenges.

1.2 NK cell effector functions

1.2.1 NK cell cytotoxicity

A characteristic function of NK cells is their ability to identify and kill infected or transformed host cells. Though they identify their targets in distinct ways, NK cells exert cytotoxicity toward target cells in a similar way to CTLs, commonly through directed-release of cytolytic granules or through the death-ligand/death receptor system. Both of these mechanisms require direct contact between an NK cell and its target and the formation of an immunological synapse. The secretion of

cytolytic granules is the primary approach used and ultimately leads to apoptosis of the target cell. Cytolytic granules are organelles similar to lysosomes that are stored in the cytoplasm of NK cells until the NK cell comes in contact with a susceptible target. Appropriate activation signals trigger the NK cell to release the cytolytic granules. This occurs in a stepwise, directed manner, beginning with rapid rearrangements of the NK cell's cytoskeleton and microtubule organising centre (MTOC) to polarise the preformed granules towards the membrane at the NK cell-target cell synapse. Upon fusion of the lytic granules with the NK cell membrane, release of the granule contents into the synapse occurs (Orange 2008).

The main components released are perforin and granzymes, which can act in synergy to induce target cell apoptosis. Perforin is a pore-forming protein, critical to NK cell cytotoxicity as it enables granzyme-mediated induction of target cell apoptosis. NK cells from perforin-deficient mice display impaired cytotoxicity *in vitro* (Kagi et al. 1994). However, the precise function of perforin remains unclear. Originally the purpose of perforin was thought to be to create pores through which granzyme could enter the cell, however granzyme uptake has been shown to occur efficiently by receptor-mediated endocytosis (Thiery et al. 2011). More recent evidence suggests that perforin may, instead, play a role in disrupting target cell endosomal trafficking (Smyth et al. 2005; Browne et al. 1999). *In vitro* evidence also suggests that perforin may function as a lytic agent, killing cells by osmotic lysis or at least disrupting target cell homeostasis leading to apoptosis or necrosis, however whether this occurs *in vivo* remains to be further investigated (Liu et al. 1986; Osinska, Popko, and Demkow 2014). Granzymes are serine proteases that directly induce target-cell apoptosis through caspase-dependent and independent mechanisms. Granzyme A and B are the best-characterised granzymes in NK cells. NK cells constitutively express granzyme A, whilst granzyme B is translated into protein within 6 hours of NK cell activation. Granzyme B acts with greater potency than granzyme A (Fehniger et al. 2007).

NK cells can also kill target cells through engagement of death ligands belonging to the tumour necrosis factor (TNF) family. NK cells can express a variety of death ligands including Fas ligand (FasL) and TNF-related apoptosis-inducing ligand (TRAIL). Engagement of these ligands with their cognate death receptor on a target cell induces target cell apoptosis (Screpanti et al. 2005). Each death receptor has an intracellular death receptor domain, which can recruit adaptor proteins, leading to the induction of target cell apoptosis. Interestingly, NK cells can induce death ligand expression on transformed cells that do not constitutively express death ligands. NK cells then kill these cells through engagement of the newly expressed death ligands with the NK cells' death receptors (Screpanti et al. 2001). (See **Fig 1.1**). NK cells can kill more than one target cell upon activation, and this is termed 'serial killing' (Bhat and Watzl 2007; Choi and Mitchison 2013). Interestingly, recent data suggests that cytotoxicity through the release of cytolytic granules and cytotoxicity through receptor-mediated apoptosis are temporally regulated during an immune response; initially NK cells primarily kill target cells through cytolytic granule release and granzyme B activity and later use the death receptor pathway (Prager and Watzl 2019; Liesche et al. 2018).

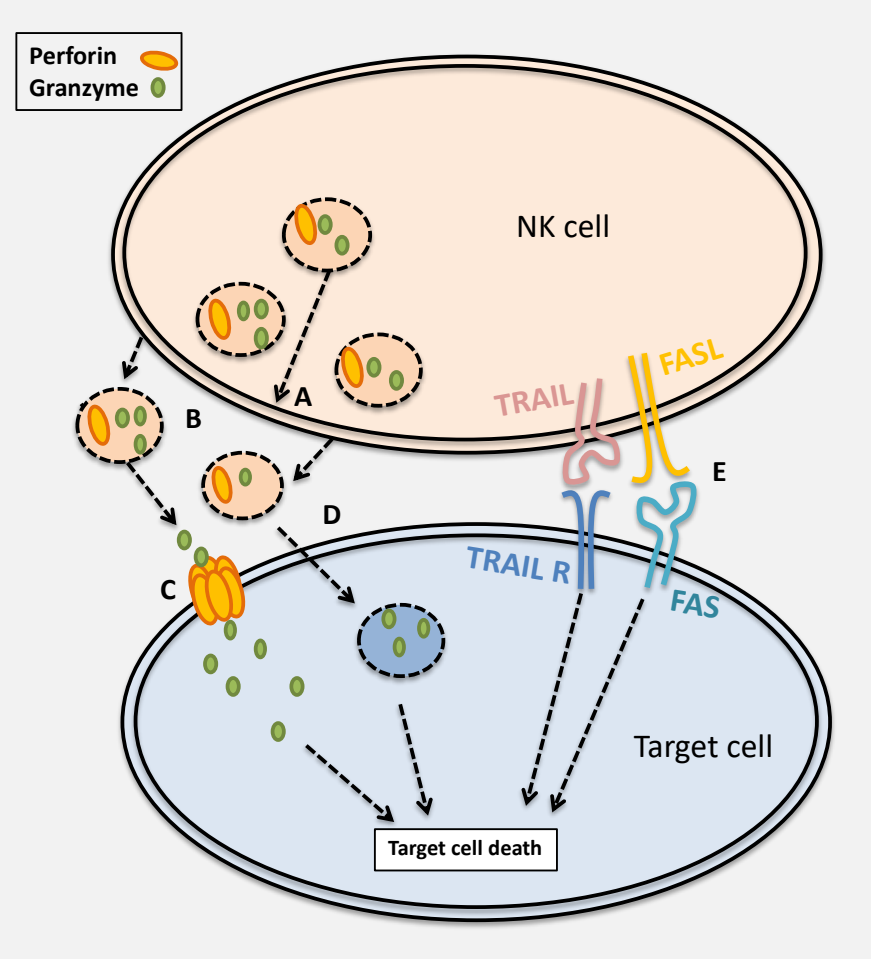

Figure 1.1 Mechanisms of NK cell cytotoxicity

NK cells can kill their target cells through the directed release of cytolytic granules containing perforin and granzyme. If an NK cell encounters a susceptible target, preformed cytolytic granules are mobilised towards the membrane at the NK cell-target cell synapse (**A**). The NK cell releases the contents of the lytic granules into the synapse (**B**). Perforin polymerises to form pores in the membrane of the target cell, which facilitates entry of granzyme (**C**). Alternatively, granzyme may be endocytosed into the target cell (**D**). Granzyme mediates target-cell apoptosis upon entry. A different mechanism by which NK cells can kill their targets is through engagement of death ligands expressed on NK cells with death receptors on target cells. Ligation of death receptors initiates a downstream signalling cascade which induces target cell death (**E**).

1.2.2 NK cell cytokine secretion

Another important effector function associated with NK cells is the production and secretion of cytokines and chemokines. NK cells can synthesise and secrete a multitude of cytokines including TNF α, IFNγ and granulocyte/macrophage colony-stimulating factor (GM-CSF) . The secretion of TNF α and IFNγ by activated NK cells can augment the functions of antigen presenting cells, including dendritic cells (DCs) and macrophages. NK cells can therefore positively-influence DC maturation and IL12 production (Gerosa et al. 2002; Piccioli et al. 2002). NK cell-derived IFNγ is crucial to the development of adaptive responses and contributes to the polarisation of CD4+ T cells towards the protective Th1 phenotype (Bihl et al. 2010; Martin-Fontecha et al. 2004). NK cells can be recruited to lymph nodes where they are proximal to the site of T cell priming by DCs. This supports the idea that NK cells can influence T cell polarisation through cytokine-production, and thus link the innate and adaptive arms of the immune response. IFNγ production by NK cells also contributes to anti-viral and anti-tumour responses, directly limiting viral spread and inducing apoptosis in tumour cells (Ikeda, Old, and Schreiber 2002; Waggoner et al. 2016). NK cells can also secrete chemokines including CCL3, CCL4, CCL5 and CXCL8 (Fauriat et al. 2010; Bluman et al. 1996; Smyth et al. 1991).

1.2.3 Additional NK cell immune regulatory functions

In conjunction with effects mediated by the cytokines they secrete, NK cells have additional regulatory roles in the immune response. For example, NK cells can affect the scale of the adaptive immune response by regulating DC numbers during DC development. NK cells are found closely associating with DCs and can kill developing DCs depending on the NK cell/DC ratio (Piccioli et al. 2002). NK cell regulation of DCs is another way they can shape adaptive T cell responses and thus influence the scale of the adaptive immune response. Furthermore, NK cells can directly control T cell numbers (Waggoner et al. 2011). For instance, NK cells have been shown to directly lyse activated CD4+ T lymphocytes in the context of viral infection, to prevent T-cell dependent immunopathology (Waggoner et al. 2011).

1.3 NK cell development

NK cell development occurs predominantly in the bone marrow and is dependent on IL15, as is demonstrated by abnormal NK cell development in mice lacking expression of IL15 or any subunits of the IL15 receptor (Kennedy et al. 2000; Vosshenrich et al. 2005). NK cells derive from common lymphoid progenitors (CLPs), which arise from haematopoietic stem cells. CLPs are capable of developing into any lymphocyte subset and it is IL15 that selectively promotes their development towards NK cells. In order to respond to IL15, cells must express CD122 (the IL2 and IL15 receptor common β chain) and CD132 (the common gamma chain). The acquisition of CD122 is thus a hallmark of the NK cell population and commits lineage-negative lymphoid precursors to the NK cell lineage. To become a functional mature NK cell, immature cells must undergo an 'education' process. This consists of NK cell inhibitory receptors engaging with cognate major histocompatibility complex (MHC) class I ligands on surrounding cells. Cells which don't ligate their inhibitory receptors during this process, become anergic as a protective mechanism to prevent NK cell self-reactivity.

1.4 NK cell homeostasis and priming

IL15 is not only important for NK cell development, but also for the survival of homeostatic NK cells in the periphery (Cooper et al. 2002; Koka et al. 2003). The mechanism behind this is thought to be through the prevention of apoptosis (Yang, Chen, et al. 2016). Under homeostatic conditions, mature NK cells are found in circulation, surveying host cells to ensure normal surface marker expression. Prior to activation, NK cells are characterised by their small cell size and lack of expression of 'activation markers' such as CD69 (Donnelly et al. 2014). Though predominantly located in peripheral blood, bone marrow and spleen during steady-state conditions, NK cells have also been described residing in the lymph nodes, liver, pancreas, lung and uterus and have the ability to migrate and undergo extravasation into most tissues in response to chemokine signalling (Shi, Ljunggren, et al. 2011). Although NK cells have been documented to have tissue-

residency at certain sites, much of our current knowledge of NK cell biology comes from the study of peripheral blood and splenic NK cells, therefore it is important to note that it is likely that tissue-resident NK cells may possess different features.

Unlike naïve T lymphocytes, NK cells, even in a resting state, are poised for activation. Although early descriptions of NK cells reported their abilities to kill without prior sensitisation (Herberman et al. 1975), it is now known that in order to become fully responsive when activated, NK cells must first be primed (Walzer, Jaeger, et al. 2007; Lucas et al. 2007; Long 2007). Priming of NK cells readies them for the rapid activation of their effector functions. Primed NK cells constitutively express perforin and granzymes and therefore can mount a cytotoxic response within minutes of activation, without the time constraints associated with translation of effector molecules (Stetson et al. 2003; Lanier 2005). Un-primed, resting NK cells from mice housed in specific-pathogen-free (SPF) conditions are minimally cytotoxic when isolated as they contain little or no granzyme or perforin protein, despite abundant mRNA transcripts (Fehniger et al. 2007). It is therefore suggested that these cells are 'pre-armed' with mRNA which can rapidly be translated into protein upon priming (Fehniger et al. 2007). It has also been previously shown that resting murine NK cells constitutively express IFNγ mRNA but not protein, which can be translated upon activation (Stetson et al. 2003; Fehniger et al. 2007). This is in contrast to studies in human NK cells, where the majority of freshly isolated PBMCs express granzyme B and perforin and are cytotoxic – these cells may already be primed however due to chronic exposure of humans to pathogens (Fehniger et al. 2007).

Though the exact mechanisms underpinning NK cell priming are yet to be fully elucidated, IL15 has been shown to be sufficient to support murine NK cell priming *in vitro* and *in vivo* (Lucas et al. 2007; Nandagopal et al. 2014). An idea is therefore posited that NK cell-receptor ligation may represent the 'trigger' that leads to directed granule release at the NK cell-target-cell synapse, whilst cytokines and other signals may stimulate granzyme and perforin translation which provides the

potential for a potent cytotoxic response (Fehniger et al. 2007). This concept is supported by a recent study which identified that in order to produce IFNγ in response to receptor-ligation, NK cells require additional cytokine-stimulation to first induce expression of IFNγ transcripts (Piersma et al. 2019).

1.5 NK cell activation

Upon recognition of malignant or pathogen-infected cells, NK cells can quickly become activated to kill target cells and to secrete pro-inflammatory cytokines. NK cells can be activated in response to a variety of signals. These include: an environment rich in inflammatory cytokines, cellular interactions with targets causing an increase in ligation of activating receptors or a decrease in ligation of inhibitory receptors, or alternatively, engagement of an NK cell's Fc receptors. NK cell activation signals do not act in isolation and therefore, unlike T or B cells, a single signalling cascade does not dominate NK cell effector functions (Lanier 2005). Calcium signalling triggered by activating receptors can initiate the cytoskeletal polarisation which positions lytic granules at the NK cell-target cell synapse – this results in highly specific killing of the target with minimal risk to surrounding cells (Screpanti et al. 2005; Wulfing et al. 2003).

1.5.1 Receptor-mediated NK cell activation

NK cells differ from adaptive T and B lymphocytes in that they do not express specific antigen receptors derived from gene recombination, and instead express an array of germ-line encoded activating and inhibitory receptors. NK cell activation is governed by the integration of signals received from both repertoires of receptor upon contact with a potential target cell. It is the net balance of signals received that can activate NK cell cytotoxicity towards the target cell or can cause the NK cell to detach. Activation can occur in response to either an increase in ligation of activating receptors, or a decrease in ligation of inhibitory receptors. Whereas, the absence of activating signals or induction of strong inhibitory signalling will inhibit the cytotoxic functions of the NK cell.

1.5.2 Activating Receptors

NK cells express a wide array of activating receptors, which recognise ligands abnormally induced on the surface of cells in response to stress or associated with pathogens. Examples of activating receptors expressed on NK cells include the Natural Cytotoxicity receptors (NCRs), NKG2D and DNAM-1. The NCRs include NKp30, NKp44 and NKp46, which are proposed to bind viral hemagglutinins and hemagglutinin neuraminidases (Mandelboim et al. 2001; Chisholm and Reyburn 2006). NCRs have also been reported to be involved in the recognition of monocytes infected with cellular pathogens (Vankayalapati et al. 2005; Garg et al. 2006). NKG2D recognises aberrant expression of the MHC class I chain-related (MIC) molecules MICA and MICB in addition to UL16-binding proteins that can be induced by viral infection and malignant transformation of cells. DNAM-1 recognises CD122 and CD155, molecules that are expressed on target cells under conditions of stress (Chan, Smyth, and Martinet 2014). Upon ligation, most activating receptors associate with adapter proteins containing immunoreceptor-tyrosine-based activation motifs (ITAMs). ITAM-containing adapter proteins serve as signal transducing molecules and once phosphorylated, recruit kinases such as Syk and ZAP70 which propagate strong activation signals downstream to induce NK cell degranulation and cytokine secretion.

In addition to the activating receptors listed above, NK cells express CD16, a low-affinity Fc receptor for IgG. CD16 binds to the Fc portion of antibody. CD16 ligation activates NK cells to lyse antibody-coated cells through a process called antibody-dependent cell-mediated cytotoxicity (ADCC). Unlike other NK cell activating receptors, which require synergistic action, activation through CD16 in isolation can stimulate NK cell activation and its ligation is sufficient to trigger both cytokine-release and cytotoxicity (Bryceson et al. 2006). Killing through ADCC is a way in which NK cells can contribute to the adaptive immune system in response to antibodies and allows NK cells to respond to monoclonal antibody (mAb) based therapies.

1.5.3 Inhibitory Receptors

As NK cell activating receptors mainly recognise self-ligands, there is the potential for NK cells to induce tissue damage. Thus, the presence of inhibitory receptors acts as a safeguard to tightly regulate NK cell activity and prevent damage to healthy cells. Activation of NK cells is tightly controlled by a myriad of inhibitory receptors that serve to tolerise NK cells towards healthy host cells. Well-documented inhibitory receptors are the killer-cell immunoglobulin-like receptors (KIRs) in humans and the LY49 family in mice. These inhibitory receptors mainly recognise a selection of class I MHC molecules constitutively expressed by healthy cells. Abnormal cells may express reduced levels of MHC class-1 (commonly as an immune escape mechanism from CTLs). These cells have been described as 'missing self' and, as such, are susceptible to NK cell killing (Karre et al. 1986). This makes NK cells particularly effective against CTL-elusive targets. Among other inhibitory receptors are the CD94 and NKG2 family, which are expressed by both human and murine NK cells and encode receptors that recognise non-classical MHC class I ligands (HLA-E in humans and Qa1 in mice) (Lanier 2005).

Inhibitory receptors, though diverse in their extracellular domains, function through common immunoreceptor-tyrosine based inhibitory motifs (ITIMs) in their cytoplasmic tails. ITIMs are tyrosine-phosphorylated upon receptor engagement, and recruit tyrosine phosphatases, that act to suppress NK cell responses through dephosphorylation of the signalling molecules downstream of activating receptors. In short, if the target cell expresses sufficient ligands to signal through inhibitory receptors, the inhibitory signals are strong enough to inhibit the triggering of cytotoxic pathways by activating receptors, thus inhibiting the induction of NK cell effector functions (Lanier 2005) (See **Fig 1.2**).

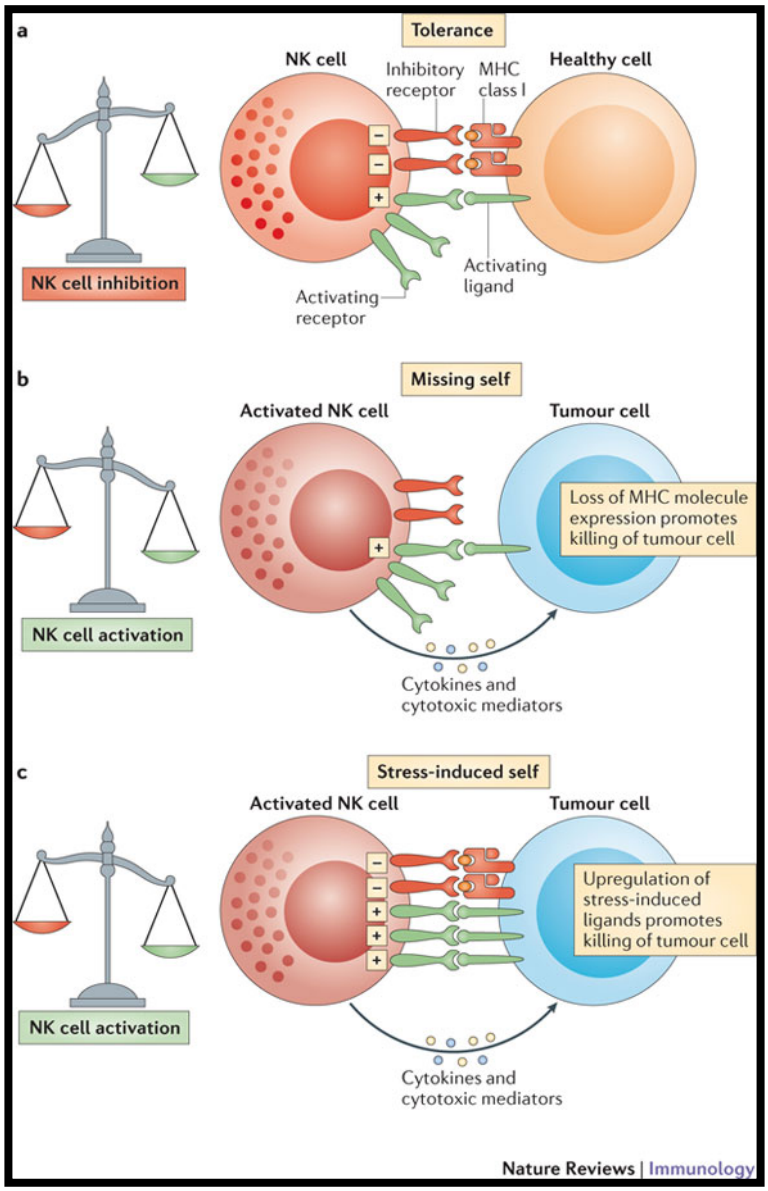

Figure 1.2 NK cell receptor signalling – balancing activation with inhibition

Whether an NK cell becomes activated upon interaction with a target cell depends on the balance of signals received through the NK cell's activating and inhibitory receptors. (**a**) If the majority of ligands on the target cell are inhibitory, the target will be tolerised. (**b**) If the target fails to engage the NK cell's inhibitory receptors the target will be killed. (**c**) Despite ligating inhibitory receptors, if the target cell expresses strong activating ligands, the NK cell is still activated to kill. Figure from: (Vivier et al. 2012).

1.5.4 Cytokine and cellular activation of NK cells

NK cell activation and the magnitude of NK cell responses can be strongly influenced by the cells and cytokines in the surrounding environment. Activation by cytokines can induce NK cell proliferation, IFNγ secretion and effector molecule production. Additionally, the death receptor TRAIL, which is only constitutively expressed on a minor subset of NK cells, is highly induced following stimulation with cytokine (Smyth et al. 2005).

NK cells can be rapidly recruited to sites of inflammation by chemokines and can become activated in response to various cytokines including IL2, IL12, IL15, IL18 and type 1 IFNs (Marcais et al. 2013). These cytokines can signal in isolation, but also synergistically to enhance NK responses. For example IL12 can induce NK cells to express the high affinity IL2 receptor (CD25), which enables them to respond even to low doses of T cell-derived IL2 (Lee, Fragoso, and Biron 2012; Bihl et al. 2010). IL2 has been used *in vitro* to activate and expand NK cells. Interestingly, IL2 is thought of as an adaptive cytokine, mainly produced by activated T cells in secondary lymphoid organs. Thus, the responsiveness of NK cells to IL2 signalling positions them to effectively respond and function alongside adaptive T cell responses (Boyman and Sprent 2012). Newly primed antigen-specific CD4+ T cells can therefore activate NK cells directly through secretion of IL2 and indirectly through the regulation of IL12 secretion by dendritic cells (DCs) (Bihl et al. 2010). In addition to being the main producers of IL12 and IL18, DCs can cross-present IL15 to both prime and activate NK cells (Lucas et al. 2007).

1.6 Role of NK cells in the immune system

1.6.1 NK cell responses against pathogens

NK cells play an important and well-described role in the anti-viral immune response (Horowitz, Stegmann, and Riley 2011). Patients lacking NK cells or with NK cells that have defective activity are more susceptible to severe herpesvirus or

papillomavirus infections (Orange 2013). As previously discussed, NK-cells are a major source of IFNγ, which can directly limit viral spread. Furthermore, a role for NK cell 'memory' has been described in response to certain viral infections. This has been characterised in detail for murine cytomegalovirus (MCMV) infection, in which a subset of NK cells expand during primary infection. Upon next exposure to the virus, these cells proliferate, secrete IFNγ and degranulate at a much greater rate than previously unexposed NK cells (Sun, Beilke, and Lanier 2009).

Human NK cells have been reported to respond to Mycobacterium tuberculosis-infected monocytes via their NCRs (Vankayalapati et al. 2005). However, in most-cases the anti-bacterial role of NK cells seems to be in response to indirect NK cell activation - through cellular interactions with APCs or through the TLR-dependent induction of cytokines such as IL12 and IL18 by APCs (Newman and Riley 2007). Thus, NK cells can also respond to bacterial infection, though their importance in the context of direct recognition and bacterial clearance is less well described (Horowitz, Stegmann, and Riley 2011).

1.6.2 NK cell anti-tumour responses

NK cells play a crucial role in tumour immunosurveillance. Cancer cell transformation can induce expression of stress-associated molecules such as MICA and MICB on the target cell surface, these serve as ligands for NK cell activating receptors. In addition, many tumour cells downregulate MHC class 1 expression, which can evade CTL recognition. In doing so, these cells become susceptible to killing by NK cells, which can eliminate these cancerous cells which are 'missing self' upon engagement. Evidence to support the role played by NK cells in immune-surveillance comes from correlative and epidemiological studies which have found that individuals whose NK cells have reduced cytotoxic activity are at a significantly higher risk of developing cancer (Imai et al. 2000; Orange 2013).

In addition to cancer immunosurveillance, NK cells have an important role in the response to haematological cancers and in prevention of tumour metastasis (Gorelik et al. 1982; Lopez-Soto et al. 2017; Talmadge et al. 1980). NK cells also have a role to play in the clearance of established malignancies, though this role is less well defined. Higher numbers of tumour-infiltrating NK cells correlate with better prognosis in cancer patients with certain solid tumours (Coca et al. 1997; Ishigami et al. 2000). NK cells have also been shown to eliminate cancer stem cells (CSCs) from melanoma cell lines *in vitro* (Pietra et al. 2009). CSCs are self-renewing, radio resistant and drug resistant cells, commonly responsible for relapses following cancer therapies. Therefore, the ability of NK cells to clear such cells is important. IFNγ may affect tumour angiogenesis, and NK cells are a potent source of IFNγ (Screpanti et al. 2005). However, NK cell effectiveness against solid tumours can be controversial – in many cases NK cells are found to be defective at tumour sites. This could be due to immunosuppressive effects of tumours, nutrient depletion in the tumour microenvironment or a failure of NK cells to infiltrate the solid tumour mass.

1.6.3 NK cell immunotherapeutic strategies

The anti-tumour function of NK cells is being harnessed for the development of immunotherapeutic strategies to treat cancer. NK cells have important roles in the anti-tumour effect of many immunotherapeutic strategies currently in the clinic. For example, many monoclonal antibodies (mAb) have been developed that are targeted towards cancer cells, including Rituximab (anti-CD20 mAb), Cetuximab (anti-EGFR mAb), Trastuzumab (anti-Her2 mAb) and Mogamulizumab (anti-CCR4 mAb) (Seidel, Schlegel, and Lang 2013; Campbell and Hasegawa 2013). NK cells can mediate the immunotherapeutic effects of monoclonal antibody therapies, as they can recognise and engage antibody coated target cells through their Fc receptors and can kill the targeted cell through ADCC.

Furthermore, adoptive transfer of NK cells as an anti-cancer therapy also holds promise. A single injection of cytokine-activated NK cells into mice with

established tumours, leads to a substantial reduction in growth of the tumour (Ni et al. 2012). For treatment of acute myeloid leukaemia (AML), NK cells have already successfully been used as adoptive transfer treatments (Aversa et al. 2005). Options are currently being explored for the introduction of *ex vivo* expanded or genetically manipulated NK cells such as NK cells engineered with chimeric antigen receptors (CAR). Improved understanding of NK cell biology, and how metabolites and nutrients regulate NK cells will allow further exploitation of NK cells in the development of these new, targeted therapies.

1.7 Immune cell metabolism

Immunometabolism refers to the study of interactions between metabolism and the immune system. This can either be at a systemic level, documenting the effects of whole body metabolism on immune functions and vice versa, or alternately can refer to cellular bioenergetics and how the metabolism of an immune cell may affect its functions. Though both are interlinked, the latter is of most relevance to this study.

Immune cells need to be able to respond to changes in their environment and to rapidly adapt from quiescence to activation. Activated immune cells change in function and morphology; they may undergo blastogenesis, proliferate, migrate through tissues and produce and secrete large amounts of effector molecules. These processes commonly require transcription and translation of a new programme of genes and proteins and thus, there is a demand for increased cellular energy and biosynthetic precursors to allow for macromolecular synthesis – this provides a metabolic challenge. In response to this, the cells must adapt their metabolic configurations. Indeed, a key feature of immune cells is the ability to adapt their metabolic profiles upon activation, to meet the energy and biosynthesis demands associated with their activated state (Pearce et al. 2013). Further to this, it has now become apparent that many immune cells rely on distinct metabolic configurations not only to fuel but also to regulate their effector functions (Loftus and Finlay 2016). Therefore, a detailed understanding of how

immune cells couple their metabolic needs to their effector functions, will provide a means to enhance or recover immune responses in disease settings and to improve immunotherapeutic treatment strategies.

1.8 Basic metabolic configurations

All cells require energy and appropriate nutrients to fuel basic cellular processes, homeostasis and survival. Adenosine triphosphate (ATP) is the main cellular energy carrier, thus, maintaining adequate levels of cellular ATP levels is an essential requirement of all cells. There are three core, integrated pathways that are dominantly used for energy production: glycolysis, the tricarboxylic acid (TCA) cycle and oxidative phosphorylation (OxPhos). These pathways cooperate to maintain energy balance and are outlined in more detail below and in (**Fig 1.3**).

1.8.1 Glycolysis

Glycolysis is a catabolic pathway that occurs in the cytosol. The glycolytic pathway metabolises one glucose molecule to two pyruvates via a series of enzymatic steps, requiring NAD+ as a co-factor and generating a net of two ATP from each glucose molecule metabolised. Glucose-derived pyruvate has one of two fates. In the presence of oxygen, it can enter the mitochondria and be further metabolised through the TCA cycle to produce reducing equivalents to fuel OxPhos (described in following section). Alternatively, pyruvate can be reduced to lactate in the cytosol by lactate dehydrogenase A (LDH-A) and removed from the cell – a reaction that doesn't require oxygen. In doing so, cellular levels of NAD+ are replenished which is important to allow the cell to sustain a high flux through glycolysis. However, the conversion of pyruvate to lactate does not only occur in conditions where oxygen is limiting (hypoxia). Many cancer cells and rapidly proliferating cells also metabolise glucose to lactate, even when oxygen is plentiful. This metabolic configuration is termed 'aerobic glycolysis'.

As aerobic glycolysis only generates a net of two ATP molecules per glucose molecule metabolised, it can be considered as energetically wasteful. Much higher

quantities of glucose must be metabolised through glycolysis than the amount needed to sustain equal ATP production when OxPhos is used. So why do some cells preferentially adopt aerobic glycolysis? It has been argued that aerobic glycolysis permits faster ATP production than OxPhos and that when there is demand for increased ATP levels, the bioenergetic costs of increasing the glycolytic machinery are less than that of upregulating the OxPhos machinery (Koppenol, Bounds, and Dang 2011; Olenchock, Rathmell, and Vander Heiden 2017). However, it is likely that the greatest benefit in utilising aerobic glycolysis is to fuel biosynthesis (Lunt and Vander Heiden 2011). High flux through glycolysis generates large quantities of glycolytic intermediates which can be siphoned from the glycolytic pathway and used as substrates for ancillary pathways involved in the synthesis of lipids, amino acids and nucleotides For example, glucose-6-phosphate (G6P), generated by the first step in glycolysis, can feed into the pentose phosphate pathway (PPP) where it can be metabolised to support nucleotide synthesis and to generate NADPH – an important reducing agent for lipid synthesis (O'Neill, Kishton, and Rathmell 2016) (**Fig 1.4**). Additional glycolytic intermediates can generate amino acids such as serine or alanine for protein synthesis (Mullarky et al. 2016; Donnelly and Finlay 2015). Therefore, in addition to granting cells oxygen-independence in hypoxic environments, this pathway has benefits for cells engaging in cellular growth and proliferation.

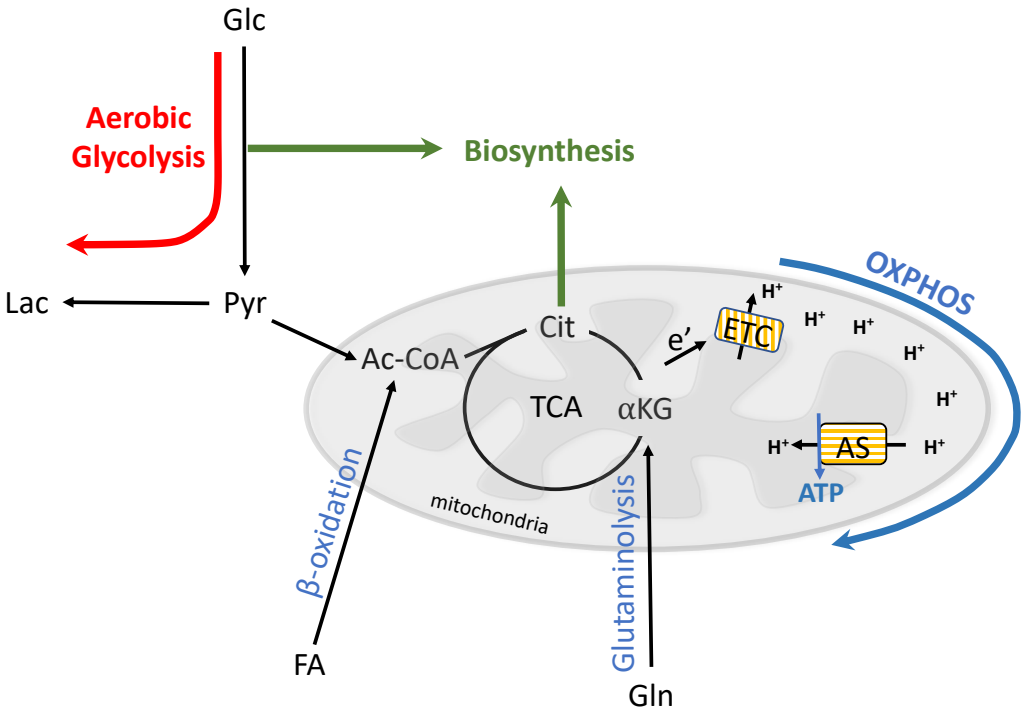

Figure 1.3 Metabolic pathways for energy homeostasis and biosynthesis

Cellular metabolism can be configured to efficiently generate energy in the form of ATP. Glucose (Glc) can be metabolised by glycolysis to pyruvate (Pyr), which can be used to fuel oxidative phosphorylation (OxPhos) in the mitochondria. Pyruvate is converted to acetyl-CoA (Ac-CoA), which feeds into the TCA cycle and generates the reducing equivalents NADH and $FADH_2$ (not shown) that transfer electrons (e') to complex I and II of the electron transport chain (ETC) leading to a proton (H^+) gradient across the mitochondrial inner membrane that is used to drive the activity of ATP synthase (AS). Additional fuels can be used for OxPhos and mitochondrial energy production. Fatty acids are broken down in the mitochondria through β-oxidation that yields acetyl-CoA. Amino acids, most notably glutamine (Gln), can also be metabolised for the purposes of ATP production. Glutamine is metabolised via glutaminolysis to αKG, which can feed into the TCA cycle. In addition to fuelling ATP synthesis, glucose and glutamine metabolism can support biosynthetic processes. Intermediates of glycolysis can be diverted into metabolic pathways to generate biosynthetic precursors important for the synthesis of lipids, nucleotides and proteins. Similarly, the TCA intermediate citrate (Cit) can be exported from the mitochondrial and metabolised to support the biosynthesis of these molecules. Cells will metabolise glucose to lactate when there is no oxygen available for OxPhos (anaerobic glycolysis, not shown). Cells with high biosynthetic demands will also metabolise glucose to lactate in the presence of oxygen (aerobic glycolysis) while also feeding pyruvate into the mitochondria to support OxPhos. This metabolic configuration is of benefit because it allows for high flux through glycolysis leading to elevated levels of glycolytic intermediates that can be diverted towards biosynthesis, while also generating large amounts of ATP. (O'Brien and Finlay 2019).

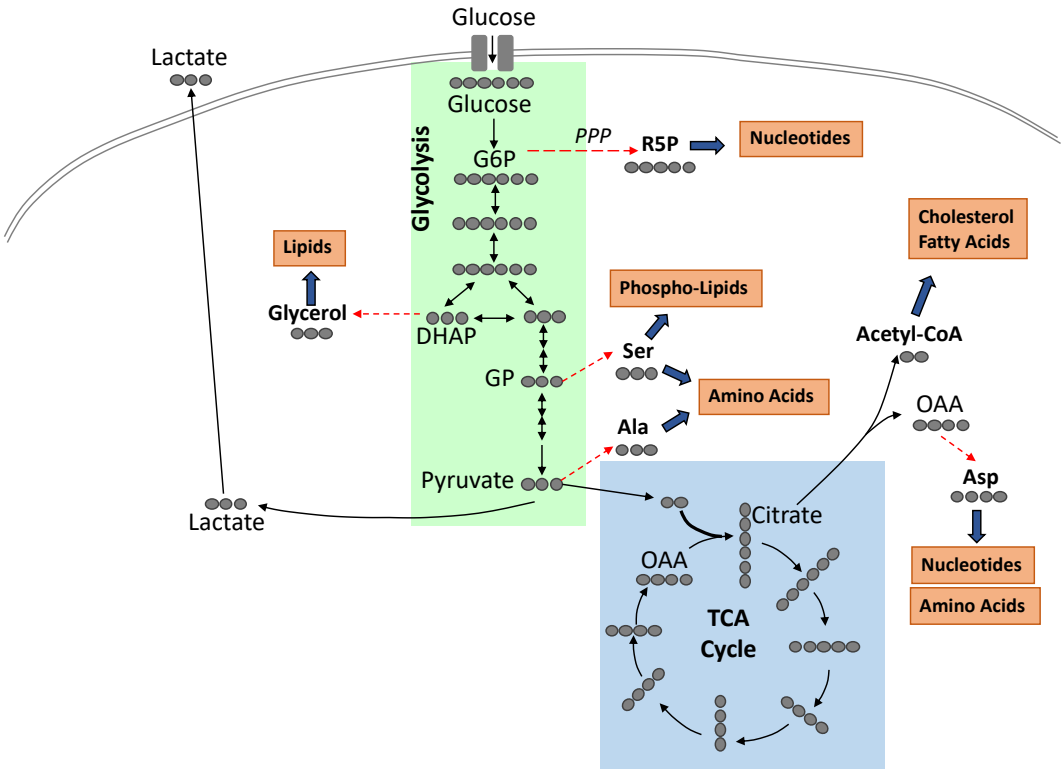

Figure 1.4 Cellular metabolism configured to fuel biosynthesis

Glucose can be used as a carbon source (grey circles represent carbon atoms) to generate biomolecules that can be used for biosynthesis. Glucose catabolism, through the glycolytic pathway (green) generates intermediates that can be siphoned from glycolysis into ancillary pathways to generate biomolecules. For instance, glucose-6-phosphate (G6P) can enter the pentose phosphate pathway (PPP) to generate ribulose-5-phosphate (R5P) for nucleotide synthesis. Dihydroxyacetone phosphate (DHAP) can be converted to glycerol, for lipid synthesis. Amino acids for protein synthesis can be generated from 3-phosphoglycerate (GP) and pyruvate. Pyruvate can enter the TCA cycle (blue) where it can be converted to citrate and then exported to generate cytosolic acetyl-coA which can be used for lipid synthesis, and oxaloacetate (OAA) which can be converted to the amino acid aspartate (Asp). Cells that synthesise large amounts of biomolecules for secretion or that undergo enhanced growth and proliferation, may adapt this metabolic profile to meet their biosynthetic needs. Figure and adapted legend from (Donnelly and Finlay 2015).

1.8.2 The TCA cycle and OxPhos

A second fate of glucose-derived pyruvate is its complete oxidation to CO_2 and H_2O in the mitochondria via OxPhos. OxPhos generates ATP through the oxidation of nicotinamide adenine dinucleotide (NADH) and flavin adenine dinucleotide ($FADH_2$). Metabolising glucose through TCA cycle and OxPhos is the more energy efficient pathway in terms of ATP production per glucose molecule. From each glucose metabolised, it generates vastly more energy (a net of 34 ATP from each glucose molecule compared to a net of 2 ATP molecules from aerobic glycolysis). Predominant use of this pathway is therefore common among cells in a quiescent, oxygen-replete state, that have limited requirements for biosynthesis and therefore primarily configure their metabolism for efficient ATP production to fuel homeostatic processes (Pearce and Pearce 2013).

OxPhos is an oxygen-dependent pathway and begins with the mitochondrial import of pyruvate, followed by its conversion to acetyl-CoA. Acetyl-CoA then joins the TCA cycle where it can be further metabolised . The main goal of the TCA cycle is to generate reducing equivalents to feed into OxPhos. Acetyl-CoA condenses with oxaloacetate (OAA) to form citrate. As citrate is further metabolised, the reducing equivalents NADH and $FADH_2$ are generated. $FADH_2$ and NADH can donate electrons to the electron transport chain (ETC) to fuel OxPhos and generate ATP. The TCA cycle can also be fuelled by amino acids such as glutamine which can be broken down by glutaminolysis to α-ketoglutarate (αKG) -a substrate that can feed into the TCA cycle. Alternatively, fatty acids can contribute to the TCA cycle following their β-oxidation in the mitochondria to generate acetyl-coA.

However, the TCA cycle is not the only route through which glucose can provide mitochondrial reducing equivalents to fuel OxPhos. The electrons from NADH generated by GAPDH in the cytosol can be transferred to the mitochondrial NADH pool through the aspartate-malate shuttle (AMS) and to mitochondrial $FADH_2$ through the glycerol-3 phosphate shuttle, thereby fuelling OxPhos and ATP production. The citrate malate shuttle (CMS) also generates mitochondrial NADH

through both the metabolism of pyruvate in the mitochondria and the transfer of electrons from cytosolic NADH to the mitochondrial NADH pool. The CMS is of most relevance to this study as it is the predominant pathway used by IL2/IL12-stimulated NK cells to fuel OxPhos (Assmann et al. 2017). The CMS is described in more detail in the next section.

1.8.3 The Citrate Malate Shuttle (CMS)

The CMS involves the import of glucose-derived pyruvate into the mitochondria. Pyruvate is metabolised to acetyl-coA (this yields one NADH molecule). Acetyl-coA combines with OAA to form citrate. Citrate can be exported from the mitochondria through Slc25a1. Slc25a1 is an obligate citrate/malate antiporter. Therefore, for each citrate molecule exported from the mitochondria, it is replaced by the entry of a cytosolic malate molecule. In the cytosol, citrate is metabolised by ATP citrate lyase (ACLY) to cytosolic acetyl-CoA and OAA which can be converted to malate in a reaction that oxidises NADH to yield NAD+. Malate re-enters the mitochondria through Slc25a1 where it is converted back to OAA yielding a second NADH molecule in the mitochondria. OAA can then react with another glucose derived acetyl-CoA to form another molecule of citrate, thus completing the cycle. Therefore, the CMS generates 2 molecules of NADH per pyruvate that enters the mitochondria. In contrast, the TCA cycle makes 5 NADH plus 1 $FADH_2$. However, use of the CMS comes with additional benefits – regeneration of cytosolic NAD+ and generation of cytosolic acetyl-coA. Maintaining NAD+ in the cytosol is essential to support glycolytic flux as it is an essential cofactor for the glycolytic enzyme GAPDH. Whereas the AMS also imports reducing equivalents into the mitochondria, the CMS has the added output of exporting acetyl-coA into the cytosol via citrate. Cytosolic acetyl-coA can be used for acetylation reactions or lipid synthesis (**Fig 1.5**)

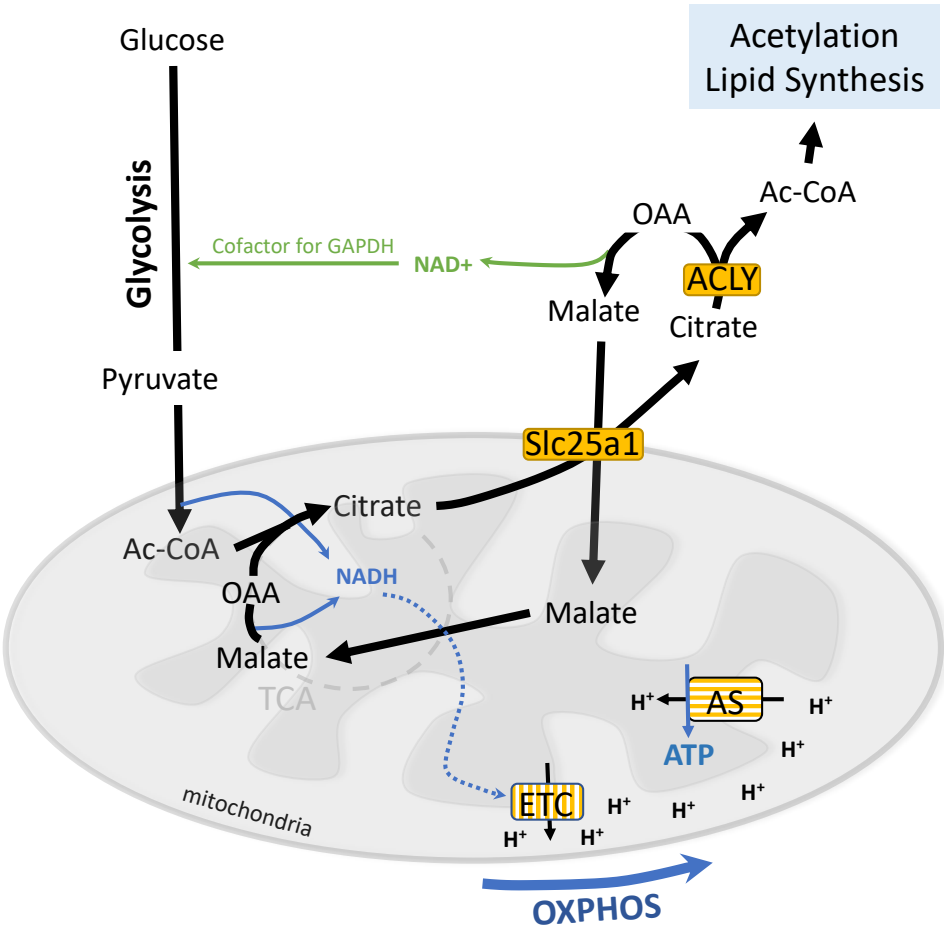

Figure 1.5 The Citrate-malate shuttle

Glucose is metabolised through glycolysis to pyruvate and then to mitochondrial acetyl-CoA (Ac-CoA) yielding one reduced NADH molecule. Ac-CoA combines with oxaloacetate (OAA) to make mitochondrial citrate, which is exported from the mitochondria through Slc25a1 - the citrate/malate antiporter. In the cytosol, citrate is metabolised by ATP citrate lyase (ACLY) to generate cytosolic Ac-CoA and OAA, which can be converted to malate in a reaction that oxidises NADH to yield NAD+. Maintaining NAD+ in the cytosol is essential for glycolysis to continue as it is a requisite cofactor for the glycolytic enzyme GAPDH. Malate re-enters the mitochondria through Slc25a1 where it is converted back to OAA yielding a second NADH molecule in the mitochondria. OAA can then react with another glucose derived Ac-CoA to form another molecule of citrate, thus completing the cycle. Therefore, the citrate malate shuttle generates 2 molecules of NADH per glucose pyruvate that enters the mitochondria that is used to drive OxPhos. In contrast, the TCA cycle makes 5 NADH plus 1 $FADH_2$. However, the citrate malate shuttle has the additional output of cytosolic Ac-CoA that can be used as the substrate for acetylation reactions or lipid synthesis (O'Brien and Finlay 2019).

1.9 Auxiliary metabolic pathways

There is a complexity of peripheral pathways that can feed into and sprout off the core metabolic pathways. A plethora of these ancillary pathways exist including the pentose phosphate pathway (PPP), lipid synthesis pathways for production of cholesterol and fatty acids, and the polyamine synthesis pathway. The PPP is an auxiliary metabolic pathway that branches from glycolysis. The PPP can be divided into an oxidative and a non-oxidative arm. The oxidative-branch converts the glycolytic intermediate, glucose-6-phosphate (G6P) into CO_2, ribulose-5-phosphate (R5P) and NADPH. R5P can be used to fuel *de novo* nucleotide synthesis. Alternatively, R5P can enter the non-oxidative arm of the PPP and cycle to G6P to re-enter the oxidative arm in a process that generates NADPH (See **Fig 1.6**).

NAPDH generated by the PPP can be used to support the *de novo* lipid synthesis, important for the biosynthesis of biological membranes. *De novo* lipid synthesis comprises of the cholesterol synthesis pathway and the fatty acid synthesis pathway, both fuelled by cytosolic acetyl-coA. For fatty acid synthesis, acetyl-CoA is carboxylated to generate malonyl-CoA by the enzyme acetyl-coA carboxylase (ACC). This is an irreversible step and thus is the first committed step of the fatty acid synthesis pathway. Fatty acid synthase (FASN) carries out the chain elongation steps through repeat condensation of two-carbon units and can use PPP-derived NADPH as a reducing equivalent.

Cholesterol biosynthesis is a complex and heavily regulated process which also stems from acetyl-CoA. Cholesterol is synthesised from two precursor acetyl-coA building blocks. The committing and rate-limiting step of cholesterol synthesis is the conversion of acetyl-coA to mevalonate via the actions of the enzyme HMG-CoA reductase. This reaction also requires NADPH. Mevalonate undergoes a huge number of enzymatic reactions which culminate in the generation of squalene. Cyclisation of squalene to form four fused rings proceeds, to form cholesterol. Cholesterol can undergo further modifications to generate oxysterols, cholesterol esters for storage or cholesterol sulfates. Cellular cholesterol levels are tightly

controlled at the level of cholesterol synthesis and efflux through reciprocal regulation of two transcription factor families – the sterol regulatory element binding proteins (SREBP) and the liver X receptors (LXR). The LXRs are a family of ligand-activated transcription factors that induce a transcriptional programme that results in cholesterol storage or cholesterol efflux. SREBP transcription factors are described in more detail in section 1.14.

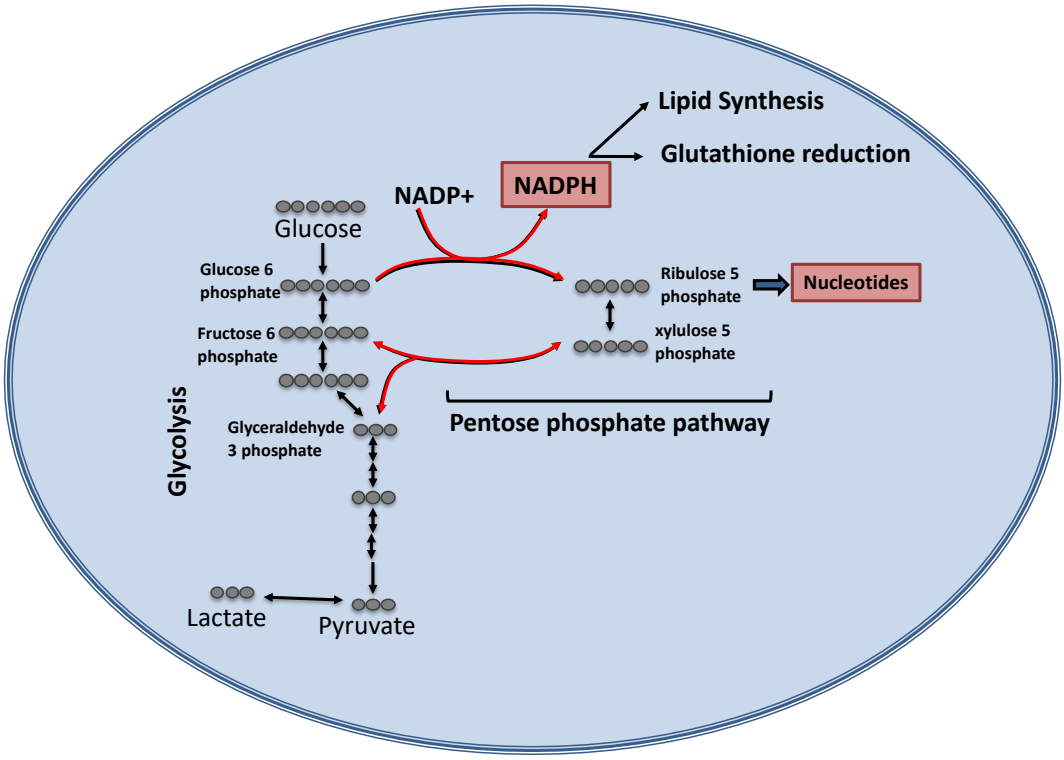

Figure 1.6 The Pentose Phosphate Pathway

The pentose phosphate pathway (PPP) is an ancillary pathway that branches from the core glycolytic pathway. Glucose is converted into glucose-6-phosphate, which feeds into the oxidative arm of the PPP. Glucose-6-phosphate is then used to generate ribulose-5-phosphate which can be further modified for the production of nucleotides. Alternatively,ribulose-5-phosphate can feed into the non-oxidative arm of the PPP to prioritise the generation of NADPH which is an important reducing equivalent and necessary for lipid synthesis.

1.9.1 The Polyamine synthesis pathway

De novo polyamine synthesis is another important auxiliary metabolic pathway. The natural polyamines (putrescine, spermidine and spermine) are small, positively charged metabolites present in all eukaryotic cells that are synthesised from the amino acid precursor – ornithine. Ornithine can be synthesised from arginine through the actions of arginase, or from glutamine as part of the urea cycle. Alternatively, ornithine can be produced from proline and glutamate by the enzyme ornithine acetyltransferase (OAT). Due to their small, cationic nature, polyamines interact with numerous important negatively charged biomolecules including proteins, phospholipids and nucleic acids. Therefore, polyamines have the means to affect a range of different cellular processes, including influencing DNA and RNA stability, protein translation, and gene expression, thereby playing roles in cellular growth, proliferation and survival (See **Fig 1.7**).

The first step of polyamine synthesis is the conversion of ornithine to putrescine by the enzyme ornithine decarboxylase (ODC) (**Fig 1.8**). This is the rate-limiting step of the pathway. The polyamine putrescine can be converted into the other polyamines -spermidine and then spermine, by the enzymes spermidine synthase or spermine synthase respectively. Alternatively spermidine can be used as a substrate for the hypusination of eukaryotic initiation factor 5A (eIF5A) .Hypusination is a unique post-translational modification and eIF5A is the only protein known to be hypusinated. Hypusine forms at a lysine residue on eIF5A. An aminobutyl moiety from spermidine is transferred to eIF5A by the enzyme DHPS. This forms deoxyhypusinated eIF5A. ($eIF5A^{DH}$). $eIF5A^{DH}$ can then be hydroxylated by DOHH to form hypusinated eIF5A ($eIF5A^{H}$). Hypusination of eIF5A is essential for its function.The polyamine content of the cell is tightly regulated at the level of enzyme expression and activity. Furthermore, polyamine levels are regulated by their catabolism. Polyamine catabolic enzymes: SSAT , PAO and SMO, can acetylate and/or oxidise polyamines leading to their interconversion or depletion from the cell.

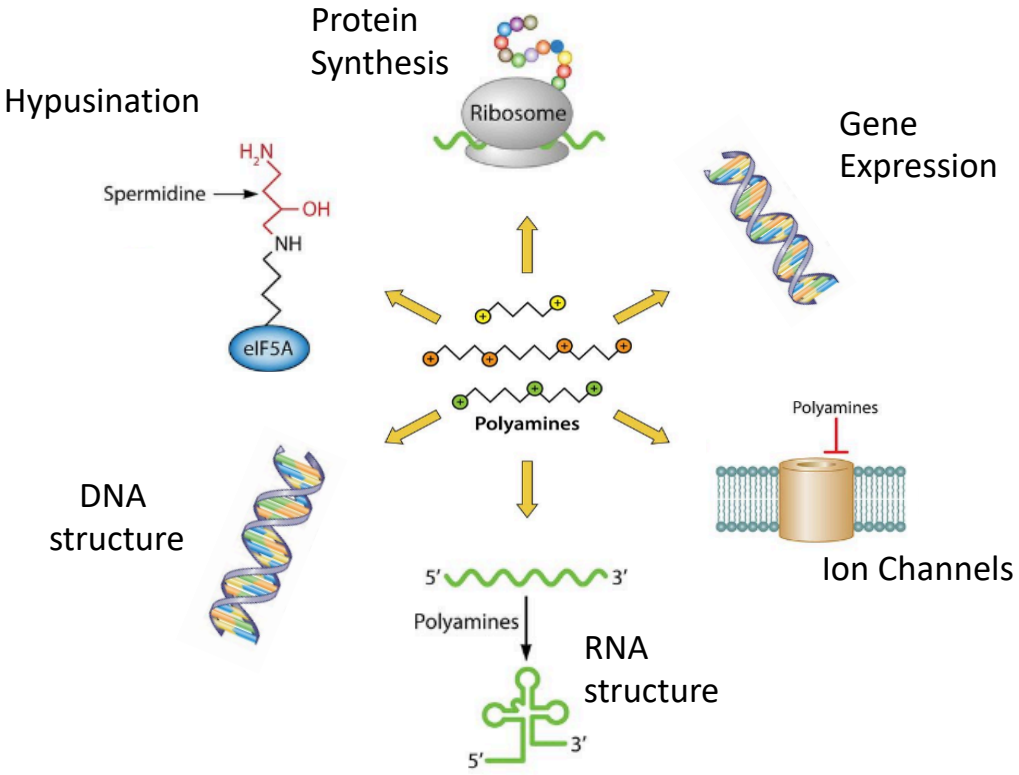

Figure 1.7 Polyamines can affect many cellular processes

Polyamines (putrescine, spermidine and spermine) are small and positively charged. Therefore, they have the ability to interact with negatively charged biomolecules and influence a diverse amount of cellular processes. Processes affected by polyamines include protein synthesis and gene expression. Polyamines can modulate ion channels. Polyamines can influence the structure of DNA and RNA. Furthermore, the polyamine spermidine, is the substrate for hypusination of the translation initiation factor – eIF5A. Figure from (Mounce et al. 2017).

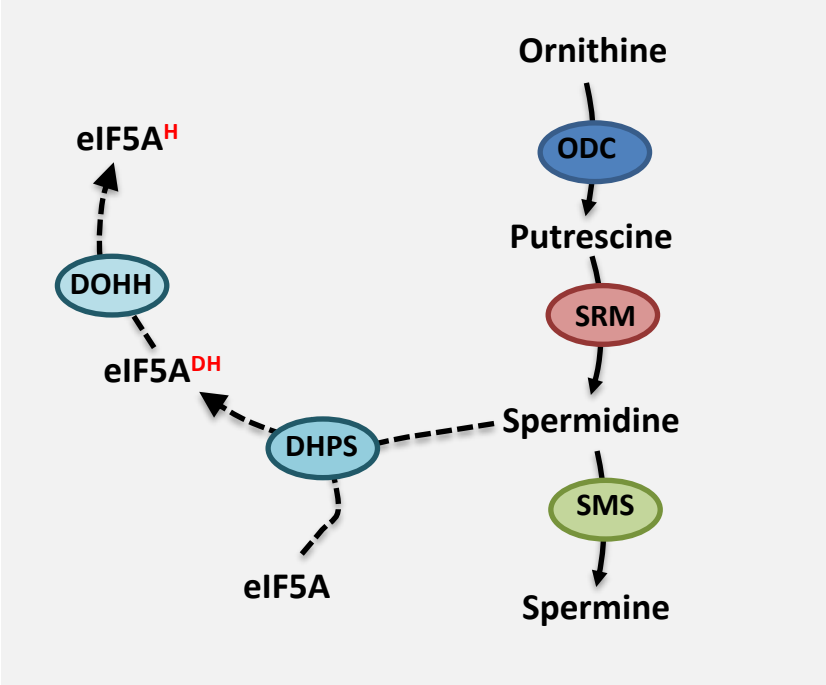

Figure 1.8 *De novo* polyamine synthesis supports hypusination

The amino acid ornithine is the precursor to polyamine synthesis. Ornithine is converted to putrescine by the enzyme ODC (this is the rate-limiting step *of de novo* polyamine synthesis). Putrescine can be converted to spermidine by SRM. Spermidine can be further converted to generate spermine by SMS. Alternatively, spermidine can be used as a substrate for the hypusination of eIF5A. An aminobutyl moiety from spermidine is transferred to eIF5A by the enzyme DHPS. This forms deoxyhypusinated eIF5A ($eIF5A^{DH}$). $eIF5A^{DH}$ is then hydroxylated by DOHH to form hypusinated eIF5A ($eIF5A^{H}$).

1.10 Metabolic reprogramming

As mentioned previously, immune cells adopt particular metabolic configurations to meet their functional needs. Additionally, many immune cells will need to adapt their metabolic profiles during their lifespans as they transition through different activation states or encounter environments rich or poor in certain fuels or nutrients. Immune cells can change their metabolism rapidly, for transient, short-term adaptations or they can metabolically reprogram to sustain longer-term metabolic changes. Metabolic reprogramming refers to complete re-

wiring/remodelling of a cell's metabolic machinery. For example, the rate of glycolysis may increase by one of two scenarios – either rapid increases due to increased efficiency of already present glycolytic machinery or due to complete metabolic reprogramming involving increased expression of glucose transporters and glycolytic enzymes. As the latter requires transcription and translation of new proteins, it takes longer to occur but results in an increased glycolytic capacity, and is thus able to sustain increased levels of glycolysis for longer periods - as may be necessary for an immune cell involved in an immune response.

1.11 NK cell metabolism

Baseline metabolic activity of resting *ex vivo* splenic NK cells is relatively low, with NK cells preferentially using OxPhos to generate ATP (Keppel et al. 2015). Furthermore, short-term stimulation does not result in any increase in rates of NK cell OxPhos or glycolysis (Keppel et al. 2015). For instance, four hours of cytokine stimulation (with IL15, IL12/IL15 or IL12/IL18) or six hours receptor ligation (with anti-NK1.1 or anti-Ly49D) does not result in increased metabolic rates (Keppel et al. 2015). However, work from our group has revealed that upon longer-term activation, NK cells undergo a metabolic switch towards a phenotype that allows for heightened flux through glycolysis in addition to increases in OxPhos (Donnelly et al. 2014; Assmann et al. 2017). Complete metabolic reprogramming facilitates this change in NK cell metabolism. 18 hours of cytokine-stimulation induces NK cells to increase expression of glucose transporters, glycolytic enzymes and nutrient transporters in addition to increases in mitochondrial mass (Donnelly et al. 2014; Marcais et al. 2014; Assmann et al. 2017). This increase in glycolytic machinery allows for increased glucose uptake and corresponds with an increase in glycolytic capacity and rate of glycolysis in activated NK cells, with the preferential conversion of glycolysis-derived pyruvate to lactate (Donnelly et al. 2014; Assmann et al. 2017). Though cytokine-stimulation also induces increased rates of OxPhos in NK cells, the overall balance of NK cell metabolism shifts from OxPhos to glycolysis (Marcais et al. 2014; Donnelly et al. 2014). Receptor-ligation alone (through NK1.1) has also been shown to trigger modest increases in the

rates of glycolysis and OxPhos after 18 hours. However, receptor ligation induces expression of CD25 – the high affinity IL2 receptor, on NK cells. Thus, ligation of NK1.1 facilitates increased NK cell responsiveness to IL2, and therefore substantial increases in glycolysis and OxPhos are observed with NK1.1 stimulation in the presence of IL2 , compared to NK cells activated with IL2 or NK1.1 alone (Kedia-Mehta et al. 2019). Thus indicating that receptor-ligation can prime NK cells for enhanced IL2-induced metabolic responses (Kedia-Mehta et al. 2019) .

Of note, in cytokine-stimulated NK cells, the pyruvate that does enter the mitochondria is not metabolised through the TCA cycle to fuel OxPhos as is the case in many other immune cell subsets. Instead, pyruvate is converted to mitochondrial citrate which is metabolised by the CMS to generate the reducing equivalents to fuel OxPhos and ATP production. Unlike the TCA cycle, which can receive inputs from multiple fuels, the CMS is fuelled exclusively by glucose. Therefore, glutamine is not an important fuel for driving OxPhos in cytokine-activated NK cells; inhibition of glutaminolysis with the glutaminase inhibitor bis-2-(5-phenylacetamido-1,3,4-thiadiazol-2-yl)ethyl sulphide (BPTES) or treating cells with 6-diazo-5-oxo-L-norleucine (DON) – an inhibitor of glutamine-utilising enzymes, had no effect on NK cell OxPhos rates (Loftus et al. 2018). Whether NK cells use fatty acids as a fuel source has not been extensively studied, partly due to the fact that there is a lack of specific tools for examining fatty acid oxidation. Etomoxir, an inhibitor commonly used to block fatty acid oxidation has recently been found to have a number of off-target effects (O'Connor et al. 2018; Yao et al. 2018; Raud et al. 2018). Of note, the accumulation of excess fatty acids (palmitate and/or oleate) within NK cells can be detrimental to NK cell metabolism (Michelet et al. 2018).

1.12 NK cell metabolism is integral to NK cell function

The importance of metabolic changes for NK cell function has been investigated using a variety of approaches to limit the flux through either glycolysis or OxPhos and it has emerged that NK cell metabolism is essential to support NK cell effector functions. For instance, although NK cells do not increase levels of glycolysis or

OxPhos following short-term cytokine or receptor-stimulation, inhibition of basal metabolic rates reduces NK cell production of IFNγ (Keppel et al. 2015). When NK cell metabolic reprogramming is blocked over longer time points, effector functions are even more dramatically impaired. Strategies that reduce metabolic rates in murine NK cells inhibit cytokine-induced proliferation and impair NK cell cytotoxicity against a range of cell lines *in vitro* (Mah et al. 2017; Assmann et al. 2017). Concentrations of the metabolic inhibitors 2-deoxyglucose (2DG) and oligomycin that limit but do not completely inhibit glycolysis and OxPhos, respectively, are found to inhibit the production of IFNγ and the expression of granzyme b in both murine and subsets of human NK cells (Keating et al. 2016; Donnelly et al. 2014). 2DG-treatment also decreases the ability of IL15-activated human NK cells to kill K562 target cells (Mah et al. 2017). Culturing NK cells in galactose, a fuel that can only support low rates of glycolysis, rather than glucose also inhibits the effector function of both human and murine NK cells (Donnelly et al. 2014; Keating et al. 2016). When 2DG is injected into mice it is preferentially taken up by highly glycolytic cells and will limit the rate of glycolysis in these cells. 2DG treatment in mice following poly I:C administration or MCMV infection results in reduced NK cell IFNγ production and in the case of MCMV infection, reduced clearance of m157 target cells and increased viral loads (Mah et al. 2017; Donnelly et al. 2014). Therefore NK cell metabolism is integrally linked to NK cell effector functions. Understanding the mechanisms underlying this link will provide greater insight into NK cell biology and may explain why NK cells are found to be defective in many pathological situations.

1.13 Regulation of NK cell metabolism

1.13.1 Role of mTORC1 in NK cell metabolic reprogramming

A key integrator of cellular metabolism and function that has been extensively explored in immune cells is the mammalian target of rapamycin complex 1 (mTORC1) (Finlay et al. 2012a). mTORC1 activity can be controlled by cytokine signalling, however mTORC1 can also acutely sense and respond to levels of

cellular nutrients (Pollizzi and Powell 2014). Through its role as a serine/threonine kinase, mTORC1 activity promotes anabolic processes including protein and lipid synthesis and shuts off catabolic processes such as autophagy. Additionally, in many cell types, mTORC1 facilitates metabolic reprogramming (Finlay et al. 2012a). This positions mTORC1 in a key position to co-ordinate environmental signals with cell responses in immune cells (Pollizzi and Powell 2014).

Indeed, mTORC1 activation is critical for inducing metabolic reprogramming in NK cells upon cytokine-activation (Donnelly et al. 2014; Marcais et al. 2014). Resting NK cells have low mTORC1 activity and stimulation with cytokine induces a robust increase in mTORC1 signalling both in murine and human NK cells (Marcais et al. 2014; Donnelly et al. 2014; Keating et al. 2016; Jensen et al. 2017). This increased mTORC1 activity is essential to support NK cell metabolism (Viel et al. 2016; Donnelly et al. 2014). mTORC1 activity is required for increased expression of nutrient transporters and glycolytic enzymes in NK cells activated either *in vitro* or *in vivo* (Nandagopal et al. 2014; Donnelly et al. 2014; Marcais et al. 2014). Inhibition of mTORC1 using the pharmacological inhibitor rapamycin results in decreased glycolysis in murine NK cells stimulated with either IL2/IL12 or high dose IL15 (Donnelly et al. 2014; Viel et al. 2016). Thus highlighting that mTORC1 activity is necessary to support increases in NK cell metabolism.

Likewise, increased mTORC1 activity is essential to promote NK cell effector functions. For instance, rapamycin-treatment impairs cytokine-induced production of effector molecules such as IFNγ and granzyme B (Donnelly et al. 2014). Furthermore, a study of mice treated with rapamycin during MCMV infection revealed reduced mTORC1 activity in NK cells was associated with reduced NK cell proliferation, IFNγ production and cytotoxicity leading to elevated viral burdens (Nandagopal et al. 2014). Cytotoxic responses of human NK cells were also shown to be mTORC1-dependent (Michelet et al. 2018).The importance of mTORC1 for NK cell responses is also evident during receptor activation of NK cells - IFNγ production and CD98 expression following ligation of the NKG2D

receptor was shown to be mTORC1-dependent (Abel et al. 2018). Likewise, NK cells stimulated through the NK1.1 receptor in the presence of IL2, have been recently shown to require mTORC1 activity for their increased glycolytic and OxPhos rates and for IFNγ and granzyme B expression (Kedia-Mehta et al. 2019).

It is worth noting that mTORC1 activity in NK cells, and also in $CD8^+$ cytotoxic T lymphocytes (CTL), is not downstream of the PI3K/Akt signalling axis but is acutely sensitive to the levels of the amino acids leucine and glutamine (Loftus et al. 2018; Sinclair et al. 2013; Finlay et al. 2012a). Thus mTORC1 is critical to the responses of cytokine-activated NK cells. Investigating the importance of downstream targets of mTORC1 is therefore critical to our understanding of NK cell metabolism and function.

1.13.2 Transcription factors controlling NK cell metabolism

The transcription factor cMYC is often considered to be controlled downstream of mTORC1. Indeed, the initial upregulation of cMYC expression in NK cells that occurs within minutes of IL2/IL12 stimulation is partially dependent on mTORC1 signalling, but cMYC expression is completely independent of mTORC1 at all timepoints after a few hours. Instead, cMYC expression is dependent on the availability of the amino acids that are required to maintain high rates of cMYC translation to offset continuous cMYC degradation (Loftus et al. 2018). While glutamine is not an important fuel for NK cells (discussed previously), glutamine is important for cMYCc signalling as it facilitates amino acid uptake through the system L-amino acid transporter Slc7a5 (see **Fig 1.9**). Withdrawal of glutamine or inhibition of amino acid uptake through Slc7a5 results in the rapid loss of cMYC protein within minutes (Loftus et al. 2018). cMYC is required for the metabolism of activated NK cells through its control of the expression of the metabolic machinery in NK cells. cMYC is required for the increased expression of glucose transporters and glycolytic enzymes to support glycolysis and for mitogenesis to provide the increased mitochondrial mass required to support high rates of OxPhos (Loftus et al. 2018). cMYC is also important for NK cell metabolism and

function following receptor ligation (NK1.1 ligation in combination with IL2) as recently demonstrated by other members of our group (Kedia-Mehta et al. 2019).

Interestingly, while in CD8+ T lymphocytes, the transcription factor HIF1α is the key transcription factor required to support elevated glycolysis, this is not the case in NK cells (Loftus et al. 2018; Finlay et al. 2012b). HIF1α-deficient NK cells have no defects in either glycolysis or OxPhos in response to cytokine-stimulation (Loftus et al. 2018). While HIF1α does not appear to be important in this context, it might be predicted that HIF1α may have a role in controlling NK cell metabolism in other contexts such as under conditions of hypoxia. The transcription factor Regulatory factor X 7 (RFX7) has been identified as a negative regulator of NK cell metabolism. Consistent with this, the rates of glycolysis and OxPhos in RFX7-deficient NK cells were increased when compared to control NK cells (Castro et al. 2018). RFX7-deficient NK cells were reduced in number and dysfunctional during immune responses indicating the importance of controlled metabolism for NK cell homeostasis (Castro et al. 2018).

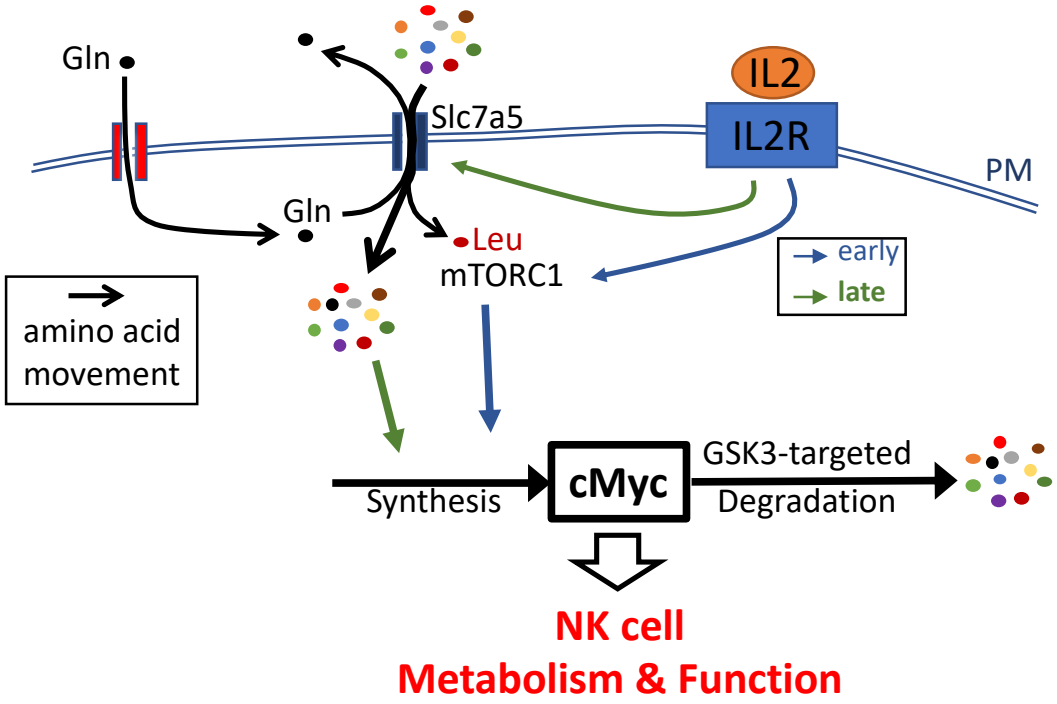

Figure 1.9 Model for the regulation of cMYC expression in NK cells.

cMYC is a transcription factor with crucial roles in the regulation of NK cell metabolism and function. Expression of cMYC is tightly controlled by a balance of cMYC protein synthesis and GSK3-targeted proteasomal degradation. At early time points following IL2/IL12 stimulation (minutes) cMYC protein levels accumulate in an mTORC1 dependent manner. mTORC1 is activated by IL2 signalling and can increase cMYC protein translation. IL2/IL12 stimulation also induces the expression and activity of the amino acid transporter SLC7A5. At later time points following IL2/IL12 stimulation (20 h), amino acid uptake through SLC7A5 is essential to sustain cMYC protein expression, while mTORC1 activity is not required. Withdrawal of the amino acid glutamine, which is essential for SLC7A5 activity, or the direct inhibition of amino acid transport through SLC7A5, both result in rapid loss of cMYC protein levels. While leucine uptake through SLC7A5 is required for mTORC1 activity, at these later time points, leucine withdrawal is not sufficient to reduce cMYC expression. Uptake of other amino acids through SLC7A5 are important in the regulation of cMYC, such as methionine, phenylalanine, tyrosine, arginine and tryptophan. Therefore, cMYC is a key regulator of NK cell metabolic and functional responses. Figure and adapted legend from (Loftus et al. 2018)

1.14 Sterol Regulatory Element Binding Proteins

In many cell types, the activity of sterol regulatory element binding proteins (SREBP) is induced downstream of mTORC1 activation (Porstmann et al. 2008). SREBP transcription factors are a group of transcription factors with an important role in the induction of lipid synthesis. SREBP transcription factors are considered to be 'master regulators' of *de novo* lipid synthesis, due to their role in controlling expression of an array of lipogenic genes, including enzymes in the synthesis pathways of cholesterol and fatty acids (Horton, Goldstein, and Brown 2002). Three SREBP isoforms exist: SREBP1a, SREBP1c and SREBP2 (Yokoyama et al. 1993; Hua et al. 1993; Shimomura et al. 1997). SREBP1a and SREBP1c are transcribed from the same gene but with alternate first exon, whilst SREBP2 is encoded by a separate gene (Horton et al. 1998). In general, all SREBP isoforms are ubiquitously expressed, however their ratios vary across different tissues (Im et al. 2011). Additionally, the activities of the three isoforms differ. SREBP1a and SREBP1c primarily activate transcription of genes involved in fatty acid synthesis whilst SREBP2 is more commonly associated with transcription of genes encoding enzymes in the cholesterol synthesis pathway (Horton, Goldstein, and Brown 2002; Horton et al. 1998). However, when over-expressed at super-physiologic levels, all SREBP isoforms can activate all described SREBP target genes. Unless otherwise stated, the use of 'SREBP' henceforth, refers to all SREBP isoforms.

Newly synthesised SREBP transcription factors are embedded in the membrane of the endoplasmic reticulum (ER). Their structure consists of an N-terminal domain, containing a bHLH-Zip region, two hydrophobic transmembrane segments and a regulatory C-terminal domain. The N-terminal segment of SREBP is the active transcription factor and in order to have effects on target genes, it must be released proteolytically from the membrane so that it can translocate to the nucleus. The release of the active SREBP involves a complicated multistep process.

1.14.1 SREBP proteolytic cleavage

Immediately following synthesis, SREBP transcription factors are inserted into the ER membrane where they associate through their C-terminal regulatory domain, with a membrane-bound escort protein called SCAP. SREBP transcription factors only have the ability to leave the ER membrane when in complex with SCAP. This occurs via the binding of SCAP to COPII proteins, which cluster the SCAP/SREBP complex into transport vesicles (Sun et al. 2007). These COPII-coated vesicles traffic from the ER to the Golgi apparatus. Here, SREBP interacts with two Golgi-resident proteases designated site-1-protease (S1P) and site-2-protease (S2P). S1P and S2P sequentially cleave the full-length, membrane bound SREBP, to release the N-terminal domain. The liberated N-terminal then translocates to the nucleus, where SREBP can recognise and bind to a 10 base-pair sequence known as a sterol regulatory element (SRE) and stimulate transcription (Smith et al. 1990) (See **Fig 1.10)**. Of note, SREBP transcription factors can also recognise and bind to E-box motifs but the extent to which SREBP activity influences transcription at these sites physiologically is unclear (Amemiya-Kudo et al. 2002; Shimano 2001).

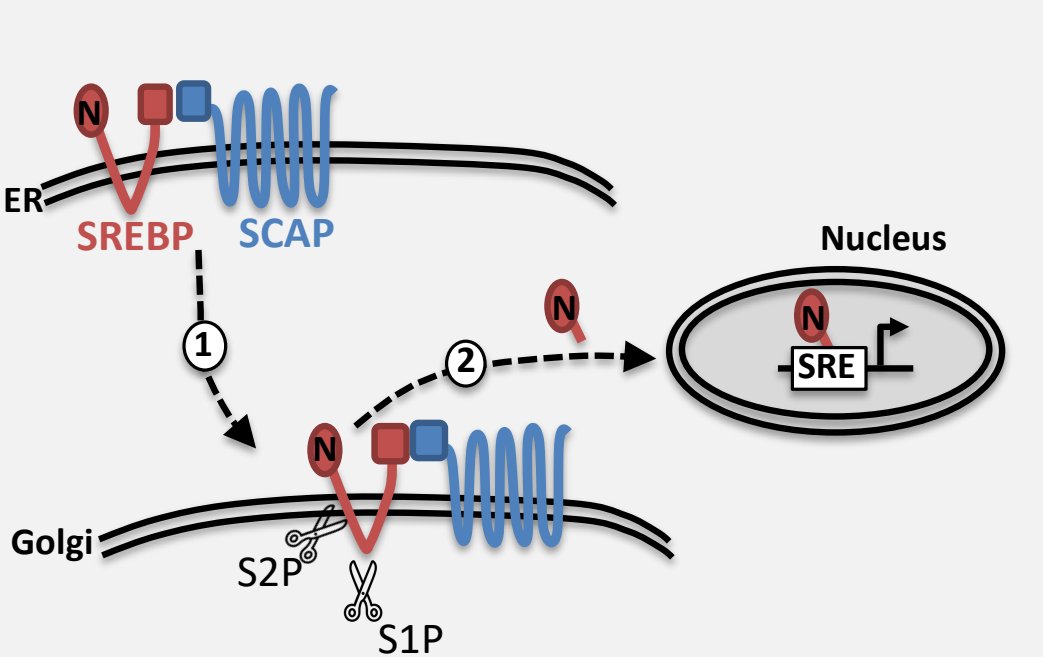

Figure 1.10 SREBP processing and activation

Newly synthesised SREBP is immediately inserted into the ER membrane. SREBP is membrane bound and its N-terminal, transcriptionally active domain cannot enter the nucleus to influence gene transcription. To enter the nucleus, the N-terminal domain of SREBP must be released from the membrane-bound full-length form. For this to occur, SREBP must be translocated from the ER to the Golgi in complex with chaperone protein SCAP (**1**). In the Golgi, the N-terminal, transcriptionally active SREBP fragment is released following 2 sequential cleavage steps by Golgi-resident proteases: site-1 protease (S1P) and site-2 protease (S2P)(**2**). Active SREBP can then enter the nucleus and bind sterol regulatory element (SRE)-containing promoters to influence transcription.

1.14.2 Regulation of SREBP proteolytic cleavage

Regulation of SREBP processing is complex. Feedback inhibition by cholesterol and cholesterol derivatives control the exit of SCAP, and therefore the exit of SREBP, from the ER (Kandutsch and Chen 1974; Radhakrishnan et al. 2007a). SCAP, in addition to its function as an escort protein for SREBP, also acts as a sterol sensor. When the cholesterol content of the ER membrane is above 4-5% of total ER lipid, a conformational change in SCAP causes it to bind to one of two ER-resident

proteins designated Insig-1 and Insig-2 (Radhakrishnan et al. 2008). The conformational change in SCAP caused by Insig-binding prevents it from interacting with COPII proteins and therefore the SCAP/SREBP complex is not incorporated into transport vesicles. Therefore, SREBP transcription factors are retained in the ER and cannot transit to the Golgi. As no proteases exist in the ER that can release its N-terminal fragment, SREBP cannot enter the nucleus (Sun et al. 2007).

Interestingly, oxysterols - oxidised forms of cholesterol - also inhibit SREBP activity, even more potently than un-oxidised cholesterol (Brown and Goldstein 1974; Kandutsch and Chen 1975). Oxysterols are short-lived oxygenated derivatives of cholesterol and have been shown to inhibit SREBP processing through a separate mechanism to cholesterol. It has been demonstrated that whereas cholesterol binds to SCAP, 25-hydroxycholesterol (25HC), a potent oxysterol, directly binds to Insig (Radhakrishnan et al. 2007b). The binding of 25HC to Insig, induces SCAP-Insig binding (Adams et al. 2004). Again, this prevents SCAP interacting with COPII proteins and therefore SREBP cannot be further processed or activated (See **Fig 1.11**).

1.14.3 Other mechanisms of SREBP regulation

In addition to sterol regulation of the proteolytic processing of SREBP transcription factors, SREBP activity can be controlled in other diverse ways, including through transcription and translation of SREBP transcription factors themselves, through degradation of SREBP in the nucleus, and through changes in levels of Insig proteins and SCAP (Brown and Goldstein 2009). Of note, mTORC1 has been shown to positively regulate the action of SREBP through several distinct mechanisms (Duvel et al. 2010; Porstmann et al. 2008). mTORC1 can induce increased SREBP expression, increase SREBP processing and can promote stabilisation and nuclear accumulation of the processed nuclear form of SREBP (Bakan and Laplante 2012; Laplante and Sabatini 2013).

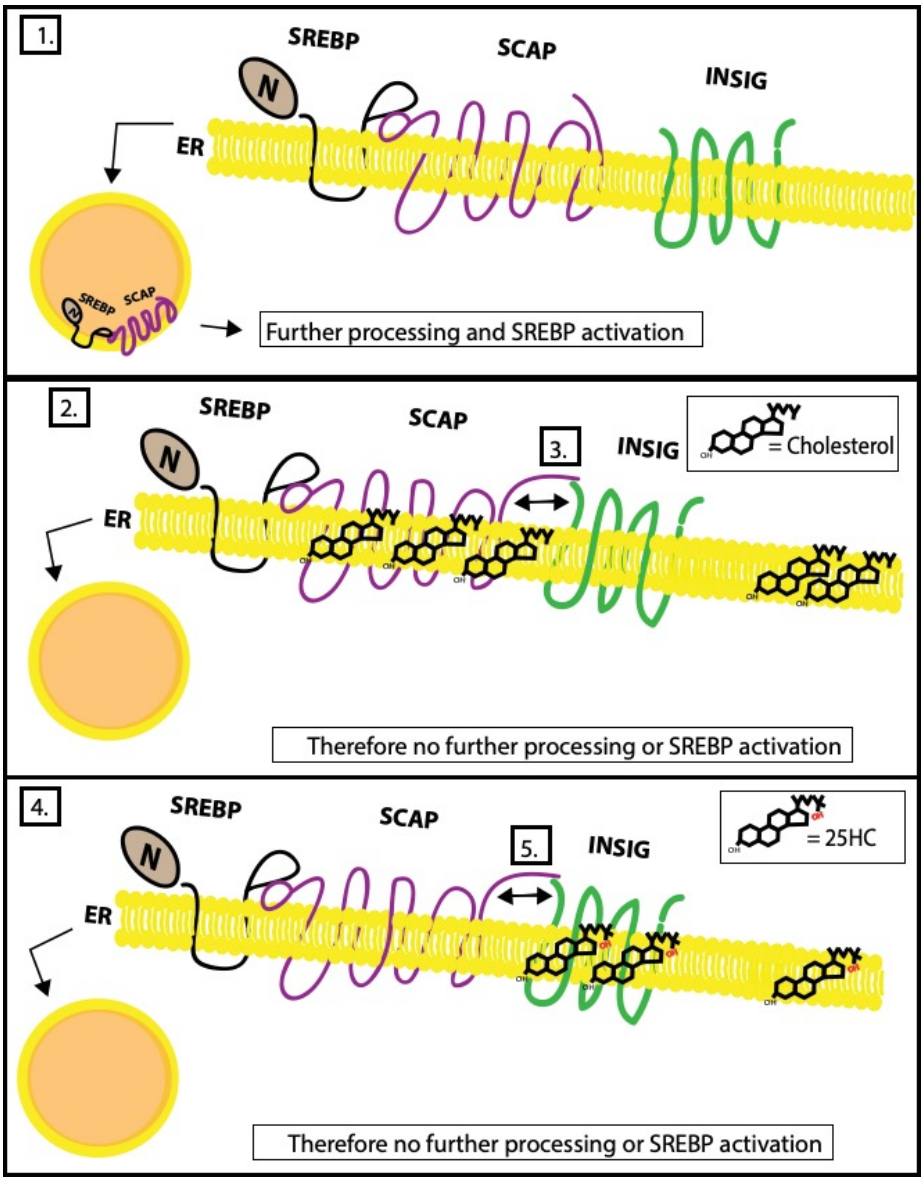

Figure 1.11 Regulation of SREBP processing by cholesterol and oxysterols

(**1**) Under conditions of low ER cholesterol, SREBP is trafficked from the ER in complex with SCAP and can be further processed into its active form. (**2**) When ER cholesterol levels rise, cholesterol binds to SCAP and changes its conformation causing it to bind Insig. (**3**) SCAP-Insig binding prevents SCAP or SREBP from being incorporated into transport vesicles and thus SREBP is retained in the ER and cannot be activated. (**4**) When ER levels of 25HC increase, 25HC binds to Insig. (**5**) Insig changes in conformation when it senses 25HC and induces a conformational change in SCAP. This prevents SCAP and SREBP from leaving the ER.

1.15 Aims and Objectives

Knowledge of NK cell metabolism has significantly expanded in recent years. At the beginning of this study nothing was published about the role for SREBP transcription factors in NK cell biology, however preliminary data generated by previous Finlay lab members identified that SREBP was important for lipid synthesis by NK cells. Surprisingly, they showed that lipid synthesis was dispensable for NK cell metabolism and function. This led to a hypothesis in the lab that SREBP transcription factors may be directly important for NK cell metabolism and function.

Overall aim:

To investigate a role for SREBP transcription factors in controlling NK cell metabolic and functional responses.

Specific objectives:

1) Investigate whether SREBP transcription factors are active in cytokine-stimulated NK cells
2) Determine the role for SREBP in controlling NK cell metabolism using pharmacological inhibitors of SREBP activation
3) Use a transgenic approach to prevent SREBP activation in NK cells and assess the impact on NK cell metabolism
4) Investigate whether SREBP plays a role in the function of NK cells

2 Materials and Methods

2.1 Materials

2.1.1 Chemicals

IL2 was purchased from NCI preclinical repository. IL12 and NK cell isolation kit II were purchased from Miltenyi Biotech. EasySep™ Mouse NK cell Isolation Kit and Robosep buffer were from Stemcell Technologies. Recombinant murine IL15 was purchased from Peprotech. Human IL15 was from NIH. IL18 was obtained from GlaxoSmithKline (GSK). Seahorse XF media and calibration buffer were purchased from Agilent technologies. RNeasy RNA purification mini kit was purchased from Qiagen. Qscript cDNA supermix was purchased from Quanta Biosciences. Golgi plug, Cytofix/Cytoperm, Calcein-AM and Perm/Wash were purchased from BD biosciences. GoTaq DNA Polymerase, 5X Green Flexi-Buffer and $MgCl_2$ were from Promega. Dulbecco's phosphate buffered saline and Penicillin-Streptomycin were purchased from Invitrogen/Biosciences. Cell-Tak™ was purchased from Corning. Heat-inactivated FCS was from Labtech International. GC7 and Immobilon™ Western Chemiluminescent HPR Substrate (ECL) blotting reagent were from Merck Millipore. Rapamycin and unstained protein maker were purchased from Fisher Scientific. PF429242 was purchased from Adoog Bioscience. DFMO and DENSPM were purchased from Tocris. 40% Acrylamide, research grade ethanol, research grade isopropanol, 1,4-Dithiothrotol (DTT), Phosphate buffered saline tablets, Tetramethylethylenediamine (TEMED), Tween-20, Ammonium persulphate (APS), Sodium dodecyl-sulphate (SDS), Tris, 4-Hydroxytamoxifen (4-OH-TMX), 25-Hydroxycholesterol (25HC), 27-Hydroxycholesterol (27HC), GW3965, Ciclopirox (Cpx), Dimethyl-sulfoxide (DMSO), 1000X Polyamine Supplement, Nancy-520, Proteinase K, Deoxynucleotide set (dNTPS), β-Mercaptoethanol (β-ME), Glucose, Galactose, 2-deoxyglucose (2DG), Ultima Gold™ LSC cocktail, Rotenone, Antimycin-A, Oligomycin, Fluoro-Carbonyl Cyanide Phenylhdrazone (FCCP), Ponseau S, Triton-X and research-grade ethanol were purchased from Sigma-Aldrich. Ethanol was purchased from school stores.

2.1.2 Equipment

Tissue culture dishes (6, 12, 24, 48 and 96 well), tissue culture flasks (25cm^2, 75cm^2 and 175cm^2), falcons (15ml, 50ml), cell strainers (70µm), Absolute qPCR seals and AB-1900 low profile PCR plates were obtained from Thermo Fisher. MicroAmp Fast 96-well Reaction plates (0.1ml) for PCR were from Applied Biosystems. Transfer pipettes were purchased from Starstedt. 96-well flat black polystyrene plates were purchased from Costar. Haemocytometers were purchased from Hausser Scientific. EasySep^{TM} magnet for column-free separation was from Stemcell Technologies. AutoMACS pro separator and LS MACS separation columns were obtained from Miltenyi Biotec. Seahorse XFe96 Analyzer, Seahorse XF24 Analyser, XF 24-well and XF 96-well microplates and cartridges were from Agilent Technologies. ^{3}Prime Thermal Cycler was from Techne. Electrophoresis running system was from Atto. XCELL II Blot Module transfer system was from Invitrogen. Nanodrop Spectrophotometer ND-1000 was from Labtech International. Steri-Cycle CO_2 Incubator was from Thermo Forma. Power Source 300 V was obtained from VWR International. FACS Canto, LSR Fortessa, 5ml FACS tubes and 5ml syringes were from Becton Dickinson (BD). ABI 7900HT Fast qRT-PCR machine and QuantStudio 3 Real-Time PCR System were from Applied Biosystems. FlowJo^{TM} software was from TreeStar. GraphPad Prism 6.00 was from GraphPad Software.

2.1.3 Mice

C57BL/6J mice were purchased from Harlan (Bicester, U.K.) or Charles River or were bred in house. Scap$^{flox/flox}$ mice (B6;129-Scaptm1Mbjg/J)(Matsuda et al. 2001) were obtained from the Jackson Laboratory. Tamox-Cre mice (Gt(ROSA)26Sortm2(cre/ERT2)Brn/Cnrm) were obtained from the EMMA archive (Hameyer et al. 2007). cMyc$^{flox/flox}$ mice were obtained from Dundee University. All mice were maintained in compliance with EU and the Health Products Regulatory Authority regulations with the approval of the University of Dublin's ethical review board.

2.1.4 *Cell lines*

K562, a human chronic myelogenous leukaemia cell line and B16-F10, a murine melanoma cell line, were originally purchased from the American Type Culture Collection (ATCC).

2.1.5 *Flow cytometry antibodies and stains*

Sources of antibodies and stains used for flow cytometry are listed in **Table 2.1.**

2.1.6 *Western blotting antibodies*

Sources of antibodies used for western blotting are listed in **Table 2.2** .

2.1.7 *Buffers and Solutions*

Various buffers and solutions were used are described in the methods used in this report. Their compositions are outlined in **Table 2.3.**

Table 2.1 Antibodies and stains used for flow cytometry

Target/Stain	Fluorophore	Clone	Source	Dilution/ Concentration
Fc block	-	2.4G2	BD Pharmingen	1/100
NK1.1	BV421	PK136	BioLegend	1/200
NKp46	Percp-eFluor 710	29A1.4	eBioSciences	1/200
CD3	FITC	145-2c11	eBioSciences	1/600
TCR-β	APC	H57-597	BD Pharmingen	1/200
TCR-β	PE	H57-597	BD Pharmingen	1/200
CD19	PeCy7	ID3	BD Pharmingen	1/200
IFNγ	APC	XMG1.2	BD Pharmingen	1/200
Granzyme B	PeCy7	NGZB	eBioSciences	1/200
CD25	APC-Cy7	PC61	BD Pharmingen	1/200
CD71	BV510	C2F2	BD Pharmingen	1/200
CFSE	CFSE	-	Molecular Probes	1/1000
LD Aqua	V500	-	ThermoFisher	1/500
LD Near-IR	APC-Cy7	-	ThermoFisher	1/500
CellTrace™ Violet	V450	-	Molecular Probes	1/1000
Zombie NIR™	APC-Cy7	-	BioLegend	1/500
MitoTracker™ Red (CMXRos)	PE-CF594	-	ThermoFisher	100nM
MitoTracker™ Green	FITC	-	ThermoFisher	100nM
TMRM	PE		ThermoFisher	100nM

Table 2.2 Western blotting primary antibodies

Antibody raised against:	Source:	Dilution:	Secondary antibody:
cMyc	Cell Signalling Technologies	1/2500	Rabbit
β-actin	Sigma	1/5000	Mouse

Table 2.3 Buffers and solutions

Media/Buffer/Solution:	Components:
NK cell culture media	RPMI medium 1640 (+) L-Glutamine, FCS (10%), Penicillin/Streptomycin (1%), 50µM β –ME
B16 culture media	DMEM Glutamax™, FCS (10%), Penicillin/Streptomycin (1%)
K562 culture media	IMDM (+) L-Glutamine, FCS (10%), Penicillin/Streptomycin (1%)
Glucose free media + supplements	Dialayzed FCS (10%), 2mM Glutamine, 1mM Sodium Pyruvate, 1x Vitamin Cocktail, 1x Selenium/Insulin Cocktail, 50µM β-ME and Penicillin/Streptomycin (1%)
FACS buffer	Dulbecco's PBS supplemented to contain 7% NK cell culture media
Ear digest buffer	25mM NaCl, 50mM Tris/HCl, 0.1% SDS
50X TAE	2M Tris, 17.4M acetic acid, 64mM EDTA
2% Agarose gel	2g agarose, 100ml 1x TAE, 20µl Nancy-520
Resolving gel	1.344ml of ddH20, 2.25ml of 1M Tris pH 8.8, 0.6ml of 1% SDS, 1.5ml of 40% Acrylamide, 300µl of 1.5% APS, 6µl of TEMED
Stacking gel (10% acrylamide)	3.12ml of ddH20, 0.625ml of 1M Tris pH 6.8, 0.5ml of 1% SDS, 0.5ml of 40% Acrylamide, 250µl of 1.5% APS, 5µl of TEMED
Cell-Tak™ for cell adhesion of cells to 24 well Seahorse plates	13µl Cell-Tak™ (Corning), 4180.5µl Sodium Bicarbonate (0.1M), 6.5µl NaOH (1M). Recipe makes enough to coat 20 wells
Cell-Tak™ for cell adhesion of cells to 96 well Seahorse plates	9.25µl Cell-Tak™ (Corning), 2986.1µl Sodium Bicarbonate (0.1M), 4.65µl NaOH (1M). Recipe makes enough to coat 96 wells
RNA lysis buffer	RLT buffer (Qiagen), β -ME (1%)
Protein lysis buffer	100mM Tris/HCl pH 6.7, 20% Glycerol, 4% SDS, 5% β -ME (5%), 0.1% bromophenol blue
Western blot running Buffer (10X)	25mM Tris, 192mM Glycine, 0.1% SDS
Western blot stripping Buffer (10X)	62.5mM Tris, 2% SDS, β -ME (0.7%)
Western blot transfer Buffer (10X)	25mM Tris, 192mM Glycine, 10% methanol
PBST	100ml 10X PBS, 900ml ddH_20, 1ml Tween

2.2 Methods

2.2.1 NK cell culture

NK Cell Expansion

Mice were sacrificed and murine spleens obtained under sterile conditions. Spleens were gently passed through a 70μm strainer, into a well of a 6-well plate containing cold NK cell culture media. The resulting cell suspension was passed back through the strainer using a Pasteur pipette until any clumps were dissipated. The suspension was then transferred to a falcon and centrifuged at 1400rpm for 4 minutes at room temperature (RT). The supernatant was discarded and cell pellet resuspended. Red blood cells were removed by osmotic lysis - sterile ddH_20 was briefly added to the pellet, followed by quick addition of NK cell culture media to prevent lysis of splenocytes. Cells were again centrifuged and supernatant discarded after which cell concentration was adjusted to $2x10^6$ cells/ml in NK cell culture media. The resulting splenocyte suspension was plated out in 6 well plates (5 ml of cell suspension/well). To selectively enrich NK cell numbers, these splenocytes were cultured for 6 days (unless otherwise stated) in the presence of IL15. IL15 was added on day 0 and then re-added on day 3. As the biological activity of murine recombinant IL15 (Peprotech) varied between batches, the optimal culturing concentration was titrated for each new lot, to ensure NK cells expanded in culture but did not become overly activated (as measured by cell size and effector molecule production). Concentrations of IL15 used varied between 5-15ng/ml. Murine recombinant IL15 (Peprotech) was substituted with human IL15 (NIH), later in the project. Human IL15 which was used at 10ng/ml .

SCAP^{KO} NK Cell Expansion

Where indicated, splenocytes were isolated from *Scap*^{KO} (*Scap*$^{fl/fl}$ × Tamox-Cre) mice or *Scap*^{WT} (*Scap*$^{+/+}$ × Tamox-Cre) mice. Splenocytes were isolated as described in section 2.2.1.2, and cultured for 3 days in low dose IL15 (Peprotech) in NK cell culture media in the presence of 4-hydroxytamoxifen (0.6 µM, Sigma) to induce Cre recombinase-mediated excision of the floxed *Scap* exon.

NK Cell Stimulation

On day 6 (apart from where stated otherwise), cells were pooled from culture, washed from culture media, and resuspended in fresh media for stimulation. For biochemical analyses, NK cells were purified by magnetic-activated cell sorting (MACS) using the NK cell isolation kit II (Miltenyi Biotech) and an AutoMACS pro separator, according to manufacturer's instructions. Alternatively, NK cells were purified manually using the EasySep^{TM} system and EasySep^{TM} mouse NK cell isolation kit according to manufacturer's instructions. Cells were stimulated with the cytokine combination IL2 (20 ng/mL, NCI preclinical repository) and IL12 (10 ng/mL, Miltenyi Biotech) or IL12 (25 ng/mL, Miltenyi Biotech), IL15 (50 ng/mL, Peprotech) and IL18 (5 ng/mL, R&D Systems). Unstimulated NK cells were maintained in low-dose IL15 (5 ng/ml) as a survival factor. Stimulations were carried out in the presence or absence of 25-hydroxycholesterol (2.5 µM, Sigma), PF429242 (10 µM, Adoog Bioscience), 2-deoxy-D-glucose (0.5, 1, 10mM Sigma), rapamycin (20nM, Fisher), oligomycin (0.4, 1, 40, 400nM, Sigma), DFMO (1mM,Tocris), DENSPM (10µM,Tocris), GW3965 (2µM), 27HC (1,2µM, Sigma) ,GC7 (9.25,46.5,92.5 µM, Merck Millipore), CPX (5,10,20 µM, Sigma) Polyamine Supplement (2X, Sigma).Appropriate vehicle controls were used where necessary. Where indicated, NK cells were stimulated in glucose-free medium supplemented with either glucose (10mM, Sigma) or galactose (10mM, Sigma). For a summary of cell treatments, vehicle controls and concentrations see **Table 2.4.**

Table 2.4 Cell treatments

Compound:	Stock Concentration:	Final Dilution:	Vehicle control used:
IL2	20µg/ml	20ng/ml	-
IL12	50µg/ml	10ng/ml	-
IL15 (culturing dose)	20µg/ml	5-15ng/ml	-
IL15 (unstim. dose)	20µg/ml	10ng/ml	-
IL15 (activating dose)	20µg/ml	50ng/ml	-
Human IL15 (culturing dose)	0.51mg/ml	10ng/ml	-
Human IL15 (unstim. dose)	0.51mg/ml	7.5ng/ml	-
IL18	100µg/ml	5ng/ml	-
25HC	1.8mg/ml	1µg/ml	DMSO
27HC	10mM	1 µM,2 µM	EtOH/DMSO
PF429242	100mM	10µM	DMSO
Rapamycin	1mM	20nM	-
2DG	1M	0.5mM,1mM,10mM	-
Glucose	1M	10mM	-
Galactose	1M	10mM	-
Oligomycin	2mM	0.4nM, 1nM, 40nM, 400nm	-
4-Hydroxytamoxifen (4-OH TMX)	6mM	0.6µM	-
DFMO	75mM	1mM	-
GW3965	4mM	2µM	DMSO
DENSPM	100mM	10 µM	-
GC7	92.5mM	9.25 µM,46.5 µM, 9.25 µM	-
CPX	150mM	5 µM,10µM, 20 µM	DMSO
Polyamine Supermix	1000x	2x	-

2.2.2 Culture of cell lines

B16-F10 murine melanoma cells were cultured in DMEM (Invitrogen/Biosciences) supplemented with 10% heat-inactivated FCS (Labtech, International), and 1% penicillin/streptomycin (Invitrogen/Biosciences). K562 human chronic myelogenous leukaemia cells were cultured in IMDM supplemented with 10% heat-inactivated FCS and 1% penicillin/streptomycin

2.2.3 RNA analysis

RNA isolation

RNA lysates were obtained from purified NK cells. Cells were resuspended and transferred to Eppendorfs, centrifuged at 1400rpm for 3 minutes, supernatant decanted, 1ml of cold PBS added, and the previous centrifugation step repeated. The supernatant was discarded and cell pellets were lysed in 600µl of RLT buffer containing 1% β-ME. RNA was isolated using the RNeasy mini kit (Qiagen) according to manufacturer's instructions. RNA preparations were assessed for quality and RNA concentration using a Nanodrop spectrophotometer (ND-1000) (NanoDrop® Technologies). RNA lysates were stored at -80°C prior to cDNA synthesis.

cDNA synthesis

20µl of cDNA was synthesized from 0.5 µg or 1µg of isolated RNA. RNA was diluted with DEPC water and cDNA was generated using 4µl of q-Script cDNA Supermix (Quanta Biosciences) according to the manufacturer's instructions. The reverse transcription required to for this process was carried out in Techne's ^{3}Prime Thermal Cycler according to temperature cycles listed in in **Table 2.5**.

Table 2.5 Temperature settings for cDNA synthesis

Duration:	Temperature:
5 minutes	25°C
30 minutes	42°C
5 minutes	85°C
Hold	4°C

Primer Design

Primers for quantitative real time PCR (qRT-PCR) were designed using Primer BLAST software located on the NCBI website (http://www.ncbi.nlm.nih.gov/tools/primer-blast/). The transcript ID for the gene of interest was entered into Primer Blast and parameters for primer design were set such that they fulfilled the following requirements:

- GC content of between 40-60%
- GC clamp at one end
- spanning an exon-exon junction
- have at least three mismatches to other sequences in the gene of interest
- to have less than 1°C between melting temperatures
- for forward and reverse primers to be of similar length

Primer sequences generated were verified using the Ensembl genome browser (http://www.ensembl.org/index.html). Sequences of primers used for RT-qPCR are listed in **Table 2.6.**

RT-qPCR

Quantitative real time PCR (qRT-PCR) was performed in triplicate in a 96-well plate using iQ SYBR Green-based detection on an ABI 7900HT Fast qRT-PCR machine (Applied Biosystems) or a QuantStudio 3 Real-Time PCR System (Applied Biosystems). Each 10µl PCR reaction consisted of 0.5µl cDNA, 5µl SYBR Green supermix, 3.7µl nuclease free water and 0.4µl each of sense and antisense primers. Plates were sealed with an Absolute qPCR seal (MSC) and run under fast cycle conditions as listed in **Table 2.7**

For analysis of qRT-PCR data, genes of interest were normalised to an internal control gene - either *Rplp0* or *Gapdh* or *HPRT*. The relative mRNA content of samples was calculated according to the following equation:

$$\text{Rel. mRNA expression} = 2^{(ct_{uc} - ct_{us})} / 2^{(ct_{rc} - ct_{rs})}$$

Where **ct** is the threshold cycle, **u** is the mRNA of interest, **r** is the reference gene, **uc** is the sample every other sample is made relative to and **s** is every other sample.

Table 2.6 PCR primer sequences

Gene name:	Primer sequence:
Acat2 forward	5’-CCAGAGCGACAAGATGAATGC-3
Acat2 reverse	5’-CCACAACCTGCCGTCAAGA-3’
Acly forward	5’-CCCCAAGATTCAGTCCCAAGTC-3’
Acly reverse	5’-GATCCCCAGTGAAAGGGTAGAC -3’
cMyc forward	5’- GCGTTGGAAACCCCGACAG -3’
cMyc reverse	5’- CTTCCAGATATCCTCACTGGGC-3’
Dhps forward	5’- GAGAGTGGGATCAACAGGATTGG-3’
Dhps reverse	5’- TATGGGCCCAATAATACACAGAGTC-3’
Fasn forward	5’-GGTATAGACGACGGGCACAG-3’
Fasn reverse	5’-GCCATTCCAGGTAAATGGGC-3’
Gapdh forward	5’-CATGGCCTTCCGTGTTCCTA-3’
Gapdh reverse	5’-CCTGCTTCACCACCTTCTTGAT-3’
Hex2 forward	5’-TCGCCTGCTTATTCACGGAG-3’
Hex2 reverse	5’-TCGCCTGCTTATTCACGGAG -3’
Hmgcs1 forward	5’-CATTGGGCGGCTAGAAGTTG-3’
Hmgcs1 reverse	5’-ACCAGAGCATATCGTCCATCC-3’
Ldha forward	5’-CTGGGAGAACATGGCGACTC-3’
Ldha reverse	5’-ATGGCCCAGGATGTGTAACC-3’
Pkf (liver) forward	5’- GTTTGGAAGCCTCTCCTCCTC-3’
Pkf (liver) reverse	5’- AGAGGTCAACACGGCGATG-3’
Pkm1 forward	5’-AAACAGCCAAGGGGGACTAC-3’
Pkm1 reverse	5’- TTATAAGAGGCCTCCACGCTG-3’
Rplp0 forward	5’-CATGTCGCTCCGAGGGAAG-3’
Rplp0 reverse	5’-CAGCAGCTGGCACCTTATTG-3’
Scap forward	5’-GCTCTGCGCATCCTATCCAATTCCC-3’
Scap reverse	5’-CAGCCGGCAAGTAACAAGGGATCCG-3’
Slc25a1 forward	5’-CTTCCTGGGGTGCCTATGTG-3’
Slc25a1 reverse	5’-CATTTAAGGCCAATGGCGGG-3’
Slc2a1 forward	5’-GGAATCGTCGTTGGCATCCT-3’
Slc2a1 reverse	5’-CGAAGCTTCTTCAGCACACTC-3’
Sms forward	5’-CCCTCTTGGCTGATGGTGAG-3’
Sms reverse	5’-TTGCCTTGCACATCACTGTC-3’
Srebp1a forward	5’- CGGTTTTGAACGACATCGAAGACATGC -3'
Srebp1a reverse	5’- TTTAAAGCAGCGGGTGCCGATG -3'
Srebp1c forward	5’- CTGACAGGTGAAATCGGCG-3'
Srepb1c reverse	5’- ACACGGACGGGTACATCTTT-3'
Srebf2 forward	5’- GACATCGACGAGATGCTACAGTTTG -3'
Srebf2 reverse	5’- AGACTTTGACCTGCAGGGCC -3'
Srm forward	5’- TTCCTACCTATCCCAGCGGC-3'
Srm reverse	5’- ATGTCATTGAGGGCCTTCCG-3'

Table 2.7 PCR run settings

Stage:	Temperature (°C)	Time (seconds)	Cycles
1	95	60	1
2	95	1	35
2	57	20	
3	95	15	1
3	55	30	1
3	95	15	1

2.2.4 Genotyping

Ear Digestion

Ear clips were placed in Eppendorf tubes and digested overnight at 55°C in the presence of 50µl ear digest buffer and 5µl of proteinase K. After digestion, 100µl of DEPC water was added to tubes and they were heated at 100°C for 7 minutes to inactivate proteinase K. Samples were stored at 4°C short-term prior to analysis.

PCR and gel

Digested ear templates were diluted 1 in 3 in DEPC water. For Tamoxifen Cre PCR, 1µl of diluted template was added to 24µl of Tamoxifen-Cre master-mix or for SCAP PCR, 1µl of diluted template was added to 19µl of SCAP master-mix. Respective master-mix components are listed in **Table 2.8**. The PCR reactions were carried out in Techne's ^{3}Prime Thermal Cycler according to the temperature cycles listed in **Table 2.9** (Cre) and **2.10** (Scap). Primer sequences are listed in **Table 2.11**. PCR products were separated on a 2% agarose gel containing 20 µl of Nancy-520.

Table 2.8 Genotyping master mix components

Component:	Tamoxifen Cre master-mix (µl)	Scap master-mix (µl)
5X Buffer	5	4
$MgCl_2$	2.5	1.6
Forward primer (pre-diluted 1/10)	0.5	2
Reverse primer (pre-diluted 1/10)	0.5	2
dNTP (10mM solution)	1	0.4
GoTaq enzyme	0.1	0.2
DEPC water	14.4	10.2

Table 2.9 Cre PCR temperature settings

Temperature (°C)	Time	Cycles
94	Hold	1
94	5min	
94	1min	35
63	2min	
72	3min	
72	5min	1
4	Hold	

Table 2.10 Scap PCR temperature settings

Temperature (°C)	Time	Cycles
94	Hold	1
94	3min	
94	30 sec	35
68	45 sec	
72	30 sec	
72	2min	1
4	Hold	

Table 2.11 Genotyping primer sequences

Gene name:	Primer sequence:
Cre forward	5'- CGGTCGATGCAACGAGTGATGAGG-3'
Cre reverse	5'- CCAGAGACGGAAATCCATCGCTCG-3'
Scap forward	5'- GCTCTGCGCATCCTATCCAATTCCC-3'
Scap reverse	5'- CAGCCGGCAAGTAACAAGGGATCCG-3'

2.2.5 Flow cytometry

For FACS analysis, NK cells were transferred to labelled FACS tubes and washed with FACS buffer to remove residual media. Cells were incubated for 5 minutes at 4 °C with Fc blocking antibody, in order to prevent non-specific binding of FACS antibodies to the cells. Subsequently, cells were stained with saturating concentrations of surface-targeted antibodies for a further 20min at 4 °C. Cells

were then washed with FACS buffer and resuspended in FACS buffer for analysis. Samples were analysed by FACS Canto 2 (BD) or FACS Fortessa (BD) using FACS Diva software and data analysed using FlowJo™ (TreeStar). Live cells were gated according to their forward scatter (FSC-A) and side scatter (SSC-A), single cells according to their FSC-W and FSC-A and cultured NK cells were identified as NK1.1+ , NKp46+ and CD3- cells. For splenocyte experiments NK cells were identified as NK1.1+ , NKp46+, CD3-, CD19- cells.

Intracellular staining

Where intracellular staining was required, GolgiPlug™ (BD Biosciences) - a protein transport inhibitor - was added to cells in culture for the final 4 hours of stimulation, to prevent secretion of proteins. Cells were surface stained as previously described (section 2.2.5), followed by fixation and permeabilization of the cells, using the Cytofix/Cytoperm kit from BD Biosciences according to manufacturer's instructions. Intracellular antibodies were added to the permeabilised cells for a further 20 minutes at 4°C, then cells were washed and analysed as described in section 2.2.5.

Viability staining

For viability analysis, NK cells were transferred to FACS tubes, washed twice with FACS buffer and then stained with either LD Aqua or LD Near-IR (ThermoFisher) or Zombie NIE (BioLegend). Staining was carried out at room temperature for 20 minutes. Cells were then washed in FACS buffer prior to further staining and analysis.

MitoTracker Staining

For mitochondrial mass experiments, cells were washed from stimulation media, transferred to FACS tubes and incubated in media containing MitoTracker™ Red CMXRos (100nM, ThermoFisher) or MitoTracker™ Green (100nM, ThermoFisher) for 30 min at 37 °C, prior to further staining and analysis.

TMRM Staining

To measure mitochondrial membrane potential, cells were washed from stimulation media, transferred to FACS tubes and incubated in media containing TMRM (100nM, ThermoFisher), for 30 min at 37 °C, prior to further staining and analysis.

CFSE labelling

For proliferation studies, NK cells were stained on day 3 of culture with the CellTrace™ CFSE kit (Molecular Probes) according to manufacturer's instructions. Cells were returned to culture for a further 2 days and analysed by flow cytometry every 24 hours. Proliferation was determined based on the dilution of CFSE.

2.2.6 Seahorse metabolic flux analysis

A Seahorse XF-24 Analyser or Seahorse XFe96 Analyser (Agilent Technologies) was used for real-time analysis of the extracellular acidification rate (ECAR) and oxygen consumption rate (OCR) of purified NK cells cultured under various conditions. Analysers were used according to manufacturer's instructions and seahorse cartridges were calibrated over-night with calibration buffer prior to use. For analysis, purified NK cells were washed from NK cell culture media and resuspended in seahorse media containing appropriate cytokines. NK cells were seeded at 200,000 NK cells/well (for Seahorse XFe96 Analyser) or 500-750,000 cells/well (for Seahorse XF24 Analyser) and adhered, using Cell-Tak™ (Corning), to a 24-well or 96-well XF Cell Culture Microplate (Agilent Technologies). The cell plate was kept at 37°C for 30 minutes in a non-CO_2 incubator before insertion into the Seahorse analyser. The Seahorse analyser sequentially measures the ECAR and the OCR of a monolayer of cells over time. Over the course of analysis, inhibitors were injected at sequential stages in order to interrogate the metabolic state of the cells (See **Fig 2.1**). The following inhibitors were injected and are listed in order of injection: oligomycin (2 μM), p-trifluoromethoxy carbonyl cyanide phenyl hydrazine (FCCP) (0.5 μM), rotenone (100 nM) plus antimycin A (4 μM), and 2DG (30 mM). Measurements following injections allowed for the calculation of basal

glycolysis, glycolytic capacity, basal mitochondrial respiration, and maximal mitochondrial respiration (see **Fig 2.1**).

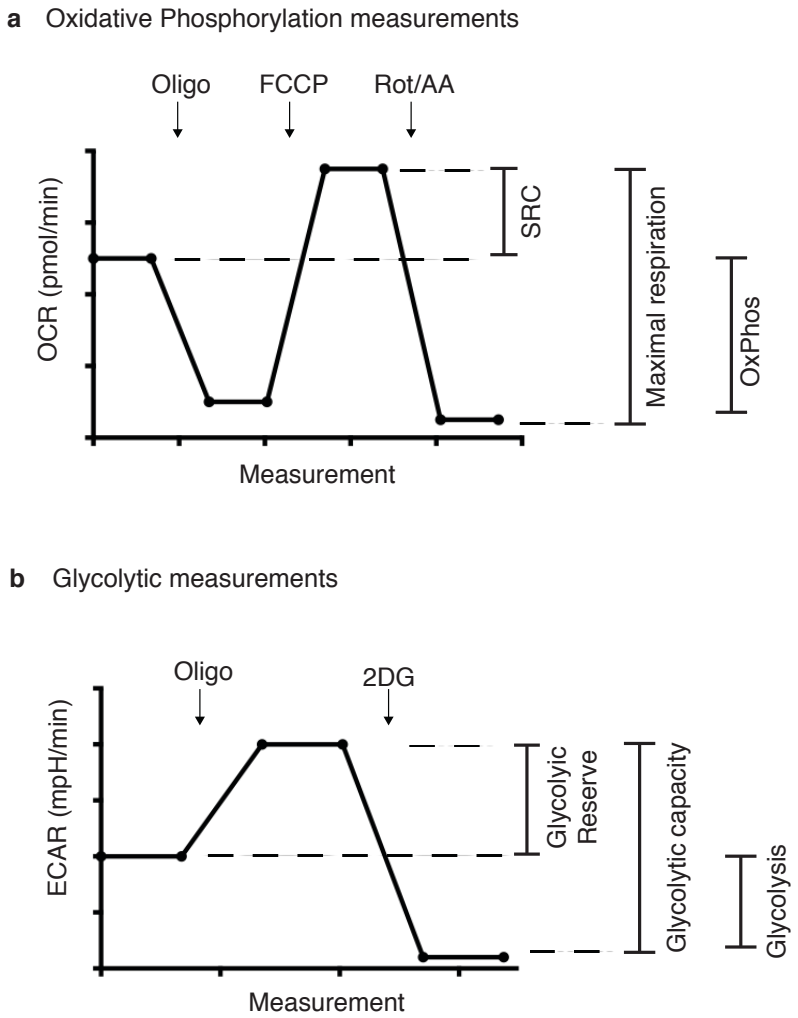

Figure 2.1 Schematic outlining interpretation of ECAR and OCR measurements

Injection of oligomycin (inhibits ATP synthase), blocks OxPhos and allows for calculation of glycolytic capacity. Injection of the uncoupling agent, FCCP, allows for calculation of maximum respiration. Antimycin A (AA) & rotenone, inhibit mitochondrial complexes 3 and 1 respectively – completely inhibits respiration and provides a control value for OCR when no respiration is occurring.2DG completely blocks glycolysis and provides a control value for the ECAR when no glycolysis is occurring.

2.2.7 *Fluorescent release cytotoxicity assay*

For measurement of NK cell cytotoxicity, NK cells were stimulated for 18h under various conditions. K562 target cells were stained with 10 µM Calcein-AM (BD Pharmingen) at 37 °C for 30 min. 30,000 stained target cells were added to a 96-well V-bottom plate and NK cells were added in a NK : target cell ratio 5:1, 2:1, and 1:1, respectively. For measurement of spontaneous release and maximum release, only target cells were added to the well or a final concentration of 0.2% Triton X-100 lysis buffer was added to target cells, respectively. Cells were incubated for 4 h at 37 °C. After incubation, the plate was spun down at 200 × g for 5 min and 75 µl of supernatant were transferred to a black 96-well plate. Fluorescence was measured on a Molecular Probes Spectra Max M3 spectrometer with an excitation wavelength of 495 nm and an emission wavelength of 515 nm. All samples were measured in triplicate and the average was used for further analysis. Experiment was only deemed valid if spontaneous release under 30%.

2.2.8 *Flow cytometry based cytotoxicity assay*

To analyse NK cell cytotoxicity, B16 target cells were labelled with CellTrace™ Violet (CTV, molecular probes) and seeded in a 48 well plate at a density of 4x104 cells/well. Purified NK cells were stimulated for 18 hours in the presence or absence of various inhibitors, after which they were washed out of cytokine and co-incubated at different effector to target ratios with the CTV-stained B16 target cells. After 4 hours, cells were harvested and stained with Live/Dead Near-IR (Thermo Fisher). Cell death of B16 cells was then analysed by flow cytometry.

2.2.9 *In vivo B16 melanoma tumour model*

B16 murine melanoma cells were used to induce tumours in C57BL/6 mice. Tumours were induced by subcutaneous (s.c.) injection of 2×10^5 B16 cells per mouse, into the right flank. On days 3, 7 and 10 post-tumour induction, mice were administered NK cells ($1.2–2 \times 10^6$ cells/mouse) or PBS, by s.c. injection into the tumour site. Injected NK cells were stimulated *in vitro* for 18 h prior to injection

with IL12 (25 ng/ml) + IL15 (50 ng/ml) + IL18 (5 ng/ml) with or without 25HC (2.5 µM). Tumour growth was assessed every 2-3 days and measurements recorded of the perpendicular diameters of the tumour using a callipers. Animals were sacrificed when tumours measured 15 mm in diameter (D) or on day 15. Tumour size was calculated using the following formula: $(D1)^2 \times (D2/2)$, D1 being the smaller value of the tumour diameter.

2.2.10 Western blotting

Protein extraction

To extract proteins, purified NK cells were resuspended and washed twice in ice-cold PBS. Supernatant was removed and cell pellets were resuspended in protein lysis buffer at a concentration of 10 million cells/ml. Cell lysates were heated for 9 minutes on a heat block to denature the protein content before analysis.

SDS-PAGE

Cell lysates were loaded into a 10 % acrylamide gel (see **table 2.3** for composition of stacking and resolving gels) and run using the AE6450 system from Atto Corporation, to separate proteins based on molecular weight.

Western blot

In order to transfer the separated protein from the gel onto PVDF membrane, gels were removed from the plates in the gel running system, placed into a 'gel-membrane sandwich', and assembled into the transfer apparatus according to the manufacturer's instructions. Transfer buffer containing 10% methanol was added to the transfer apparatus and the PVDF membrane was pre-activated in methanol. Proteins were transferred overnight at 15V, with the transfer apparatus in an ice box. Following transfer, membranes were carefully moved and stained with Ponseau S solution in order to confirm quality and conformity of the transfer and to allow annotation of the unstained protein ladder. Ponseau was then rinsed with ddH_2O. Membranes were blocked with 5% milk (in PBST) at RT for 40 minutes on a roller. Membranes were then incubated for a further 4 hours at RT in primary

antibody (see **Table 2.2** for dilutions). Membranes were then washed in PBST 3 times for 5 minutes each before probing with an appropriate secondary antibody for a further 45 minutes at RT. Wash steps with PBST were repeated 3 times. ECL was added to the membrane to allow visualisation of antibodies. A GelDoc XR+ System was used to assess the luminescence.

2.2.11 Metabolomics

The metabolomics data in this report was generated by Dr Nadine Assmann in collaboration with the University of Regensburg . Purified NK cells were stimulated with IL2 (20 ng/ml) plus IL12 (10 ng/ml) in the presence or absence of 25HC (2.5μm). At the appropriate time-point, cells were harvested and washed three times with ice-cold PBS. Metabolites were extracted from the cell pellet and cell culture supernatant by adding 80% aqueous methanol. Extracts were dried using a centrifugal evaporator (GeneVac EZ-2, SP Scientific) and were stored at −80 °C until further processing as described previously (Assmann et al. 2017). For polyamine quantification, metabolites were then analysed by liquid chromatography–tandem mass spectrometry (LC-MS/MS) as previously described (Stevens et al. 2010).

2.2.12 Proteomics Dataset

A Finlay lab quantitative-proteomics data set was generated at the University of Dundee on 6-day cultured IL2/IL12-stimulated NK cells provided by Dr Nadine Assmann. This dataset is available to members of our research group to probe and provides information on the copy number of each protein expressed in an 18h IL2/IL12-stimulated NK cell. For the generation of the dataset, 500,00 purified NK cells were stimulated for 18 h in the presence of IL2 (20 ng/ml) plus IL12 (10 ng/ml). To remove dead cells, a density gradient (Lymphoprep, Axis-Shield) was used. Cells were spun down and stored at −80 °C until further preparation. Proteomics analysis was then carried out at the University of Dundee according to the method described previously (Loftus et al. 2018).

2.2.13 Statistical analysis

GraphPad Prism 6.00 (GraphPad Software) was used for statistical analysis. A one-way ANOVA test was used for the comparison of more than 2 groups throughout with a Tukey post-test for multiple comparisons. Analysis of data with 2 factors were analysed by a two-way ANOVA with Sidak test for multiple comparison. A two-tailed Students t-test was used when there were only 2 groups for analysis. For comparison of relative values a one-sample t-test was used to calculate p values with the theoretical value set to 1.00. A p-value ≤ 0.05 was considered as statistically significant. In all figures, *p ≤ 0.05, **p ≤ 0.01, ***p ≤ 0.001 and ****p ≤ 0.0001.

3 SREBP controls metabolism in IL2/IL12-stimulated NK cells

3.1 Introduction

Previous publications from our group have demonstrated that mTORC1 signalling is critical for cytokine-induced activation of both murine and human NK cells (Donnelly et al. 2014; Keating et al. 2016). In many cell types, SREBP transcription factors act downstream of mTORC1 signalling (Porstmann et al. 2008). It was therefore hypothesised by our group that SREBP transcription factors might be active downstream of mTORC1 in cytokine-stimulated NK cells and that SREBP activity may important for regulating NK cell biology.

3.2 SREBP transcription factors are active in IL2/IL12-stimulated NK cells

Initial experiments were performed to determine whether SREBP transcription factors are expressed and are active in cytokine-stimulated NK cells. To obtain sufficient cell numbers for these biochemical analysis, murine splenocytes were expanded for 6 days in low dose IL15, to enrich for NK cells (referred to as cultured NK cells henceforth)(Zhao and French 2012; Donnelly et al. 2014). These cultured NK cells have previously been shown to have a similar profile to *ex vivo* splenocytes, yet are primed to respond robustly to further stimulation (Donnelly et al. 2014).Cultured NK cells were either left in the presence of low dose IL15 as a survival factor (referred to as unstimulated cells henceforth), or activated with the cytokine combination of IL2/IL12, for 18 hours, prior to analysis of mRNA transcript levels by RT-qPCR. mRNA transcripts encoding all three SREBP isoforms (SREBP1a, SREBP1c and SREBP 2) increased in response to IL2/IL12 cytokine stimulation (**Fig3.1a**) and these increased levels of expression were seen as early as 8 hours post-stimulation (**Fig 3.1 b-c**). To investigate SREBP transcriptional activity, the expression of a number of established SREBP target genes was measured; fatty acid synthase (*Fasn*), 3-Hydroxy-3-Methylglutaryl-CoA Synthase 1 (*Hmgcs1*) and Acetyl-CoA Acetyltransferase 2 (*Acat2*). The expression of all target genes robustly increased following 18 hours IL2/IL12 cytokine-stimulation (**Fig 3.2**). To confirm that these increases were SREBP-dependent, two

pharmacological inhibitors, with distinct mechanisms of action, were used to block SREBP activation: 25-hydroxycholesterol (25HC) and PF429242 (**Fig 3.3**). 25HC inhibits SREBP translocation to the Golgi thus preventing SREBP processing and activation, and PF429242 inhibits site-1 protease (S1P), required for cleavage of SREBP in the Golgi, thereby also preventing SREBP processing and activation (Radhakrishnan et al. 2007a; Hawkins et al. 2008)(**Fig 3.3**) NK cells stimulated with IL2/IL12 for 18 hours in the presence of either 25HC or PF429242 failed to increase expression of *Fasn, Hmgcs1* or *Acat2* (**Fig 3.2**).

The expression of SREBP transcription factors and these target genes was confirmed by interrogating a Finlay-lab whole cell, quantitative proteomics dataset, which had been generated by University of Dundee on samples provided by Dr Nadine Assmann. This data set provides information on the copy number of each protein per NK cell, following 18 hours IL2/IL12 cytokine-stimulation. NK cells expressed the proteins encoded by both *Srebf1* , *Srebf2* (**Fig 3.4a**). Copy numbers of SREBP transcription factors were comparable to levels of cMyc – a transcription factor previously shown to have an important role in IL2/IL12-stimulated NK cells - and were substantially increased when compared to HIF1α - a transcription factor previously shown to play no role in IL2/IL12-stimulated NK cells (Loftus et al. 2018) (**Fig 3.4a**). Furthermore, we compared copy numbers of SREBP target genes, to proteins found in other metabolic pathways known to be active in IL2/IL12-stimulated NK cells – namely the pentose phosphate pathway (PPP) and the TCA cycle (Assmann et al. 2017). Proteins encoded by SREBP-target genes were expressed at similar levels to these pathways(**Fig 3.5**). Given the link between mTORC1 and SREBP in other cell types, it was next investigated whether SREBP activity is dependent on mTORC1 signalling in NK cells (Porstmann et al. 2008). Indeed, the highly specific mTORC1 inhibitor, rapamycin, significantly reduced the expression of SREBP target genes in IL2/IL12 stimulated NK cells (**Fig 3.6**). Combined, these data demonstrate that SREBP activity is induced upon NK cell stimulation with IL2/IL12, in an mTORC1-dependent manner.

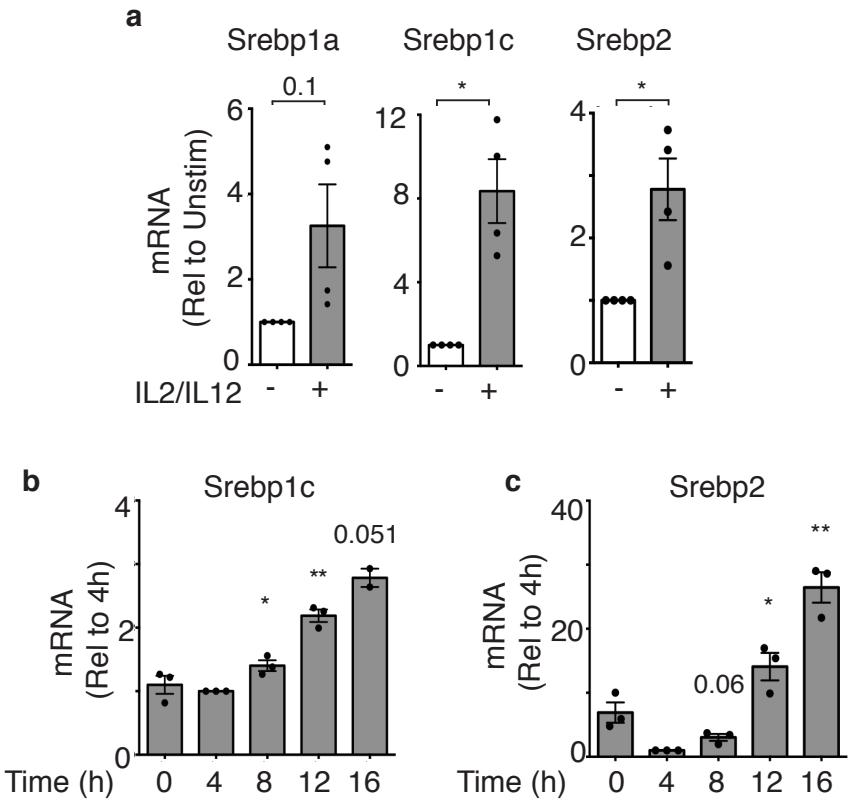

Figure 3.1 IL2/IL12 stimulated NK cells increase expression of mRNA encoding SREBP transcription factors

NK cells were cultured from splenocytes, purified and left unstimulated (white bars) or stimulated (grey bars) with IL2 (20ng/ml) + IL12 (10ng/ml), for 18 h (**a**) or as indicated (**b-c**), and the cells lysed and analysed by qRT-PCR for mRNA encoding SREBP1 (SREBP1a and SREBP1c isoforms) or SREBP2. Data is normalised to levels of control genes *Gapdh* **(a)** or *Rplp0* (**b-c)** and presented relative to mRNA expression in unstimulated **(a)** or 4h stimulated (**b-c)** NK cells. Data is mean +/- S.E.M of 2-3 (**b-c**) or 4 (**a)** independent experiments. Statistical analysis was performed using a one sample t-test versus a theoretical value of 1 (*p<0.05, **p<0.01).

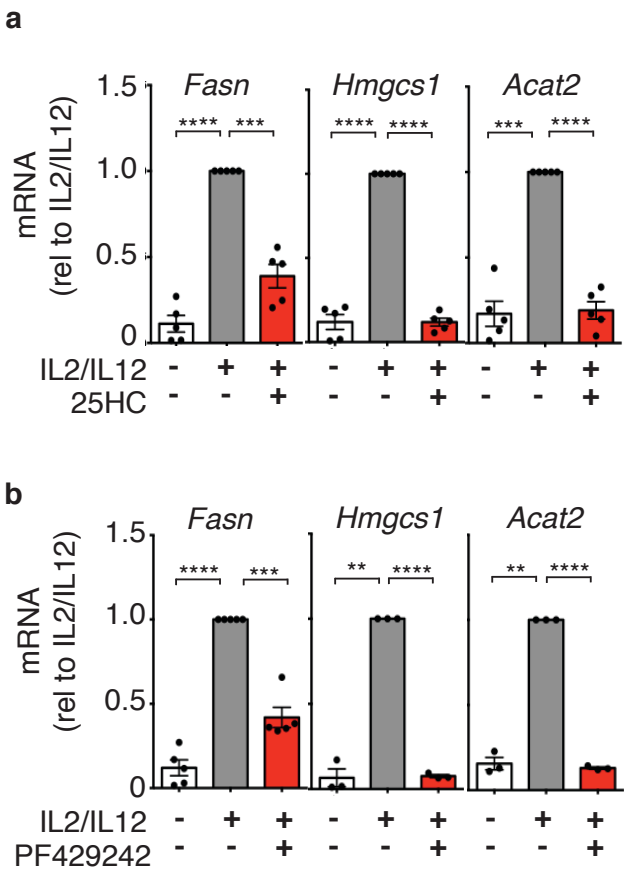

Figure 3.2 IL2/IL12 stimulated NK cells increase SREBP target gene expression

Cultured NK cells were purified and then stimulated with IL2 (20ng/ml) + IL12 (10ng/ml) in the presence or absence of 25HC (2.5 μM) (**a**) or PF429242 (10μM) (**b**) for 18 h, or alternatively left unstimulated, and the cells lysed and analysed by qRT-PCR for *Fasn*, *Hmgcs1* and *Acat2* mRNA expression. Data is normalised to levels of control gene *Rplp0* and presented relative to levels in IL2/IL12-stimulated NK cells. Data is mean +/- S.E.M of 3 or 5 independent experiments. Statistical analysis was performed using a one sample t-test versus a theoretical value of 1 (**p<0.01, ***p<0.001, ****p<0.0001).

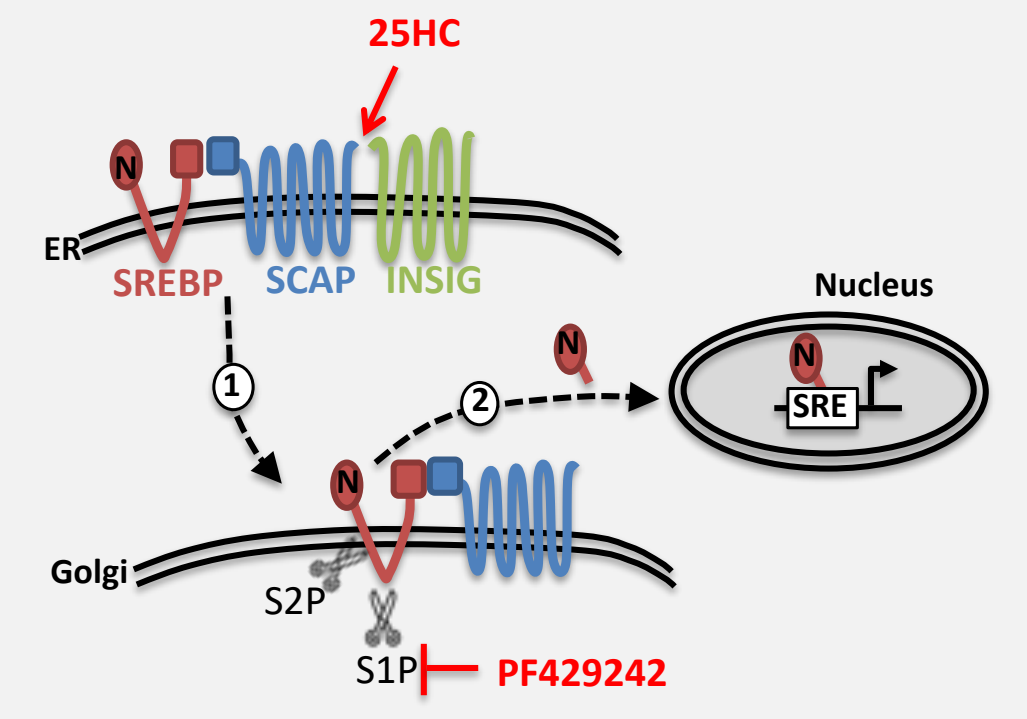

Figure 3.3 Schematic illustrating the mechanism of SREBP activation and inhibition with the inhibitors 25HC and PF429242

Upon synthesis, SREBP is immediately inserted in the ER membrane. Whilst membrane bound, SREBP is inactive as a transcription factor. In order to influence transcription, the N-terminal, transcriptionally-active domain of SREBP must be released from the membrane-bound full-length form. For this to occur, SREBP must be translocated from the ER to the Golgi in complex with chaperone protein SCAP (**1**). In the Golgi, the N-terminal, transcriptionally active SREBP fragment is released following 2 sequential cleavage steps by Golgi-resident proteases: site-1 protease (S1P) and site-2 protease (S2P)(**2**). Active SREBP can then enter the nucleus and bind sterol regulatory element (SRE)-containing promoters. 25HC promotes binding of SCAP to ER-resident protein INSIG, thus retaining the SCAP-SREBP complex in the ER, and preventing SREBP activation. In the absence of SCAP, SREBP activation is inhibited as SREBP cannot translocate to the Golgi for activation. PF429242 inhibits S1P and thus prevents SREBP processing and release from the Golgi membrane.

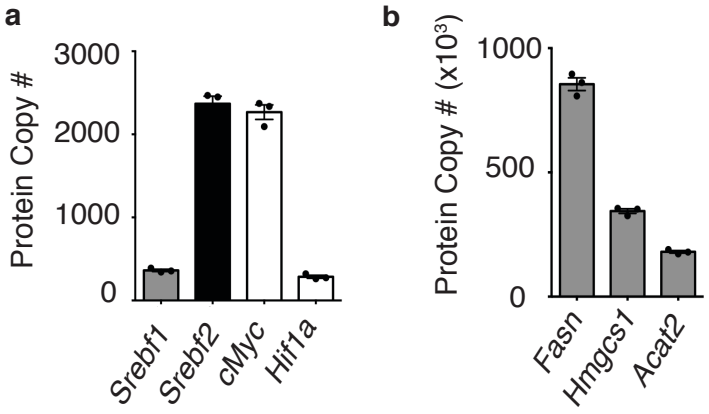

Figure 3.4 IL2/IL12 stimulated NK cells express SREBP and SREBP-target genes at protein level

Cultured NK cells were activated with IL2 (20ng/ml) + IL12 (10ng /ml) for 18 h and copy numbers of the proteins encoded by *Srebf1*, *Srebf2*, *Fasn, Hmgcs1* and *Acat2* were determined using quantitative proteomic analysis. Data is mean +/- S.E.M of 3 experiments. (*Proteomic dataset was generated by the University of Dundee on samples provided by Dr Nadine Assmann*)

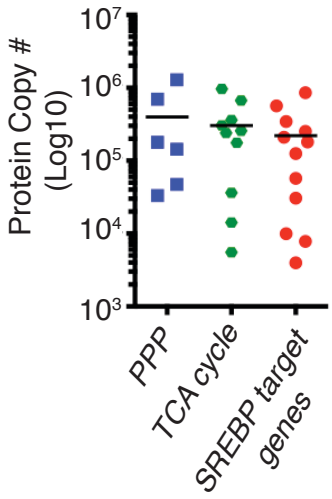

Figure 3.5 Protein expression levels of SREBP target genes is comparable with expression of enzymes in other pathways known to be active in IL2/IL12-stimulated NK cells

Cultured NK cells were activated with IL2 (20ng/ml) + IL12 (10ng /ml) for 18 h and copy numbers of proteins involved in the PPP (blue), in the TCA cycle (green) and encoded by SREBP target genes (red) were determined using quantitative proteomic analysis. Data is mean +/- S.E.M of 3 experiments. (*Proteomic dataset was generated by the University of Dundee on samples provided by Dr Nadine Assmann*)

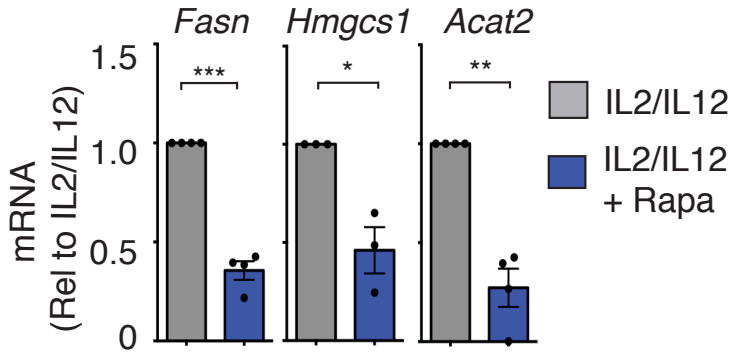

Figure 3.6 IL2/IL12-induction of SREBP activity in NK cells is dependent on mTORC1 signalling.

NK cells were cultured from splenocytes, purified and then stimulated with IL2 (20ng/ml) + IL12 (10ng/ml) in the presence or absence of rapamycin (20 nM) for 18h, and the cells lysed and analysed by qRT-PCR for *Fasn*, *Hmgcs1* and *Acat2* mRNA expression. Data is normalised to levels of control gene *Rplp0* and presented relative to levels in IL2/IL12 activated NK cells. Data is mean +/- S.E.M of 3-4 independent experiments. Statistical analysis was performed using a one sample t-test versus a theoretical value of 1 (*p<0.05,**p<0.01, ***p<0.001)

3.3 SREBP activity is required for IL2/IL12-induced NK cell growth & proliferation

Following IL2/IL12 stimulation, NK cells induce cellular growth to increase cell size within 24 hours, as measured by an increase in forward scatter (FSC-A) by flow cytometry (Donnelly et al. 2014) (**Fig 3.7**). This phase of cellular growth is followed by cellular proliferation 24 to 48 hours post-stimulation, which can be measured as the dilution of fluorescent CFSE dye (**Fig 3.7**). The role for IL2/IL12-induced SREBP activity in these growth and proliferative responses was investigated. Inhibiting SREBP activity with 25HC reduced NK cell growth and proliferation in response to IL2/IL12-stimulation. 25HC-treated NK cells were smaller in size after 24 hours and showed less dilution of CFSE, indicating less proliferation, after 48 hours(**Fig 3.8)**.

To further investigate the role for SREBP in cytokine-induced NK cell growth and proliferation, a genetic model was developed to prevent SREBP activation in NK cells: inducible *Scap* knock-out mice. SCAP is an integral membrane protein, that acts as a SREBP chaperone protein and is essential for the proteolytic activation of all three SREBP isoforms. Without SCAP, SREBP cannot be translocated from the ER to the Golgi for cleavage, therefore cells lacking SCAP cannot activate SREBP (**Fig 3.3)** (Moon et al. 2012). Mice with LoxP sites flanking exon 1 of the *Scap* gene were crossed to transgenic mice expressing a tamoxifen-inducible cre recombinase, resulting in inducible $Scap^{flox/flox}$ xTamox-cre mice, hereafter referred to as $SCAP^{KO}$ mice (Horton, Goldstein, and Brown 2002; Hameyer et al. 2007).To delete *Scap* in splenic NK cells from these mice, 4-hydroxytamoxifen (4-OH TMX) was added to NK cell cultures on day 0 to induce cre recombinase-mediated excision of the floxed exon 1 of *Scap* (**Fig 3.9**). After 4 days in culture, $SCAP^{KO}$ NK cells and $Scap^{WT}$ ($Scap^{WT/WT}$ x Tamox-Cre) NK cells, that were similarly treated with 4-OH TMX, were purified and analysed by RT-qPCR. $SCAP^{KO}$ NK cells had significantly reduced expression of *Scap* **(Fig3.10a)** and SREBP target genes (**Fig 3.10b**) as compared to levels from $Scap^{WT}$ NK cells. Upon 18 hours stimulation with IL2/IL12, $SCAP^{KO}$ NK cells also failed to increase the expression of *Scap* or

SREBP target genes, whereas a strong induction of SREBP activity was observed in stimulated $SCAP^{WT}$ NK cells (**Fig 3.10 c-d**).

Having validated that $Scap^{KO}$ NK cells lack SREBP activity, this model was used to address whether SREBP transcription factors are important for NK cell growth and proliferation. Unstimulated $Scap^{KO}$ NK cells were equivalent in size to unstimulated $Scap^{WT}$ NK cells, but $Scap^{KO}$ NK cells were significantly smaller than $Scap^{WT}$ control NK cells following IL2/IL12 stimulation (**Fig 3.11**). Additionally, IL2/IL12-stimulated NK cells lacking *Scap* proliferated less than $Scap^{WT}$ NK cells over the course of 48 hours (**Fig 3.12**).

To further investigate the role of SREBP in NK cells, the viability of NK cells lacking SREBP activity was assessed. Interestingly, viability of $Scap^{KO}$ NK cells was equivalent to $Scap^{WT}$ control NK cells when unstimulated at 24 and 48 hours, whilst upon IL2/IL12-stimulation $Scap^{KO}$ NK cells had decreased viability compared to $Scap^{WT}$ counterparts at 48 hours (**Fig 3.13**). Of note, both $Scap^{KO}$ and $Scap^{WT}$ NK cells had reduced viability at 48 hours. We attributed this to be an off-target effect of the tamoxifen-cre system, based on observations from our lab and others using other tamoxifen-cre models, whereby non-specific actions of the cre-recombinase lowered viability of cell cultures (Loonstra et al. 2001; Bersell et al. 2013). To avoid this caveat, the viability of IL2/IL12-activated NK cells at 48 hours was further investigated by pharmacologically inhibiting SREBP activation with either 25HC or PF429242. These experiments confirmed that cells lacking SREBP activity had significant viability defects after 48 hours of cytokine -stimulation (**Fig 3.14a**). Taken together, these data demonstrate that SREBP activity is essential for cytokine-induced NK cell growth and proliferation, and that SREBP-activity is essential for the long-term viability of IL2/IL12-stimulated NK cells. Given that at 18 hours post-stimulation there was no significant impact of SREBP inhibition on NK cell viability, the metabolism of NK cells at this timepoint was further explored in the rest of this study (**Fig 3.14b**).

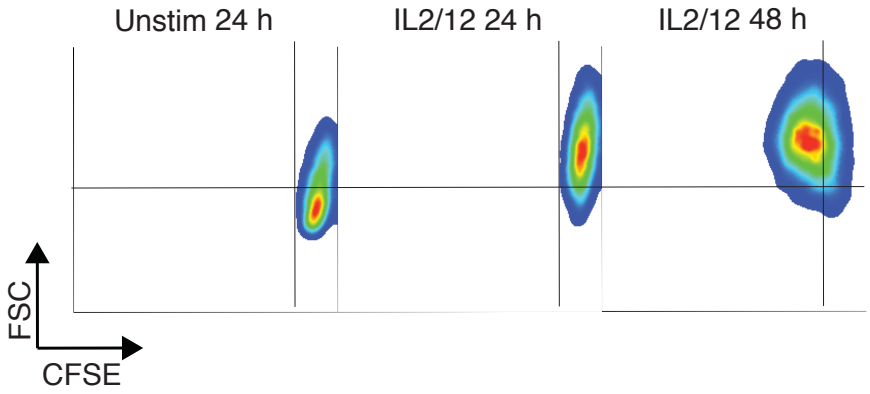

Figure 3.7 IL2/IL12 stimulation induces NK cell growth and proliferation

NK cells were cultured from splenocytes for 3 days, then CFSE-stained and left unstimulated or stimulated with IL2 (20ng/ml) + IL12 (10ng/ml) for 24 h or 48 h. Cells were analysed by flow cytometry for FSC-A as a measure of size and CFSE-dilution as a read-out of proliferation. Plots shown are representative of at least 6 experiments.

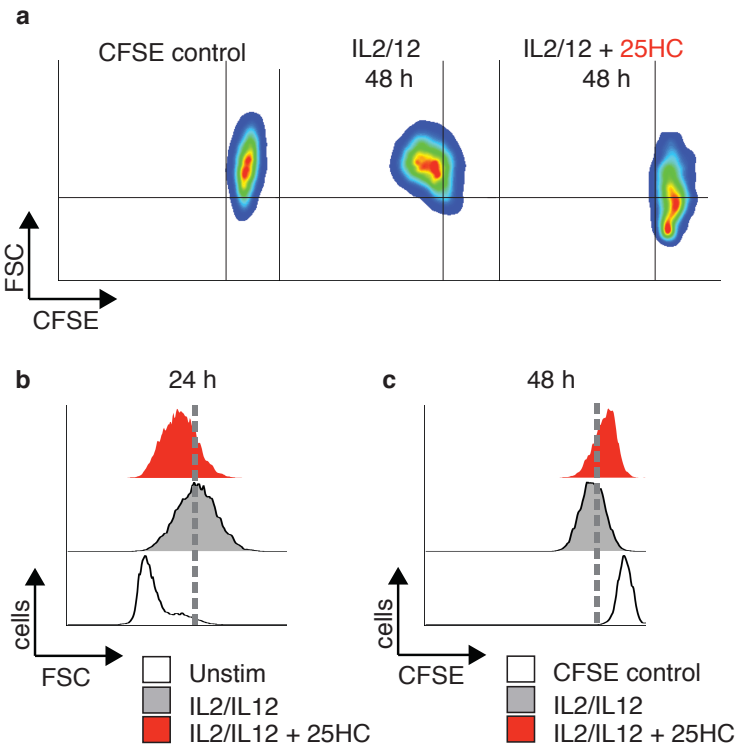

Figure 3.8 Inhibiting SREBP activity impairs NK cell growth and proliferation in response to IL2/IL12 stimulation

NK cells were cultured from splenocytes for 3 days then CFSE-stained and left unstimulated or stimulated with IL2 (20ng/ml) + IL12 (10ng /ml) for 24 h or 48 h in the presence or absence of 25HC (2.5 μM). Cells were analysed by flow cytometry for FSC-A (**a**,**b**) as a measure of size and CFSE-dilution (**a,c**) as a read-out of proliferation. Data presented is representative of 2 independent experiments.

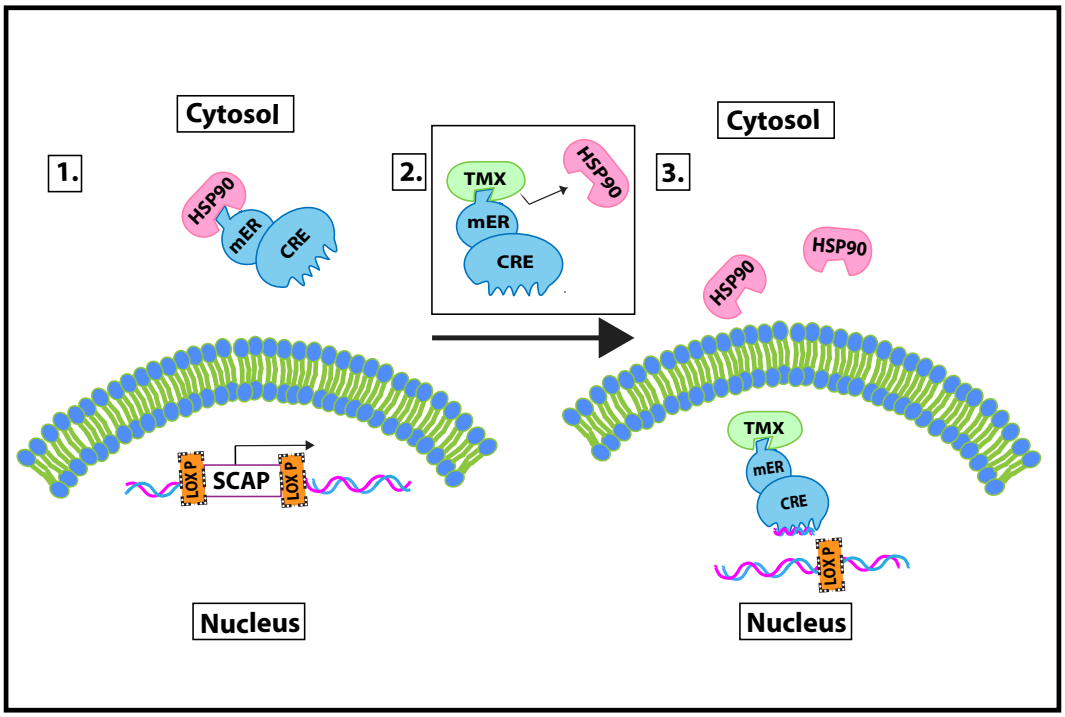

Figure 3.9 4-OH TMX inducible cre recombinase system for *Scap* deletion

(**1**) Scap^{KO} (*Scap*$^{flox/flox}$ x Tamox-Cre) mice express a fusion protein comprised of a cre recombinase and modified estrogen receptor (mER). The mER interacts with HSP90 which holds the mER-cre fusion protein in the cytosol. The mER has specificity to bind 4-OH TMX. (**2**) Upon 4-OH TMX addition, HSP90 is displaced from the receptor. (**3**) The mER-cre fusion protein is no longer held in the cytosol and translocates into the nucleus. Here the cre recombinase recognises and catalyses the recombination of LoxP sites flanking the first exon of the *Scap* gene. This results in the excision of the first exon of *Scap* so that the gene can no longer be transcribed.

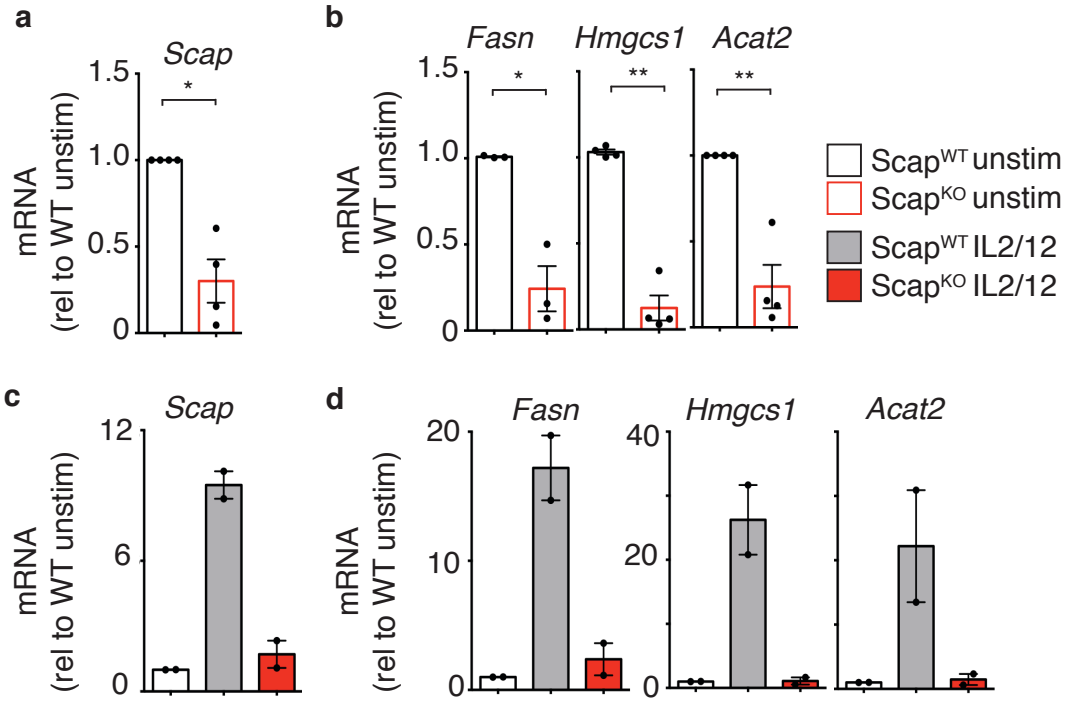

Figure 3.10 4-OH TMX induces deletion of *Scap* from Scap^{KO} (Scap$^{flox/flox}$ x Tamox-Cre) NK cells

NK cells from either Scap^{KO} (*Scap*$^{flox/flox}$ x Tamox-Cre) or Scap^{WT} (*Scap*$^{WT/WT}$ x Tamox-Cre) mice, were cultured from splenocytes for 3 days in the presence of 4-OH TMX (0.6 μM). Cells were left unstimulated (**a-b**) or stimulated with IL2 (20ng/ml) + IL12 (10ng /ml) (b)for a further 18h prior to purification and cells lysed and analysed by qRT-PCR for mRNA levels of *Scap* (**a,c**), or *Fasn*, *Hmgcs1* and *Acat2* (**b,d**). Data is mean +/- S.E.M of 2(**c-d**) or 4(**a-b**) independent experiments. Statistical analysis was performed using a one sample t-test versus a theoretical value of 1 (*p<0.05, **p<0.01).

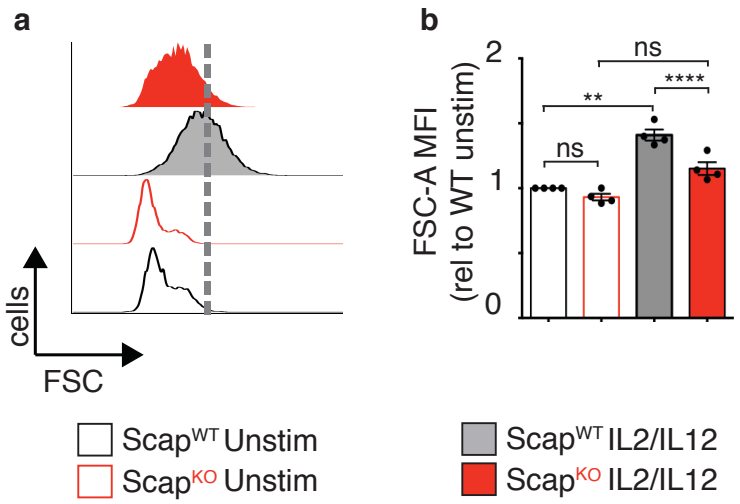

Figure 3.11 Scap^{KO} NK cells have impaired growth

Scap^{KO} (*Scap$^{flox/flox}$* x Tamox-Cre) or Scap^{WT} (*Scap$^{WT/WT}$* x Tamox-Cre) NK cells were cultured for 3 days in the presence of 4-OH TMX (0.6 μM), then left unstimulated or stimulated with IL2 (20ng/ml) + IL12 (10ng/ml) for 24 hours. FSC-A was analysed by flow cytometry. Data is representative (**a**) or mean +/- S.E.M (**b)** of 4 independent experiments. Statistical analysis was performed by one-way ANOVA with Tukey's multiple comparisons test (ns: non-significant, **p<0.01, ****p<0.0001).

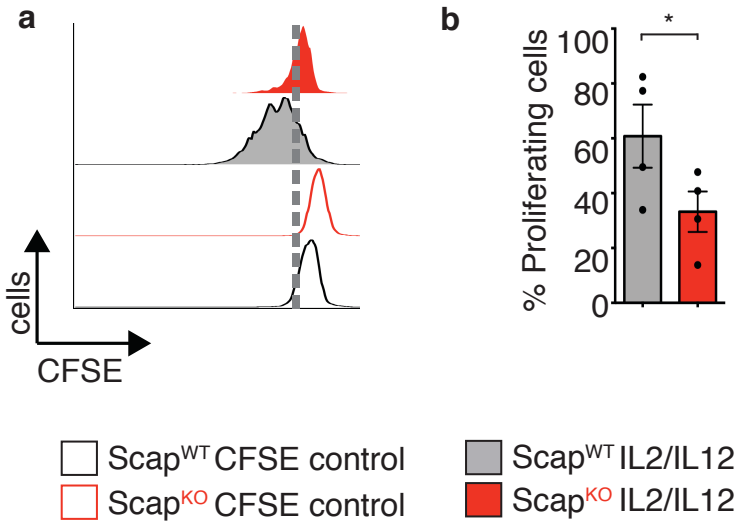

Figure 3.12 Scap^{KO} NK cells have impaired proliferation

Scap^{KO} (*Scap$^{flox/flox}$* x Tamox-Cre) or Scap^{WT} (*Scap$^{WT/WT}$* x Tamox-Cre) NK cells were cultured for 3 days in the presence of 4-OH TMX (0.6 μM), then CFSE-stained and stimulated with IL2 (20ng/ml) + IL12 (10ng/ml) for 48h hours. Cells were analysed by flow cytometry for CFSE-dilution as a read-out of proliferation. Data is representative (**a**) or mean +/- S.E.M (**b)** of 4 independent experiments. Statistical analysis was performed using a paired two-tailed t-test (*p<0.05).

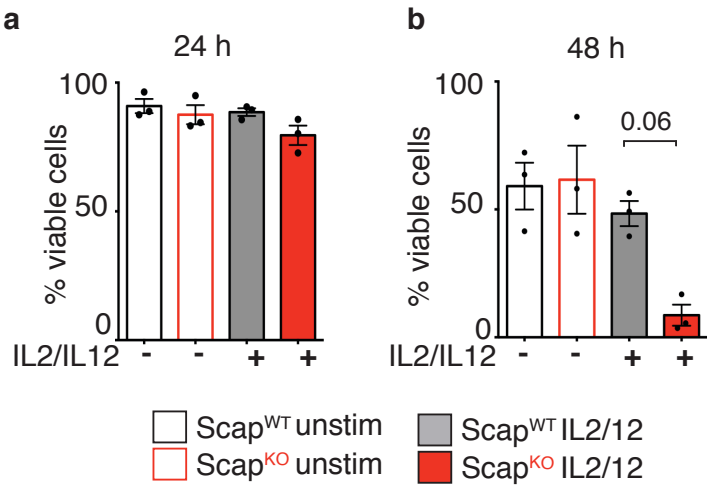

Figure 3.13 SREBP activity is required for NK cell survival following IL2/IL12 stimulation

$Scap^{KO}$ (*Scap*$^{flox/flox}$ x Tamox-Cre) or $Scap^{WT}$ (*Scap*$^{WT/WT}$ x Tamox-Cre) NK cells were cultured from splenocytes for 3 days in the presence of 4-OH TMX (0.6 μM), then left unstimulated or stimulated with IL2 (20ng/ml) + IL12 (10ng/ml) for 24 h (**a**) or 48 h (**b**) NK cell viability was analysed by flow cytometry following Live/Dead staining. Data is mean +/- S.E.M of 3 independent experiments. Statistical analysis was performed by one-way ANOVA with Tukey's post-test.

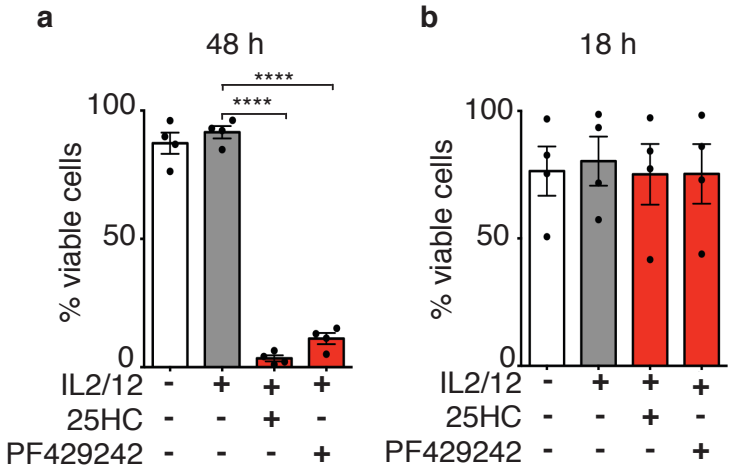

Figure 3.14 SREBP activity is required for NK cell survival following IL2/IL12 stimulation

NK cells were left unstimulated (white bars) or stimulated with IL2 (20ng/ml) + IL12 (10ng/ml) in the presence (red bars) or absence (grey bars) of 25HC (2.5 μM) or PF429242 (10μM) for 48 h (**a**) or 18 h (**b**). NK cell viability was analysed by flow cytometry following Live/Dead staining. Data is mean +/- S.E.M of 4 independent experiments. Statistical analysis was performed by one-way ANOVA with Tukey's post-test (****p<0.0001).

3.4 SREBP activity is required for IL2/IL12-induced NK cell glycolysis & OxPhos

SREBP activity is classically known to support *de novo* lipid synthesis. However work by other members of the Finlay research group has shown that lipid synthesis is not required for NK cell growth and proliferation (Assmann et al. 2017). Given that direct inhibition of lipid synthesis pathways did not mirror the defects in NK cell growth and proliferation observed with SREBP inhibition, it was proposed that SREBP transcription factors had a novel function in NK cells, outside of their classical role in regulating lipogenesis. Previous work from our lab found that 18 hours IL2/IL12 stimulation induces metabolic reprogramming in NK cells, resulting in increased glucose metabolism with elevated rates of glycolysis and OxPhos (Donnelly et al. 2014). In these studies, multiple approaches were used to limit glycolysis and all resulted in decreased cell size (Donnelly et al. 2014). To expand on these experiments, the involvement of glycolysis and OxPhos in cytokine-induced NK cell proliferation was investigated. Firstly, the rate of glycolysis was manipulated using various approaches. Low doses of the glycolytic inhibitor 2-deoxyglucose (2DG) were used to reduce glycolytic flux without completely blocking glycolysis, as described previously (Sukumar et al. 2013; Donnelly et al. 2014; Shi, Wang, et al. 2011). 2DG is a glucose analogue, it is taken up by cells but cannot be further metabolised downstream of hexokinase. 2DG treatment impaired IL2/IL12-stimulated NK cell growth and proliferation in a dose-dependent manner (**Fig. 3.15**). To confirm that elevated glycolysis is required for NK cell growth and proliferation a second, complementary strategy was used to limit the rate of glycolysis in NK cells. For these experiments glucose was replaced with galactose. Galactose is an alternative fuel source which is metabolised through the Leloir pathway to glucose-6-phosphate before entering glycolysis. However, the conversion rate of galactose to glucose-6-phosphate is slow and therefore importantly, galactose only supports low levels of glycolysis (Donnelly et al. 2014; Frey 1996). NK cells stimulated in galactose instead of glucose displayed impaired proliferation and reduced cellular growth **(Fig. 3.16).**

Having observed similar defects in growth and proliferation with SREBP inhibition as with inhibition of glycolysis, it was posited that SREBP activity might be required for elevated glycolysis in activated NK cells. Using Seahorse Metabolic flux analysis, experiments were conducted to investigate the metabolic state of NK cells lacking SREBP activity. It was found that after 18 hours IL2/IL12 stimulation, purified $Scap^{KO}$ NK cells had substantially reduced rates of glycolysis (measured as extracellular acidification rate, ECAR) compared to IL2/IL12-stimualted $Scap^{WT}$ control cells (**Fig 3.17**). Additionally, $Scap^{KO}$ NK cells had a significantly reduced glycolytic capacity (**Fig 3.17**). Our lab has previously shown that in IL2/IL12 stimulated NK cells, increased glycolysis is associated with increased expression of key glycolytic-associated genes (Donnelly et al. 2014). It was therefore investigated whether the defects in glycolysis observed in the absence of SREBP activity were due to an impairment in upregulating the glycolytic machinery. However, blocking SREBP activity with 25HC or PF429242 had no significant impact upon the mRNA levels of glycolytic enzymes or the glucose transporter Slc2a1 (**Fig 3.18**). Therefore, the glycolytic impairment in NK cells lacking SREBP activity was not due to a decrease in expression of glycolytic enzymes.

Leading on from this I looked at the impact of OxPhos inhibition on NK cell growth and proliferation. Low doses of the ATP synthase inhibitor oligomycin have been shown to disrupt TCR stimulated $CD4^{+}$ T cell proliferation and also to disrupt the function of human NK cells (Chang et al. 2013; Keating et al. 2016). In these experiments I investigated the impact of low doses of oligomycin, which partially inhibit ATP synthesis and OxPhos, on IL2/IL12-induced NK cell growth and proliferation (Keating et al. 2016) . Limiting OxPhos impaired NK cell growth and proliferation in IL2/IL12-stimulated NK cells in a dose dependent manner (**Fig 3.19).** It was therefore investigated whether increased OxPhos was dependent upon SREBP activity. Indeed, Seahorse metabolic flux analysis revealed that the oxygen consumption rate (OCR) of purified IL2/IL12-stimulated NK cells lacking *Scap* was significantly reduced compared to OCR levels of $SCAP^{WT}$ controls (**Fig 3.20).** In 3 out of 4 experiments, a substantial decrease in NK cell respiratory

capacity was also observed (**Fig 3.20)**. These experiments were repeated with the pharmacological inhibitor of SREBP activation, 25HC. Inhibition of SREBP activity with 25HC resulted in significantly impaired basal levels of glycolysis and glycolytic capacity and impaired basal OxPhos and respiratory capacity in IL2/IL12 activated NK cells(**Fig 3.21)**. When SREBP activity was inhibited with PF429242, a similar pattern of decreased metabolism was observed (**Fig 3.22)**.

Increased OxPhos levels upon IL2/IL12-stimulation are associated with increased NK cell mitochondrial mass (Loftus et al. 2018). It was therefore investigated whether SREBP was required for increased mitochondrial abundance following IL2/IL12 stimulation. These experiments were carried out using MitoTracker^{TM} Red - a mitochondrial-specific dye: inhibition of SREBP activity with either 25HC or PF429242 had no effect on IL2/IL12-induced increases in NK cell mitochondrial mass (**Fig 3.23**). Taken together, these results describe a novel role for SREBP in controlling NK cell glycolysis and OxPhos, though the mechanisms involved were not initially clear.

Parallel work by others in our group revealed cytokine-stimulated NK cells adopt a distinct metabolic profile called the citrate-malate-shuttle (CMS)(Assmann et al. 2017). Glycolysis-derived pyruvate is typically considered to promote mitochondrial OxPhos by fuelling the TCA cycle. The TCA cycle then feeds electrons into the electron transport chain (ETC) via NADH and $FADH_2$ reducing equivalents (**Fig 3.24 left**). However, cytokine activated NK cells primarily drive OxPhos using the CMS, and not the TCA cycle (**Fig 3.24 right**) (Assmann et al. 2017). In other cell types SREBP transcription factors are known to control the expression of the two key components of the CMS: Slc25a1 and ACLY. Therefore the expression of *Acly* and *Slc25a1* mRNA levels in cytokine-stimulated Scap^{KO} NK cells was assessed. 18 hours IL2/IL12 stimulation increased both *Acly* and *Slc25a1* levels in Scap^{WT} NK cells. However, cytokine-activated Scap^{KO} NK cells failed to express comparable levels of either gene (**Fig3.25**). These data argue that the metabolic defects

observed in cytokine-stimulated, $Scap^{KO}$ NK cells, are due, at least in part, to impaired upregulation of the CMS machinery.

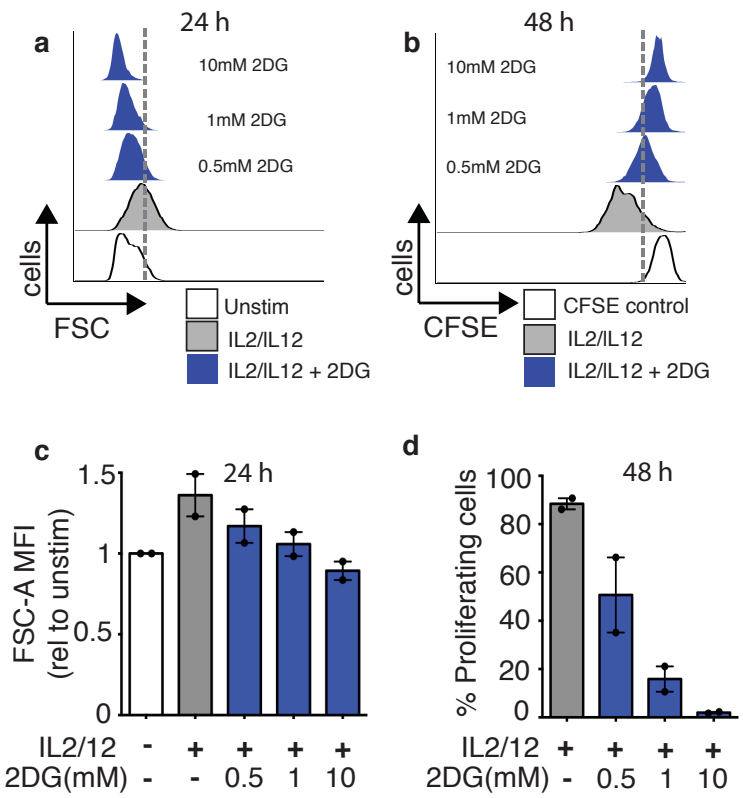

Figure 3.15 Limiting the rate of glycolysis impairs NK cell growth & proliferation

NK cells were cultured for 3 days, then CFSE-stained and left unstimulated or stimulated with IL2 (20ng/ml) + IL12 (10ng/ml), for 24 h or 48 h in the presence or absence of a range of low concentrations of 2DG (0.5mM, 1mM, or 10mM). NK cells were analysed by flow cytometry for FSC-A as a readout of size (**a,c**) and CFSE-dilution as a readout of proliferation (**b,d**). Data is mean +/- S.E.M (**c,d)** or representative (**a,b**) of 2 independent experiments.

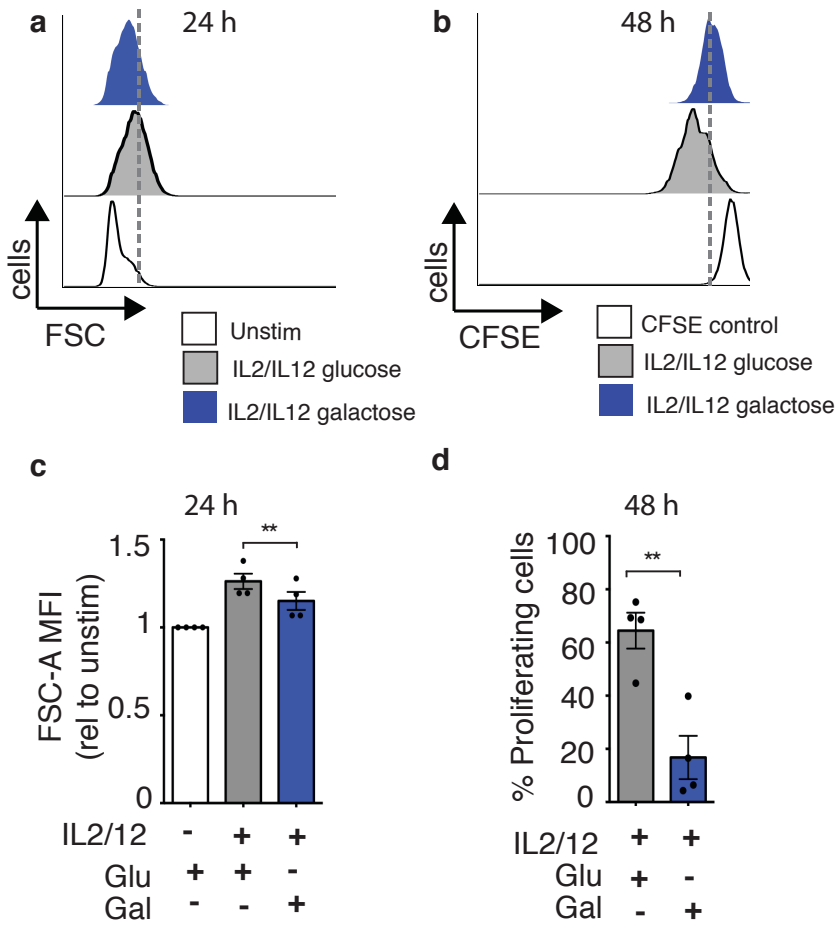

Figure 3.16 Replacing glucose with galactose impairs NK cell growth & proliferation

NK cells were cultured for 3 days, then CFSE-stained and left unstimulated or stimulated with IL2 (20ng/ml) + IL12 (10ng/ml), for 24 h or 48 h in media supplemented with pyruvate and either glucose or galactose. Cells were analysed by flow cytometry for FSC-A as a readout of size (**a,c**) an CFSE-dilution as a readout of proliferation(**b,d**). Data is representative (**a,b**) or mean +/- S.E.M (**c,d**) of 3 independent experiments. Statistical analysis was performed using a paired two-tailed t-test (**p<0.01).

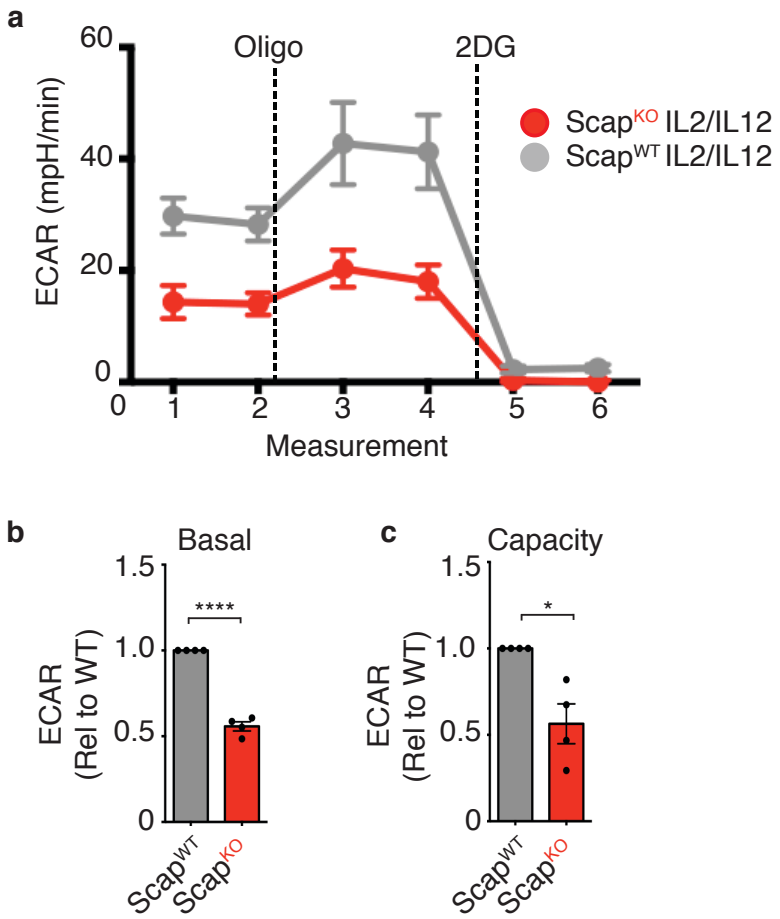

Figure 3.17 Decreased glycolysis in IL2/IL12-stimulated NK cells lacking SREBP activity

Splenic NK cells were cultured from either Scap^{KO} (*Scap*$^{flox/flox}$ x Tamox-Cre) or Scap^{WT} (*Scap*$^{WT/WT}$ x Tamox-Cre) mice then purified and stimulated with IL2 (20ng/ml) + IL12 (10ng/ml) for 18h. Extracellular acidification rate (ECAR) was measured as a readout of glycolysis. Representative trace (**a**) and pooled measurements are shown for basal glycolytic rate (**b**) and glycolytic capacity (**c**). Data is representative of (**a**) or mean +/- S.E.M (**b,c**)of 4 experiments. Statistical analysis was performed using a one sample t-test versus a theoretical value of 1 (* $p<0.05$, ***$p<0.0001$).

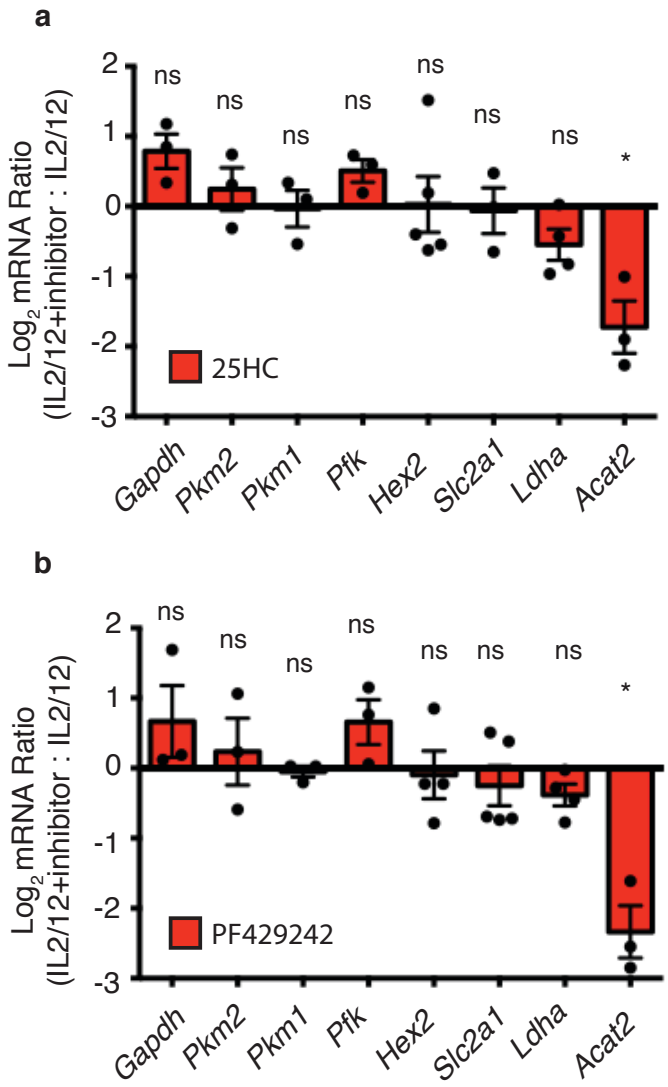

Figure 3.18 Inhibition of SRBP activity has no significant effect on expression of the glycolytic machinery

Cultured NK cells were purified and then stimulated with IL2 (20ng/ml) + IL12 (10ng /ml), for 18 h in the presence or absence of 25HC (2.5 μM)(a) or PF429242 (10μM)(b). Cells were lysed and analysed by qRT-PCR for the expression of *Gapdh*, *Pkm2*, *Pkm1*, *Pfk*, *Hex2, Slc2a1* and *Ldha* mRNA. *Acat2* is a known SREBP target gene so *Acat2* mRNA was also measured as a positive control. All results were normalised to levels of control gene *Rplp0.* Data is mean +/- S.E.M of 3-7 experiments analysed by column statistics versus a theoretical value of 1 (ns, non-significant,* $p<0.05$).

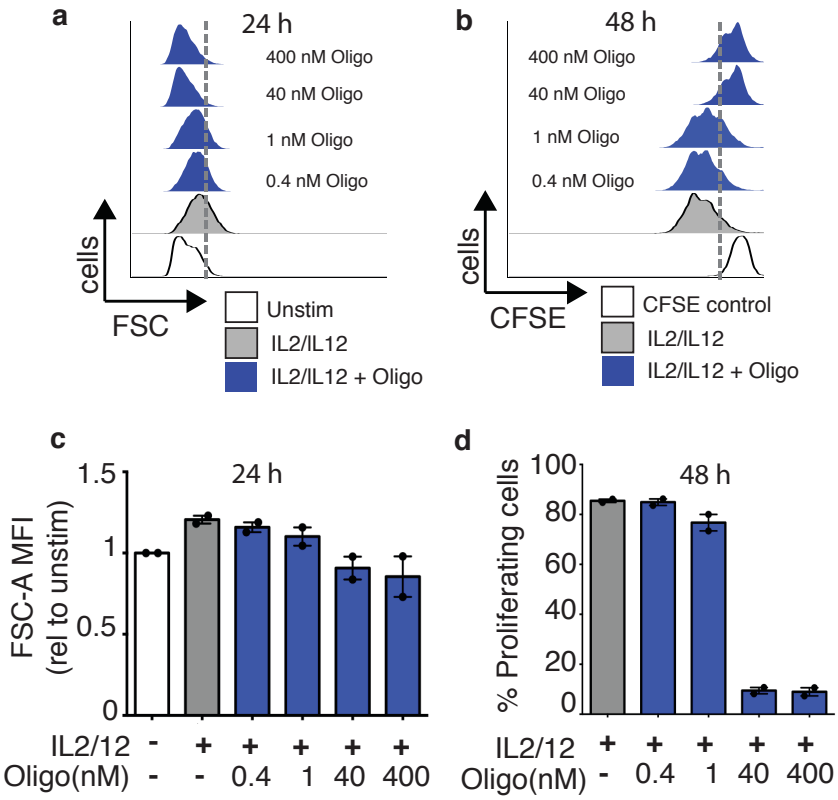

Figure 3.19 Limiting OxPhos impairs growth & proliferation of IL2/IL12 stimulated NK cells

NK cells were cultured for 3 days, then CFSE-stained and left unstimulated or stimulated with IL2 (20ng/ml) + IL12 (10ng/ml), for 24 h (**a,c**) or 48 h (**b,d**) in the presence or absence of a range of concentrations of oligomycin (0.4nM, 1nM, 40nM or 400nM). Cells were analysed by flow cytometry for FSC-A as a readout of size (**a,c**) and CFSE-dilution (**b,d**) as a readout of proliferation. Data is representative or mean +/- S.E.M of 2 independent experiments.

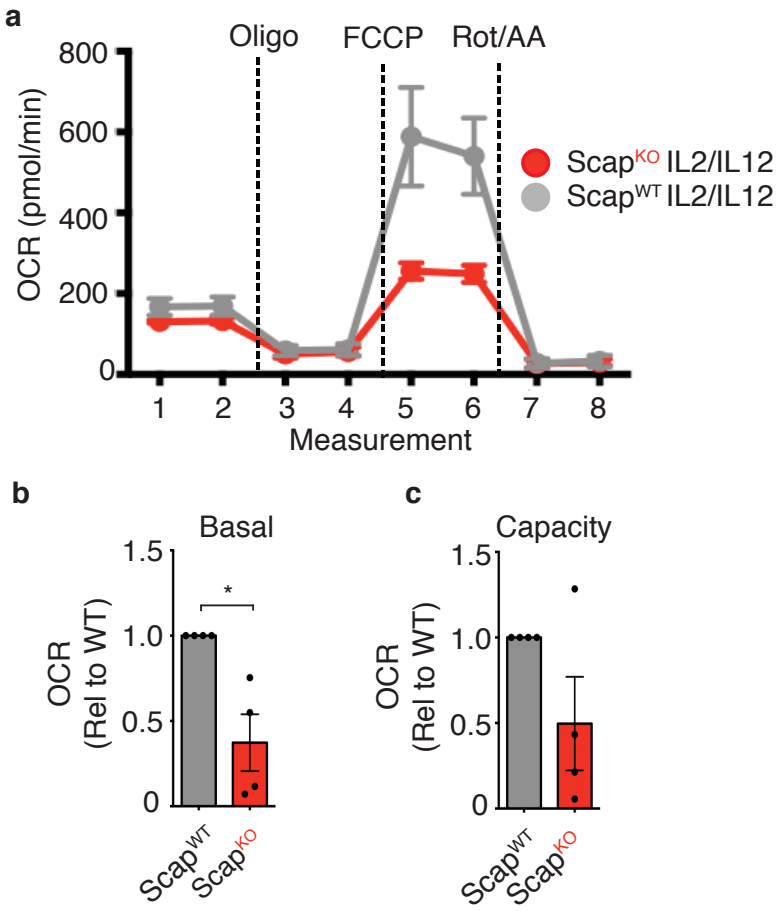

Figure 3.20 Impaired OxPhos in IL2/IL12 stimulated NK cells lacking SREBP activity

Splenic NK cells were cultured from either Scap^{KO} (*Scap*$^{flox/flox}$ x Tamox-Cre) or Scap^{WT} (*Scap*$^{WT/WT}$ x Tamox-Cre) mice then purified and stimulated with IL2 (20ng/ml) + IL12 (10ng/ml) for 18h. Oxygen consumption rate (OCR) was measured as a readout of OxPhos. Representative trace (**a**) and pooled measurements are shown for basal OxPhos (**b**) and respiratory capacity (**c**). Data is presented relative to OCR levels in Scap^{WT} NK cells and is representative of (**a**) or mean +/- S.E.M (**b,c**) of 4 independent experiments. Statistical analysis was performed using a two-tailed one sample t-test versus a theoretical value of 1 (* $p<0.05$).

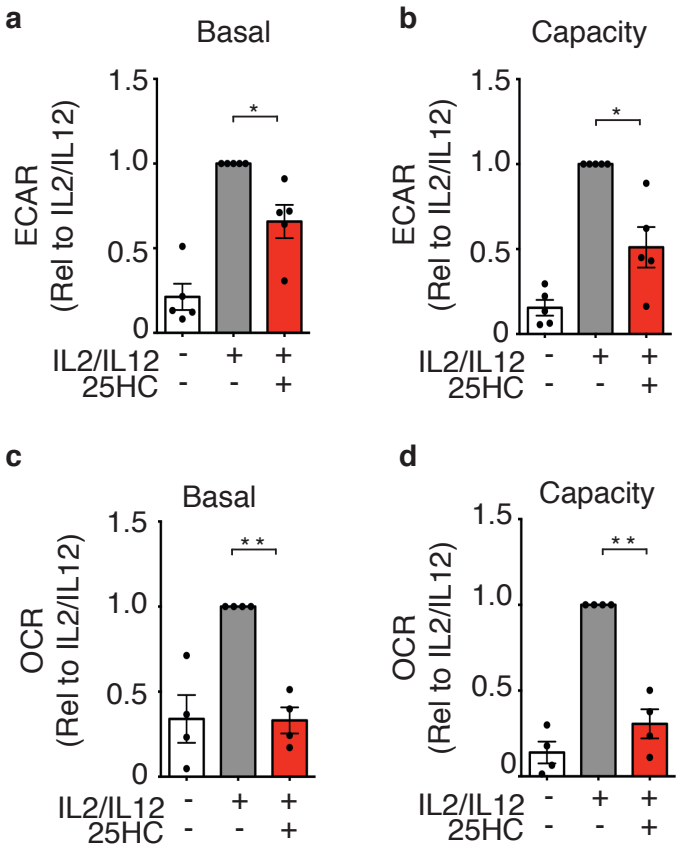

Figure 3.21 Inhibition of SREBP activity with 25HC impairs glycolysis and OxPhos in IL2/IL12-stimulated NK cells

Cultured NK cells were purified and left unstimulated or stimulated with IL2 (20ng/ml) + IL12 (10ng/ml) for 18h in the presence or absence of 25HC (2.5 μM). ECAR and OCR rates were measured by Seahorse extracellular flux analysis. Pooled measurements are shown for basal glycolysis (**a**) glycolytic capacity (**b**) basal OxPhos (**c**) and respiratory capacity (**d**). Data is presented relative to levels in IL2/IL12-stimulated NK cells and is mean +/- S.E.M of 4 (**c-d**) or 5 (**a-b**) experiments. Statistical analysis was performed using a two-tailed one sample t-test versus a theoretical value of 1 (* $p<0.05$, ** $p<0.01$).

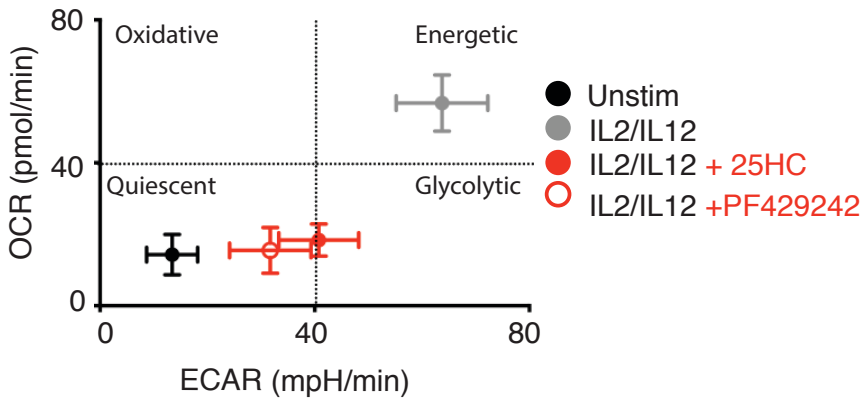

Figure 3.22 Inhibition of SREBP activity with either 25HC or PF429242 impairs metabolism in IL2/IL12-stimulated NK cells

Cultured NK cells were purified and left unstimulated or stimulated with IL2 (20ng/ml) + IL12 (10ng /ml), for 18 h in the presence or absence of 25HC (2.5 μM) or PF429242 (10μM). OCR was measured as a readout of OxPhos and ECAR was measured as a readout of glycolysis. Data is presented on an energy map of ECAR versus OCR rates and is mean +/- S.E.M of pooled data from 2-5 experiments.

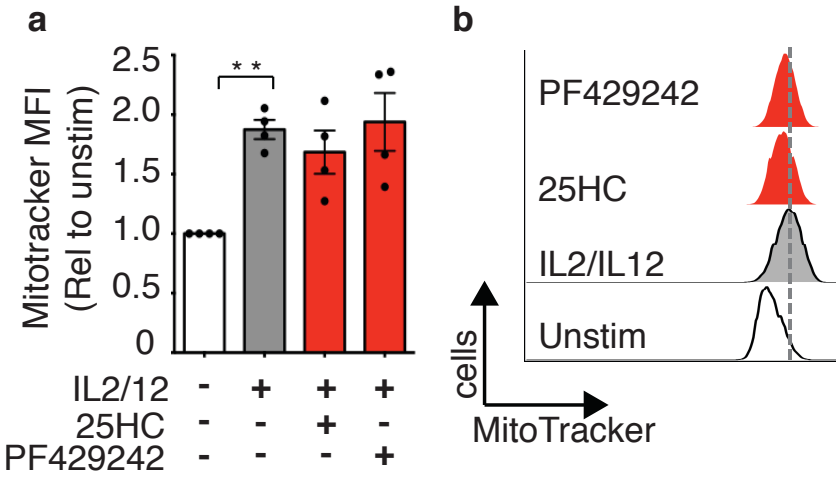

Figure 3.23 Inhibition of SREBP activity has no effect on mitochondrial mass

NK cells were cultured from splenocytes and stimulated with IL2 (20ng/ml) + IL12 (10ng/ml) for 18 h in the presence or absence of 25HC (2.5μM) or PF429242 (10μM). Mitochondrial mass was measured by flow cytometry using MitoTracker™ Red dye which stains mitochondria. Data presented is mean fluorescence intensity (MFI) relative to unstimulated NK cells. Data is mean +/- S.E.M of 4 independent experiments analysed by a one sample t-test versus a theoretical value of 1 or a paired two-tailed t-test (**p<0.01).

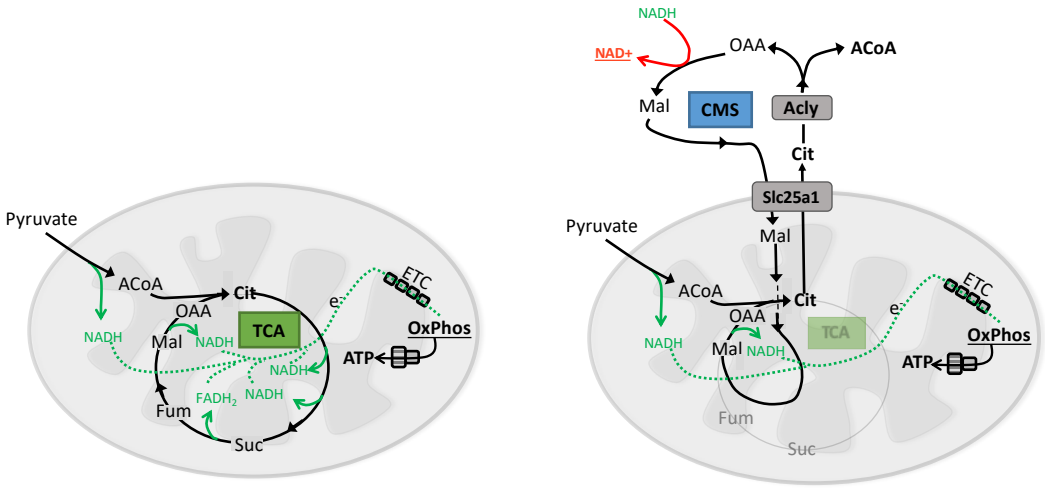

Figure 3.24 NK cells use a novel metabolic configuration known as the Citrate Malate Shuttle (CMS)

(**Left**) Glycolysis-derived pyruvate is typically considered to promote mitochondrial OxPhos by fuelling the TCA cycle. The TCA cycle feeds electrons into the electron transport chain (ETC) via NADH and $FADH_2$ reducing equivalents.

(**Right**) Cytokine-activated NK cells adopt a distinct metabolic configuration called the CMS. Pyruvate is metabolised to acetyl-CoA, generating 1 molecule of NADH, and this acetyl-CoA is combined with oxaloacetate (OAA) to generate citrate. This mitochondrial citrate is then exported into the cytoplasm through Slc25a1. Slc25a1 is an obligate antiporter and so to sustain citrate export, malate must be imported into the mitochondria. In the cytoplasm, citrate is cleaved by ACLY into acetyl-CoA and OAA. OAA is further metabolised to generate malate, regenerating NAD+ in the cytosol, and this malate is imported into the mitochondria to be converted back to OAA, generating another NADH in the mitochondria and completing the cycle. Cytokine activated NK cells primarily use the CMS, and not the TCA cycle, to drive OxPhos.

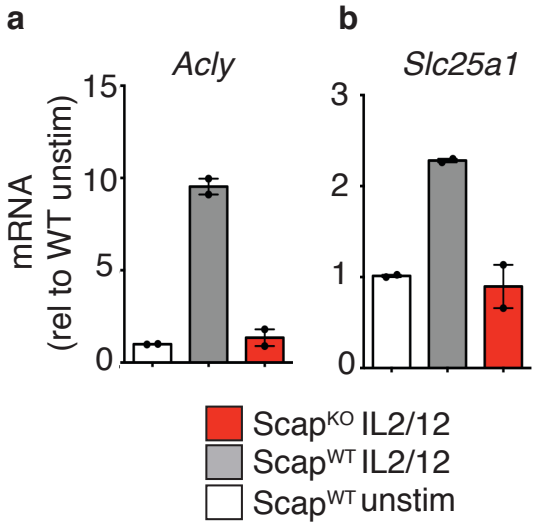

Figure 3.25 SREBP controls the expression of key components of the citrate malate shuttle - *Acly* and *Slc25a1*

NK cells from either Scap^{KO} or Scap^{WT} mice, were cultured from splenocytes for 3 days in the presence of 4-OH TMX (0.6 μM). NK cells were purified and left unstimulated or stimulated with IL2 (20ng/ml) + IL12 (10ng/ml) for 18 h and analysed by qRT-PCR for mRNA levels of *Slc25a1* or *Acly.* Data is mean +/- S.E.M. of 2 experiments. Data is normalised to control gene *Rplp0* and presented relative to mRNA abundance in unstimulated Scap^{WT} NK cells.

3.5 Discussion of chapter 3

Data presented in this chapter reveal a new and unexpected role for SREBP transcription factors as essential regulators of growth and proliferation and glucose metabolism in cytokine-activated NK cells. This is a novel role for SREBP transcription factors which are classically considered as master regulators of *de novo* lipid synthesis due to their ability to induce transcription of the complete panel of enzymes involved in the synthesis of fatty acids and cholesterol (Horton, Goldstein, and Brown 2002; Horton et al. 2003).

Cytokine-stimulation of NK cells with IL2/IL12 triggered increases in expression and activity of SREBP transcription factors. The increase in SREBP activity was dependent on mTORC1 signalling. This is in line with a number of published studies carried out in other cell types linking mTORC1 activity to SREBP activation (Porstmann et al. 2008; Duvel et al. 2010; Peng, Golub, and Sabatini 2002).For instance, when CD8+ T lymphocytes stimulated with anti-CD3 and anti-CD28 were pre-treated with the mTORC1 inhibitor rapamycin, the processing and nuclear accumulation of SREBP transcription factors was prevented. This was associated with decreased expression of a number of SREBP target genes (Kidani et al. 2013). Similarly, $CD4^+$ T cells in which regulatory-associated protein of mTOR (raptor) is deleted, have a reduced ability to process and activate SREBP when stimulated with anti-CD3 and anti-CD28 and co-ordinately cannot upregulate expression of SREBP target genes (Yang et al. 2013).

mTORC1 is known to be an essential regulator of both NK cell development and NK cell activation (Donnelly et al. 2014; Marcais et al. 2014; Nandagopal et al. 2014). Developing NK cells undergo several stages of maturation in the bone marrow that can be identified based on surface expression levels of CD11b and CD27 (Chiossone et al. 2009). mTORC1 activity is highest in $CD11b^{lo}$-$CD27^{hi}$ pre-NK cells and decreases as cells mature (Marcais et al. 2014). Interrogation of the bone marrow scRNAseq data set generated by the Tabula Muris consortium reveals that these $CD11b^{lo}$-$CD27^{hi}$ pre-NK cells express higher mRNA levels for a range of SREBP

target genes compared to the immature ($CD11b^{hi}$-$CD27^{hi}$) and mature ($CD11b^{hi}$-$CD27^{lo}$) NK cell subsets (Tabula Muris Consortium 2018). For example pre-NK cells express higher mRNA levels of *Fasn* and *Acly* – two established SREBP target genes. There is therefore a correlation between high mTORC1 activity and SREBP target gene expression in developing NK cells. There is a further link between SREBP activity and mTORC1 signalling in activated NK cells. Resting NK cells have low mTORC1 activity and mTORC1 signalling increases robustly following cytokine activation (Donnelly et al. 2014). When mTORC1 signalling is inhibited with rapamycin during stimulation, NK cells have impaired metabolism and reduced cellular growth (Donnelly et al. 2014; Viel et al. 2016). Reduced mTORC1 activity is also associated with reduced proliferation –administration of rapamycin to mice during murine cytomegalovirus (MCMV) infection, significantly impairs NK cell expansion in response to the virus (Nandagopal et al. 2014). In this chapter I demonstrated that metabolism and cellular growth and proliferation were also reduced when SREBP was inhibited. Therefore, my research argues that some effects of mTORC1 inhibition, may be due to downstream inhibition of SREBP activity.

Studies in other cell types – mainly epithelial cells- have revealed that there are numerous ways that mTORC1 signalling can promote SREBP activity, though specific mechanisms are still unclear and are likely to be cell-type specific. mTORC1-mediated activation of SREBP can be mediated by both p70 S6 ribosomal protein kinase (S6K) dependent and independent mechanisms (Duvel et al. 2010; Li, Brown, and Goldstein 2010; Li et al. 2011). mTORC1-signalling can induce processing and activation of SREBP post-transcriptionally (Porstmann et al. 2008; Duvel et al. 2010). Experiments carried out in TSC1 or TSC2 knockout cell lines suggest that sustained mTORC1 signalling can promote ER-stress which leads to induction of the unfolded protein response (UPR) – which can also promote SREBP processing and activation (Ozcan et al. 2008; Colgan et al. 2007; Lee and Ye 2004). The UPR is a signalling pathway that induces temporary inhibition of translation and an upregulation of ER chaperones in order to deal with the adverse effects of

ER stress. The UPR can lead to SREBP activation, through enhanced SREBP processing (Kammoun et al. 2009; Colgan et al. 2007; Lee and Ye 2004; Werstuck et al. 2001). SREBP activation can also be controlled at the level of transport into the nucleus where the phosphatase lipin-1 is known to have a regulatory role. mTORC1 can phosphorylate and thus impair lipin-1 from negatively regulating SREBP transcription (Peterson et al. 2011). Which of these mTORC1-driven processes contribute to SREBP activation in cytokine-stimulated NK cells remains to be determined.

The PI3K/AKT signalling axis can also influence SREBP activation (Porstmann et al. 2008).Pre-treatment with the PI3K inhibitor LY294002, before activation with anti-CD3 and anti-CD28 reduced SREBP target gene expression in CD8+ T cells. However data generated using this inhibitor must be interpreted with caution as it can also potently inhibit mTORC1 signalling (Kidani et al. 2013; Feldman and Shokat 2010). A common misconception is that mTORC1 acts downstream of PI3K/AKT signalling in all cell types. However, this is not the case in IL2/IL12-activated NK cells or some other lymphocyte subsets (Loftus et al. 2018; Finlay et al. 2012a). Furthermore, inhibition of AKT in IL2/IL12-stimulated NK cells has no effect on NK cell growth, which argues that it is not acting upstream of SREBP activity in NK cells (Loftus et al. 2018). Taken together, in IL2/12 stimulated NK cells, mTORC1 signalling is required for SREBP activity, though identifying the exact signalling involved requires further investigation.

The pharmacological inhibitors used to investigate SREBP activity in this study - 25HC and PF429242 – inhibit SREBP processing and activation through different mechanisms. 25HC prevents translocation of membrane-bound SREBP from the ER to the Golgi for cleavage, whilst PF429242 inhibits the Golgi resident S1P, thus preventing cleavage of membrane-bound SREBP. Both inhibitors impaired SREBP transcriptional activity in IL2/IL12-stimulated NK cells as shown by a decrease in the expression of a number of SREBP target genes. However, both inhibitors can have additional actions on the cell. Therefore, it is important to consider whether

the results observed using these inhibitors can be attributed to inhibition of SREBP activity alone or could be due to off-target effects of either inhibitor.

25HC can ligate and activate the liver X receptor (LXR). The LXR is a ligand-activated transcription factor whose ligands include various oxysterol species and intermediates derived from the cholesterol synthesis pathway. The transcriptional programme induced upon LXR ligation leads to expression of genes involved in cholesterol storage and cholesterol efflux, which ultimately would lead to activation of SREBP. Thus, LXR activation in our system, would be expected to cause an increase, and not a decrease, in SREBP activity. In contrast 25HC, treatment significantly impaired SREBP activity in NK cells. Additionally, the promoter of the gene encoding SREBP1 harbours an LXR-response element (Chen et al. 2004; Repa et al. 2000).Therefore upon LXR-ligation with 25HC one would expect to observe an induction of SREBP1 expression. Taken together this argues that 25HC is not activating the LXR in IL2/IL12-activated NK cells. Furthermore, PF429242, the alternate pharmacological inhibitor used in this study, is not an LXR ligand. However, through its inhibition of S1P, it also can have non-specific effects as the ER-stress sensor, Activating Transcription Factor 6 (ATF6), also requires S1P for cleavage and activation. ATF6 plays an important role in the UPR. ATF6 is central to the regulation of GRP78 -a ubiquitously expressed ER-chaperone protein. GRP78 represses ER-stress induced UPR activation by preventing activation of ATF6, IRE1alpha and PERK – key members of the UPR. Inhibition of ATF6 activity by PF429242 has been reported to induce the UPR, even in the absence of additional ER-stress-inducing stimuli (Lebeau et al. 2018) Activation of ER stress sensor, and IRE1α substrate, XBP1 has been reported to supress T cell OxPhos levels and induce immune checkpoint and exhaustion markers on $CD8^+$ T cells (Ma et al. 2019; Song et al. 2018). However in NK cells IRE1α-XBP1 has been shown to be necessary to support OxPhos(Dong et al. 2019). Expression of the OxPhos machinery was downregulated in NK cells lacking IRE1α- as was basal and maximal OxPhos levels (Dong et al. 2019). The same study shows that XBP1 also facilitates NK cell growth and proliferation (Dong et al. 2019). Thus it is unlikely

that off-target induction of this pathway is causing the inhibitory effects on NK cell metabolism and growth and proliferation observed with PF429242. The fact that similar results were obtained in this study when SREBP was inhibited using either 25HC or PF429242 provides confidence that findings in this report are due to SREBP inactivation. Crucially, the additional use of the genetic $SCAP^{KO}$ model – further argues that SREBP plays a key role in controlling NK cell metabolism. It is accepted that the tamoxifen-inducible cre recombinase system comes with its own caveats. Non-specific cre effects can cause DNA damage (Bersell et al. 2013; Loonstra et al. 2001). For this reason cre positive $SCAP^{WT}$ controls were used for all experiments. The fact that similar results were obtained in this study when SREBP was inhibited using 25HC, PF429242 or following *Scap* deletion, provides confidence that findings using these methods are due to SREBP inactivation.

Data from this chapter identified that activation of SREBP transcription factors is necessary for cytokine-induced NK cell growth and proliferation. These results are consistent with research in T cells, which revealed that SREBP activation is essential for the increased proliferation that occurs upon TCR-stimulation (Chen, Heiniger, and Kandutsch 1975; Kidani et al. 2013). $SCAP^{KO}$ $CD8^{+}$ T cells -which lack SREBP activity- displayed impaired growth and proliferation in response to a panel of different stimuli (Kidani et al. 2013). In contrast, in B lymphocytes research has shown that the SREBP inhibitor 25HC has no effect on proliferation of B220+ splenic B cells in response to stimulation with LPS,TGFβ and IL2 or IL5 for 56 hours (Bauman et al. 2009). However treatment with 25HC reduces IL-2-mediated B proliferation after 7 days (Bauman et al. 2009). It is worth noting that LXR ligation by 25HC may also be involved here as it has been reported that LXR ligation impairs proliferation of mitogen-activated B cells (Bensinger et al. 2008).

As SREBP transcription factors are classically known to be involved in the control of *de novo* lipid synthesis it was considered that lipid synthesis may be important for NK cell growth and proliferation. Indeed, lipid synthesis had been shown to be essential for growth and proliferation in other immune cells. The proliferation

defects in $SCAP^{KO}$ CD8+ T lymphocytes were attributed to a reduction of SREBP-induced *de novo* cholesterol synthesis; proliferation defects observed in $SCAP^{KO}$ $CD8^+$ T cells could be recovered upon addition of exogenous cholesterol (Kidani et al. 2013). Building from this, Yang et al identified that modulating cholesterol metabolism, through inhibition of the cholesterol esterification enzyme -ACAT2- could enhance CD8+ T cell proliferation (Yang, Bai, et al. 2016). A separate study showed that inhibition of fatty acid synthesis with the inhibitor C75, reduced proliferation of CD8+ T cells *in vitro* in response to IL2 (O'Sullivan et al. 2014). Furthermore, Lee et al. show that *de novo* fatty acid synthesis is necessary for $CD8^+$ T cell proliferation in response to bacterial infection (Lee et al. 2014).T cell specific deletion of acetyl coA carboxylase (ACC1) – the enzyme required to produce malonyl coA – an essential step for fatty acid synthesis – resulted in impaired antigen-specific proliferation of CD8+ T cells in response to infection with listeria-OVA (Lee et al. 2014). Additionally in CD4+ T lymphocytes, *de novo* fatty acid synthesis has been shown to be essential for proliferation of the T_H17 subset (Berod et al. 2014). Therefore it was unanticipated and intriguing when parallel work from other researchers in our group identified that lipid synthesis is dispensable for NK cell growth and proliferation (Assmann et al. 2017). In contrast with studies in $CD8^+$ T cells, when the inhibitors C75 or TOFA, were used in NK cells to block either fatty acid or cholesterol synthesis directly, cytokine-stimulated NK cells increased in size and proliferated equivalently to control NK cells (Assmann et al. 2017). The finding that *de novo* lipid synthesis pathways are not important for NK cell growth and proliferation is surprising. Lipids are the most abundant species in every cell membrane and growing cells must double their membrane lipids in preparation for cellular division (Jackowski, Wang, and Baburina 2000). Cellular lipid requirements can be met by a combination of lipid synthesis and lipid import. While NK cells do utilise SREBP-dependent lipid synthesis, it has been shown that this *de novo* lipid synthesis is not essential for NK cell growth or proliferation (Assmann et al. 2017). It is therefore tempting to speculate that when lipid synthesis is inhibited in NK cells, they meet their demands for lipid through uptake from their extracellular environment. Indeed, it has been shown that NK

cells readily take up free fatty acids from supplemented culture media (Michelet et al. 2018). However accumulation of excess lipids within NK cells was found to be detrimental to NK cell metabolism and function (Michelet et al. 2018).This would suggest that NK cells have the plasticity to alternate between lipid uptake and lipid synthesis to meet proliferative demands depending on their circumstance. This would contrast with $CD4^+$ T cells, where the source of lipid defines differentiation and function of the cellular subtype – T regulatory (Treg) cells take up exogenous fatty acids whilst Th17 cells utilise *de novo* lipid synthesis to support proliferation (Berod et al. 2014). Inhibiting *de novo* fatty acid synthesis in $CD4^+$ T cells prevents TH17 cell development and instead favours induction of Tregs. A separate study profiled the differences in fatty acid and cholesterol uptake by CD8+ T memory and T effector cells (O'Sullivan et al. 2014). CD8+ T memory cells incorporated much less exogenous fatty acids than CD8+ T effector cells both *in vitro* and *in vivo* whilst LDL uptake between the two subsets were similar(O'Sullivan et al. 2014). Of note, inhibition of fatty acid synthesis with C75 in the T memory subset triggered a significant decrease in cell survival whilst viability of T effector cells was unaffected when treated with the same dose of C75 (O'Sullivan et al. 2014). Therefore the fact that SREBP activity but not lipid synthesis was required for NK cell proliferative responses was intriguing.

A question that remained was why IL2/IL12-activated NK cells might rely on SREBP activity for growth and proliferation, if not for lipid synthesis. Experiments in this chapter demonstrated that IL2/IL12-activated NK cells required both glycolysis and OxPhos for optimal growth and proliferation – when either pathway was perturbed, NK cells were smaller, and proliferated less. It is already known that increased NK cell metabolism following IL2/IL12-stimulation is accompanied by complete metabolic reprogramming: NK cells increase expression of glucose transporters and glycolytic enzymes, increase glucose uptake and increase flux through glycolysis (Donnelly et al. 2014; Assmann et al. 2017). One output of such glycolytic reprogramming is the production of biosynthetic precursors. Glycolytic and TCA cycle intermediates can be siphoned into different pathways to provide

building blocks such as amino acids, lipids and nucleotides - all essential for cellular expansion (Hume et al. 1978; Vander Heiden, Cantley, and Thompson 2009). The crucial discovery was that SREBP activity is required for cytokine-induced increases in both glycolysis and OxPhos in NK cells, and thereby for NK cell growth and proliferation. This posed the question as to what mechanism is linking SREBP activation NK cell glycolysis and OxPhos? Kidani *et al* reported that SREBP inhibition prevented metabolic reprogramming in CD8+ T cells, with activated $SCAP^{KO}$ T cells unable to achieve ECAR or OCR rates similar to $SCAP^{WT}$ control T cells (Kidani et al. 2013). SREBP inhibition had no effect on the mitochondrial mass of activated CD8+ T cells in the aforementioned study. Similarly, the increased mitochondrial mass, induced upon IL2/12-activation of NK cells, is shown to be unaffected when SREBP activity is impaired. In other cell types SREBP is reported to induce transcription of a number of mitochondrial enzymes (Reed et al. 2008; Feng, Tsui, and Juang 2005). Whether SREBP is controlling expression of mitochondrial enzymes in cytokine-activated NK cells is yet to be determined. Meanwhile in other cell types, SREBP transcription factors have been linked to expression of glycolytic enzymes (Gosmain et al. 2004; Kidani et al. 2013). $SCAP^{KO}$ CD8+T cells had significantly lower expression of a number of key glycolysis-associated genes, including glycolytic enzymes (*Pkm2, Hk2, Gapdh*), the glucose transporter - *Slc2a1* - and *Ldha* (Kidani et al. 2013). This is in contrast to the data presented herein, which demonstrate that in NK cells, cytokine-induced up-regulation of numerous glycolytic enzymes, as well as *Ldha* and *Slc2a1* are unaffected when SREBP activity is inhibited. Therefore, though SREBP transcription factors are shown to be crucial for increased glucose metabolism upon activation of both NK cells and CD8+ T cells, SREBPs appear to drive glycolysis in both cell types, at least in part, through separate mechanisms.

During the course of this study, it was identified by other researchers in our group, that IL2/IL12-activated NK cells use the CMS rather than the TCA cycle to support OxPhos (Assmann et al. 2017). Data presented herein confirm that expression of the two key components of the CMS – Acly and Slc25a1 – are controlled by SREBP

transcription factors. Thus, providing a link between SREBP activity and NK cell glucose metabolism. It is important to note that the TCA cycle is still present in IL2/IL12-activated NK cells (Loftus et al. 2018). The relative contributions of both the TCA cycle and the CMS to NK cell metabolism were investigated by another member of the Finlay lab and it was identified that the CMS is mainly driven by glucose to fuel OxPhos, and glutamine feeds into the TCA cycle, which makes minimal contribution to overall OxPhos levels (Loftus et al. 2018). It is likely that other immune cell subsets may make use of the CMS to varying degrees. For instance, metabolic flux analysis of CD4+ T cells differentiated under Th1 polarising conditions revealed a similar pattern of glucose flux as seen in IL2/IL12 activated NK cells using the CMS (Peng et al. 2016; Assmann et al. 2017). It would be interesting to investigate whether the metabolic defects observed when SREBP was inhibited in CD8+ T cells, are also in part due to CMS inhibition (Kidani et al. 2013).

The are several possible reasons as to why NK cells preferentially use the CMS. Firstly, the CMS regenerates cytosolic NAD+ - an important co-factor for sustaining the activity of the glycolytic enzyme GAPDH, thus sustaining elevated glycolysis. Another important output of the CMS, is cytosolic acetyl-CoA. In most eukaryotic cells, acetyl-coA is primarily generated in the mitochondrial matrix. Cytosolic acetyl-CoA, in addition to being a substrate for lipid synthesis, can influence the activity of multiple enzymes and therefore control numerous cellular processes – either directly or via the epigenetic regulation of gene expression. Acetyl CoA acts is the substrate for acetylation reactions. Multiple proteins are acetylated as a post-translational modification to control their function – including nearly all the enzymes involved in glycolysis, OxPhos and the TCA cycle (Guan and Xiong 2011). For example the glycolytic enzyme - GAPDH - is acetylated to increase its catalytic activity, which has been shown to be essential for optimising memory CD8+ T lymphocyte responses (Li et al. 2014; Balmer et al. 2016). Additionally, more than 20% of mitochondrial proteins are acetylated (Kim et al. 2006; Samant et al. 2014). Protein acetylation has been ascribed an important role in maintaining

mitochondrial homeostasis, biogenesis, fusion and fission (Webster et al. 2013; Webster et al. 2014). As shown in this chapter, NK cells increase mitochondrial mass upon activation and it is known that maintenance of mitochondrial fitness is essential for NK cell longevity (O'Sullivan et al. 2015).

Furthermore, acetyl groups donated from acetyl-coA allow for the acetylation of histones which influences chromatin accessibility (Wellen et al. 2009). There is a correlation between high levels of histone acetylation at a locus and transcriptional activity, whilst conversely, reduced acetylation is linked to gene silencing. For instance, in naïve T lymphocytes the loci of the IL4 and IFNγ genes have low levels of acetylation, whereas TCR stimulation leads to rapid acetylation of histones H3 and H4 of respective genes depending on TH1 or TH2 polarisation (Fields, Kim, and Flavell 2002; Avni et al. 2002). Therefore acetyl-coA can be directly linked to the control of gene expression. Histone acetylation of promoters is necessary for transcription of many genes. For instance the *Ifnγ* gene in NK cells contains an array of histone acetylation domains (Chang and Aune 2005).

It is emerging that NK cells can exhibit innate immune memory (Cerwenka and Lanier 2016). For example, trained NK cells – which are pre-activated with cytokine – have enhanced responses upon re-stimulation (Romee et al. 2012; Keppel, Yang, and Cooper 2013; Cooper et al. 2009). Epigenetic mechanisms are likely to effect NK cell training and memory (Cooper et al. 2009; Cerwenka and Lanier 2016). For example NK cells from HCMV-infected humans exhibit hyper-methylation of DNA at certain sites (Lee et al. 2015). Furthermore expression of the activating receptor NKG2D is regulated epigenetically through histone acetylation (Fernandez-Sanchez et al. 2013). Indeed, unpublished work from other members of our group has indicated that enhanced histone acetylation can be associated with cytokine-induced NK cell memory. Acetylation of histones is important for facilitating epigenetic changes. Therefore an exciting implication from this work is that cytokine-activated NK cells may engage in the CMS to provide acetyl-coA to support epigenetic reprogramming and promote NK cell training. Taken together,

findings from this chapter demonstrate a novel role for SREBP transcription factors as important regulators of NK cell metabolism in IL2/IL12-activated NK cells.

4 SREBP is required for the effector functions of IL2/IL12-stimulated NK cells

4.1 Introduction

Data presented in chapter 3 illustrates that SREBP activity is essential for the induction of optimal NK cell metabolic responses. Previous work from our group has demonstrated that NK cell metabolism is integrally linked to NK cell effector functions (Donnelly et al. 2014). When essential NK cell metabolic regulators such as cMyc or mTORC1 are inhibited, NK cell effector functions are compromised (Loftus et al. 2018; Donnelly et al. 2014).With this in mind, and having defined SREBP as a novel regulator of metabolism in NK cells, the impact of failed metabolism – due to the loss of SREBP activity- on NK cell effector responses was investigated.

4.2 SREBP activity is required for IL2/IL12-induced NK cell effector functions

Using 25HC and PF429242 to inhibit SREBP activation, IFNγ and granzyme B expression in IL2/IL12-activated NK cells was measured by flow-cytometry. After 20h stimulation, both IFNγ (**Fig 4.1**) and granzyme B (**Fig 4.2)** levels were significantly reduced in NK cells stimulated in the presence of either inhibitor of SREBP activation. To further confirm the importance of SREBP activity for NK cell effector function, cytokine-induced NK cell responses were investigated using $SCAP^{KO}$ mice. IL2/IL12-stimulated NK cells lacking *Scap* expression also displayed decreased IFNγ and granzyme B expression when compared to $SCAP^{WT}$ controls (**Fig 4.3)** Leading on from these findings, the capacity of NK cells lacking SREBP activity to kill target cells was investigated. NK cells activated in the presence of either 25HC or PF429242 were substantially impaired in their ability to kill both K562 or B16 tumour target cells *in vitro* (**Fig 4.4**).

A property of 25HC, which is shared with a number of other oxysterols, is that it can also ligate the liver X receptor (LXR) (Janowski et al. 1996). LXRs are ligand-activated transcription factors, involved in regulating cholesterol homeostasis. In order to confirm that 25HC was not affecting NK cell function through activating

LXR signalling, we investigated the function of NK cells treated with the synthetic LXR agonist - GW3965 (Collins et al. 2002). NK cells stimulated with IL2/IL12 in the presence of GW3965 for 18 hours showed no significant changes in IFNγ production (**Fig 4.5)** or granzyme B expression (**Fig 4.6**) compared to NK cells activated in the absence of the agonist. In addition, GW3965 did not affect cytokine-induced NK cell blastogenesis (**Fig 4.7**). 27-hydroxysterol (27HC) is another oxysterol that acts as an LXR agonist. While 27HC had not widely been considered to be potent inhibitor of SREBP activation, a recent report found that 27HC inhibits SREBP activity in hepatocytes (Li, Long, et al. 2018). NK cells stimulated in the presence of 27HC showed decreased IFNγ production (**Fig 4.8**). and granzyme B expression (**Fig 4.9**). compared to control NK cells, thus mirroring the phenotype of NK cells stimulated in the presence of 25HC. Interestingly, work in the Finlay lab has recently shown that 27HC does inhibit SREBP activation in cytokine stimulated NK cells. Taken together these data demonstrate that 25HC-mediated inhibition of SREBP and not 25HC-mediated LXR ligation accounts for the impact of 25HC on NK cell metabolism and function.

The experiments described so far in this study were carried out in cultured NK cells which were IL15-primed and expanded. Next we wanted to study NK cells isolated from the spleen and stimulated with cytokine directly *ex vivo*. IFNγ production was significantly reduced in splenic NK cells activated in the presence of the SREBP inhibitor, 25HC (**Fig 4.10**). Similarly, there was a trend towards decreased granzyme B production in SREBP inhibited NK cells activated directly *ex vivo*. (**Fig 4.11**)

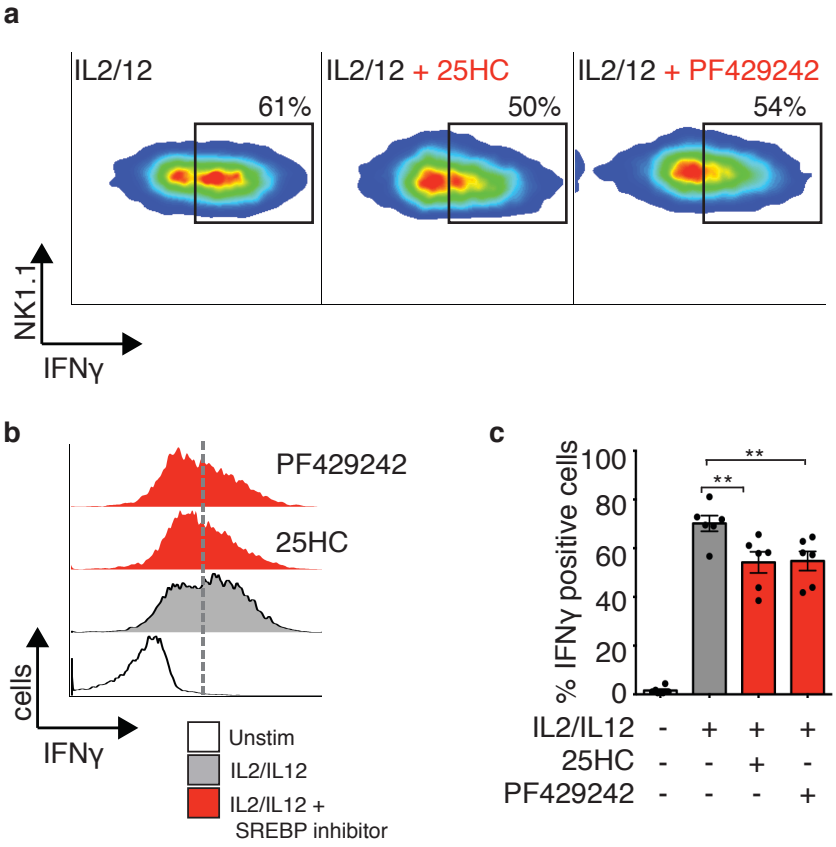

Figure 4.1 SREBP activity is required for NK cell IFNγ production in response to IL2/IL12 stimulation

Cultured NK cells were either left unstimulated or were activated with IL2 (20ng/ml) + IL12 (10ng/ml), in the presence or absence of 25HC (2.5μM) or PF429242 (10μM) for 20h. Expression of IFNγ was measured by flow cytometry. Data is representative or mean +/- S.E.M of 6 experiments. Statistical analysis was performed using a one-way ANOVA with Tukey's post-test (**p<0.01).

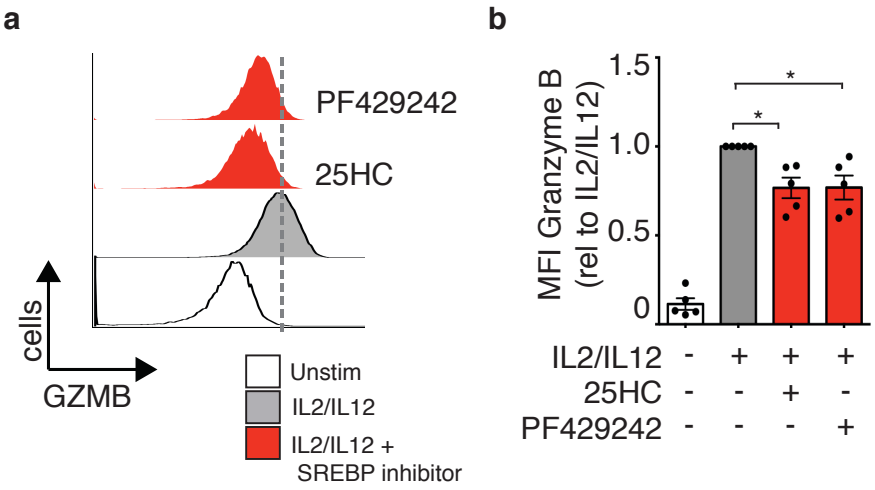

Figure 4.2 SREBP activity is required for NK cell Gzmb production in response to IL2/IL12 stimulation

Cultured NK cells were either unstimulated or were activated with IL2 (20ng/ml) + IL12 (10ng/ml), in the presence or absence of 25HC (2.5 μM) or PF429242 (10μM) for 20h. Granzyme B expression was measured by flow cytometry. Data is representative (**a**) or mean +/- S.E.M (**b**) of 5 experiments. Statistical analysis was performed using a two-tailed one sample t-test versus a theoretical value of 1 (* $p<0.05$).

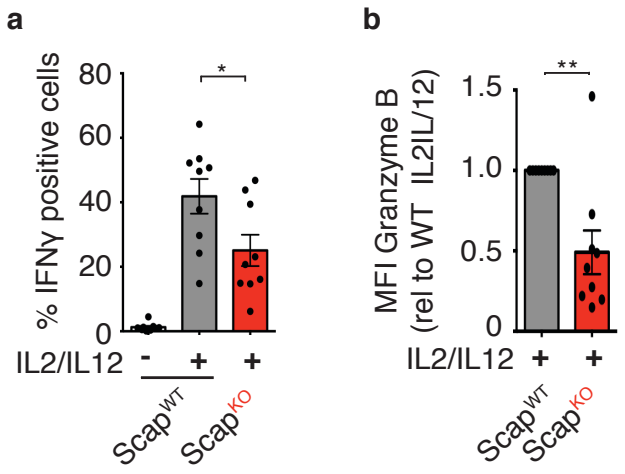

Figure 4.3 SCAP^{KO} NK cells have impaired effector functions

NK cells cultured from Scap^{KO} (*Scap*$^{flox/flox}$ x Tamox-Cre) or Scap^{WT} (*Scap*$^{WT/WT}$ x Tamox-Cre) spleens were left unstimulated or stimulated with IL2 (20ng/ml) + IL12 (10ng /ml) for 20h before measuring expression of IFNγ (**a**) and granzyme B (**b**) by flow cytometry. Data is mean +/- S.E.M of 9 independent experiments. Statistical analysis was performed using a one-way ANOVA with Tukey's post-test (**a)** or column statistics relative to a theoretical value of one (**b**) (*p<0.05, (**p<0.01).

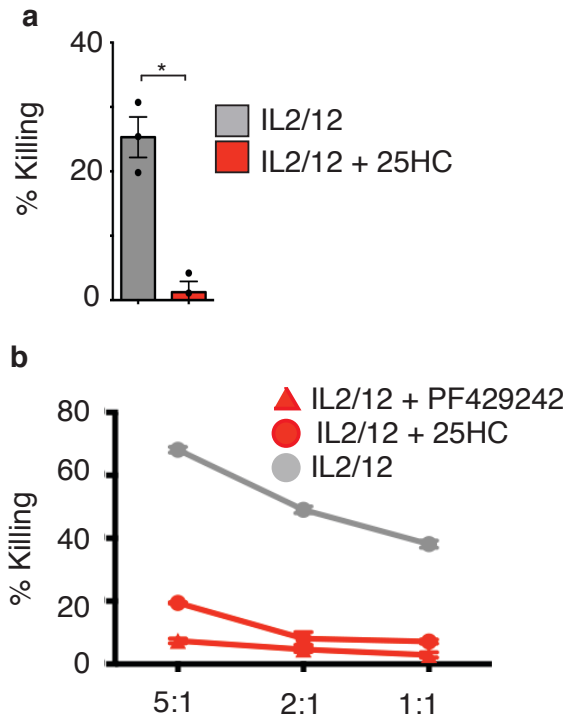

Figure 4.4 SREBP activity is required for NK cell in cytotoxicity *in vitro*

Cultured NK cells were activated with IL2 (20ng/ml) + IL12 (10ng/ml) in the presence or absence of 25HC (2.5 μM) or PF429242 (10μM) for 18 h prior to assessing *in vitro* cytotoxicity towards tumour cells. Cytotoxicity was measured following co-incubation of NK cells with either B16 (**a**) or K562 (**b**) target cells, for 4 hours at a ratio of 10 NK cells to 1 target cell (**a**) or as indicated (**b**). Percentage killing analysed by flow cytometry (**a**) or by a fluorescence release assay (**b**) and is presented as proportion of target cells killed. Data is mean +/- S.E.M (**a**) or representative (**b)** of 3 independent experiments. Statistical analysis was performed using a paired two-tailed t-test (*p<0.05)

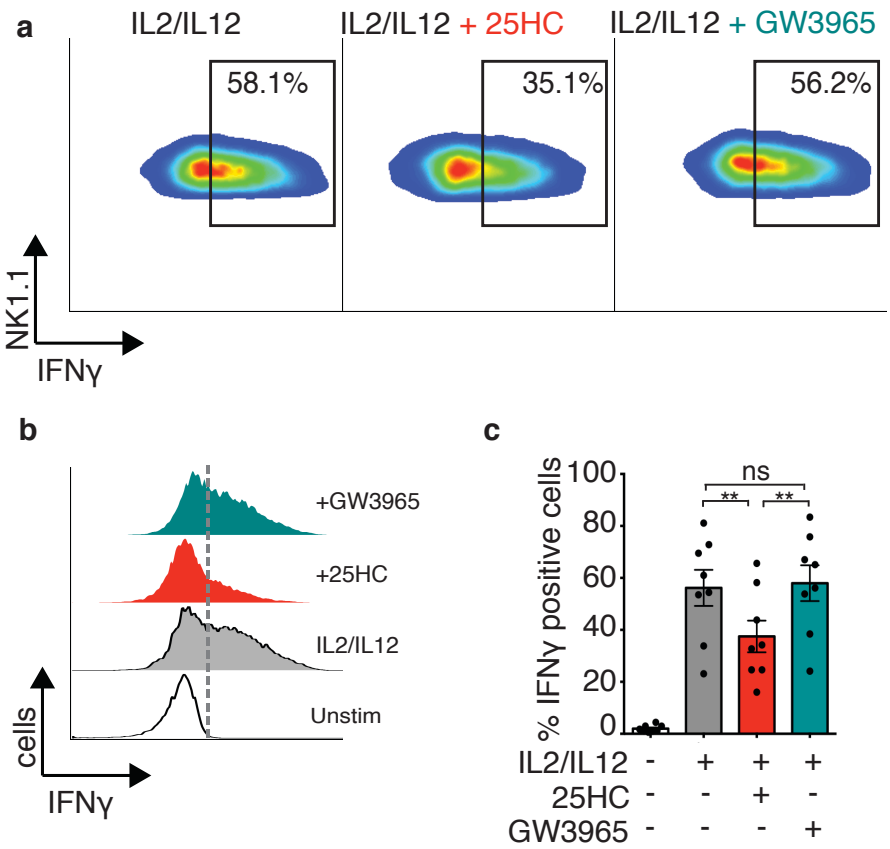

Figure 4.5 Ligation of the LXR has no effect on IFNγ production by IL2/IL12-stimulated NK cells

Cultured NK cells were either left unstimulated or were activated with IL2 (20ng/ml) + IL12 (10ng/ml), in the presence or absence of 25HC (2.5 μM) or GW3965 (2μM) for 20h. Expression of IFNγ was measured by flow cytometry. Data is representative or mean +/- S.E.M of 8 experiments. Statistical analysis was performed using a one-way ANOVA with Tukey's post-test. (ns= non-significant, **p<0.01).

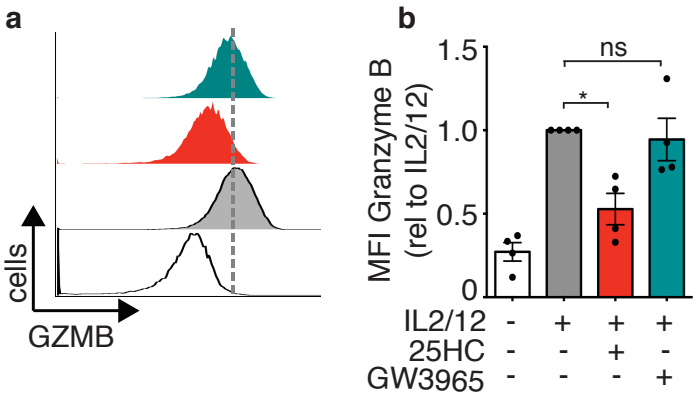

Figure 4.6 Ligation of the LXR does not significantly affect granzyme B expression by IL2/IL12-stimulated NK cells

Cultured NK cells were either left unstimulated or were activated with IL2 (20ng/ml) + IL12 (10ng/ml), in the presence or absence of 25HC (2.5 μM) or GW3965 (2μM)for 20h. Expression of granzyme B was measured by flow cytometry. Data is representative or mean +/- S.E.M of 4 experiments. Statistical analysis was performed using column statistics relative to a theoretical value of one (ns= non-significant, *p<0.05).

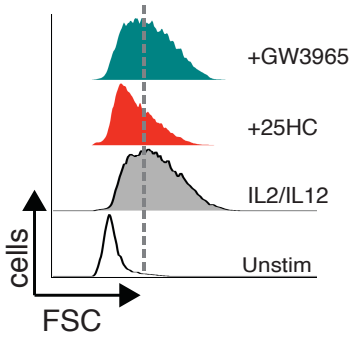

Figure 4.7 Ligation of the LXR does not impair NK cell growth by IL2/IL12-stimulated NK cells

Cultured NK cells were either left unstimulated or were activated with IL2 (20ng/ml) + IL12 (10ng/ml), in the presence or absence of 25HC (2.5 μM) or GW3965 (2μM) for 20h. NK cell FSC-A was measured by flow cytometry, as a surrogate of cell size. Data is representative of 4 independent experiments.

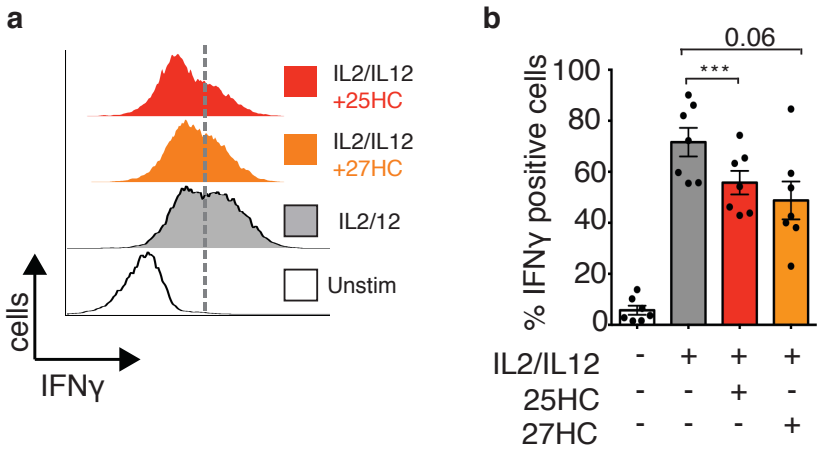

Figure 4.8 27HC impairs IFNγ production in IL2/12-stimulated NK cells

Cultured NK cells were either left unstimulated or were activated with IL2 (20ng/ml) + IL12 (10ng/ml), in the presence or absence of 25HC (2.5 μM) or 27HC (1 or 2 μM) for 20h. Cells were intracellularly stained and IFNγ production was measured by flow cytometry. Data is representative or mean +/- S.E.M of 7 independent experiments. Statistical analysis was performed using a one-way ANOVA with Tukey's post-test (ns= non-significant, ***$p<0.001$). (Chloe Choi contributed some replicates to this figure).

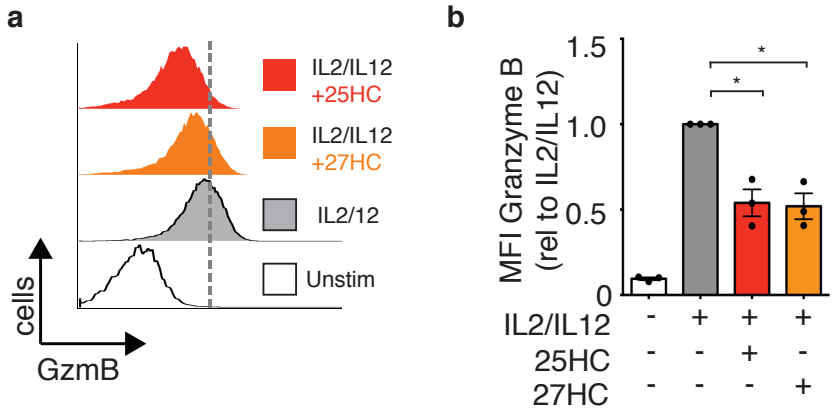

Figure 4.9 27HC reduces granzyme B production in IL2/IL12 stimulated NK cells

Cultured NK cells were either left unstimulated or were activated with IL2 (20ng/ml) + IL12 (10ng/ml), in the presence or absence of 25HC (2.5 μM) or 27HC (1μM)for 20h. Cells were intracellularly stained and granzyme B expression was measured by flow cytometry. Data is representative (**a**) or mean +/- S.E.M (**b**) of 3 experiments. Statistical analysis was performed using column statistics relative to a theoretical value of one (*p<0.05).

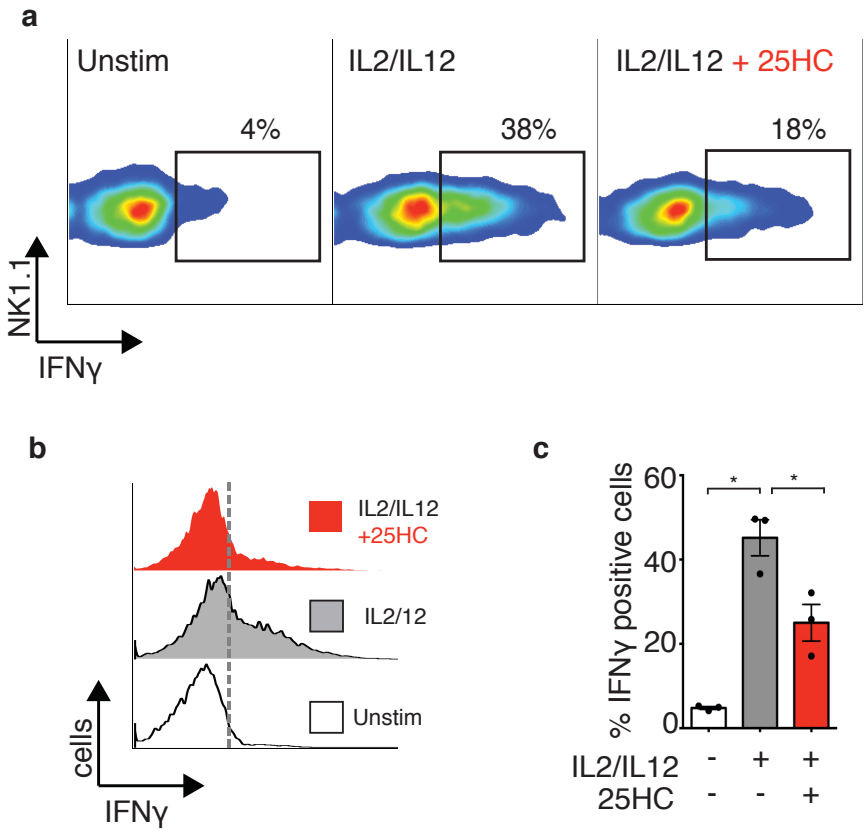

Figure 4.10 IFNγ production is dependent on SREBP activity in splenic NK cells stimulated *ex vivo*

Freshly isolated splenocytes were either left unstimulated or were activated with IL2 (20ng/ml) + IL12 (10ng/ml), in the presence or absence of 25HC (2.5 μM) for 20h. Cells were intracellularly stained and IFNγ production was measured by flow cytometry. Data is representative (**a-b**) or mean +/- S.E.M (**c**) of 3 experiments. Statistical analysis was performed using a one-way ANOVA with Tukey's post-test. (, *p<0.01).

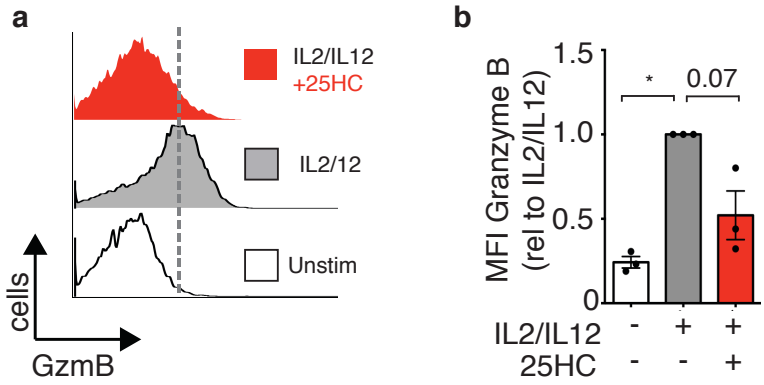

Figure 4.11 Granzyme B production is dependent on SREBP activity in splenic NK cells stimulated *ex vivo*

Freshly isolated splenocytes were either left unstimulated or were activated with IL2 (20ng/ml) + IL12 (10ng/ml), in the presence or absence of 25HC (2.5 μM) for 20h. Cells were intracellularly stained and production of granzyme B was measured by flow cytometry. Data is representative or mean +/- S.E.M of 3 experiments. Statistical analysis was performed using a one-way ANOVA with Tukey's post-test. (*p<0.01).

4.3 SREBP activity is required for NK cell therapeutic responses *in vivo*

Various approaches are being developed to use NK cells therapeutically to treat cancer. One such approach involves adoptive transfer of *in vitro*-activated NK cells to the patient. The cytokine combination of IL12/IL15/IL18 is a promising stimulation for this purpose as it has been shown to sustain robust anti-tumour responses (Guillerey, Huntington, and Smyth 2016; Ni et al. 2012). IL12/IL15/IL18-stimulation promotes very high expression of the high affinity IL2 receptor -CD25. This allows NK cells to respond to low concentrations of IL2 produced *in vivo* (Leong et al. 2014; Ni et al. 2012). Following 20 hour stimulation with IL12/IL15/IL18, NK cells increase in size **(Fig 4.12)** and express increased levels of CD25 compared to unstimulated or IL2/IL12 stimulated NK cells (**Fig 4.13**). They similarly increase expression of IFNγ (**Fig 4.14**), whilst expression of granzyme B is comparable to levels observed in IL2/IL12-stimulated NK cells(**Fig 4.15**). With this in mind, the importance of SREBP signalling for NK cell effector functions in response to the IL12/IL15/IL18 cytokine combination was investigated. Indeed, IL12/IL15/IL18-induced IFNγ production (**Fig 4.16**) and granzyme B expression (**Fig 4.17)** was substantially reduced when SREBP activity was inhibited by 25HC. Likewise, when SREBP activity was inhibited in IL12/IL15/IL18-stimulated NK cells they were smaller in size (**Fig 4.18**) and failed to increase CD25 expression to the same extent as control NK cells (**Fig 4.19**). Additionally, NK cell killing of B16 or K562 tumour target cells was dramatically inhibited when SREBP activity was prevented, as measured by *in vitro* cytotoxicity assays (**Fig 4.20**). To verify that SREBP inhibition and not LXR ligation was responsible for the effects of 25HC on IL12/IL15/IL18-induced NK cell responses, NK cells were stimulated in the presence of LXR agonist GW3965. LXR activation was found to have no effect on CD25 expression (**Fig 4.21**) or cell size (**Fig 4.22**) following IL12/IL15/IL18-stimulation. Furthermore, IFNγ production (**Fig 4.23**) and granzyme B expression (**Fig 4.24**) were unaltered in IL12/15/18 stimulated NK cells following LXR ligation.

Therefore the impaired responses observed with 25HC in IL12/15/18-stimulated NK cells were attributed to SREBP inhibition and not to LXR ligation.

Having confirmed that SREBP activation is critical for the anti-tumour response of IL12/IL15/IL18-activated NK cells *in vitro*, it was next sought to investigate the anti-tumour actions of these NK cells *in vivo*. Using the B16 mouse-model of melanoma, the importance of SREBP signalling for the therapeutic anti-tumour effects of adoptively transferred IL12/15/18-stimulated NK cells was measured. For these experiments, B16 tumour cells were injected subcutaneously into the flanks of C57Bl/6 mice on day 0, followed by injection of *in vitro* stimulated NK cells on days 3, 7 and 10 post-tumour induction (**Fig 4.25:** *sub-cutaneous injections were performed by Dr Lydia Dyck, Lynch Lab, TCD*). The injection of IL12/IL15/IL18 stimulated NK cells significantly slowed the rate of tumour growth when compared to control mice that received PBS injections (**Fig 4.26**). However, this therapeutic effect was lost when NK cells were stimulated with IL12/IL15/IL18 in the presence of the SREBP inhibitor, 25HC. Mice receiving injections of NK cells stimulated with IL12/IL15/IL18 in combination with 25HC showed tumour growth that was comparable to that of the control mice (**Fig 4.26**). Altogether, these data show that SREBP activity in NK cells is required for acquiring a metabolic phenotype that facilitates NK cell anti-tumour responses *in vivo*.

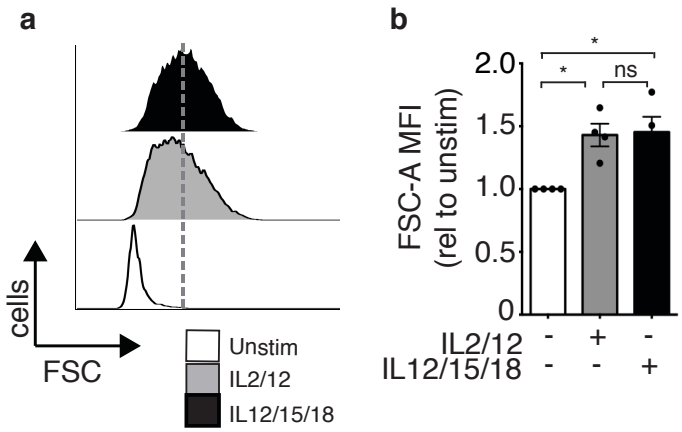

Figure 4.12 IL12/IL15/IL18-stimulated NK cells increase in size to a similar extent as IL2/IL12-stimulated NK cells

Cultured NK cells were left unstimulated or activated with a cytokine combination of either IL2 (20ng/ml) + IL12 (10ng /ml) or IL12 (25ng/ml), IL15 (50ng/ml) and IL18 (5ng/ml) before measuring expression of IFNγ by flow cytometry. Data is representative of (**a**) or mean +/- S.E.M of (**b**) of 4 experiments. Statistical analysis was performed using column statistics relative to a theoretical value of one or a paired two-tailed t-test (ns=non-significant,*p<0.05,). (Some n numbers from the IL12/IL15/18-stimulated condition overlap with the IL12/IL15/18-stimulated condition in Fig 4.18)

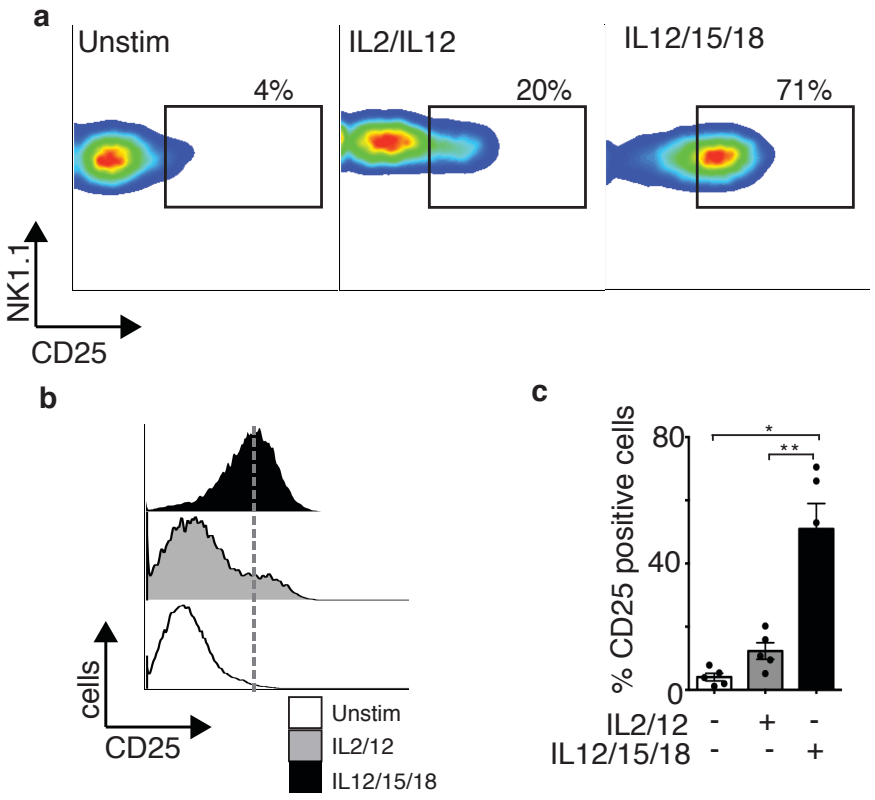

Figure 4.13 IL12/IL15/IL18-stimulated NK cells have enhanced CD25 expression

Cultured NK cells were left unstimulated or activated with a cytokine combination of either IL2 (20ng/ml) + IL12 (10ng /ml) or IL12 (25ng/ml), IL15 (50ng/ml) and IL18 (5ng/ml). Expression of CD25 was measured by flow cytometry. Data is representative or mean +/- S.E.M of 5 experiments. Statistical analysis was performed using a one-way anova with Tukey's post-test. (ns= non-significant, *p<0.05, **p<0.01).(Some n numbers from the IL12/IL15/18-stimulated condition overlap with the IL12/IL15/18-stimulated condition in Fig 4.19)

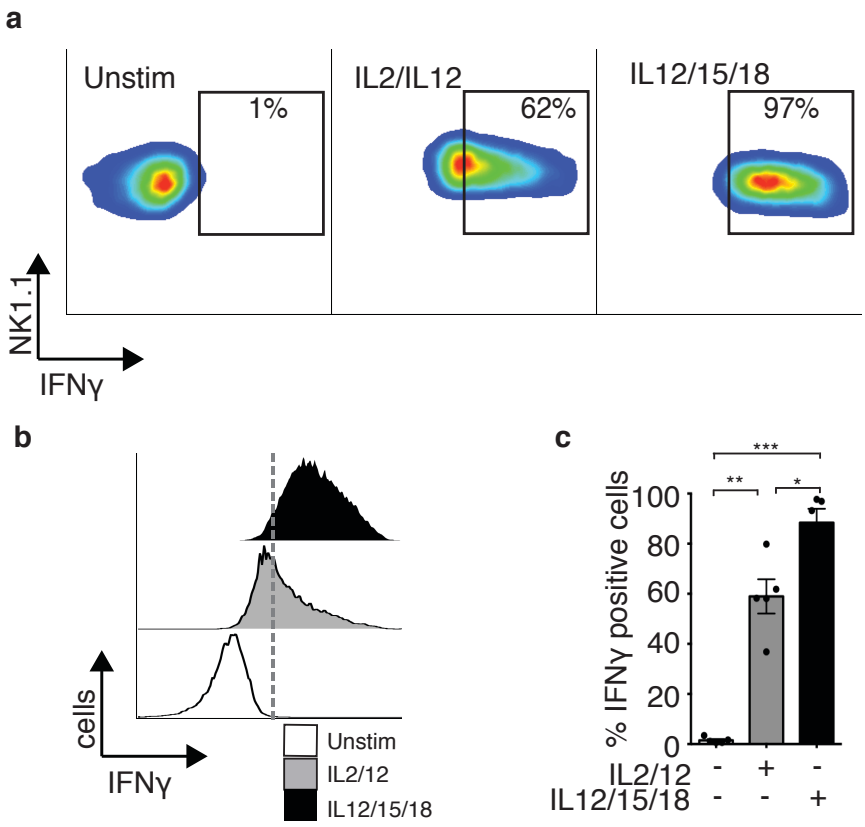

Figure 4.14 NK cells have enhanced IFNγ production following IL12/IL15/IL18 stimulation

Cultured NK cells were left unstimulated or activated with a cytokine combination of either IL2 (20ng/ml) + IL12 (10ng /ml) or IL12 (25ng/ml), IL15 (50ng/ml) and IL18 (5ng/ml). Expression of IFNγ was measured by flow cytometry. Data is representative of at least 6 independent experiments. Statistical analysis was performed using column statistics relative to a theoretical value of one or a paired two-tailed t-test (*p<0.05,**p<0.01) (Some n numbers from the IL12/IL15/18-stimulated condition overlap with the IL12/IL15/18-stimulated condition in Fig 4.16).

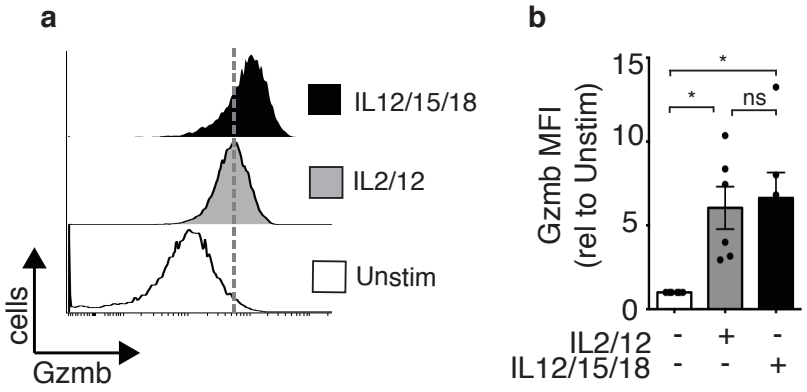

Figure 4.15 IL12/IL15/IL18-stimulation induces robust granzyme B expression

Cultured NK cells were left unstimulated or activated with a cytokine combination of either IL2 (20ng/ml) + IL12 (10ng /ml) or IL12 (25ng/ml), IL15 (50ng/ml) and IL18 (5ng/ml) for 20 h. Expression of granzyme B was measured by flow cytometry. Data is representative (**a**) or mean +/- S.E.M of 6 experiments. Statistical analysis was performed using column statistics versus a theoretical value of 1 (to compare unstimulated condition with stimulated conditions) or by a paired two-tailed t-test (to compare IL2/IL12 stimulated cells with IL12/IL15/IL18-stimulated cells) (ns =non-significant,*$p<0.05$).

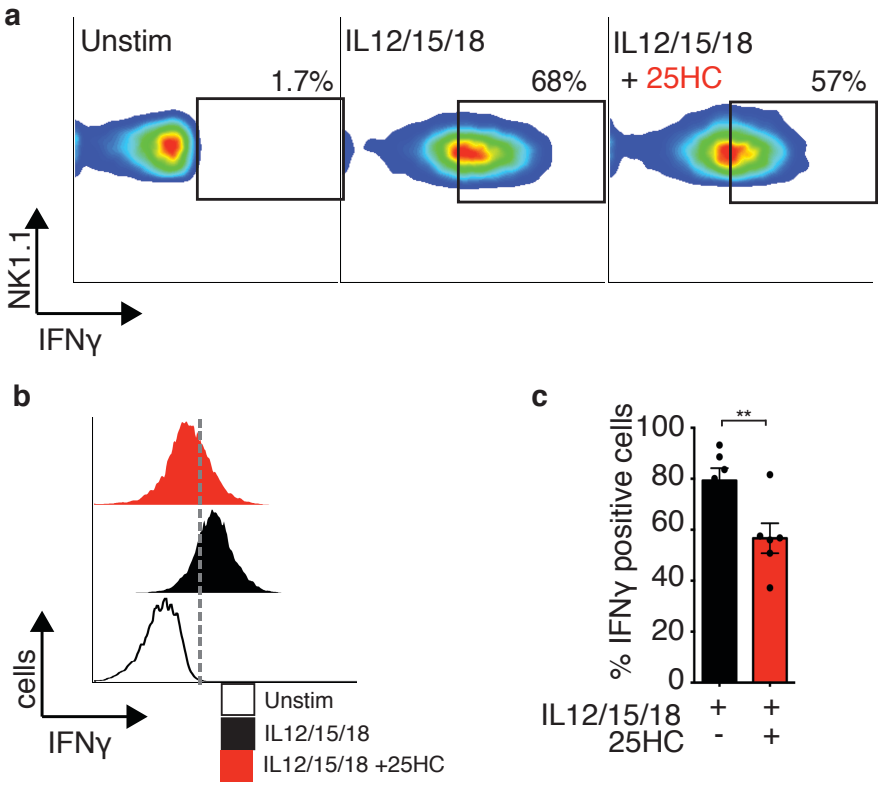

Figure 4.16 IL12/IL15/IL18-induced IFNγ responses are SREBP dependent

Cultured NK cells were left unstimulated or activated with IL12 (25ng/ml), IL15 (50ng/ml) and IL18 (5ng/ml) in the presence or absence of 25HC (2.5 μM) for 20 h. Expression of IFNγ was measured by flow cytometry. Data is representative (**a-b**) or mean +/- S.E.M of 6 independent experiments. Statistical analysis was performed using a two-tailed paired t-test (**p<0.01).

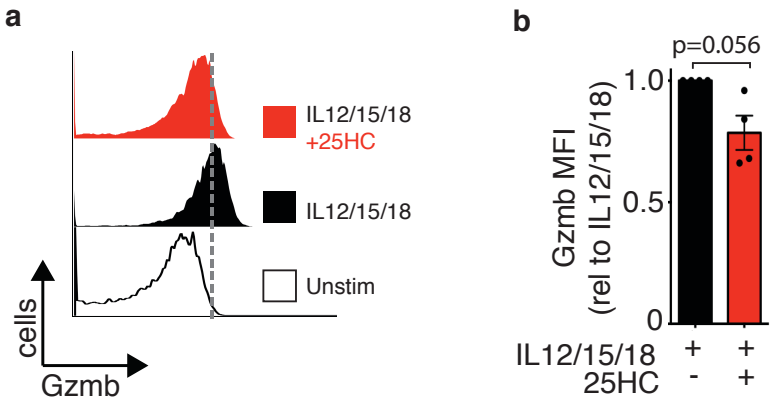

Figure 4.17 IL12/IL15/IL18-induced granzyme B responses are SREBP dependent

Cultured NK cells were left unstimulated or activated with IL12 (25ng/ml), IL15 (50ng/ml) and IL18 (5ng/ml) in the presence or absence of 25HC (2.5 μM) for 20 h. Expression of granzyme B was measured by flow cytometry. Data is representative (**a**) or mean +/- S.E.M (**b**) of 4 experiments. Statistical analysis was performed using column statistics versus a theoretical value of 1.

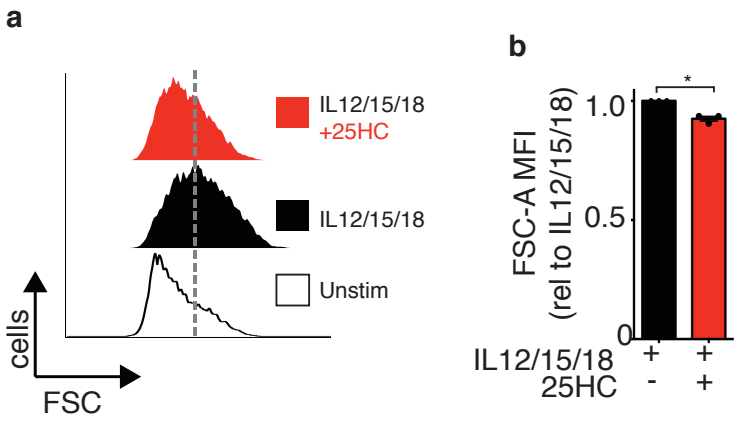

Figure 4.18 Inhibition of SREBP activity during IL12/IL15/IL18-stimulation reduces NK cell size

Cultured NK cells were left unstimulated or activated with IL12 (25ng/ml), IL15 (50ng/ml) and IL18 (5ng/ml) in the presence or absence of 25HC (2.5 μM) for 20 h. FSC-A was measured by flow cytometry as a readout of cell size. Data is representative (**a**) or mean +/- S.E.M (**b**) of 3 experiments. Statistical analysis was performed using column statistics versus a theoretical value of 1.(*$p<0.05$).

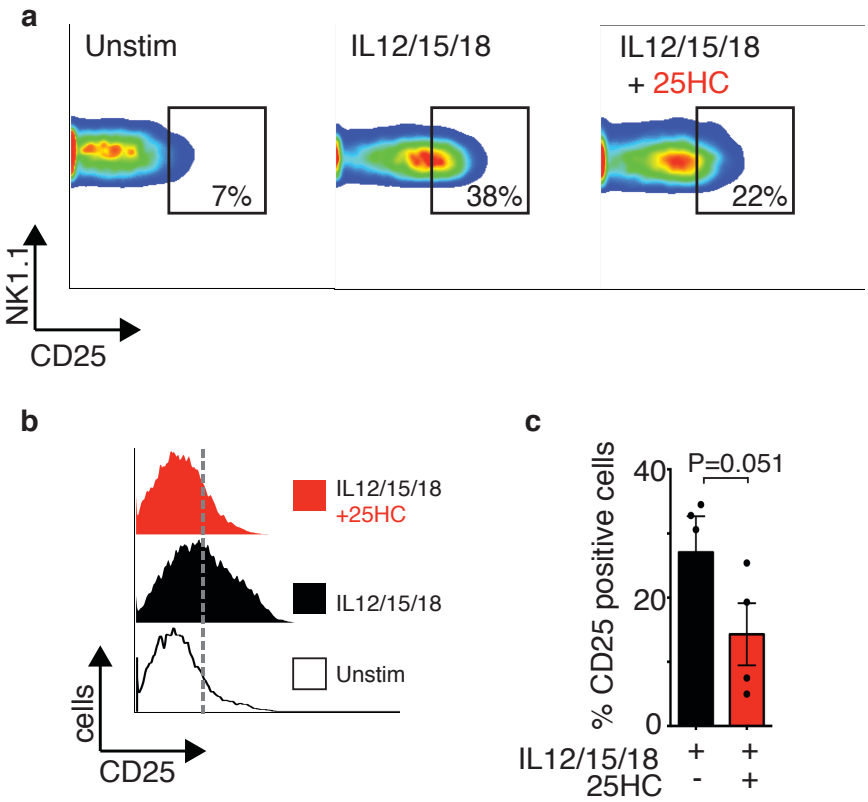

Figure 4.19 IL12/IL15/IL18-induced CD25 expression is SREBP dependent

Cultured NK cells were left unstimulated or activated with IL12 (25ng/ml), IL15 (50ng/ml) and IL18 (5ng/ml) in the presence or absence of 25HC (2.5 μM) for 20 h. Cells were surface stained and CD25 expression was measured by flow cytometry. Data is representative of (**a-b**) or mean +/- S.E.M (**c**) of 4 experiments. Statistical analysis was performed using a paired two-tailed t-test.

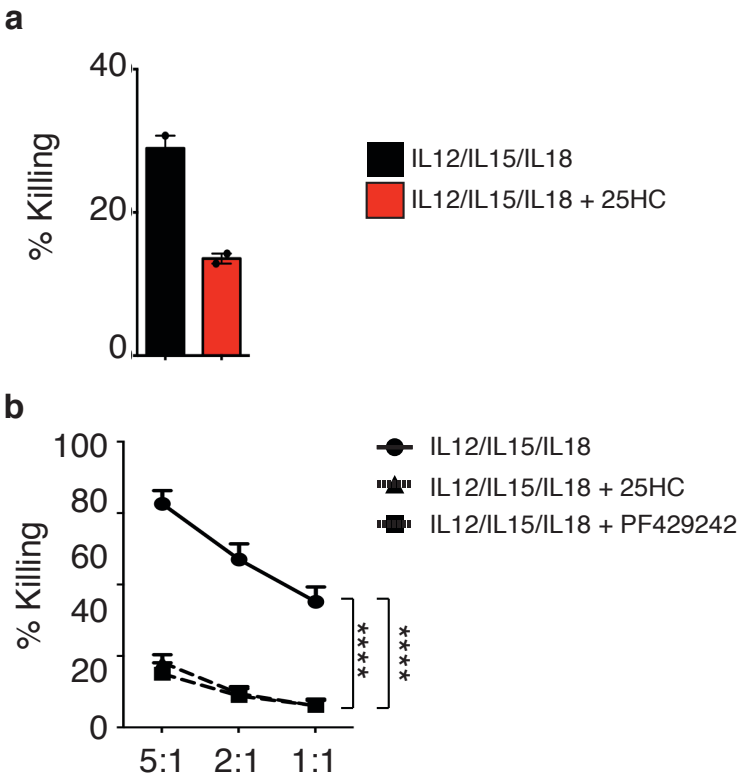

Figure 4.20 SREBP activity is important for NK cell cytotoxicity *in vitro* in response to IL12/IL15/IL18 stimulation

Cultured NK cells were activated with IL12 (25ng/ml), IL15 (50ng/ml) and IL18 (5ng/ml), in the presence or absence of 25HC (2.5 μM) or PF429242 (10 μM) for 18 h prior to assessing *in vitro* cytotoxicity towards tumour cells. Cytotoxicity was measured following co-incubation of NK cells with either B16 (**a**) or K562 (**b**) target cells, for 4 hours at a ratio of 10 NK cells to 1 target cell (**a**) or as indicated (**b**). Percentage killing analysed by flow cytometry (**a**) or by a fluorescence release assay (**b**) and is presented as proportion of target cells killed. Data is mean +/- S.E.M of 2 (**a**) or 4 (**b**) independent experiments. Statistical analysis was performed using a 2-way ANOVA with Sidak post-test (****p<0.0001). (*Fluorescence release assay (**b**) was performed by Dr Nadine Assmann.)*

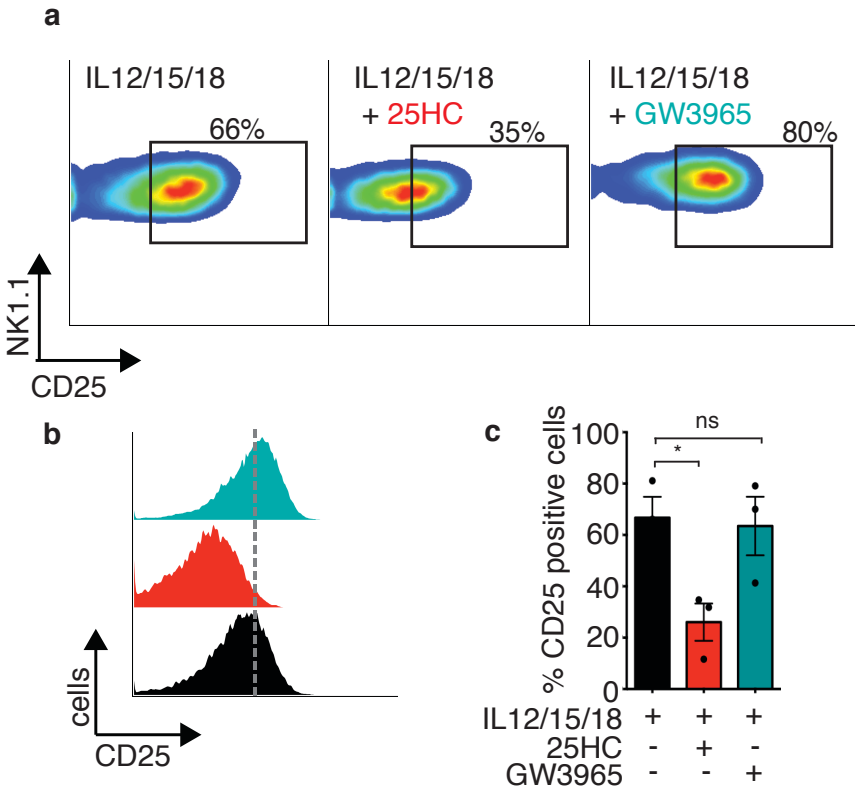

Figure 4.21 LXR ligation does not decrease NK cell CD25 expression following IL12/IL15/IL18-stimulation

Cultured NK cells were left unstimulated or activated with IL12 (25ng/ml), IL15 (50ng/ml) and IL18 (5ng/ml) in the presence or absence of 25HC (2.5 μM)or GW3964 (2 μM). Expression of CD25 was measured by flow cytometry. Data is representative or mean +/- S.E.M of 3 experiments. Statistical analysis was performed using a one-way ANOVA with Tukey's multiple comparisons test (ns =non-significant,*$p<0.05$).

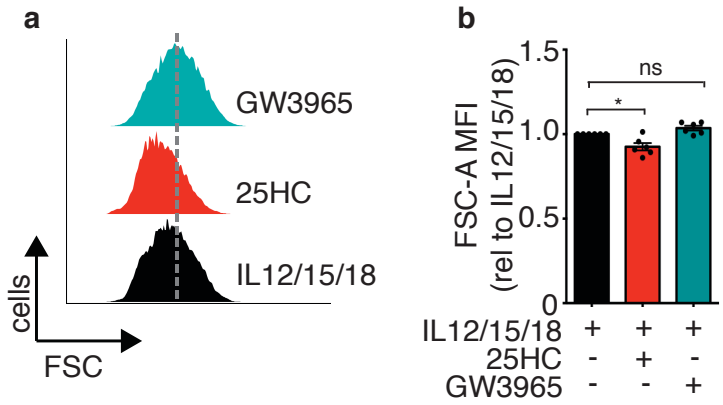

Figure 4.22 LXR ligation does not impair NK cell growth following IL12/IL15/IL18-stimulation

Cultured NK cells were left unstimulated or activated with IL12 (25ng/ml), IL15 (50ng/ml) and IL18 (5ng/ml) in the presence or absence of 25HC (2.5 μM) or GW3964 (2 μM). FSC-A was measured by flow cytometry as a readout of cell size. Data is representative or mean +/- S.E.M of 6 experiments. Statistical analysis was performed using a column statistics versus a theoretical value of 1 (ns =non-significant,*p<0.05).

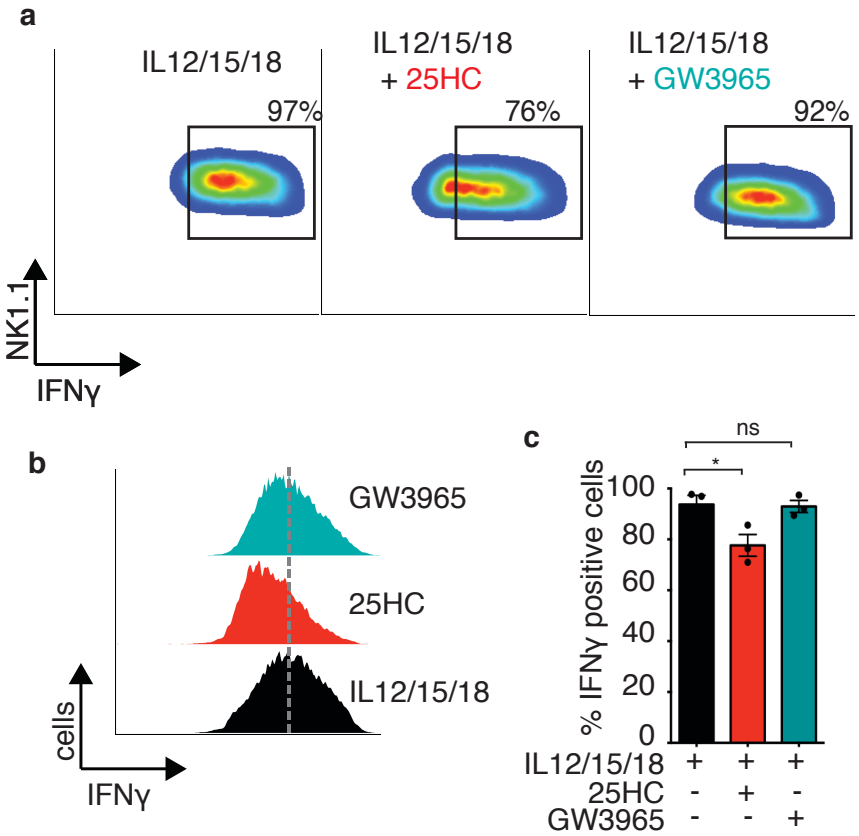

Figure 4.23 LXR ligation does not impact NK cell IFNγ production following IL12/IL15/IL18-stimulation

Cultured NK cells were left unstimulated or activated with IL12 (25ng/ml), IL15 (50ng/ml) and IL18 (5ng/ml) in the presence or absence of 25HC (2.5 μM) or GW3964 (2μM). Expression of IFNγ was measured by flow cytometry. Data is representative of or mean +/- S.E.M of 3 experiments. Statistical analysis was performed using a one-way ANOVA with Tukey's post-test. (ns=non-significant,*p<0.05).

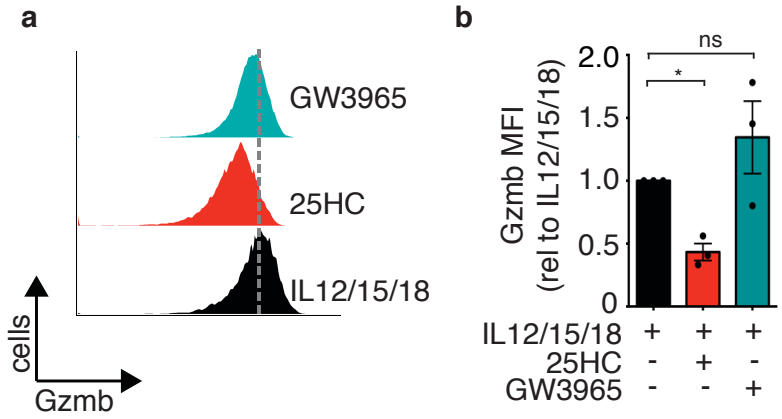

Figure 4.24 LXR ligation does not impact NK cell Gzmb production following IL12/IL15/IL18-stimulation

Cultured NK cells were left unstimulated or activated with IL12 (25ng/ml), IL15 (50ng/ml) and IL18 (5ng/ml) in the presence or absence of 25HC (2.5 μM) or GW3964 (2μM). Granzyme B expression was measured by flow cytometry. Data representative (**a**) or mean +/- S.E.M (b) of 3 experiments. Statistical analysis was performed using a column statistics versus a theoretical value of 1 (ns =non-significant,*p<0.05).

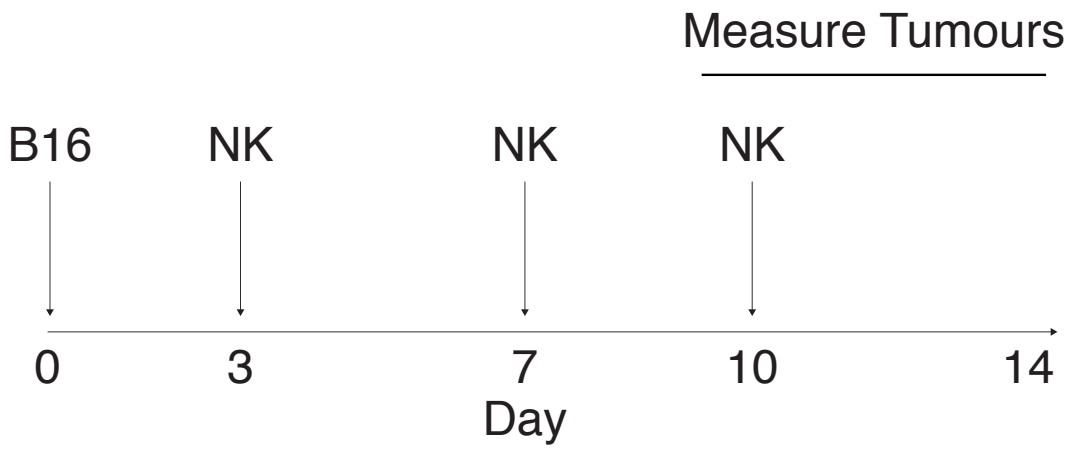

Figure 4.25 Timeline for experiment investigating NK cell anti-tumour responses *in vivo*

Schematic outlining the experimental design for investigating NK cell anti-tumour responses *in vivo*. B16 tumour cells were injected subcutaneously into the flanks of C57Bl/6 mice on day 0, followed by injections on day 3, 7 and 10, of cultured, purified, NK cells after overnight *in vitro* stimulation with IL12/15/18 in the presence or absence of 25HC. Alternatively mice were injected with PBS instead of NK cells as a control. (*Experiment was designed in collaboration with Dr Lydia Dyck.)*

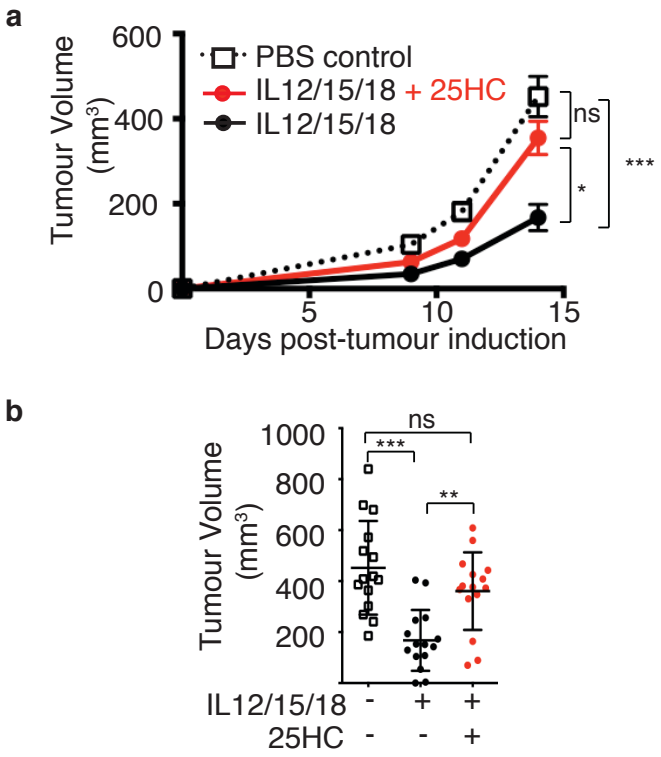

Figure 4.26 SREBP activity is important for therapeutic NK cell anti-tumour responses *in vivo*

C57Bl/6 mice were injected with B16 tumour cells on day 0, followed by injections of purified, *in vitro*-activated, NK cells stimulated overnight with IL12 (25ng/ml), IL15 (50ng/ml) and IL18 (5ng/ml) in the presence or absence of 25HC (2.5 μM). Alternatively, control mice were injected with PBS instead of NK cells. Tumour volume was calculated on days 9, 11 and 14. Shown is pooled data (**a**) and measurements from individual mice on day 14 (**b**). Data presented is for 15 mice per group. Statistical analysis was performed by 2-way ANOVA (**a**) or one-way ANOVA with Tukey's post-test (**b**) (ns, non-significant,* $p<0.05$, ** $p<0.01$, ***$p<0.001$). (*Sub-cutaneous injections were performed by Dr Lydia Dyck.)*

4.4 Discussion of chapter 4

Numerous studies have established that cellular metabolism is integrally linked to immune cell function. As such, different immune cell types adopt specific metabolic configurations to support their unique functional demands (Loftus and Finlay 2016). Previous work from the Finlay group highlighted that IL2/IL12-activated NK cells depend on increased metabolism to support cytokine-induced effector responses such as increased expression of granzyme B and IFNγ (Donnelly et al. 2014). It has also been demonstrated that when central regulators of NK cell metabolism - such as mTORC1 or cMYC - are inhibited, there is a dramatic functional consequence; NK cells lose their ability to produce effector molecules, have reduced cytotoxicity against target cells *in vitro* and have impaired responses to viral infections *in vivo* (Loftus et al. 2018; Donnelly et al. 2014; Marcais et al. 2014; Nandagopal et al. 2014). Data presented in chapter three revealed the importance of SREBP transcription factors as central regulators of metabolism in IL2/IL12-activated NK cells. It was therefore hypothesised that SREBP activity would be required for NK cell effector functions. Indeed, findings from this chapter highlight the importance of SREBP activity for optimal cytokine-induced NK cell effector responses. Thus identifying SREBP transcription factors as critical regulators of NK cell metabolism and function.

Data in this report highlight the importance of SREBP transcription factors for optimal NK cell effector responses when activated with the cytokine-combination of IL2/IL12 or alternatively with IL12/IL15/IL18. NK cells with impaired SREBP activity displayed defective production of granzyme B and IFNγ, and had reduced cytotoxic capacities against B16 and K562 target cells *in vitro*. A crucial finding was that the *in vivo* anti-tumour functions of NK cells was also dependant on the actions of SREBP. When SREBP was inhibited in *ex vivo*-activated NK cells, they lost their ability to control tumour growth when adoptively transferred into tumour-bearing mice.

My findings linking SREBP activity to NK cell function in this chapter add to a growing body of evidence linking SREBP activity and *de novo* lipid synthesis to the functions of other immune cell subsets. For example, *de novo* fatty acid synthesis is essential for the development of CD4+ T helper 17 (T_H17) cells (Berod et al. 2014). Pharmacologically inhibiting fatty acid synthesis through inhibition of ACC1, favours the polarisation of naïve CD4+ T cells towards regulatory T cells (Tregs) as opposed to IL17-producing TH17 cells (Berod et al. 2014). Another group found that mice that lack the ability to produce the SREBP-inhibitor 25HC, have increased frequencies of IL17A production by T cells in their lymph nodes and spleens (Reboldi et al. 2014) A separate study carried out in CD4+ T cells by the Zang group reported that SREBP1 directly binds to the *Il17* gene promoter and results in inhibition of IL17 production, thus identifying a direct link between SREBP activity and IL17 expression (Cui et al. 2011). Furthermore, $SCAP^{KO}$ CD8+ T cells - which lack SREBP activity - produce reduced amounts of IFNγ and TNFα as compared to wild-type controls when challenged with antigen *ex vivo* (Kidani et al. 2013). The same study shows that when SREBP activity is inhibited in the T cell compartment, mice have a diminished antiviral response to LCMV infection (Kidani et al. 2013).

The importance of SREBP transcription factors in CD8+ T cell activation is likely due -at least in part - to an increased demand for cholesterol by activated CD8+ T cells. Stimulation of CD8+ T cells with phytohemagglutinin or with anti-CD3 and anti-CD8 triggers a SREBP-dependent increase in levels of cholesterol, both intracellularly and in the plasma membrane (Yang, Bai, et al. 2016; Chen, Heiniger, and Kandutsch 1975). In line with this, direct inhibition of either cholesterol synthesis, or cholesterol transport, caused a significant impairment in IFNγ ,TNFα and granzyme B production by CD8+ T cells activated through CD3 and CD28 (Yang, Bai, et al. 2016). Similarly, modulating cholesterol metabolism in $CD8^+$ T cells by preventing cholesterol esterification improves T cell effector functions (Yang, Bai, et al. 2016). Genetic or pharmacological inhibition of ACAT1 (a key enzyme involved in the esterification of free cholesterol to cholesteryl esters for storage) improves the ability of CD8+ T lymphocytes to produce IFNγ, granzyme B and TNFα. Correspondingly, $ACAT1^{KO}$ CD8+ T cells have an enhanced ability to control

tumour growth in mice *in vivo* (Yang, Bai, et al. 2016). An additional study revealed that exogenous addition of the cholesterol precursor, mevalonate, can rescue the defects observed when cholesterol homeostasis is perturbed in CD8+ T cells (Bensinger et al. 2008). Of note, deletion of ACAT1 in the CD4+ T cell subset had no effect on function (Yang, Bai, et al. 2016). SREBP activity has also been linked to B cell effector responses. The oxysterols 25HC and 27HC can supress the class switch recombination required for naïve B cells to switch from IgM production to IgA secretion (Bauman et al. 2009). Arguably, and in contrast to studies in T cells, this was not due to inhibition of cholesterol synthesis as IgA production could not be rescued by supplementation with exogenous cholesterol (Bauman et al. 2009). LXR ligands had no effect on class switching in this study which suggests that the results observed were mediated through SREBP inhibition, however the authors did not directly address this question (Bauman et al. 2009).

The impact of SREBP on the immune system is not confined to lymphocytes. In macrophages, SREBP has been shown to control expression of IL1β and IL18 although the mechanism involved has not been fully elucidated (Reboldi et al. 2014; Im et al. 2011). $SCAP^{KO}$ BMDMs, which lack SREBP activity, even when unstimulated, spontaneously engage a type I IFN response characterised by increased expression *Ifnb1* and interferon-stimulated genes (York et al. 2015). Decreasing *de novo* cholesterol synthesis in BMDMs can also drive type 1 IFN responses, through a yet undefined mechanism that is dependent on the cytosolic DNA sensor: STING (York et al. 2015). BMDMs that have been modified to lack the ability to produce the SREBP-inhibitor, 25HC, have increased IL1β at both protein and transcript levels compared to wild-type macrophages (Reboldi et al. 2014). Macrophages lacking 25HC production interestingly had elevated secretion of IL18, in the absence of differences at the mRNA level, suggesting increased inflammasome activity in cells with heightened SREBP activity (Reboldi et al. 2014). In fact, in another report SREBP has been reported to modulate the gene encoding the inflammasome component, NLR family pyrin domain containing 1A (Nlrp1a) (Im et al. 2011). A feed-back loop may be at play here as a recent study in monocytes and monocyte-derived macrophages has highlighted that siRNA-

silencing of NLRP3 decreases SREBP1 levels and that IL1β can induce SREBP1 expression (Varghese, Patel, and Yadav 2019).

This body of evidence highlights that the link between SREBP activity and effector responses is not limited to cytokine-activated NK cells. Furthermore, in cells of the immune system, SREBP transcription factors are not confined to their role as 'master regulators' of the enzymes involved in cholesterol and lipid synthesis; SREBP activity can additionally both directly and indirectly regulate genes encoding immune effector molecules. Taken together, these reports highlight an emerging and complicated role for SREBP transcription factors in controlling both the innate and adaptive arms of the immune system. Therefore any manipulation of SREBP activity systemically *in vivo* is likely to greatly affect the overall immune response.

In many of the aforementioned reports, the importance of SREBP transcription factors in controlling the immune response were due - at least in part – to SREBP controlled fatty acid or cholesterol synthesis. This is in contrast to the role found for SREBP transcription factors in IL2/IL12-stimulated NK cells. Inhibition of *de novo* fatty acid or cholesterol synthesis had no effect on NK cell IFNγ production, granzyme B expression, or target cell killing, as shown by other members of our group (Assmann et al. 2017). As mentioned in chapter 3, inhibition of lipid synthesis also had no effects on the metabolism of IL2/IL12-stimualted NK cells (Assmann et al. 2017).Thus, SREBP transcription factors have a novel role in NK cells, as they can control NK cell metabolism and function completely independently to their control of lipogenic pathways.

In other immune subsets, SREBP and LXR activation can be reciprocally regulated. For instance, TCR-stimulated CD8+ T cells co-ordinately silence LXR activity whilst inducing SREBP activity (Bensinger et al. 2008; Kidani et al. 2013). Antigen-induced expansion of CD8+ T lymphocytes is negatively regulated by LXR activity (Bensinger et al. 2008). Ma et al have shown that cholesterol can inhibit the anti-tumour activity of the IL-9 producing CD8+ T cell subset through an LXR-dependent manner (Ma et al. 2018). IL9 producing CD8+ T cells have been reported to have

stronger anti-tumour effects than the better characterised CTLs (Lu et al. 2014). Treatment with cholesterol, 25HC and other oxysterols reduced the mRNA expression of IL9 by this CD8+ T cell subset. Furthermore, the LXR agonist - GW3965 - inhibited IL9 expression (Ma et al. 2018). As 25HC can act as an LXR ligand, it was considered that LXR ligation may be responsible for some of the decreases in effector molecule production observed by NK cells activated in the presence of this oxysterol. This question was addressed by activating NK cells in the presence of GW3965 and measuring effector molecule production. Ligation of the LXR did not mirror the defects in IFNγ or granzyme B production observed with 25HC treatment in NK cells. Therefore, arguing that LXR activity does not play an inhibitory role in NK cells. However, interestingly, 27HC – another oxysterol which is able to ligate the LXR - inhibited IFNγ and granzyme B production in IL2/IL12-activated NK cells in this study. 27HC however has been reported to inhibit SREBP activation in hepatocytes (Li, Long, et al. 2018). Indeed, work from another member of the Finlay group has recently shown that 27HC can inhibit induction of SREBP-target genes to a similar extent as 25HC (data unpublished).

The finding that SREBP is a key regulator of NK cell function provides further insight into environments where NK cells may be dysfunctional. For instance, NK cells are found to be dysfunctional in numerous settings such as in patients with cancer or chronic infections and in obese individuals. Increased levels of cholesterol or oxysterols are common to all of the above conditions. Therefore, the ability of 25HC and 27HC to inhibit SREBP and thus NK cell function sheds light on a possible mechanism that could contribute to causing NK cell dysfunction.

NK cells play an important role in tumour immunosurveillance and in prevention of cancer growth and metastasis (Lopez-Soto et al. 2017; Morvan and Lanier 2016). Immune evasion is a known hallmark of cancer progression and tumours are known to acquire mechanisms to evade and escape immune responses (Hanahan and Weinberg 2011). Immune cells can be conditioned and curtailed by inhibitory molecules in their environment. Cholesterol levels can be enriched in the tumour microenvironment (TME) (Ma et al. 2019). Furthermore 27HC and 25HC can be secreted by tumours (Raccosta et al. 2013). The enzymes responsible

for the synthesis of 25HC and 27HC from cholesterol: cholesterol-25-hydroxylase (CH25H) and CYP27A1, respectively, can be expressed by cancer cells and thus many cancer cells secrete 25HC and 27HC, into the TME. Early studies investigating the link between cancer growth and increased levels of cholesterol and oxysterols, focused on the direct effects of these metabolites on cancer cells – for example, 25HC and 27HC were shown to directly stimulate the proliferation of ER+ breast cancer cells (Wu et al. 2013). However, it is now emerging that cholesterol and oxysterols in the TME can have suppressive effects on immune responses. Cholesterol has recently been linked to the exhaustion of CD8+ T lymphocytes in the TME through the induction of ER stress (Ma et al. 2019). In a separate study, Raccosta et al identified a mechanism whereby tumour-derived oxysterols can recruit pro-tumour neutrophils into the TME (Raccosta et al. 2013). Another study identified that tumour-derived oxysterols can inhibit the anti-tumour effects of DCs in a murine model, by preventing their migration to lymphoid organs to carry out their antigen presentation functions (Villablanca et al. 2010). Therefore it is plausible that elevated 25HC and 27HC in the TME could be suppressing SREBP activity in NK cells, thus leading to the dysfunctional phenotype observed in NK cells isolated from cancer patients. However, of relevance, CH25H-derived 25HC has been reported to have a beneficial effect in certain settings – 25HC is reported to alter cellular membrane fluidity and thus prevent uptake of tumour-derived extracellular vesicles (Ortiz et al. 2019). An additional complexity comes with the report that lower than average CH25H expression in leukocytes from melanoma patients is correlated with poor disease outcome (Ortiz et al. 2019).

Obesity is another scenario in which NK cells are known to be defective. Obesity is also associated with increased cancer risk (Calle and Kaaks 2004). NK cells are commonly found to be reduced in number and dysfunctional in obese patients (O'Shea et al. 2010; Lynch et al. 2009; Tobin et al. 2017). Furthermore, NK cells isolated from obese mice and humans have substantially reduced cytotoxic abilities (Smith et al. 2007; Michelet et al. 2018). High cholesterol is a co-morbidity associated with obesity (Gostynski et al. 2004; Must et al. 1999). Circulating levels

of 25HC, among other oxysterols, are significantly higher in subjects with metabolic syndrome, compared to age and sex-matched healthy subjects (Tremblay-Franco et al. 2015). As hypocholesteraemia and metabolic syndrome are commonly associated with obesity, obese patients may also have high levels of oxysterols and thus it is possible that the dysfunctional NK cells from these patients may have impaired SREBP activity. Indeed, data from a small cohort of obese patients found SREBP mRNA levels were markedly lower in adipose tissue of obese patients compared to normal weight control subjects (Kolehmainen et al. 2001). Furthermore, NK cells isolated from obese donors express increased cell surface expression of the scavenger receptor involved in lipid uptake - CD36 and take up more exogenous lipid than lean donors (Michelet et al. 2018).

As mentioned in chapter 3, activated NK cells utilise SREBP-dependent lipid synthesis (Assmann et al. 2017). However, when *de novo* lipid synthesis is inhibited in NK cells they can increase in mass and proliferate without impairment, arguing that in response to lipid synthesis inhibition, NK cells meet their requirements for lipid through uptake of exogenous lipid. It would therefore be of interest to determine whether impaired SREBP-activity and thus *de novo* lipid synthesis, contributes to the induction of lipid uptake machinery in NK cells isolated from obese subjects. It would be also interesting to determine whether compromised SREBP activity underlies functional and metabolic defects in NK cells isolated from obese individuals. Cholesterol and oxysterols can be elevated at a whole body level in people with hypercholesterolaemia. Elevated cholesterol and oxysterol levels systemically also promote cancer progression (Nelson et al. 2013; Boyd and McGuire 1990). Levels of 25HC are also commonly elevated in hypercholesteraemic serum (Lappano et al. 2011). It would therefore be of interest to investigate NK cell responses from these cohorts, to determine whether elevated systemic-levels of cholesterol and oxysterols correlate with decreased SREBP activity in circulating NK cells, and whether NK cell metabolism and function are effected in these cells. Depleting or modulating cholesterol levels in patients has been suggested as a strategy to improve T cell-based

immunotherapies (Ma et al. 2019; Yang, Bai, et al. 2016). Excitingly a phase III clinical trial involving over 8,000 patients receiving endocrine therapy for hormone receptor positive breast cancer, found that cholesterol-lowering medication improved the disease-free survival of these patients (Borgquist et al. 2017). The data presented herein would suggest that reducing cholesterol and oxysterol levels may also improve NK cell based immunotherapeutic strategies.

As previously described, CH25H is an enzyme which generates 25HC through the oxidation of cholesterol. Excluding tumour tissue, the expression of CH25H is restricted to a small subset of cells – DCs, macrophages and lymph node epithelial cells (Heng and Painter 2008). CH25H expression and production of 25HC by macrophages and DCs is induced in response to a range of inflammatory stimuli, in a type 1 IFN-dependent manner (Zou et al. 2011; Diczfalusy et al. 2009; Park and Scott 2010; Dennis et al. 2010; Bauman et al. 2009). Peritoneal macrophages, BMDMs and the RAW264.6 macrophage cell line substantially increase *Ch25h* mRNA expression and produce elevated levels of 25HC upon stimulation with 3-deoxy-d-manno-octulosonic acid-lipid A (KLA) – the active component of LPS (Dennis et al. 2010; Bauman et al. 2009). Similarly, LPS stimulation induces enhanced CH25H expression and 25HC production (Diczfalusy et al. 2009). Induction of CH25H expression is not unique to stimulation through TLR4 – selective agonists for TLR2 and TLR3 also induced CH25H expression (Bauman et al. 2009). Furthermore, type 1 IFN also induces CH25h expression(Park and Scott 2010). Increased expression of CH25H mRNA and protein has been shown *in vivo* in mice injected intraperitoneally with TLR ligands (Bauman et al. 2009). Of note, the increased CH25H expression was not restricted to the site of injection and was observed systemically in all tissues measured in the study. The increase in CH25H expression correlated with increased serum levels of 25HC, which was shown to be CH25H dependent (Bauman et al. 2009). Interestingly, the tissues with highest induction of CH25H were those known to harbour resident macrophage populations – for example the liver and the lung. Why innate immune cells might increase CH25H expression and 25HC production in response to type 1 IFN

signalling poses an interesting question. 25HC is described to have a protective role in the prevention of viral entry into cells (Li et al. 2017; Liu et al. 2013). Additionally, although type 1 IFN are best known for their antiviral effects, they are also known to supress immunity to prevent uncontrolled inflammation and bystander damage to the host. One could speculate that 25HC production by macrophages and DCs could also serve to prevent overactivation of NK cells. This may be of particular importance given the important role NK cells have in shaping the adaptive immune response.

In a study where mice were injected intraperitoneally with KLA, CH25H expression was induced at mRNA and protein level. Consistent with this, serum levels of 25HC were increased as was 25HC abundance in the lungs – thus highlighting a systemic effect (Bauman et al. 2009). Furthermore, humans injected with LPS increase serum levels of 25HC (Diczfalusy et al. 2009). Therefore 25HC production by macrophages may provide a mechanism to allow both local and systemic regulation of NK cell immune responses *in vivo,* to prevent exaggerated responses. This idea is supported by the finding that $CH25H^{KO}$ mice are more susceptible to septic shock and have worsened symptoms of the mouse model of multiple sclerosis (MS) - experimental autoimmune encephalomyelitis (EAE) (Reboldi et al. 2014). This study showed that activated macrophages isolated from $CH25H^{KO}$ mice overproduce IL1β. Individuals with relapsing-remitting stage of MS were also shown to have a reduction in serum 25HC compared to control patients (Crick et al. 2017). Taken together, these data suggest that a physiological role for 25HC production by the immune system *in vivo* may be to modulate and prevent the induction of an over-activated immune response. The fact that NK cell functions are so dramatically impaired in the presence of 25HC would suggest that NK cell function may be regulated by macrophages and dendritic cells in this manner.
Considered together, the results described in this chapter identify SREBP transcription factors as key regulators of NK cell function. Thus, identifying oxysterols and cholesterol – which inhibit SREBP activation – as physiological modulators of NK cell activity.

5 Polyamine synthesis and hypusination are required for NK cell metabolic and functional responses

5.1 Introduction

Polyamine synthesis is an ancillary metabolic pathway which uses the amino acid ornithine, to generate putrescine, spermidine and spermine – the three naturally occurring polyamines. Polyamines are ubiquitously found in eukaryotes and have a range of reported functions – mostly linked to cellular growth and proliferation. Polyamine synthesis is a tightly regulated process and depends on the rate-limiting enzyme, ornithine decarboxylase (ODC). The majority of polyamine research to date has been in the cancer field and a role for polyamines in NK cells has not yet been extensively explored.

The data presented in chapters three and four highlighted a novel role for SREBP transcription factors in facilitating NK cell metabolism and robust NK cell effector function in response to cytokine-stimulation. The importance of SREBP activity was independent of the classical role played by SREBP transcription factors in the control of lipid synthesis. In fact, lipid synthesis has been shown by others in our group, to be dispensable for NK cell metabolism and effector functions in cytokine-activated NK cells (Assmann et al. 2017). SREBP-activity was required for the expression of ACLY and SLC25A1 – two essential components of the Citrate Malate Shuttle (CMS) – the key metabolic circuit used by cytokine activated NK cells. Despite this, we questioned whether the dramatic functional and metabolic defects observed when SREBP activity was inhibited in NK cells was solely due to its impact on the CMS. NK cells still utilise the TCA cycle – do NK cells not have the plasticity to increase flux through the TCA cycle to supply the reducing equivalents for OxPhos when the CMS was inhibited? This observation led us to investigate whether SREBP was required for any further unexpected processes in NK cells which could contribute to the dramatic decrease in metabolism and function when SREBP was inhibited .

5.2 SREBP activity is required for polyamine synthesis in NK cells

To address whether SREBP activity may be influencing another pathway in cytokine-activated NK cells, metabolomic analysis was carried out. For these experiments cultured NK cells were left unstimulated or were activated for 18 hours with IL2/IL12 in the presence or absence of 25HC, to inhibit SREBP activation. Metabolites were then analysed by liquid chromatography–tandem mass spectrometry (LC-MS/MS) as previously described (Stevens et al. 2010). Quantification of metabolites revealed that upon stimulation, an increase in the levels of all three naturally occurring polyamines (putrescine, spermidine and spermine) was observed (**Fig 5.1 a-c** – data for this figure was generated by Dr Nadine Assmann, in collaboration with the University of Regensberg). The abundance of ornithine – the amino acid precursor used for polyamine synthesis, was also increased in NK cells upon cytokine stimulation (**Fig 5.1 d)**. Surprisingly, preventing SREBP activation with 25HC during stimulation altered abundance of polyamines. Of note, 25HC-treatment resulted in a significant decrease in the amount of the polyamine putrescine in NK cells (**Fig 5.1a**), whilst there was no significant change in the levels of spermidine or spermine (**Fig 5.1 b-c**). This pattern in the three polyamine species is consistent with what is observed in other cell types when *de novo* polyamine synthesis is inhibited by directly blocking activity of ornithine decarboxylase (ODC) – the initial and rate-limiting enzyme of the polyamine biosynthesis pathway (Levin et al. 1992; Poso and Pegg 1982; Mamont et al. 1978) (**Fig 5.2**). 25HC-treatment caused no depletion in the abundance of ornithine in NK cells, indicating that SREBP activity was not necessary for generation of the precursor necessary to support production of polyamines (**Fig 5.1d**). Therefore, it was considered that, SREBP transcription factors may be controlling *de novo* polyamine synthesis in cytokine-activated NK cells.

At this point the role of *de novo* polyamine synthesis in activated NK cells was unknown. To confirm that IL2/IL12-stimulated NK cells express the polyamine synthesis machinery, the previously generated, Finlay lab quantitative proteomics

dataset of IL2/IL12-activated NK cells was consulted (described in chapter 3). The first step of polyamine synthesis is catalysed by ODC, which forms the diamine: putrescine from ornithine. Putrescine can be further metabolised into spermidine and then spermine via addition of amine groups by the enzymes spermidine synthase (SRM) and spermine synthase (SMS), respectively (**Fig 5.2).** Proteomics data revealed that all three enzymes involved in *de nov*o polyamine synthesis were expressed in IL2/IL12-stimulated NK cells (**Fig 5.3**).

To investigate whether SREBP activity was required for expression of any of these enzymes, SREBP activity was inhibited with either 25HC or PF429242 for 18 hours mRNA transcript levels of *Odc*, *Srm* and *Sms* were measured by RT-qPCR. In-line with my hypothesis, mRNA levels of the gene encoding ODC was reduced when SREBP activity was inhibited (**Fig 5.4a**). The expression data for Srm and Sms mRNA following 25HC or PF429242 treatment was more variable and did not convincingly support a role for SREBP in the control of these genes. Taken together, these data argue that *de novo* polyamine synthesis is used by IL2/IL12-activated NK cells and controlled by SREBP transcription factors.

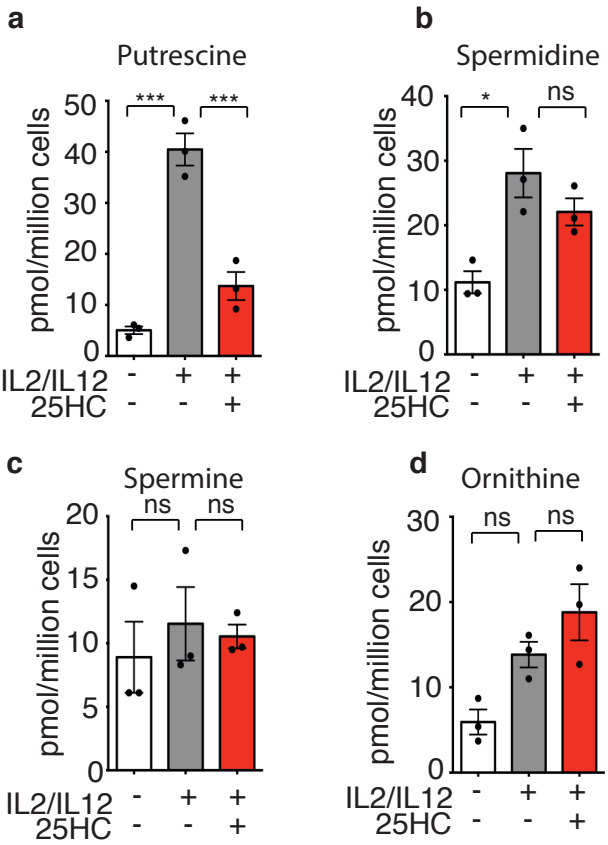

Figure 5.1 Increased polyamine synthesis with IL2/IL12 stimulation is influenced by SREBP activity

Cultured NK cells were purified and left unstimulated or stimulated with IL2 (20ng/ml) + IL12 (10ng/ml) for 18h in the presence or absence of 25HC (2.5 μM). Metabolites were then extracted and quantified by LC-MS/MS. Data is mean +/- S.E.M of 3 separate experiments. Statistical analysis was performed using a one-way ANOVA with Tukey's post-test (ns=non-significant, *p<0.05, ***p<0.001).(*This dataset was generated by Dr Nadine Assmann in collaboration with the University of Regensburg*)

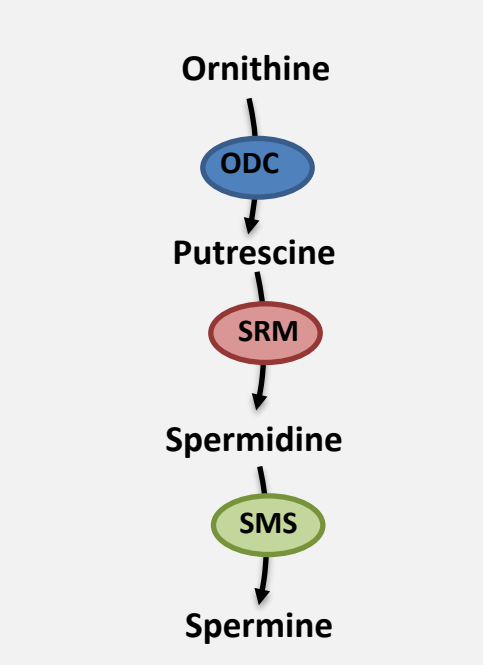

Figure 5.2 Schematic of the polyamine synthesis pathway

The amino acid, ornithine, is the precursor to polyamine synthesis. The first step of polyamine synthesis is catalysed by the rate-limiting enzyme ODC, which catalyses the formation of the diamine putrescine from ornithine. Putrescine can then be further metabolised into spermidine through the addition of an amine group by the next enzyme in the pathway, SRM. Spermidine can be further metabolised into the tetraamine, spermine via addition of an amine group by SMS.

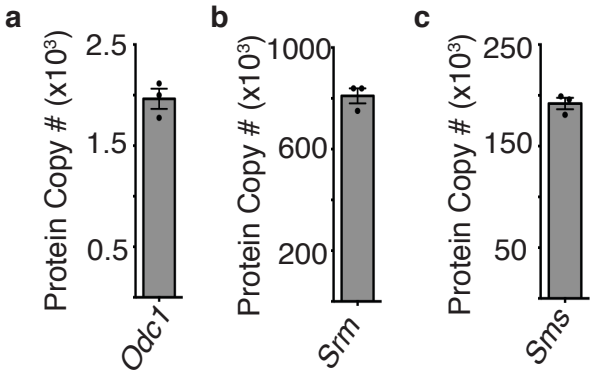

Figure 5.3 IL2/IL12 activated NK cells express enzymes of the *de novo* polyamine synthesis pathway

Cultured NK cells were activated with IL2 (20ng/ml) + IL12 (10ng /ml) for 18h. Cells were lysed and copy numbers of the proteins encoded by *Odc1*, *Srm* and *Sms* were determined using quantitative proteomic analysis. Data is mean +/- S.E.M of 3 separate experiments. (*Proteomic dataset was generated by the University of Dundee on samples provided by Dr Nadine Assmann*)

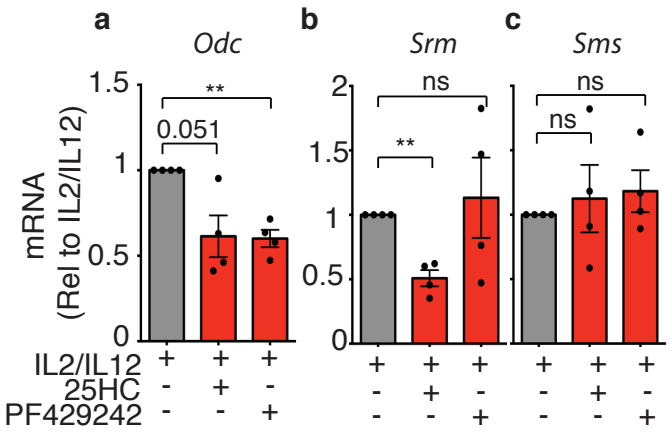

Figure 5.4 SREBP activity is required for expression of enzymes involved in the polyamine synthesis pathway

Cultured NK cells were activated with IL2 (20ng/ml) + IL12 (10ng /ml) for 18 h in the presence or absence of 25HC (2.5μm) or PF429242 (10μm) and the cells lysed and analysed by qRT-PCR for mRNA encoding ODC1, SRM and SMS. Data is normalised to levels of control gene *Rplp0* and presented relative to mRNA expression in IL2/IL12-stimulated NK cells. Data is mean +/- S.E.M of 4 independent experiments. Statistical analysis was performed using a one sample t-test versus a theoretical value of 1 (ns=non-significant, **p<0.01).

5.3 *De novo* polyamine synthesis is required for NK cell growth and proliferation

Having identified that SREBP transcription factors may control *de novo* polyamine synthesis in IL2/IL12-activated NK cell cells, the importance of polyamine biosynthesis for NK cell responses was further investigated. Due to their structural characteristics (they are small and positively charged), polyamines can interact with many important biological molecules including nucleic acids, phospholipids and proteins. Therefore polyamines have the means to affect a multitude of different cellular processes. Despite this, the functional and mechanistic consequences of many of these interactions remain poorly defined. Cellular growth and proliferation are two of the most-well described processes that have been shown to require polyamines. Data provided in chapter three identified that SREBP activity is essential for NK cell growth and proliferation in response to IL2/12-stimulation. Experiments in this chapter suggest that SREBP activation is required for polyamine synthesis in NK cells. Therefore, I questioned whether the reduced growth and proliferation observed when SREBP activity was inhibited were, at least in part, due to depletion of polyamines.

To dissect out the role of polyamine synthesis in the control of cellular growth and proliferation, the inhibitor - 2-difluoromethylornithine (DFMO) was used to irreversibly inhibit ODC – the rate-limiting enzyme of *de novo* polyamine synthesis (Poulin et al. 1992) (**Fig 5.5**). As described in chapter 3, IL2/IL12-stimulation triggers NK cell blastogenesis and proliferation. However, when polyamine synthesis was inhibited with DFMO, NK cells exhibited a significant reduction in cell growth (**Fig 5.6**). Proliferation was also impaired when NK cells were stimulated in the presence of DFMO, as measured by reduced CFSE dilution 48 hours post-stimulation (**Fig 5.7**). To confirm the importance of polyamines for NK cell growth and proliferation we undertook an additional approach. Polyamines can be interconverted or degraded via catabolic pathways, which can lead to polyamine depletion from the cell. In order to address whether polyamine depletion, through induction of their catabolism, could affect NK cell growth and

proliferation, we made use of the spermine analogue – diethylnorspermine (DENSPM). DENSPM is known to induce the polyamine catabolising enzymes – spermidine/spermine-N(1)-acetyltransferase (SSAT) and spermine oxidase (SMO), thus DENSPM can be used as an alternate pharmacological tool for the depletion of polyamines through a distinct mechanism (**Fig 5.5)** (Fogel-Petrovic et al. 1997; Stanic et al. 2009).

Interestingly, IL2/IL12-stimulation of NK cells in the presence of DENSPM had no effect on NK cell size at 24 hours (**Fig 5.8**). However stimulation in the presence of DENSPM did significantly reduce NK cell proliferation (**Fig 5.9**). Although in these experiments the difference in the frequency of cells proliferating was minor, there was a clear reduction in the dilution of CFSE by the cells that did proliferate, suggesting that they can expand, albeit at a slower rate (**Fig 5.9).** Progressing from these experiments, the viability of NK cells following IL2/IL12-stimulation in the presence of either DFMO or DENSPM was assessed by flow cytometry following Live/Dead staining. No reduction in NK cell viability was observed when cells were treated with either DFMO or DENSPM up to 48 hours post-stimulation (**Fig 5.10**). Taken together, this data identifies an important role for polyamines for NK cell growth and proliferative responses, without being required for viability.

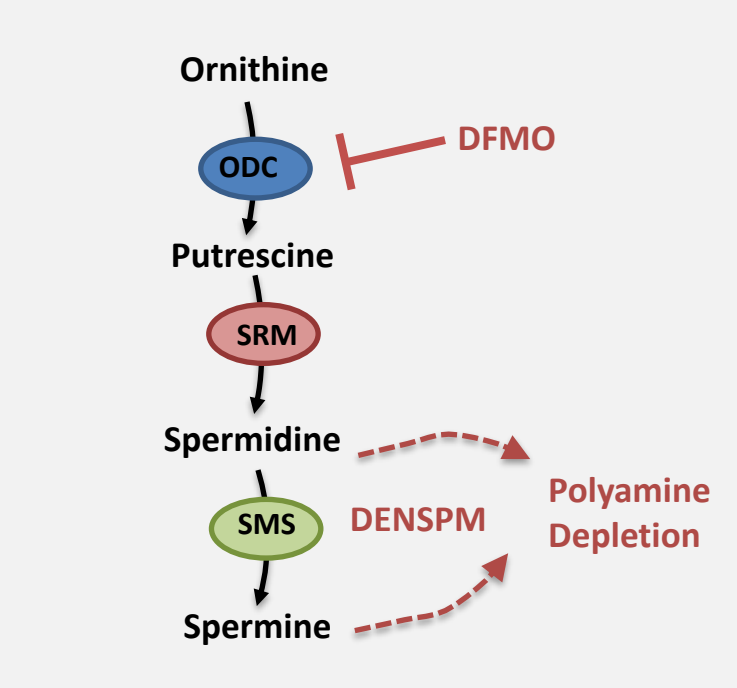

Figure 5.5 Schematic of pharmacological tools used to inhibit polyamine synthesis

(**a**) DFMO is a highly specific and an irreversible inhibitor of ODC, the rate-limiting enzyme in the de novo polyamine biosynthesis pathway. ODC catalyses the decarboxylation of amino acid ornithine to diamine putrescine.

(**b)** The spermine analogue DENSPM, induces polyamine catabolism through SSAT and SAO induction (not shown). SSAT and SAO are two-enzymes involved in the catabolism of spermine and/or spermidine and induction of these enzymes by DENSPM can lead to polyamine depletion from the cell.

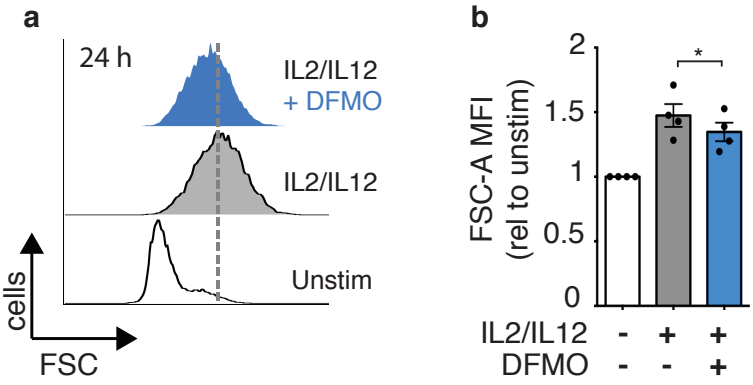

Figure 5.6 *De novo* polyamine synthesis is important for IL2/IL12 induced NK cell growth

NK cells were cultured for 3 days, then CFSE-stained and left unstimulated (white bar) or stimulated with IL2 (20ng/ml) + IL12 (10ng/ml), for 24 h in the presence (blue bar) or absence (grey bar) of DFMO (1mM). Cells were analysed by flow cytometry for FSC-A as a readout of size. Data is representative (**a**) or mean +/- S.E.M (**b**) of 4 independent experiments. Statistical analysis was performed using a paired two-tailed t-test (*p<0.05).

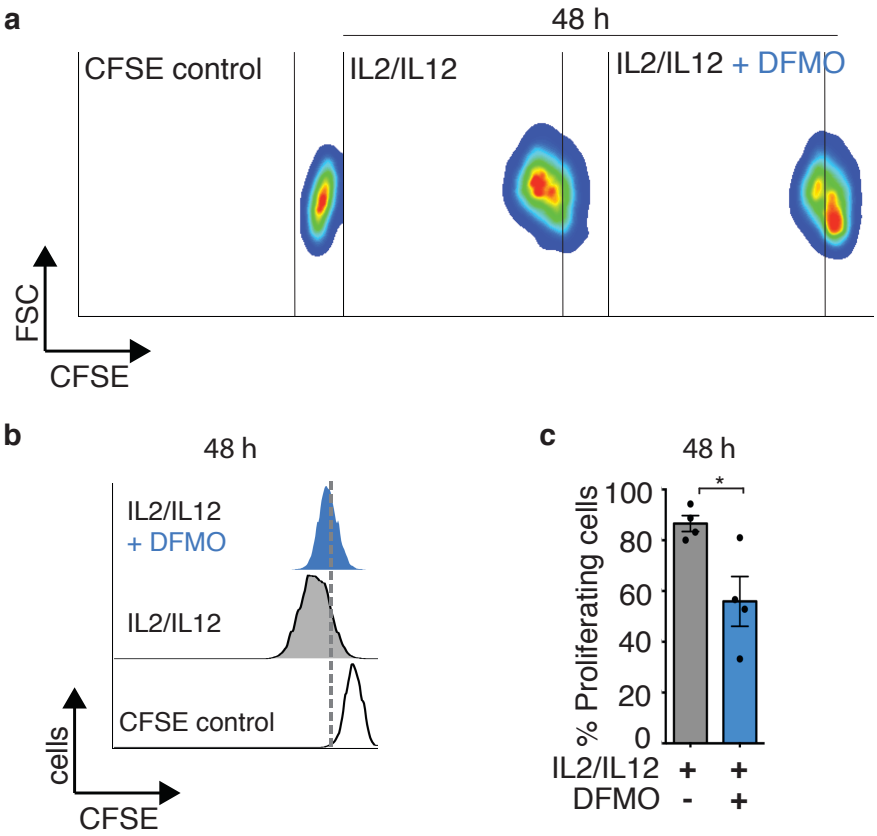

Figure 5.7 *De novo* polyamine synthesis is important for IL2/IL12 induced NK proliferation

NK cells were cultured for 3 days, then CFSE-stained and stimulated with IL2 (20ng/ml) + IL12 (10ng/ml) for 48 h in the presence (blue bar) or absence (grey bar) of DFMO (1mM). Cells were analysed by flow cytometry for CFSE-dilution as a readout of proliferation. Data is representative (**a,b**) or mean +/- S.E.M (**c**) of 4 independent experiments. Statistical analysis was performed using a paired two-tailed t-test (*p<0.05).

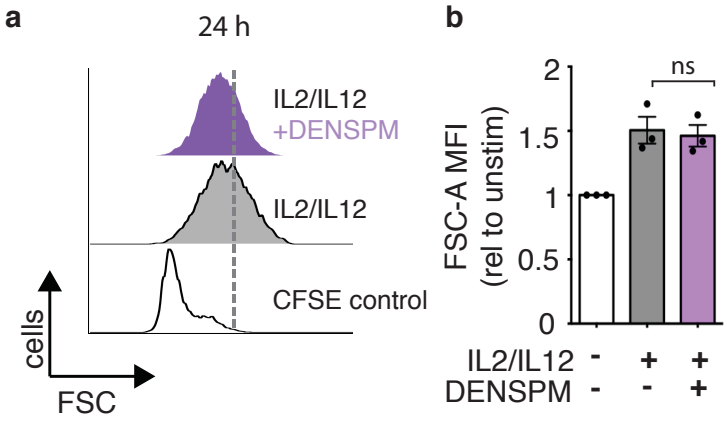

Figure 5.8 Induction of polyamine catabolism has no significant effect on IL2/IL12-induced NK cell growth

NK cells were cultured for 3 days, then CFSE-stained and left unstimulated (white bar) or stimulated with IL2 (20ng/ml) + IL12 (10ng/ml), for 24 h in the presence (purple bar) or absence (grey bar) of DENSPM (10μM). Cells were analysed by flow cytometry for FSC-A as a readout of size. Data is representative (**a**) or mean +/- S.E.M (**b**) of 3 independent experiments. Statistical analysis was performed using a paired two-tailed t-test (ns=non-significant).

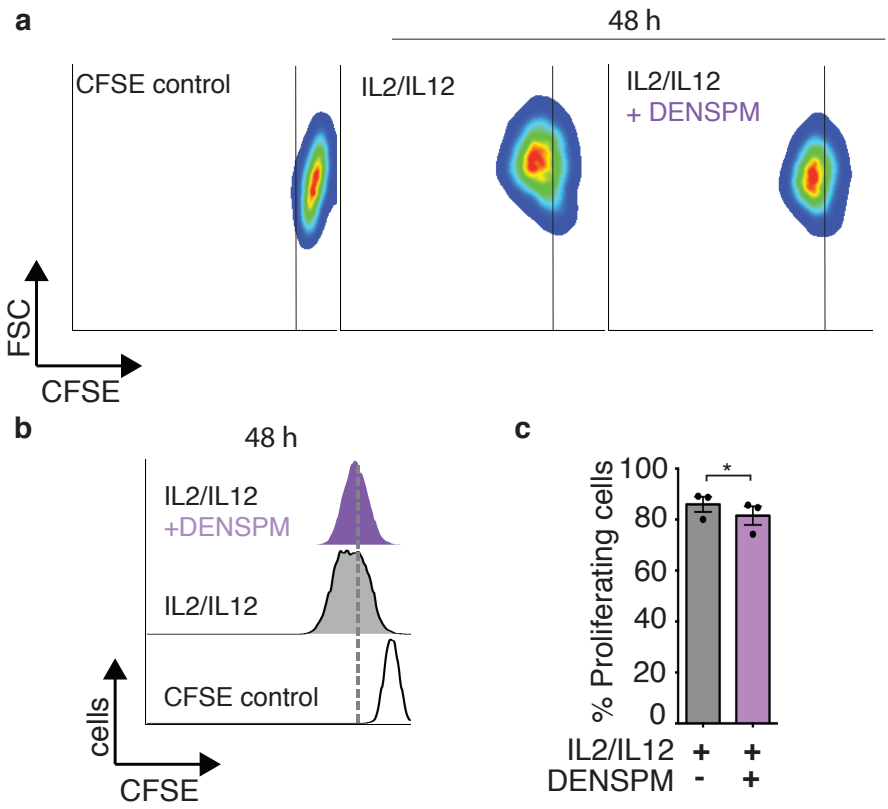

Figure 5.9 Inducing polyamine catabolism impairs IL2/IL12-induced NK proliferation

NK cells were cultured for 3 days, then CFSE-stained and stimulated with IL2 (20ng/ml) + IL12 (10ng/ml) for 48 h in the presence (purple bar) or absence (grey bar) of DENSPM (10μM). Cells were analysed by flow cytometry for CFSE-dilution as a readout of proliferation. Data is representative (**a,b**) or mean +/- S.E.M (**c**) of 3 independent experiments. Statistical analysis was performed using a paired two-tailed t-test (*p<0.05).

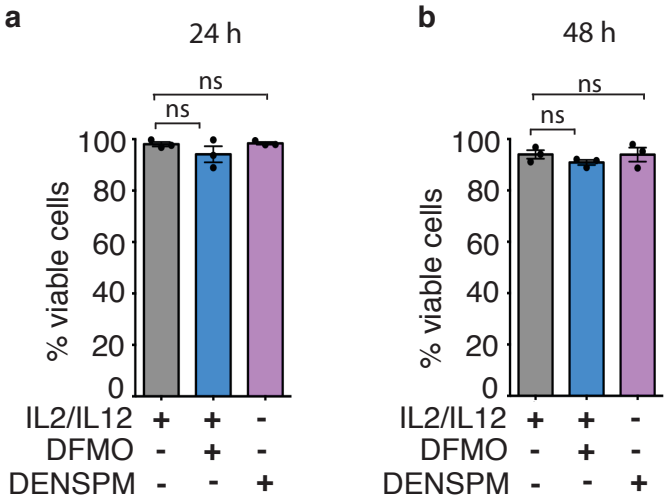

Figure 5.10 Perturbation of the polyamine synthesis pathways does not affect viability of IL2/IL12-stimulated NK cells

NK cells were cultured for 3 days, then CFSE-stained and stimulated with IL2 (20ng/ml) + IL12 (10ng/ml) for 24 h (**a**) or 48 h (**b**) in the presence or absence (grey bar) of DFMO (1mM) (blue bar) or DENSPM (10μM)(purple bar). NK cell viability was analysed by flow-cytometry following Live/Dead staining. Data is mean +/- S.E.M of 3 independent experiments. Statistical analysis was performed using a one-way ANOVA with Tukey's post-test (ns = non-significant).

5.4 De novo polyamine synthesis is required for NK cell metabolism and function

Data presented in chapter 3 demonstrated that defects in growth and proliferation can result from inhibition of glycolysis or OxPhos. As this chapter identified that polyamines are essential for NK cell growth and proliferation, I hypothesised that polyamines may be important for NK cell metabolism. Whether polyamine biosynthesis was required for NK cell metabolism in response to IL2/IL12 stimulation was therefore investigated via seahorse extracellular flux analysis. NK cells that were activated for 18 hours in the presence of DFMO displayed significantly impaired glycolysis and glycolytic capacity compared to control IL2/IL12-stimulated NK cells (**Fig 5.11**). Similarly, basal OxPhos was also impaired in DFMO-treated NK cells, with a trend toward reduced respiratory capacity also being observed (**Fig 5.12**). ECAR and OCR rates were also measured when NK cells were activated in the presence of DENSPM and a similar reduction in energy profile was observed (**Fig 5.13**).

As NK cell metabolism and effector function are integrally linked, upon uncovering that polyamines were required for NK cell metabolism, it was hypothesised that polyamines may be important for NK cell effector responses. Indeed, blocking *de novo* polyamine synthesis with DFMO, impaired IFNγ and granzyme B production in IL2/IL12-stimulated NK cells, as measured by flow cytometry (**Fig5.14**). Similarly, stimulation of NK cells in the presence of DENSPM, in order to reduce polyamine levels, also resulted in impaired IFNγ and granzyme B production after 18 hours (**Fig 5.14**). Collectively, these data demonstrate that *de novo* polyamine synthesis is important for NK cell metabolic and functional responses to IL2/IL12-stimulation.

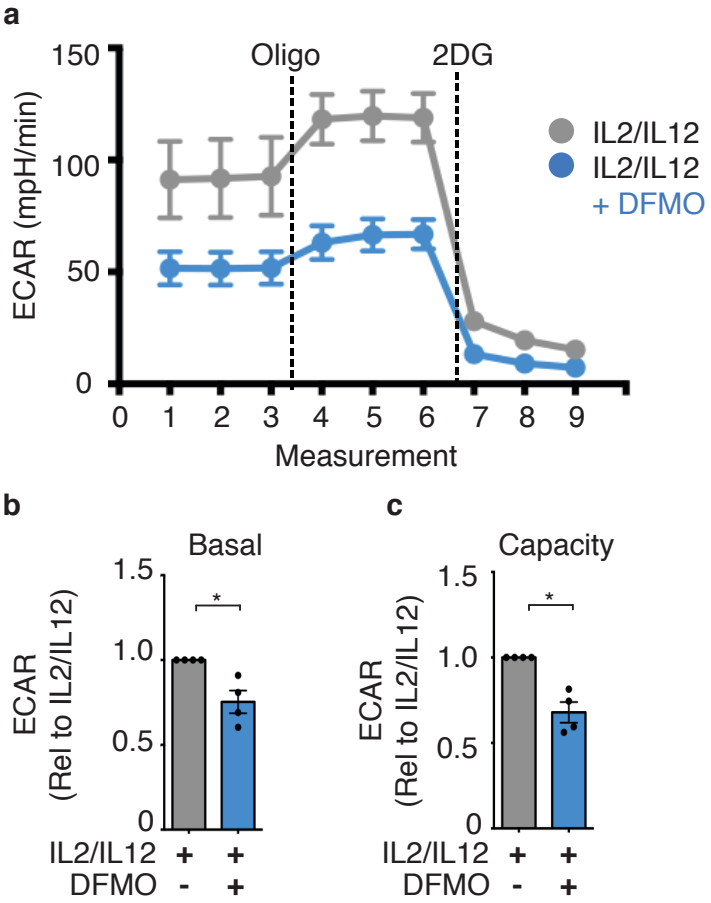

Figure 5.11 *De novo* polyamine synthesis is required for NK cell glycolysis

Cultured NK cells were purified and stimulated with IL2 (20ng/ml) + IL12 (10ng/ml) for 18h in the presence (blue) or absence (grey) of DFMO (1mM).Extracellular acidification rate (ECAR) was measured as a readout of glycolysis. Representative trace (**a**) and pooled measurements are shown for basal glycolytic rate (**b**) and glycolytic capacity (**c**). Pooled data is presented relative to ECAR levels in IL2/IL12-stimulated NK cells. Data is representative (**a**) or mean +/- S.E.M (**b,c**) of 4 independent experiments. Statistical analysis was performed using a two-tailed one sample t-test versus a theoretical value of 1 (* $p<0.05$).

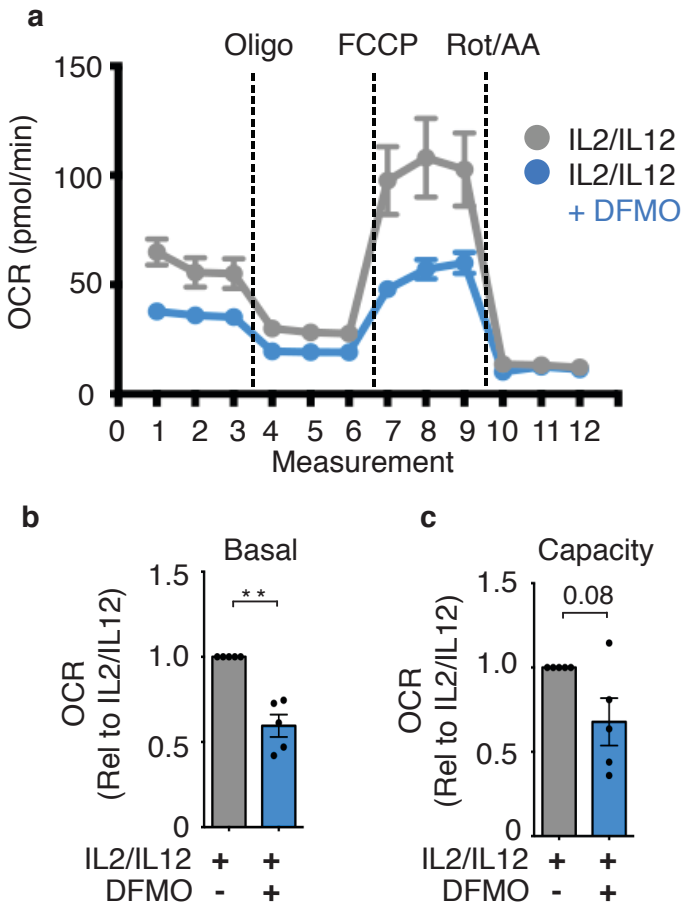

Figure 5.12 *De novo* polyamine synthesis is required for NK cell Oxphos

Cultured NK cells were purified and stimulated with IL2 (20ng/ml) + IL12 (10ng/ml) for 18h in the presence or absence of DFMO (1mM). Oxygen consumption rate (OCR) was measured as a readout of OxPhos. Representative trace (**a**) and pooled measurements are shown for basal OxPhos (**b**) and respiratory capacity (**c**). Data is representative (**a**) or mean +/- S.E.M (**b,c**) of 4 independent experiments. Pooled data is presented relative to OCR levels in IL2/IL12-stimulated NK cells. Statistical analysis was performed using a two-tailed one sample t-test versus a theoretical value of 1 (** $p<0.01$).

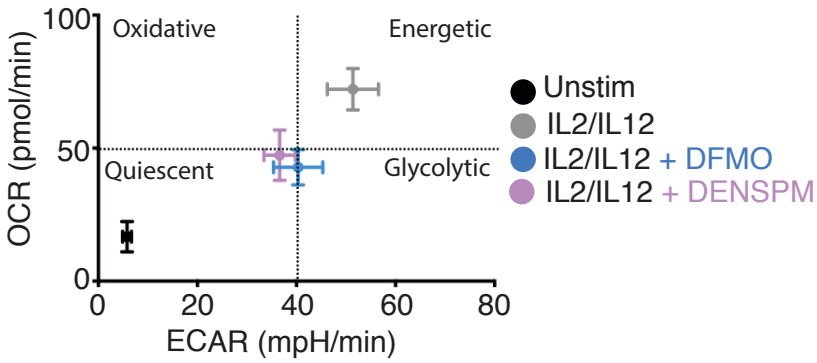

Figure 5.13 Perturbation of *de novo* synthesis levels wither either DFMO or DENSPM, impairs both OCR and ECAR levels in IL2/IL12-activated NK cells

Cultured NK cells were purified and left unstimulated or stimulated with IL2 (20ng/ml) + IL12 (10ng /ml), for 18 h in the presence or absence of DFMO (1 mM) or DENSPM (10μM). OCR was measured as a readout of OxPhos and ECAR was measured as a readout of glycolysis. Data is presented on an energy map of ECAR versus OCR rates and is mean +/- S.E.M of 5 independent experiments.

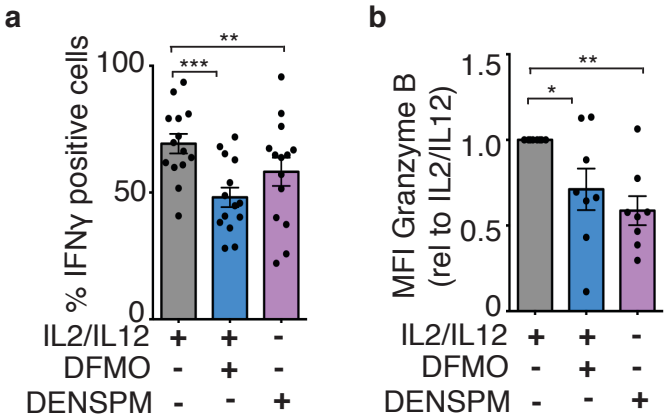

Figure 5.14 Interfering with the polyamine content of IL2/IL12-stimulated NK cells impairs IFNγ and granzyme B expression

Cultured NK cells were stimulated with IL2 (20ng/ml) + IL12 (10ng /ml), for 18 h in the presence or absence of DFMO (1 μM) or DENSPM (10μM). NK cells were intracellularly stained for IFNγ and granzyme B and analysed by flow cytometry. Data is mean +/- S.E.M of 14 (**a**) or 8 (**b**) independent experiments. Statistical analysis was performed using a one-way ANOVA with Tukey's post-test (**a)** or paired two-tailed t-test against a theoretical value of 1 (**b)** (*p<0.05, ,**p<0.01,***p<0.001)

5.5 Hypusination is important for growth and proliferation of NK cells

Having identified that polyamines were important for NK cell proliferation, metabolism and function, I questioned how they were controlling these processes. As previously mentioned, low-molecular weight, positively charged polyamines can interact with a number of molecules in the cell and are reported to influence a range of cellular processes. For instance polyamines are involved in processes including chromatin stabilisation, ion channel regulation, autophagy, and protection from oxidative stress. Additionally, the polyamine spermidine, is necessary for a unique post-translational modification known as hypusination. The only known example of hypusination occurs at a lysine residue on eukaryotic initiation factor 5A (eIF5A) (Park, Cooper, and Folk 1981). eIF5A was first thought to have a role in translation initiation, but since been assigned roles in translation elongation and termination, with its role in the translation of mRNAs being sequence-specific (Schuller et al. 2017; Gutierrez et al. 2013; Kang and Hershey 1994). Notably , expression of hypusinated eIF5A (eIF5A^{H}) has been linked to growth and proliferation (Preukschas et al. 2012; Epis et al. 2012). As SREBP activity and polyamine synthesis were essential for IL2/IL12-induced NK cell growth and proliferation, I considered that hypusination may also be important for these processes.

Upon interrogation of the Finlay lab quantitative proteomics dataset (generated by Nadine Assmann, as previously described in chapter 3) it was identified that indeed, IL2/IL12-activated NK cells express substantial protein copy numbers of eIF5A and both of the specialised enzymes involved in hypusine formation - deoxyhypusine synthase (Dhps) and deoxyhypusine hydroxylase (Dohh) (**Fig 5.15**). Hypusination formation occurs via the sequential actions of Dhps and Dohh. Dhps catalyses the transfer of the 4-aminobutyl moiety from the polyamine spermidine to a specific lysine residue on eIF5A. This reaction forms deoxyhypusinated eIF5a, which is then hydroxylated by Dohh to generate hypusinated eIF5A (**Fig 5.16**). We identified whether expression of *Dhps* at mRNA level was SREBP dependent.

SREBP activity was inhibited with either 25HC or PF429242 for 18 hours and analysis of mRNA transcript levels of the gene encoding DHPS measured by RT-qPCR. mRNA levels of the gene were substantially reduced when NK cells were activated in the presence of 25HC, and there was also a trend towards reduced Dhps mRNA in PF429242 treated NK cells (**Fig 5.17**). This provided an unexpected link between SREBP activity and hypusination.

Leading on from this, whether hypusination was required for NK cell responses was investigated. For these experiments, NK cells were cultured for three days, then CFSE-stained and activated in the presence or absence of different doses of the specific DHPS inhibitor – N1-guanyl-1,7-diaminoheptane (GC7). Inhibiting hypusination with GC7 significantly reduced growth and proliferation by IL2/IL12-activated NK cells (**Fig 5.18-5.19**). To further assess the role of hypusination in NK cell responses, we assessed NK cell viability when the hypusination machinery was inhibited with GC7. Of note, no significant reduction in NK cell viability was observed at either 24 hours or 48 hours post-stimulation (**Fig 5.20**). In order to further validate these results, another inhibitor of hypusination was used - ciclopirox (CPX). CPX has been described to inhibit DOHH -the second enzyme in the hypusination process (Clement et al. 2002). Proliferation was reduced when NK cells were activated in the presence of CPX (**Fig 5.21**) However, in contrast to the experiments with GC7, the viability of NK cells activated in the presence of CPX was dramatically reduced after 48 hours (**Fig 5.22**). Therefore, the DHPS inhibitor – GC7 was used to inhibit hypusination of eIF5A in subsequent experiments.

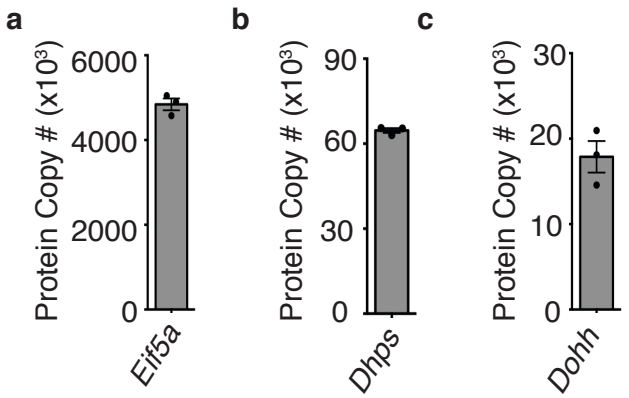

Figure 5.15 IL2/IL12-activated NK cells express eIF5a & hypusination enzymes

Cultured NK cells were activated with IL2 (20ng/ml) + IL12 (10ng /ml) for 18 h and copy number per cell of the proteins encoded by *Eif5a*, *Dhps* and, *Dohh*, determined using quantitative proteomic analysis. Data is mean +/- S.E.M of 3 independent experiments. (*Proteomic dataset was generated by the University of Dundee on samples provided by Dr Nadine Assmann*)

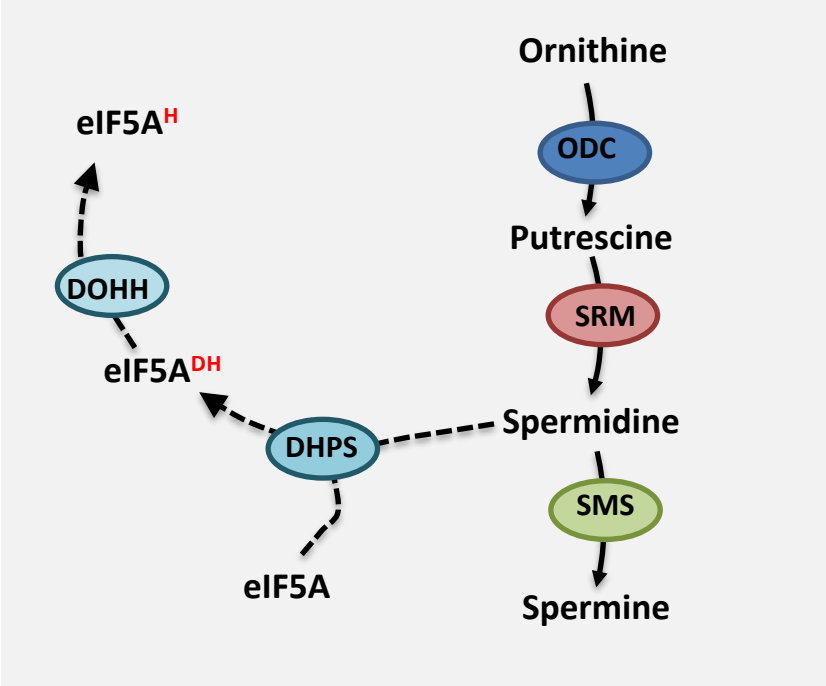

Figure 5.16 Spermidine is the substrate for hypusination of eIF5A

Hypusination formation occurs via the sequential actions of the enzymes DHPP and DOHH. DHPS catalyses the transfer of the 4-aminobutyl moiety from the polyamine spermidine to a specific lysine residue on eIF5A. This reaction forms deoxyhypusinated eIF5a ($eIF5A^{DH}$). $eIF5A^{DH}$ is then hydroxylated by DOHH to generate hypusinated eIF5A ($eIF5A^{H}$).

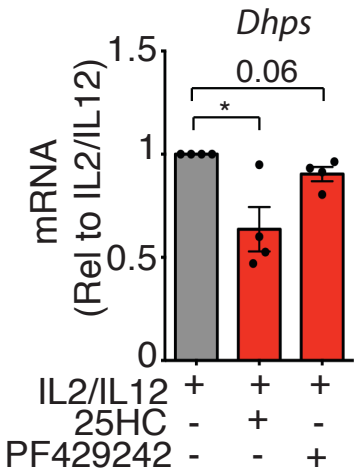

Figure 5.17 SREBP activity influences *Dhps* expression

Cultured NK cells were activated with IL2 (20ng/ml) + IL12 (10ng /ml) for 18 h in the presence or absence of 25HC (2.5μm) or PF429242 (10μm) and the cells lysed and analysed by qRT-PCR for mRNA encoding DHPS. Data is normalised to levels of control gene *Rplp0* and presented relative to mRNA expression in IL2/IL12-stimulated NK cells. Data is mean +/- S.E.M of 4 independent experiments. Statistical analysis was performed using a column statistics versus a theoretical value of 1 (ns=non-significant, *p<0.01).

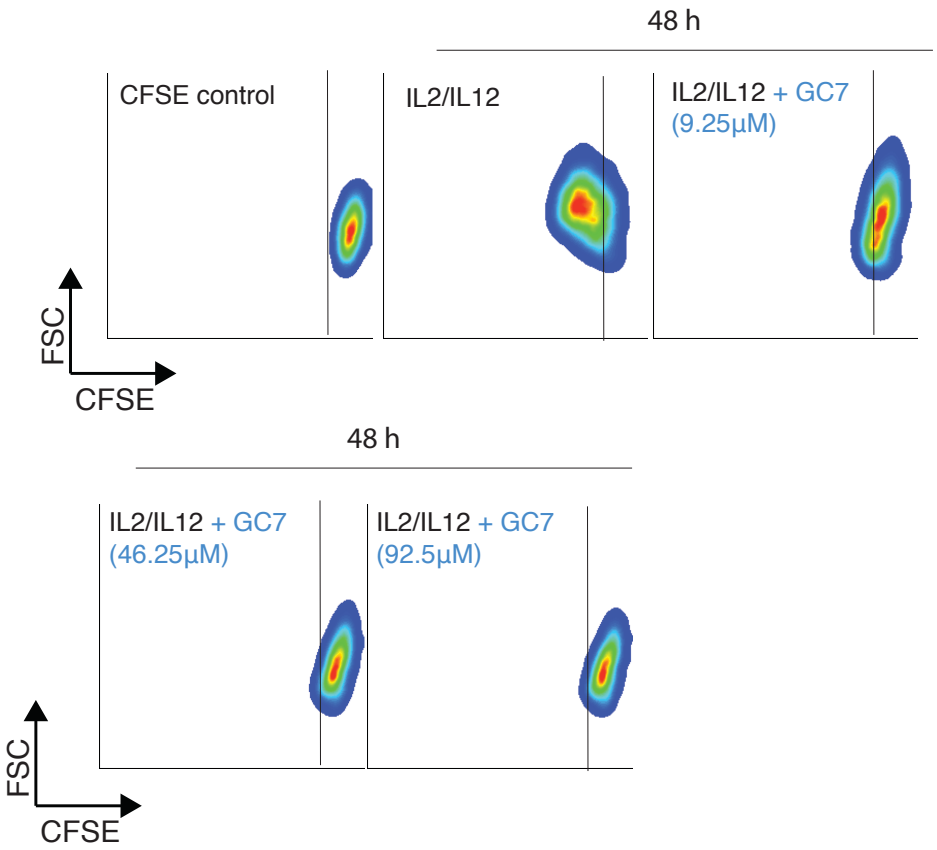

Figure 5.18 Hypusination is important for growth and proliferation of IL2/IL12-activated NK cells

NK cells were cultured for 3 days, then CFSE-stained and stimulated with IL2 (20ng/ml) + IL12 (10ng/ml) for 48 h in the presence or absence of varying doses (9.25µM,46.25µM or 92.5µM) of the hypusination inhibitor, GC7. Cells were analysed by flow cytometry for CFSE-dilution as a readout of proliferation and FSC as a readout of cell growth. Data is representative of 3 experiments.

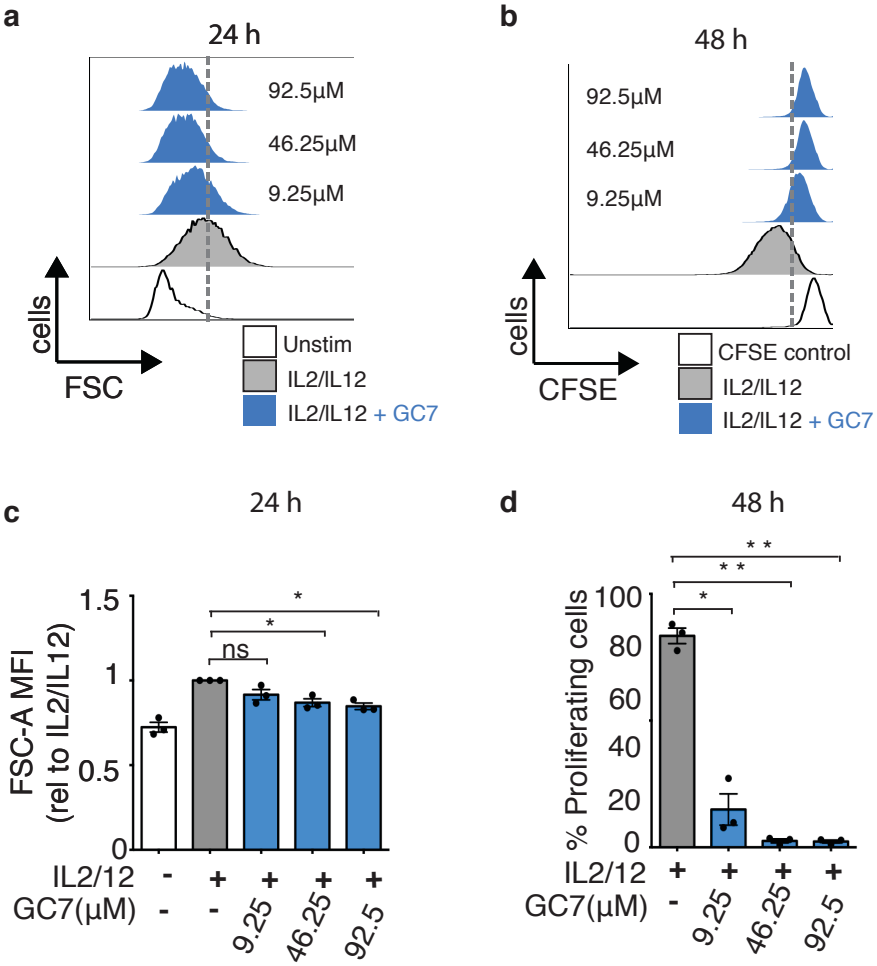

Figure 5.19 Hypusination is important for IL2/IL12-induced NK cell growth and proliferation

NK cells were cultured for 3 days, then CFSE-stained and stimulated with IL2 (20ng/ml) + IL12 (10ng/ml) for 24 h or 48 h in the presence or absence of varying doses of the hypusination inhibitor GC7 (9.25µM,46.25µM or 92.5µM). NK cells were analysed by flow cytometry for FSC-A (**a,c)** as a readout of size or CFSE-dilution (**b,d)** as a measure of proliferation. Data is representative or mean +/- S.E.M of 3 independent experiments. Statistical analysis was performed using column statistics versus a theoretical value of 1(**c**) or a one-way ANOVA with Tukey's post-test (**d)** (ns=non-significant, *p<0.01, **p<0.01).

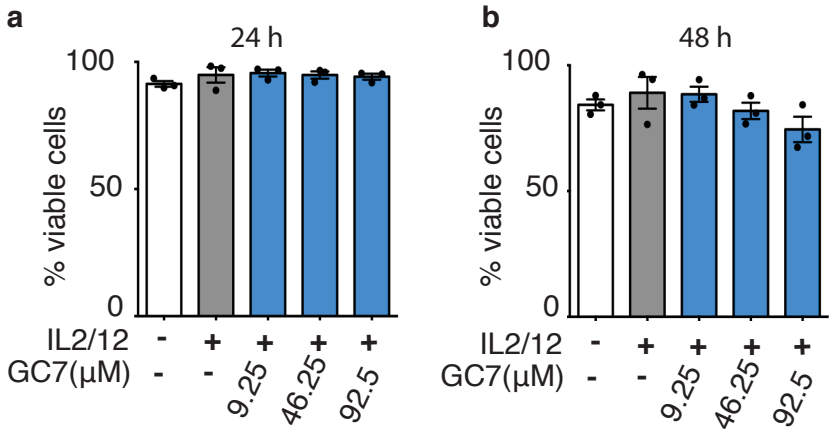

Figure 5.20 GC7 does not significantly reduce viability of IL2/IL12-activated NK cells at 24h or 48h

NK cells were cultured for 3 days, then CFSE-stained and stimulated with IL2 (20ng/ml) + IL12 (10ng/ml) for 24 h or 48 h in the presence or absence of varying doses of the hypusination inhibitor GC7 (9.25μM,46.25μM or 92.5μM). NK cells were live/dead stained and analysed by flow cytometry to assess cell-viability. Data is representative or mean +/- S.E.M of 3 independent experiments. Statistical analysis was performed using a one-way ANOVA with Tukey's post-test. (no significant differences were observed between values).

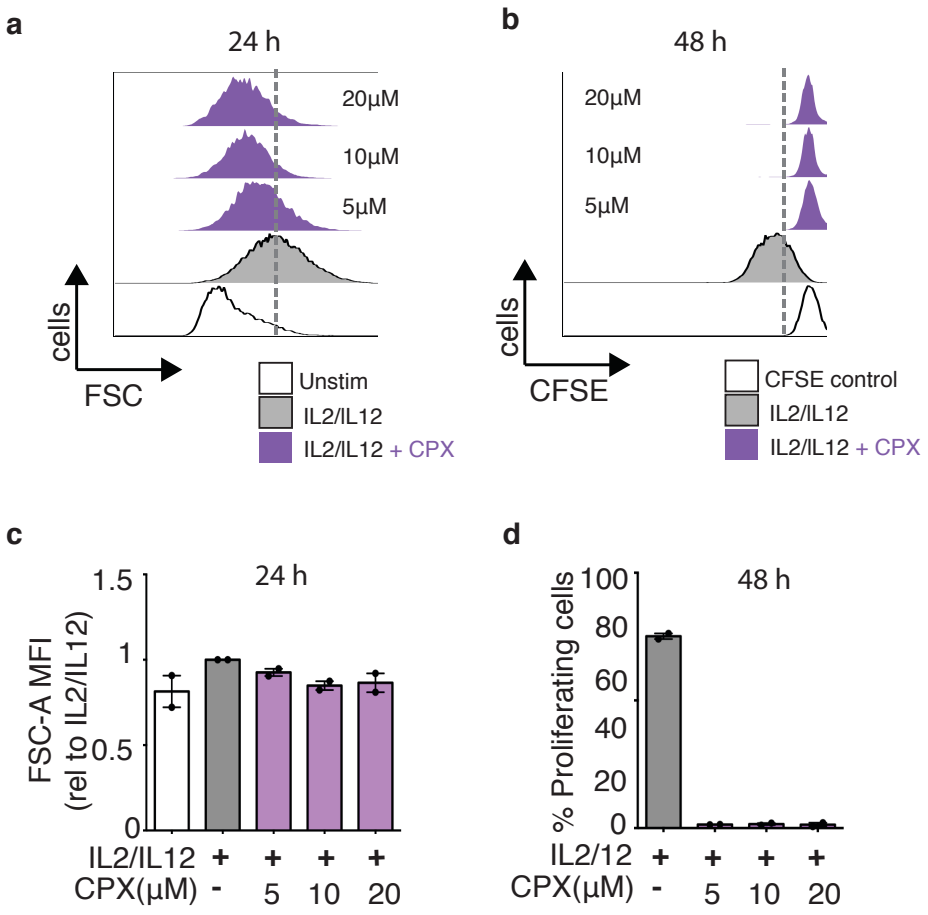

Figure 5.21 CPX-tretment impairs IL2/IL12-induced NK cell growth and proliferation

NK cells were cultured for 3 days, then CFSE-stained and stimulated with IL2 (20ng/ml) + IL12 (10ng/ml) for 24 h or 48 h in the presence or absence of varying doses (5μM,10μM or 20μM) of CPX. NK cells were analysed by flow cytometry for FSC-A (**a,c)** as a readout of size or CFSE-dilution (**b,d)** as a measure of proliferation. Data is representative (**a,b**) or mean +/- S.E.M (**c,d**) of 2 independent experiments.

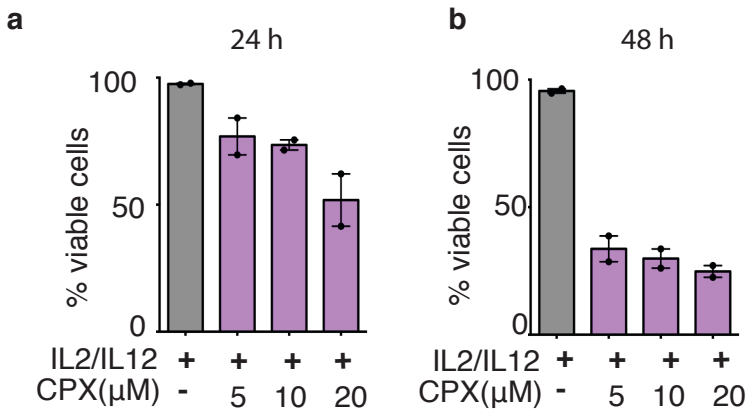

Figure 5.22 CPX reduces viability of IL2/IL12-activated NK cells

NK cells were cultured for 3 days, then CFSE-stained and stimulated with IL2 (20ng/ml) + IL12 (10ng/ml) for 24 h or 48 h in the presence (purple bar) or absence (grey bar) of varying doses (5μM,10μM or 20μM) of CPX. NK cells were live/dead stained and analysed by flow cytometry to assess cell-viability. Data is mean +/- S.E.M of 2 independent experiments.

5.6 Hypusination is important for the metabolism and of NK cells

Findings illustrated in this report thus far have demonstrated that defects in cellular metabolism can underlie cases where cellular growth and proliferation are perturbed. As inhibition of hypusination had an anti-proliferative effect on IL2/IL12-stimulated NK cells, I therefore hypothesised that hypusination may also be needed to support metabolism in cytokine-activated NK cells. The importance of hypusination for NK cell metabolism was investigated using Seahorse extracellular flux analysis. Interestingly, NK cells activated in the presence of the hypusination inhibitor, GC7, displayed no significant change in their rate of basal glycolysis, though there was a trend towards increased ECAR values (**Fig 5.23**). However, strikingly, upon further analysis it was identified that NK cells activated in the presence of GC7 had no glycolytic reserve – i.e. they could not further increase their glycolytic rate in response to addition of oligomycin. (**Fig 5.23 c,d).** IL2/IL12-stimulated NK cells activated in the absence of inhibitor, increase their glycolytic rate upon addition of oligomycin, demonstrating metabolic plasticity and the ability to adapt to the energy stress caused by reduced OxPhos.

As NK cells activated in the presence of GC7 could not further increase their glycolytic capacity in response to oligomycin, it suggested that when hypusination was inhibited in NK cells, OxPhos may be basally impaired. Indeed, IL2/IL12-stimulated NK cells activated in the presence of GC7 had strikingly reduced levels of basal OxPhos, respiratory capacity and spare respiratory capacity (**Fig 5.24).** These dramatic defects in OxPhos levels led us to consider whether inhibiting hypusination negatively affected mitochondrial health of IL2/IL12-activated NK cells. To further investigate this, NK cells were activated with IL2/IL12 in the presence or absence of GC7 and then stained with TMRM and MitoTracker Green to assess mitochondrial membrane potential and mitochondrial mass. Mitochondrial membrane potential was found to be significantly reduced in NK

cells activated in the presence of GC7, whilst no significant changes in mitochondrial mass were observed (**Fig 5.25)**.

Having identified that hypusination was important for OxPhos levels in IL2/IL12-activated NK cells. Whether this metabolic impairment impacted NK cell effector function was explored. It was found that production of IFNγ (**Fig 5.26)** and granzyme B (**Fig 5.27**) were both dependent on hypusination in IL2/IL12-stimulated NK cells. Furthermore, the cytotoxic abilities of IL2/IL12-stimualted NK cells activated in the presence of the hypusination inhibitor GC7 were investigated. NK cells activated in the presence of GC7 had impaired cytotoxicity *in vitro* towards K562 target cells (**Fig 5.28**), this defect was significant at higher concentrations (**Fig 5.28.b**).

Combined, these data unveil an important role for hypusination and thus, polyamine synthesis in the control of metabolism and function in IL2/IL12-stimulated NK cells.

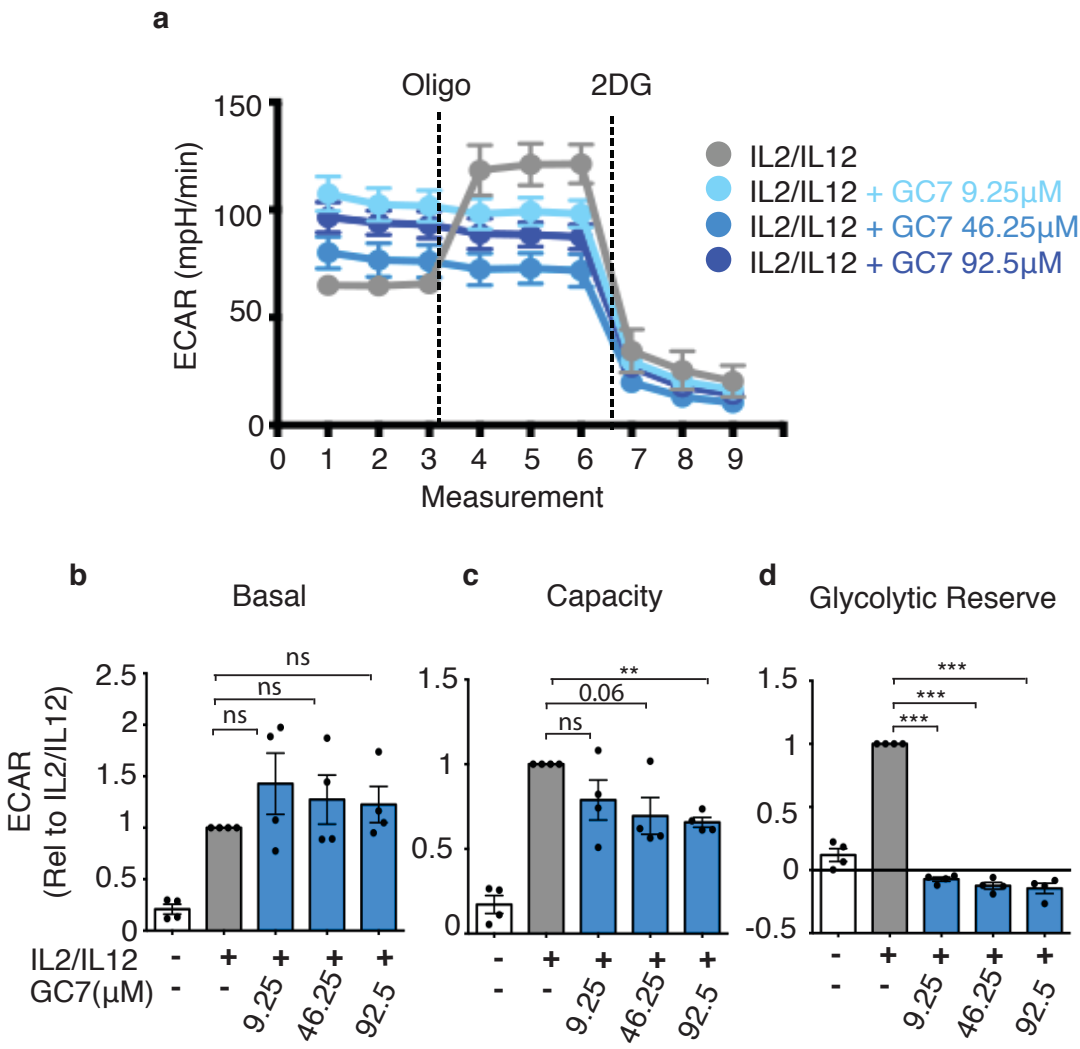

Figure 5.23 Glycolytic profile of NK cells activated with IL2/I12 in the presence or absence of DHPS inhibitor, GC7

Cultured NK cells were purified and left unstimulated or stimulated with IL2 (20ng/ml) + IL12 (10ng/ml) for 18h in the presence or absence of varying doses (9.25µM,46.25µM or 92.5µM) of GC7.Extracellular acidification rate (ECAR) was measured as a readout of glycolysis. Representative trace (**a**) and pooled measurements are shown for basal glycolytic rate (**b**) and glycolytic capacity (**c**) and spare glycolytic reserve (**d**). Data is representative (**a**) or mean +/- S.E.M (**b-d**) of 4 independent experiments. Statistical analysis was performed using a two-tailed one sample t-test versus a theoretical value of 1 (ns, non-significant,* $p<0.05$, ** $p<0.01$, ***$p<0.001$)

.

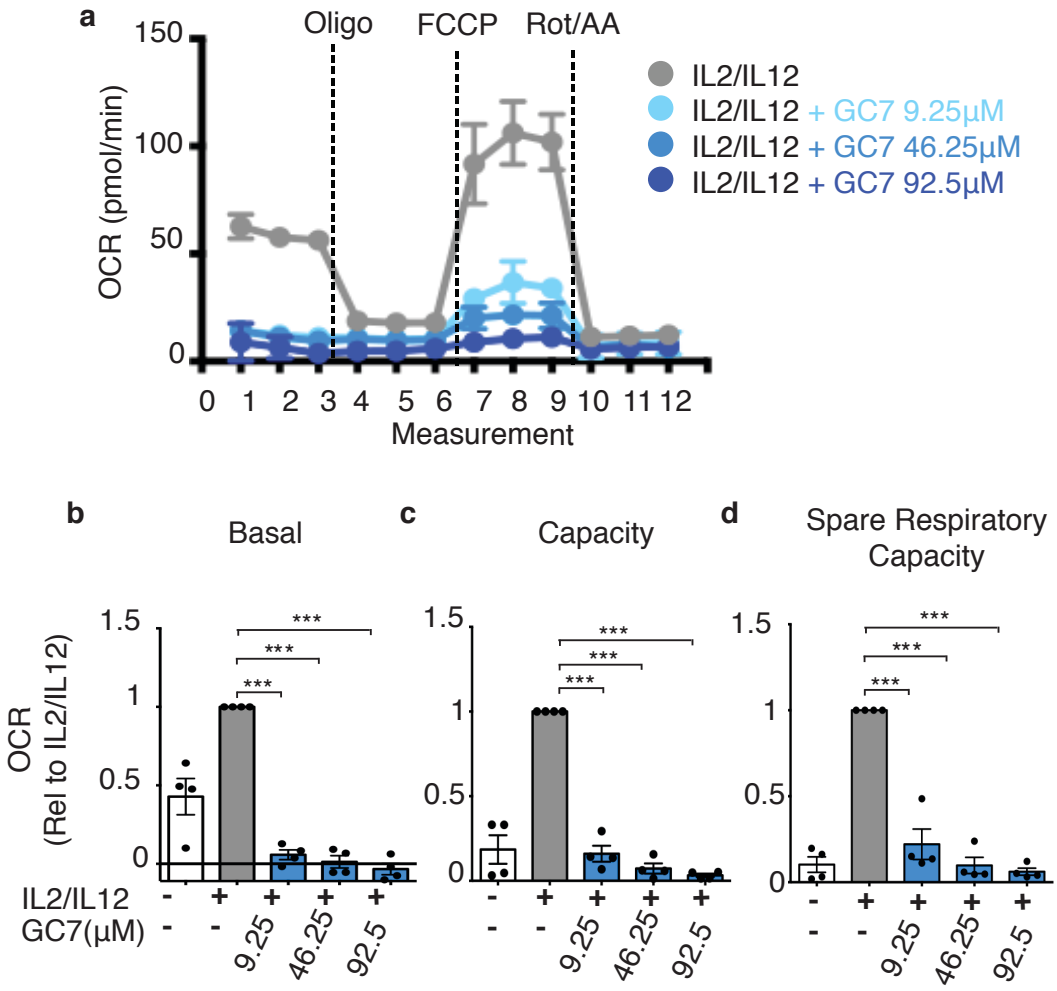

Figure5.24 OxPhos levels in NK cells activated with IL2/IL12 in the presence or absence of DHPS inhibitor, GC7

Cultured NK cells were purified and left unstimulated or stimulated with IL2 (20ng/ml) + IL12 (10ng/ml) for 18h in the presence or absence of varying doses (9.25µM,46.25µM or 92.5µM) of GC7. OCR was measured as a readout of OxPhos. Representative trace (**a**) and pooled measurements are shown for basal respiratory rate (**b**) respiratory capacity (**c**) and spare respiratory capacity (**d).** Data is representative (**a**) or mean +/- S.E.M (**b-d**) of 4 independent experiments. Statistical analysis was performed using a two-tailed one sample t-test versus a theoretical value of 1 (***p<0.001).

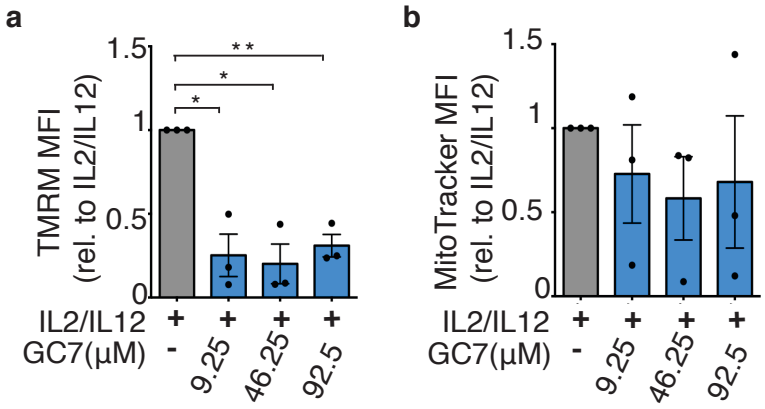

Figure 5.25 Inhibition of hypusination effects mitochondrial fitness in IL2/IL12 stimulated NK cells

Cultured NK cells were stimulated with IL2 (20ng/ml) + IL12 (10ng/ml) for 18h in the presence (blue bars) or absence (grey bar) of varying doses (9.25μM,46.25μM or 92.5μM) of the hypusination inhibitor GC7. Cells were stained with TMRM (100nM) (**a**) or MitoTracker (100nM)(**b**). NK cells were analysed by flow cytometry and data is presented relative to MFI values for IL2/IL12-stimulated NK cells. Data is mean +/- S.E.M of 3 independent experiments. Statistical analysis was performed using column statistics versus a theoretical value of 1 (*$p<0.05$, ** $p<0.01$).

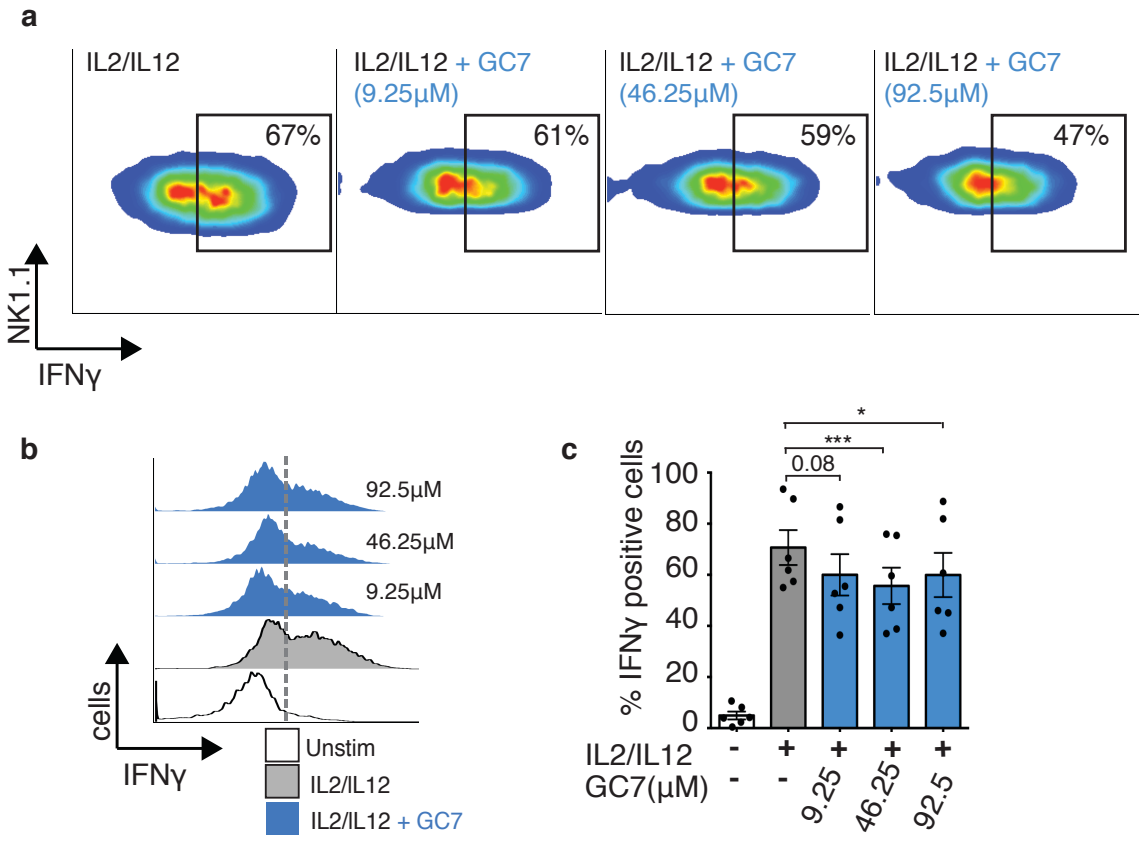

Figure 5.26 Hypusination is necessary for optimal IFNγ expression by IL2/IL12-activated NK cells

Cultured NK cells were activated with IL2 (20ng/ml) + IL12 (10ng/ml) in the presence or absence of GC7 (9.25µM, 46.25µM or 92.5µM) for 18 h. Cells were intracellularly stained for IFNγ and analysed by flow cytometry. Data is representative (**a,b)** or mean +/- S.E.M (**c**) of 6 independent experiments. Statistical analysis was performed using a paired two-tailed t-test against a theoretical value of 1 (*p<0.05, ***p<0.001)

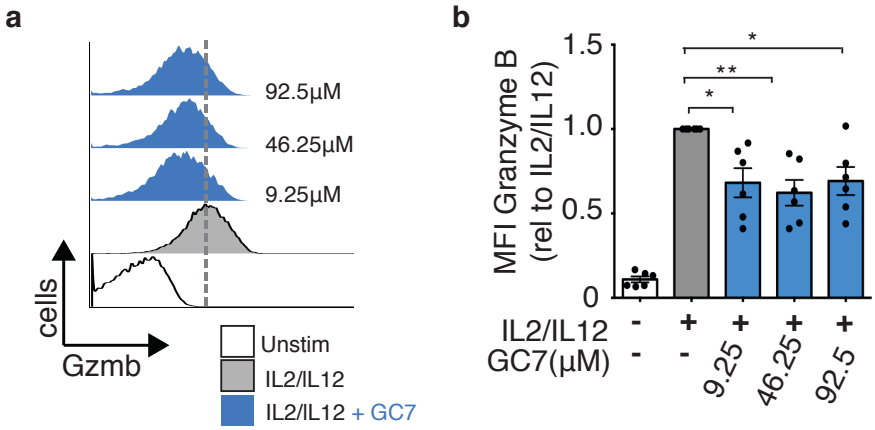

Figure 5.27 Hypusination is necessary for optimal granzyme B production in IL2/IL12-activated NK cells

Cultured NK cells were activated with IL2 (20ng/ml) + IL12 (10ng/ml) in the presence or absence of GC7 (9.25µM, 46.25µM or 92.5µM) for 18 h prior to intracellular staining for granzyme B production. Cells were analysed by flow cytometry and granzyme B production quantified. Data is representative (**a)** or mean +/- S.E.M (**b**) of 6 independent experiments. Statistical analysis was performed using a paired two-tailed t-test against a theoretical value of 1 (*p<0.05, **p<0.01)

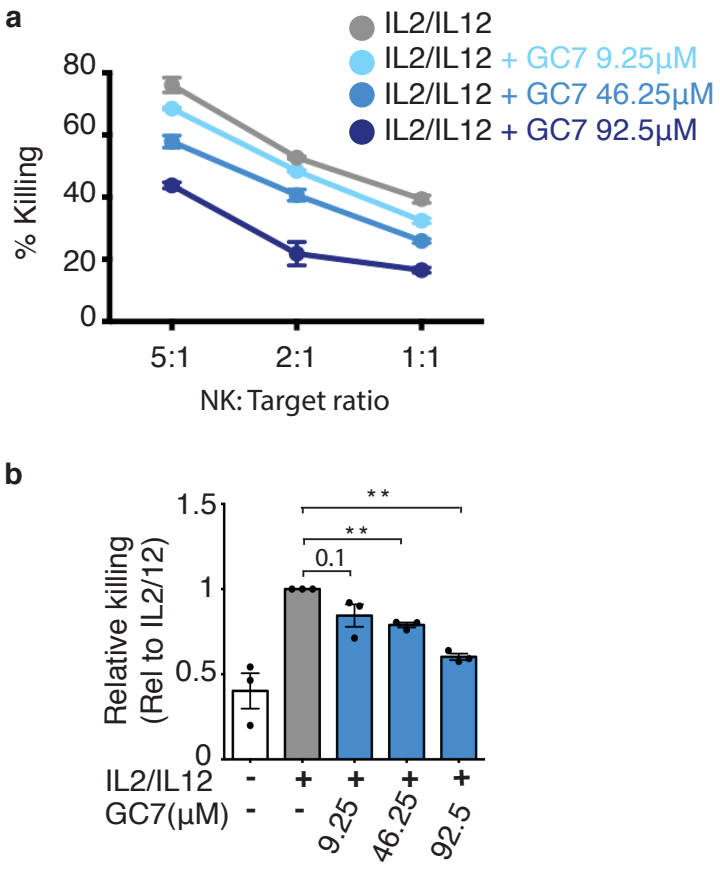

Figure 5.28 Hypusination is required for optimal NK cell cytotoxicity in IL2/IL12-stimualted NK cells

Cultured NK cells were activated with IL2 (20ng/ml) + IL12 (10ng/ml) in the presence or absence of GC7 (9.25µM, 46.25µM or 92.5µM) for 18 h prior to assessing *in vitro* cytotoxicity towards tumour K562 cells. Cytotoxicity was measured following co-incubation of NK cells with K562 target cells for 4 hours at ratios as indicated (**a**) or at 5:1 (**b**). Percentage killing was analysed by fluorescence release assay and is presented as proportion of target cells killed. Data is representative (**a**) or mean +/- S.E.M (**b**) of 3 independent experiments. Data in (**b**) is presented relative to percentage killing by IL2/IL12-stimulated NK cells. Statistical analysis was performed column statistics against a theoretical value of 1 (**p<0.01) .

5.7 Supplementation with exogenous polyamines can rescue effector molecule production, but not metabolism, in 25HC-treated NK cells

Results described in chapter three and chapter four identified SREBP transcription factors as novel regulators of NK cell metabolism and function. Advancing from this, data from this chapter reveal that SREBP activity is important for controlling the polyamine content of IL2/IL12-stimulated NK cells, likely through the control of *de novo* polyamine synthesis. Polyamine synthesis, and hypusination (which demands for adequate levels of the polyamine, spermidine) were essential for NK cell metabolism and function. Whether the requirement for SREBP activity by IL2/IL12-activated NK cells, was to generate the polyamines required to support metabolism and function was therefore further explored.

It is known that supplementation with exogenous polyamines leads to increased intracellular polyamine levels (Eisenberg et al. 2009). Therefore, to address whether polyamine production was the essential output of SREBP activity in IL2/IL12-stimulated NK cells, experiments were designed whereby SREBP activity was inhibited with 25HC and the cells supplemented with a mixture of exogenous polyamines, as previously described (Wang et al. 2011). This would allow us to dissect out whether NK cells could support metabolism and function, in the absence of other SREBP-controlled processes, once they were supplied with sufficient amounts of polyamines. However, polyamine supplementation could not rescue the metabolic defects observed when SREBP activity was inhibited in NK cells (**Fig 5.29).** NK cells stimulated in the presence of 25HC and exogenous polyamines, had no significant improvement in their rates of glycolysis (**Fig 5.29a)** or OxPhos **(Fig 5.29b)** as compared to NK cells activated in the presence of 25HC alone. This indicated that polyamine synthesis was not underpinning SREBP-mediated control of NK-cell glucose metabolism, i.e. glycolysis and OxPhos.

As extensively demonstrated throughout this chapter, NK cell metabolism is integrally linked to NK cell function. As the metabolic defects that occurred when

SREBP activity was impaired could not be rescued by the addition of exogenous polyamines, it was expected that polyamine supplementation would be unable to salvage the impaired functional responses in SREBP-inhibited NK cells either. Surprisingly, the application of exogenous polyamines significantly restored both IFNγ production **(Fig 5.30)** and granzyme B expression **(Fig 5.31)** by IL2/IL12-activated, SREBP-inhibited NK cells. Considered together, these results support the idea that in IL2/IL12-activated NK cells, SREBP activity supports metabolism in more ways than through the control of polyamine synthesis.

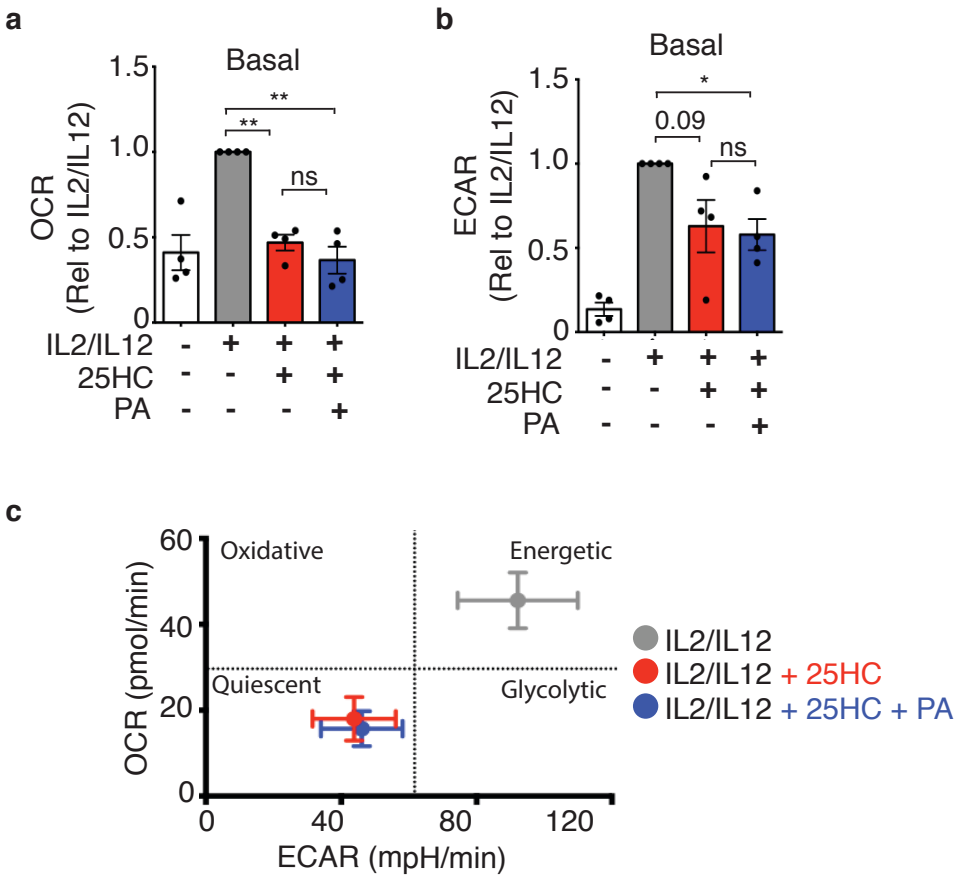

Figure 5.29 Polyamine supplementation does not rescue metabolic defects in cells lacking SREBP activity

Cultured NK cells were purified and left unstimulated or stimulated with IL2 (20ng/ml) + IL12 (10ng /ml), for 18 h in the presence or absence of 25HC (2.5μM) or 25HC (2.5 μM) plus 2x polyamine supplement. OCR was measured as a readout of OxPhos and ECAR was measured as a readout of glycolysis. Data is presented relative to levels in IL2/12-stimualted NK cells (**a-b**) or as an energy map of ECAR versus OCR rates (**c**) and is mean +/- S.E.M of 4 independent experiments.

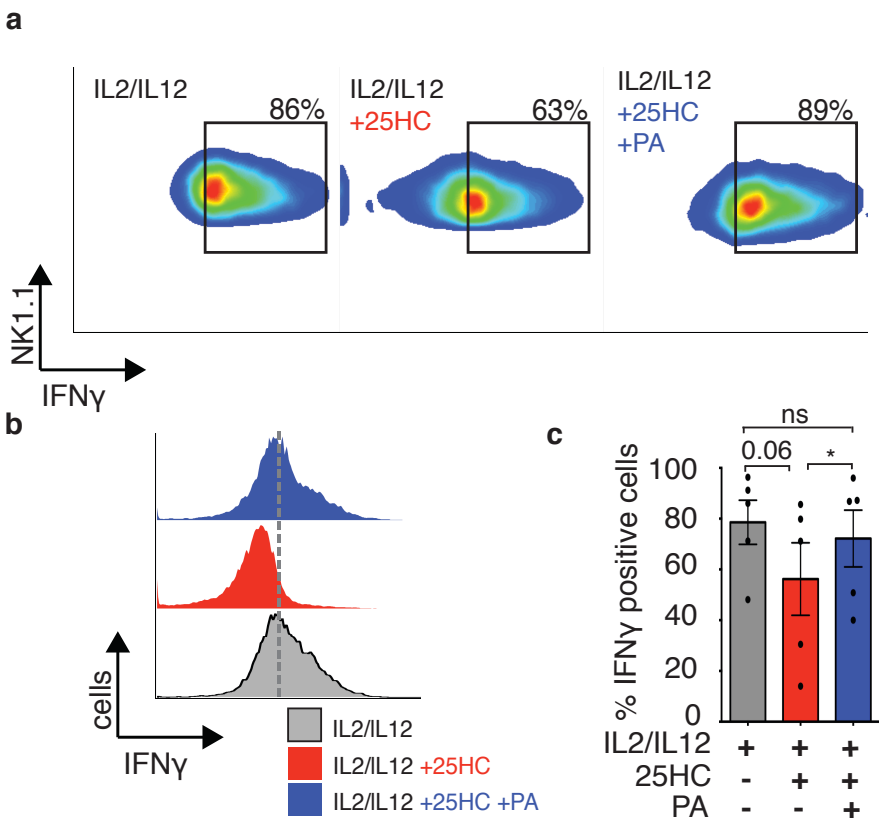

Figure 5.30 Exogenous polyamines restore IFNγ production in 25HC-treated NK cells

Cultured NK cells were activated with IL2 (20ng/ml) + IL12 (10ng/ml), in the presence or absence of 25HC (2.5μM), with or without additional supplementation with 2X polyamine (PA) supermix. Cells were intracellularly stained for expression of IFNγ, and analysed by flow cytometry. Data is representative (**a,b**) or mean +/- S.E.M (**c**) of 5 independent experiments. Statistical analysis was performed using a one-way ANOVA with Tukey's post-test (ns=non-significant, *p<0.05).

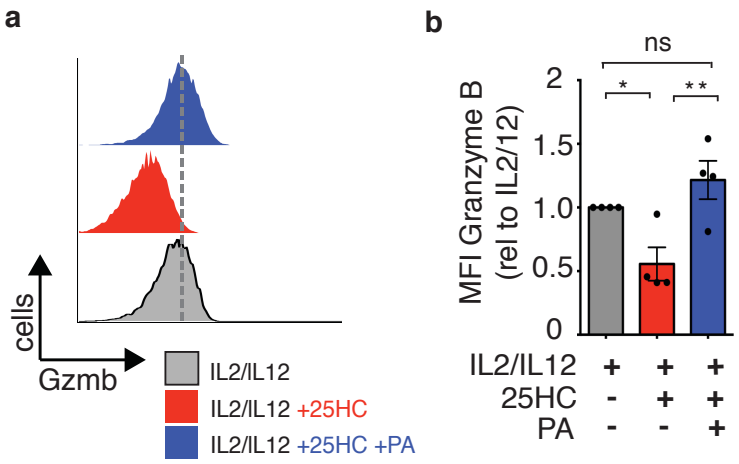

Figure 5.31 Exogenous polyamines restore granzyme B expression in 25HC-treated NK cells

Cultured NK cells were activated with IL2 (20ng/ml) + IL12 (10ng/ml), in the presence or absence of 25HC (2.5μM), with or without additional supplementation with 2X polyamine (PA) supermix. Cells were intracellularly stained for expression of granzyme B, and analysed by flow cytometry. Data is representative (**a,b**) or mean +/- S.E.M (**c**) of 4 experiments. Data is presented relative to granzyme B MFI in IL2/12-stimualted NK cells (**c**)**.** Statistical analysis was performed using column statistics against a theoretical value of 1 (ns=non-significant, *p<0.5, ** p<0.01).

5.8 SREBP activity promotes cMYC expression in IL2/IL12-stimulated NK cells

Given the novel findings that SREBP activity influences polyamine synthesis in IL2/IL12-stimulated NK cells, and that polyamines were essential for NK cell metabolism and effector function, the mechanism by which SREBP activity was controlling polyamine production was of interest. No direct link between SREBP activity and polyamine biosynthesis stood out in the literature. However, another key transcriptional regulator of NK cell metabolism and function – cMYC – has been extensively linked to *de novo* polyamine synthesis in other cell types. In fact, ODC, the first, and rate-limiting enzyme in the de novo polyamine synthesis pathway, is a direct cMYC target-gene (Wagner et al. 1993; Bello-Fernandez, Packham, and Cleveland 1993). Indeed, IL2/IL12-stimulated NK cells from Myc^{KO} (*Myc*$^{flox/flox}$ × Tamox-Cre) mice had reduced expression of *Odc1* transcripts as compared to NK cells from Myc^{WT} (*Myc*$^{WT/WT}$ Tamox-Cre) Myc^{WT} mice (**Fig 5.32**). Earlier results from this chapter identified that SREBP activity is required for the expression of *Odc1* mRNA. Whether SREBP activity was influencing ODC expression through regulation of cMYC was therefore considered.

The transferrin receptor, CD71, is a cMYC target gene and surface expression of CD71 has been confirmed to be cMYC-dependent in IL2/IL12-stimulated NK cells (Loftus et al. 2018; O'Donnell et al. 2006). To explore whether cMYC activity may be impaired in NK cells lacking SREBP activity, surface CD71 expression was measured by flow cytometry. Interestingly, CD71 expression by IL2/IL12-stimulated, NK cells was decreased if cells were activated in the presence of either PF429242 or 25HC to inhibit SREBP activation (**Fig 5.33a).** Furthermore, stimulation of NK cells from $SCAP^{KO}$ mice, which lack SREBP activity, resulted in reduced CD71 expression compared to $SCAP^{WT}$ controls **(Fig 5.33b).** This suggested SREBP transcription factors might be required for cMYC activity in IL2/IL12-activated NK cells. mRNA levels of cMYC were measured in NK cells with impaired SREBP activity and 25HC was found to decrease cMYC transcripts, though this was not true for PF429242. However, cMYC is known to be primarily regulated post-

transcriptionally in activated NK cells and other activated lymphocytes (Loftus et al. 2018; Preston et al. 2015; Swamy et al. 2016). Therefore, whether SREBP-activity influences the expression of cMYC protein was explored. Interestingly, when SREBP-activity was impaired with either 25HC or PF429242, the induction of cMYC expression following IL2/IL12-stimulation was substantially impaired (**Fig 5.34**). These findings argue that SREBP-activity can control the expression of cMYC in cytokine-activated NK cells.

In summary, data presented in this results chapter highlight a novel role for SREBP transcription factors in the control of polyamine biosynthesis by cytokine-stimulated NK cells. SREBP activity was required for optimal cMYC expression following NK cell activation, providing a possible mechanism linking SREBP activity to expression of the polyamine biosynthesis machinery. Furthermore, *de novo* polyamine synthesis and hypusination were shown to be important pathways for acquisition of increased metabolism and effector functions by IL2/IL12-stimulated NK cells.

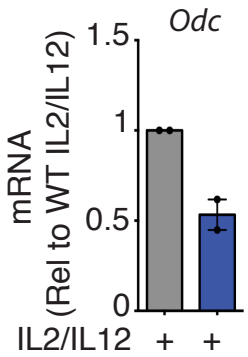

Figure 5.32 IL2/IL12-stimulated cMyc^{KO} NK cells have reduced expression of *Odc* mRNA compared to cMyc^{WT} controls

NK cells isolated from Myc^{KO} (*Myc*$^{flox/flox}$ × Tamox-Cre) (blue bar) or Myc^{WT} (*Myc*$^{WT/WT}$ Tamox-Cre) (grey bar) spleens were cultured in the presence of 4-OH TMX (0.6 μM), then purified and stimulated for a further 20 h with IL2 (20ng/ml) + IL12 (10ng /ml.).Cells were lysed and mRNA levels were quantified by qRT-PCR . Data is normalised to averaged levels of control gene *Rplp0, Gapdh and Hprt* and presented relative to mRNA expression in IL2/IL12-stimulated Myc^{WT} NK cells. Data is mean +/- S.E.M of 2 independent experiments.

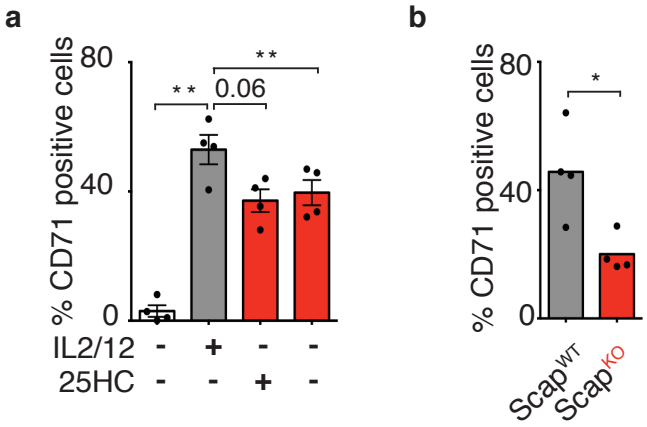

Figure 5.33 Impairing SREBP activity reduces CD71 expression on IL2/IL12-stimulated NK cell

Cultured NK cells were either left unstimulated or were activated with IL2 (20ng/ml) + IL12 (10ng/ml), in the presence or absence of 25HC (2.5μM) or PF429242 (10μM) for 20h (**a**).NK cells from $Scap^{KO}$ (*Scap*$^{flox/flox}$ x Tamox-Cre) or $Scap^{WT}$ (*Scap*$^{WT/WT}$ x Tamox-Cre) spleens were cultured in the presence of 4-OH TMX (0.6 μM), then stimulated for a further 20 h with IL2 (20ng/ml) + IL12 (10ng /ml) (**b**). Cells were stained for CD71 expression and analysed by flow cytometry. Data is representative or mean +/- S.E.M of 4 independent experiments. Statistical analysis was performed using a one-way ANOVA with Tukey's post-test (**a**) or paired two-tailed t-test (**b**) (*<0.05, **p<0.01).

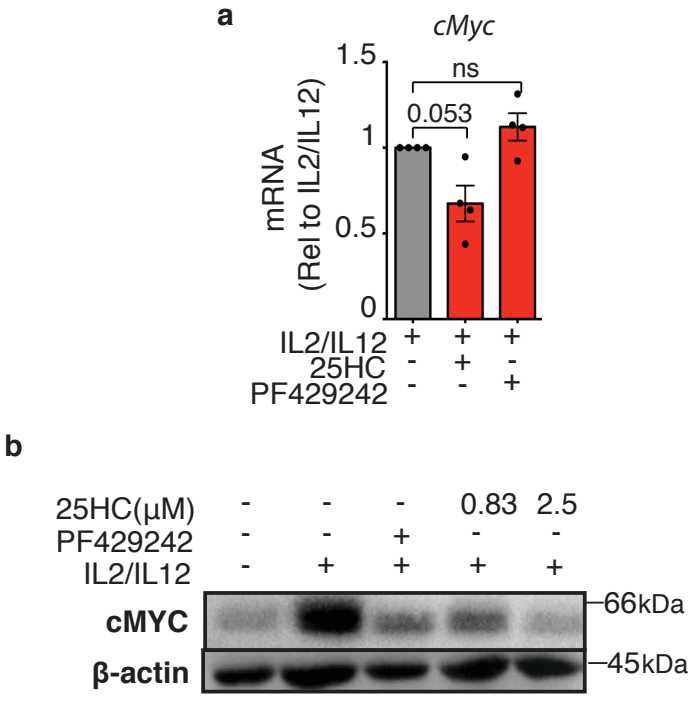

Figure 5.34 cMYC mRNA and protein expression is dependent on SREBP activity in IL2/IL12-stimulated NK cells

Cultured NK cells were activated with IL2 (20ng/ml) + IL12 (10ng /ml) for 18 h in the presence or absence of 25HC (0.83 or 2.5μm) or PF429242 (10μm) and the cells lysed for RNA **(a)** or protein (**b).** *cMyc* mRNA levels were quantified by qRT-PCR and data normalised to levels of control gene *Rplp0* and presented relative to mRNA expression in IL2/IL12-stimulated NK cells (**a**). Levels of cMYC or β-actin protein were assessed by immunoblot analysis (**b**). Data is mean +/- S.E.M (**a**) or representative (**b)** of 4 (**a**) or 3 (**b**) independent experiments. (PF429242 replicate in (**b**) is representative of n=1). Statistical analysis was performed using a column statistics versus a theoretical value of 1 (ns=non-significant).

5.9 Discussion

The three natural polyamines (putrescine, spermidine and spermine) are ubiquitously expressed in all mammalian cells, and function in a range of cellular processes including cellular proliferation, autophagy, ion channel modulation and protection from oxidative damage. Furthermore, the polyamine spermidine serves as the substrate for a post-translational modification known as hypusination. eIF5A is the only protein known to be hypusinated and hypusination is essential for its functions, which mainly promote protein synthesis (Park, Cooper, and Folk 1981; Park et al. 2010). Polyamine concentrations are frequently elevated in cancers and increased expression of eIF5A has been reported in some malignancies (Nakanishi and Cleveland 2016). For this reason polyamines and eIF5A have been extensively studied in the context of tumour growth and cancer progression. Despite numerous indications suggesting a role for polyamines in the immune system, their role in many immune cell types has not been broadly investigated. Data included in this chapter highlighted that in response to activation with IL2/IL12, NK cells increase cellular polyamine concentrations. Interfering with *de novo* polyamine synthesis or inhibiting the hypusination of eIF5A was detrimental to NK cell metabolism and function. Therefore, identifying the polyamine-hypusine axis as a novel pathway required for NK cell metabolic reprogramming and functional responses.

To ascertain the importance of *de novo* polyamine synthesis in cytokine-induced NK cells, the specific inhibitor, DFMO was used. DFMO irreversibly inhibits ODC (the first enzyme of polyamine biosynthesis) and is widely used to study the polyamine pathway (Poulin et al. 1992).To compliment the use of DFMO another pharmacological inhibitor – DENSPM - was used. DENSPM is a spermine analogue which can induce the catabolism of polyamines through induction of SSAT and SMO – two-enzymes involved in polyamine degradation. Therefore, DENSPM does not directly inhibit polyamine synthesis, but instead serves to deplete the pool of intracellular polyamines (Stanic et al. 2009; Fogel-Petrovic et al. 1997). DENSPM has no direct effects on *de novo* polyamine synthesis, therefore its use in this study

is simply to enhance our understanding of global polyamine depletion on NK cell responses and we would not necessarily expect to obtain identical results, as with direct inhibition of polyamine synthesis by DFMO.

Activation of NK cells in the presence of DFMO, impaired their growth and proliferation. The finding that *de novo* polyamine synthesis was required for NK cell growth and proliferation was not a surprising one. Polyamines have been extensively linked to cellular proliferation and numerous studies in cancer cells have demonstrated the anti-proliferative effects of DFMO. However, in contrast to the defects observed when NK cells were activated in the presence of DFMO, cellular growth was unaffected in NK cells activated in the presence DENSPM, and cellular proliferation was inhibited to a lesser extent. Therefore, the *de novo* synthesis of polyamines is essential for the growth and proliferative responses of NK cells, and induction of polyamine catabolism has small but significant effects on NK cell proliferation.

The importance polyamine synthesis for NK cell expansion parallels work carried out in T cells. Early studies identified that DFMO inhibits lymphocyte proliferation in response to IL2 (Bowlin et al. 1987). These studies were more recently expanded upon and it was identified that DFMO inhibits proliferation of T lymphocytes both *in vitro* and in immunised mice *in vivo* (Wang et al. 2011). Of note, supplementation with exogenous polyamines could completely restore proliferation by CD4+ and CD8+ T lymphocytes treated with DFMO (Wang et al. 2011). To date a precise mechanism linking polyamines to cellular growth has not been identified (Pegg 2016). Therefore, T cells and NK cells both require polyamine synthesis for cell growth and proliferation, though the molecular mechanisms linking polyamines to proliferation in either cell type has yet to be determined.

As previously mentioned, an important output of polyamine biosynthesis is the generation spermidine – the substrate used for hypusination of eIF5A. All reported functions of eIF5A require its hypusination (Park et al. 2010). In cancer cells, eIF5A^{H}

promotes cellular proliferation (Epis et al. 2012; Preukschas et al. 2012). Furthermore, data presented in this chapter suggests that hypusination is important for the growth and proliferation of cytokine-activated NK cells. Inhibition of hypusination with either GC7 (which inhibits DHPS, the first enzyme involved in the formation of hypusine) or CPX (which inhibits DOHH, the second enzyme involved in the formation of hypusine), substantially impaired the ability of NK cells to proliferate in response to IL2/IL12-stimulation. This argues that the defects in proliferation observed when polyamine synthesis was inhibited in NK cells could be due to a reduction in spermidine concentration and thus impaired hypusination of eIF5A. Interestingly, eIF5a is expressed at low levels in quiescent T cells but is inducible upon T cell stimulation (Bevec et al. 1994). GC7 treatment blocks the proliferation of CD4+ T cells *in vitro* in response to stimulation with anti-CD3 and anti-CD28 in combination with IL2, with a concomitant increase in the frequency of CD4+ Treg cells (Colvin et al. 2013). It would therefore be of interest to further determine the context specific role $eIF5A^{H}$ in the proliferation of different CD4+ T cells subtypes and indeed in CD8+ T cell responses. Furthermore, these results argue that the reason NK cells require polyamines for proliferation is to provide the substrate, spermidine to allow for the hypusination of $eIF5A^{H}$.

Further insight into how polyamines may influence NK cell growth and proliferation comes with the identification that polyamine synthesis is important NK cell metabolism. As illustrated in chapter 3, NK cells require both glycolysis and OxPhos to support their proliferation in response to IL2/IL12-stimulation. Data presented in this chapter identify that pharmacologically inhibiting *de novo* polyamine synthesis with DFMO significantly reduced rates of glycolysis and OxPhos in cytokine-activated NK cells. Interfering with the polyamine content of NK cells by using DENSPM to induce polyamine catabolism, also impaired the rates of both glycolysis and OxPhos, mirroring the energetic profile observed with DFMO treatment. This indicates that maintaining sufficient levels of polyamines is essential for NK cell metabolic reprogramming. This finding is of interest as polyamines have not been extensively studied in the context of energy-

metabolism. One group reported that DFMO inhibited glycolytic metabolism in neuroblastoma cells *in vivo* in patients and a recent study by Puleston et al. identified a role for polyamines in the metabolism of un-transformed cells (Lozier et al. 2015; Puleston et al. 2019). Murine embryonic fibroblasts (MEFs), treated with DFMO or DENSPM displayed significantly reduced basal OxPhos levels. A small reduction in glycolysis was observed in MEFs treated with DFMO however no impact on basal ECAR was induced by DENSPM in these cells (Puleston et al. 2019).Therefore results herein are adding to a new but growing body of evidence describing an emerging role for polyamine synthesis in the control of cellular metabolism.

The aforementioned publication hypothesised that the polyamine requirement for metabolism in MEFs was to provide spermidine for eIF5A hypusination (Puleston et al. 2019). This hypothesis was investigated in detail in MEFs and indeed when eIF5A^{H} was inhibited with either GC7 or CPX, with siRNA against eIF5A, OxPhos levels were dampened. These results were expanded upon to confirm a role for eIF5A^{H} in controlling OxPhos rates in numerous cell types including BMDMs (Puleston et al. 2019). This is in line with findings in this report, which identify that GC7-treatment impaired NK cell OxPhos in response to IL2/IL12-stimulation. When NK cells were activated in the presence of GC7, to inhibit DHPS and thus hypusination, OxPhos rates were dramatically impaired. Furthermore, when hypusination was inhibited not only did NK cells display extremely low levels of basal OxPhos, they were also unable to substantially increase their respiratory rates in response to FCCP addition (which uncouples OxPhos). This was further investigated and it was identified that NK cells that were activated in the presence of GC7 also had reduced mitochondrial membrane potential ($\Delta\Psi_m$) as measured by uptake of the $\Delta\Psi_m$-dependent dye, TMRM. Taken together, these results reveal an essential role for eIF5a^{H} for NK cell mitochondrial respiration.

A mechanism linking hypusination of eIF5a to OxPhos was also uncovered in the study by Puleston et al. who identified that eIF5a^{H} is required for the translation of a set of mitochondrial enzymes involved in the TCA cycle and electron transport chain, whilst having no effect on enzymes involved in glycolysis (Puleston et al. 2019). As IL2/IL12-activated NK cells mainly fuel OxPhos through the CMS, it would be more likely that reduction in electron transport chain machinery would affect NK cell OxPhos levels. It would be of future interest to examine the impact of hypusination on expression of the electron transport chain machinery in IL2/IL12-activated NK cells. Consequently, the previously discussed reliance on polyamine synthesis for optimal levels of OxPhos, is likely to provide spermidine to hypusinate eIF5a. The reduction in OxPhos rates was much greater when hypusination was inhibited directly with GC7 as compared to global inhibition of polyamine synthesis – this might argue that some hypusination is still taking place. A further discrepancy is that directly inhibiting hypusination with GC7 in NK cells dramatically abrogated NK cell OxPhos rates without effecting the ability of IL2/IL12-activated NK cells to engage in glycolysis. In contrast, inhibition of de novo polyamine synthesis impaired OxPhos but also glycolytic rates. Therefore it is likely that polyamines are acting through another mechanism to support NK cell glycolysis.

Given the importance of polyamine synthesis and hypusination for NK cell metabolism, the importance of the polyamine-hypusine axis for NK cell effector functions was investigated. With the established link between NK cell metabolism and NK cell effector function, it was not surprising that inhibition of either polyamine synthesis or hypusination, which both impaired NK cell metabolism, also reduced NK cell effector responses. Treatment with DFMO or DENSPM to reduce the polyamine content of the cell, or treatment with GC7 to block hypusination, impaired the ability of NK cells to express IFNγ or granzyme B. Furthermore, the ability of NK cells to lyse target cells *in vitro* appears to depend on hypusination, as activation of NK cells in the presence of GC7, reduced NK cell

cytotoxicity against K562 target cells. This is one of the first examples linking polyamine metabolism and hypusination to lymphocyte immune functions.

Despite numerous reports that polyamine synthesis and eIF5A are upregulated in T lymphocytes upon activation, the importance of polyamines or hypusination for immune cell effector responses has not been extensively investigated (Wang et al. 2011; Hukelmann et al. 2016; Bevec et al. 1994). It is well-documented that in response to activation, T cells dramatically increase activity of polyamine synthesis enzymes and increase intracellular concentrations of polyamines (Wang et al. 2011; Bevec et al. 1994). Furthermore, Doreen Cantrell's group identified that eIF5A is one of the top-20 most highly expressed proteins in CD8+ T lymphocytes (Hukelmann et al. 2016; Puleston, Villa, and Pearce 2017). The gene encoding eIF5A is upregulated in the PBMCs from HIV infected patients compared to healthy controls (Bevec et al. 1994). Interestingly, administration of spermidine boosted memory responses of CD8+ T cells and improved vaccination responses (Puleston et al. 2014). Furthermore early studies identified that DFMO inhibited cytotoxicity of mixed lymphocyte cultures against P815 tumour cell line (Schall et al. 1991). Therefore it is emerging that the polyamine-hypusine axis can influence functions of other lymphocytes apart from NK cells.

Interestingly, Puleston et al highlighted the importance of hypusination for macrophage alternative-activation. They identify that classically activated (LPS and IFNγ) BMDMs do not increase eIF5a^{H} following stimulation, whilst alternatively-activated (IL4-activated) BMDMs strongly induced levels of enzymes required for hypusination and of eIF5a^{H} protein (Puleston et al. 2019). Furthermore, the protective effect against *Heligmosomoides polygyrus* – a helminth parasite, by alternatively activated macrophages was lost *in vivo* when mice were pre-treated with GC7 (Puleston et al. 2019). This is in-line with the idea that hypusinated eIF5A is essential for OxPhos, as OxPhos is known to be important for macrophage alternative activation (Huang et al. 2014; Van den Bossche et al. 2016; Puleston et al. 2019). Indeed, inhibition of hypusination had

no effect on classically activated macrophages *in vivo*, which are known to have less reliance on OxPhos (Puleston et al. 2019). This has led to the idea that hypusination may be important for immune subsets that rely on OxPhos (Puleston et al. 2019). For example memory CD8+ T cells require OxPhos and interestingly administration of spermidine (the substrate for hypusination) boosted memory responses of CD8+ T cells and improved vaccination responses (van der Windt et al. 2012; Puleston et al. 2014). Hypusination was not directly investigated in this study however it is plausible that spermidine addition enhanced hypusination and thus supported elevated OxPhos by these cells.

A number of additional studies in myeloid cells has identified a role for polyamine synthesis and hypusination. Hypusination of eIF5A is required to allow for the maturation of human DCs in vitro and their subsequent ability to stimulate and activate T lymphocytes (Kruse et al. 2000). Major reductions in the DC marker CD83 was observed along with minor reductions in CD80 and CD86, when immature DCs were treated with GC7. DCs are essential for stimulating potent T cell responses – however if DCs were pre-treated with GC7, they displayed a reduced allostimulatory capacity and induced reduced T cell proliferation (Kruse et al. 2000). Macrophages induce ODC expression at an mRNA level and also increase ODC enzymatic activity in response to infection with *H.pylori* (Gobert et al. 2002). Furthermore mice injected intraperitoneally with LPS, or given LPS intranasally as a model of acute lung injury, to induce inflammation, survived better if they were treated with siRNA against eIF5A (Moore et al. 2008). Silencing of eIF5A in this model, reduced proinflammatory cytokines in the serum. Taken together the results described in this chapter add to a growing body of evidence linking polyamines and hypusination of eIF5A to immune cell function.

A novel finding from this chapter was the influence of SREBP activity on polyamine levels in cytokine-stimulated NK cells. Inhibition of SREBP activity with 25HC, reduced the polyamine content of NK cells. Importantly, a dramatic and significant reduction in putrescine was identified, despite no decrease in the concentration

of ornithine, the precursor required for polyamine synthesis, and minimal effects on the polyamines further along the synthesis pathway: spermidine and spermine. Depletion of putrescine with lesser effects on spermidine and spermine, is a pattern of metabolite depletion commonly observed when de novo polyamine synthesis is directly inhibited with DFMO (Levin et al. 1992; Poso and Pegg 1982; Mamont et al. 1978). This suggested that SREBP activity was required for de novo polyamine synthesis. This hypothesis is supported by the finding that mRNA expression of ODC is significantly reduced in NK cells when SREBP activity is inhibited.

The results presented in chapter 3 and chapter 4 of this thesis identified an essential role for SREBP transcription factors in the control of NK cell metabolism and effector responses. SREBP-activity controls activity of the CMS to support NK cell metabolism and function. Therefore whether the SREBP controlled-CMS or SREBP-controlled polyamine synthesis played a greater role in NK cell metabolism was investigated. If the main output of SREBP activity was to produce polyamines for metabolism, I hypothesised that supplementation with exogenous polyamines would be able to rescue metabolism in NK cells in which SREBP activity had been depleted with 25HC. However addition of exogenous polyamines could not rescue defects in either ECAR or OCR. This suggests that although SREBP-controlled polyamine synthesis is important for NK cell metabolism, it is not the only SREBP-controlled process necessary to support metabolism. This finding is not surprising as defects in the CMS following SREBP inhibition is likely to also account for major defects in metabolic rates. The surprising result from these experiments was that although supplementation with exogenous polyamines could not rescue the metabolic defects observed in NK cells lacking SREBP activity, addition of exogenous polyamines succeeded in restoring effector molecule production. When NK cells are stimulated in the presence of 25HC to inhibit SREBP, they have impaired production of both granzyme B and IFNγ. However when a mixture of exogenous polyamines was added to SREBP inhibited cells, it significantly restored production of these molecules. This result was surprising. Data from this thesis, in

addition to extensive work from our group and others has highlighted that enhanced metabolic responses are an essential requirement for acquisition of effector functions by cytokine-stimulated NK cells. When NK cell metabolism is pharmacologically or genetically inhibited, it seems to always correlate with decreased NK cell function (Assmann et al. 2017; Donnelly et al. 2014; Viel et al. 2016; Marcais et al. 2014; Loftus et al. 2018). However, the precise mechanism or mechanisms, linking NK cell metabolism to effector responses are yet to be identified. This data would suggest that enhanced metabolism is required in NK cells to provide polyamines to support effector molecule production. Precisely how polyamines fulfil this role is difficult to gauge and would require an additional body of work. Furthermore, whether polyamines can rescue other NK cell functions remains to be assessed. However, due to the high energy demand required for processes such as cytotoxicity it is unlikely that polyamine supplementation alone would be sufficient to replace the metabolic requirement of complex NK cell functions *in vivo*.

Another exciting finding from this chapter is the identification that SREBP is required for the expression of cMYC in IL2/IL12-activated NK cells. cMYC was reduced at both mRNA and protein level when NK cells were activated in the presence of SREBP. No established link between SREBP activity and cMYC expression has been previously identified in immune cells, however work carried out in prostate cancer cells identified that SREBP2 can bind directly to the cMYC promoter to drive its expression(Li et al. 2016). Given the complex regulation of cMYC protein expression through tight regulation of its synthesis and degradation, it will require future studies to investigate the precise link between SREBP and cMYC in NK cells. However the finding that SREBP controls cMYC expression in cytokine-activated NK cells provides a plausible mechanism for how SREBP activity could be controlling *de novo* polyamine synthesis. The rate-limiting enzyme of the polyamine biosynthetic pathway - ODC - is one of the best characterised direct targets of cMYC (Bello-Fernandez, Packham, and Cleveland 1993; Wagner et al. 1993). Furthermore, cMYC-deficient T lymphocytes fail to induce expression of

ODC and other polyamines synthesis enzymes in response to activation (Wang et al. 2011). cMYC has previously been shown by our group to be essential to the metabolic and functional responses of cytokine-activated NK cells (Loftus et al. 2018). Therefore it is tempting to speculate that some of the results previously obtained when cMYC activity was blocked in NK cells, could be due to perturbations in polyamine synthesis and hypusination.

Examined together, data presented in this chapter identify a novel link between SREBP-activity and cMYC expression in IL2/IL12-activated NK cells. Cytokine-induced upregulation of polyamine synthesis in NK cells was dependent on SREBP-activity and we propose that SREBP transcription factors mediate upregulation of the polyamine synthesis machinery through the regulation of cMYC expression. Furthermore, the upregulation of polyamine biosynthesis was shown to be essential for NK cell metabolic and functional responses following IL2/IL12-stimulation. Polyamine synthesis was required at least in part, to support hypusination of eIF5A and hypusination was also essential for NK cell metabolic and functional responses. This suggests that peripheral metabolic pathways can have essential roles in the metabolism and function of immune cells, and their roles should not be overlooked.

6 Overall Discussion

The field of immunometabolism has rapidly expanded in recent years. It is now widely established that cellular metabolism is integral to the effective functioning of immune cells and that different immune cell types adopt distinct metabolic configurations to support their specialised functions. The ability to reprogram their metabolic profiles in response to stimulation is not only essential for sufficient energy production by immune cells, but also to generate biosynthetic precursors for cell growth, proliferation , effector molecule production, and to engage in cell-type specific immune effector functions.

NK cells are no exception, recent research has highlighted that both murine and human NK cells undergo extensive metabolic changes in response to various stimuli (O'Brien and Finlay 2019). These changes are dynamically regulated by cMYC and mTORC1 (Donnelly et al. 2014; Loftus et al. 2018; Kedia-Mehta et al. 2019; Marcais et al. 2014). As mTORC1 signalling can induce SREBP activity, which is important for the function of other immune cells, it was hypothesised that SREBP transcription factors may be important for NK cell responses. Indeed, data presented throughout this thesis has identified a novel role for SREBP transcription factors as central regulators of metabolism and function in cytokine-stimulated NK cells. Furthermore, activation-induced increases in *de novo* polyamine synthesis and hypusination of eIF5A were identified as essential processes that support robust NK cell metabolic and functional responses. There is accumulating evidence illustrating that impaired cellular metabolism is a crucial factor leading to dysfunctional NK cells in a range of chronic diseases including obesity and cancer. NK cells are best characterised for their anti-viral and anti-cancer activities. Therefore, if we can understand in detail how metabolic pathways and metabolic regulators impact upon NK cell metabolism and function, we can then consider ways to exploit these findings for therapeutic gain.

The importance of NK cells in the immune response is illustrated by increased cancer burdens and increased susceptibility to infection in individuals harbouring defective NK cells (Orange 2013; Biron, Byron, and Sullivan 1989). Furthermore,

NK cells are known to be dysfunctional in a number of chronic conditions including in obesity, chronic viral infection and cancer (O'Shea et al. 2010; Lynch et al. 2009; Caras et al. 2004; Heiberg et al. 2015). The identification that metabolism is essential for NK cell functions has led to an emerging paradigm that dysfunctional metabolism can underlie these functional impairments. For instance, altered NK cell metabolism has been identified as an important factor underlying the impaired effector functions of NK cells isolated from the peripheral blood of patients with metastatic breast cancer (Slattery et al. 2019). Defects in NK cells from these patients include reduced rates of glycolysis and OxPhos in addition to altered mitochondrial morphology (Slattery et al. 2019). This parallels with work linking defective cellular metabolism to dysfunctional NK cell responses in the context of obesity. Defects in NK cells isolated from obese adults and obese children correlate with dysregulated cellular metabolism in these cells (Michelet et al. 2018; Tobin et al. 2017). The profound metabolic and functional dysfunction in NK cells in obese individuals almost certainly contributes to their increased risk of developing cancer. Although to date, the metabolism of dysfunctional NK cells from patients harbouring chronic viral infections, has not been assessed in detail, I would hypothesise that these NK cells would also be metabolically impaired. This idea is supported by evidence generated by Mala Maini's group which identified that exhausted virus-specific CD8+T cells have metabolic defects (Schurich et al. 2016). Therefore, defective metabolism is emerging as a key contributing factor to NK cell dysfunction.

Work from this report combined with recent studies from the field, has started to shed light on the mechanisms disrupting NK cell metabolism in cancer and obesity (**Fig 6.1**). For instance, it is well established that the tumour microenvironment (TME) has a suppressive effect on NK cell functions. It is interesting to note that many of the ways by which tumours can inhibit NK cell activity, can involve inhibition of NK cell metabolism. For example, lactate produced in the TME can lead to mitochondrial dysfunction and apoptosis in NK cells in the context of colorectal liver metastasis (Harmon et al. 2019). Immunosuppressive cytokines

such as TGF-β can be secreted by tumour cells and TGF-β can induce inhibit NK cells metabolism and cause functional defects (Viel et al. 2016; Zaiatz-Bittencourt, Finlay, and Gardiner 2018). In the context of lung cancer, TGF-β has been described to inhibit NK cell function through induction of fructose-1,6-bisphosphatase (FBP1), which impairs glycolysis (Cong et al. 2018). Of note, the impact of TGF-β on NK cell metabolism in cancer patients is not limited to NK cells in the TME, TGF-β can also impact peripheral NK cells. It has recently been shown by Slattery et al. that neutralising TGF-β can rescue some of the metabolic and functional defects found in NK cells from the peripheral blood of metastatic breast cancer patients (Slattery et al. 2019).

The immunomodulatory nature of the TME may contribute to why NK cell therapies are less efficacious against solid tumours than haematological malignancies. Furthermore, the TME can lead to competition for nutrients (Kedia-Mehta and Finlay 2019). Excessive glucose consumption by cancer cells in a mouse sarcoma model was shown to restrict the metabolism of CD8+ T cells and thus permit tumour progression (Chang et al. 2015). It is likely that this could also be the case for NK cells. Nutrient depletion is known to negatively impact NK cell function (Loftus et al. 2018; Donnelly et al. 2014). Glucose depletion impairs NK cell metabolism, as does depletion of amino acids (Donnelly and Finlay 2015; Loftus et al. 2018). The metabolic regulator cMYC is acutely sensitive to amino acids, in particular glutamine which supports transport through SLC7A5 to sustain expression of cMYC (Loftus et al. 2018). Data presented in this report revealed that the activity of SREBP transcription factors is also essential for coordinating NK cell metabolic and functional responses. As SREBP activity is post-translationally regulated by the presence of high concentrations of cholesterol and oxysterols, increased production of these molecules in the TME are likely to effect NK cell metabolism and function. Indeed it has been shown that CD8+ T cells undergo exhaustion due to heightened cholesterol levels in the TME (Ma et al. 2019). Furthermore data presented in this thesis show oxysterols such as 25HC and 27HC can inhibit NK cell metabolism and function. Of note, both of these oxysterol

species can be produced by cancer cells (Eibinger et al. 2013; Nelson et al. 2013). Hypercholesterolemia is often a co-morbidity associated with obesity. Whether the defects in circulating NK cells in obese individuals are due to increased cholesterol and oxysterols remains to be determined. However, it is known that excess lipids can cause NK cell defects (Michelet et al. 2018). Free-fatty acids, which are enriched in the plasma of obese individuals, can induce PPAR signalling and lipid accumulation in NK cells, which is detrimental to NK cell metabolism and function through negative actions on mTORC1 signalling (Boden and Shulman 2002; Michelet et al. 2018). These findings along with further understanding of how NK cell metabolism and function is being dysregulated in these cases, will shed light on possible ways to counteract these defects to improve patient therapies.

An example of where immune cells are increasingly used as therapies is in the context of cancer. For instance, the development of chimeric antigen receptor (CAR) engineered immune cells has shown promise in the treatment of a number of cancers. CAR engineering involves introducing artificial receptors which are specific for tumour-antigen, onto immune cells. Until recently, the majority of efforts investigating CAR-based therapies were directed towards T cells. Indeed, CAR-T cell therapies have been successful in the treatment of certain cancers (Grupp et al. 2013; Maude et al. 2014). However, more recently, CAR-NK cells have been investigated in the context of cancer therapy (Li, Hermanson, et al. 2018). There are multiple benefits that make the development of CAR NK cells an attractive therapeutic target. For instance, in contrast with CAR-T cell counterparts, NK cells display an enhanced safety profile, in-part due to their short-lived nature. Furthermore, the need to generate autologous patient CAR-T cells limits their use as an 'off-the-shelf' treatment. Conversely, CAR-NK cells can be used allogenically, as they are not at risk of inducing graft-versus-host disease (GvHD) or cytokine-release syndrome, common safety concerns associated with CAR-T cell therapies (Rezvani et al. 2017). Indeed, Li et al. compared the toxicities of CAR-T and CAR-NK cell therapies in a mouse ovarian cancer xenograft model

and found that despite both therapies reducing tumour burden to the same extent, CAR-NK cell treatment resulted in far less pathology than that caused by CAR-T cell therapy (Li, Hermanson, et al. 2018). Furthermore, the ability to expand induced pluripotent stem cell (iPSC)-derived NK cells and NK cell lines such as NK92 cells with ease, provides an opportunity to provide engineered CAR-NK cells 'off-the shelf' (Suck et al. 2016; Li, Hermanson, et al. 2018). Therefore, CAR-NK cell therapies are an attractive an exciting new avenue to explore in the immunotherapeutic field.

However, a barrier to the success of these NK cell-based immunotherapies, is the immunosuppressive mechanisms that can be encountered upon their administration to cancer patients. Therefore it is valuable to consider potential ways to combat these hurdles when developing new therapies to harness the immune system. A promising route to address this problem is to further artificially engineer CAR-NK cells, to make them more robust in the context of restrictive tumour environments and to make them resistant to the metabolically restrictive TME and immunosuppressive tumour-derived products. Drawing from our knowledge of the challenges the TME poses to NK cell metabolism and function a number of strategies could be employed. For example, data in this thesis identified that SREBP transcription factors are essential for NK cell metabolism and function, and given the knowledge that oxysterols that inhibit SREBP can be produced in the TME, inducing a form of SREBP that is resistant to oxysterol inhibition could be beneficial. This could be achieved through transgenic expression of the cleaved-terminal portion of SREBP, that lacks a membrane bound portion (Shimano et al. 1997). This would mean that SREBP could translocate freely to the nucleus, even in the presence of high concentrations of cholesterol and oxysterols. This approach may apply not only improve CAR-NK responses in the TME but also may prevent metastasis as NK cells in circulation may also come across increased cholesterol and oxysterol concentrations. This is especially true for immunotherapies being administered to patients with hypercholesterolemia.

This is just one of many possible strategies that could be harnessed to enhance NK cell metabolism and function for immunotherapies. However such ideas for therapeutics must be considered carefully as chronic metabolic activation has been shown to be detrimental to NK cell survival (Castro et al. 2018). This is of importance as many strategies are being developed aimed at enhancing NK cell functions through enhanced signalling (Miller and Lanier 2019). For instance, IL15 has become an attractive target due its well documented role in NK cell survival, with the added benefit that IL15 does not stimulate Tregs as IL2 does. Clinical trials using recombinant IL15 as a cancer treatment are underway (Conlon et al. 2015; Miller et al. 2018). However, it has recently been shown that chronic exposure of human NK cells to IL15 cytokine *in vitro* results in reduced NK cell metabolic rates (Felices et al. 2018). It is also important to consider that although many studies are focusing on cytokine administration or engineering receptors to drive NK cell activation in the TME through enhanced signalling, if NK cell metabolism is fundamentally impaired downstream of the signalling pathways involved, these efforts may be futile. This is significant as many of the inhibitors of NK cell metabolism discussed previously, bypass NK cell signalling and act directly on metabolic regulators or metabolic pathways. Therefore it may be worth focusing on engineering ways to make NK cells more resilient in the harsh tumour environment the encounter.

Much of research into the development of pharmacologic cancer therapies to date, focuses on the impact of drugs on the growth and proliferation of cancer cells. However it is necessary to highlight that many pathways identified to be important for tumour cell growth and proliferation also have important roles in immune cells. For instance, targeting cellular metabolism has been proposed as a strategy to specifically treat cancer cells as they have a higher metabolic demands to 'normal' quiescent cells. However, it is now clear that immune cells would also be affected and that this strategy is therefore not specific (Luengo, Gui, and Vander Heiden 2017). Therefore, effects on both the immune cell and the cancer cell must be considered. This concept was highlighted in a study by Bottos et al,

who identify that inhibition of the JAK pathway – with the aim of reducing breast cancer metastasis, actually resulted in enhanced metastatic burden due to unwanted NK cell inhibition (Bottos et al. 2016).

Data from this report have identified other proposed treatments that may have unwanted inhibitory effects on NK cells. For instance, the important role for polyamine synthesis and hypusination in cancer cells has led to these pathways becoming attractive targets for cell therapies. Indeed, DFMO, which inhibits *de novo* polyamine synthesis, is undergoing clinical trials for use in neuroblastoma and colorectal cancer treatment (LoGiudice et al. 2018). Of note, DFMO has also been approved by the FDA for the treatment of African sleeping sickness (LoGiudice et al. 2018). Similarly, inhibition of hypusination has been suggested as a promising route for cancer treatment (Nakanishi and Cleveland 2016). Given the findings of this thesis, I would argue that such treatments may be detrimental to the anti-tumour immune response and therefore should be considered with care. This is especially true with the growing movement towards the use of combination therapies. Any use of these inhibitors with immunotherapies involving NK cells may negate their activity.

A surge in growth in the field of immunometabolism has identified that cellular metabolism and immune cell functions are integrally linked. However, the majority of studies have focused on the roles of the major bioenergetic pathways such as glycolysis and OxPhos in immune cells. Data presented in this thesis highlights that peripheral metabolic pathways can also have major contributions to the metabolism and function of immune cells and therefore should not be overlooked. The key lesson learned from this body of work is that we need to understand the metabolism and key regulatory nodes involved in cells of the immune system in order to be fully informed on the benefits and drawbacks of certain treatment approaches - only then can we provide efficient strategies to direct beneficial immune responses.

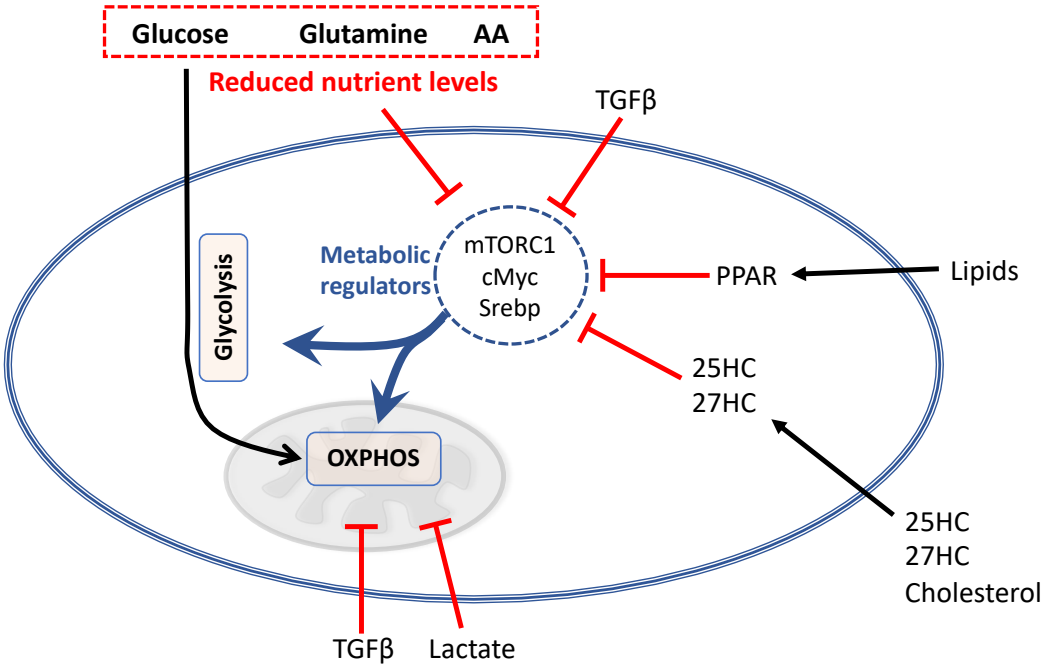

Figure 6.1 Mechanisms disrupting NK cell metabolism in cancer and obesity

In cancer, low levels of nutrients (red box) in the tumour microenvironment can impair NK cell metabolism. Limiting glucose, the key fuel for NK cells, will directly impact upon glycolysis and OxPhos rates. Restricted availability of glucose, glutamine or amino acids (AA), such as leucine, can impact upon the activity metabolic regulators mTORC1 and cMYC and so inhibit NK cell metabolism. TGFβ can inhibit NK cell metabolism through multiple mechanisms; the inhibition of mTORC1, inhibition of mitochondrial metabolism through canonical TGFβ signalling,. Cholesterol and oxysterols such as 25HC and 27HC are elevated in certain cancers and can inhibit SREBP activation, which would lead to inhibition NK cell metabolism. High concentrations of lactate in the TME can impact upon mitochondrial fitness and impair OxPhos levels. In obesity, PPAR activation by lipid ligands leads to lipid accumulation in NK cells, the inhibition of mTORC1 signalling and a state of metabolic paralysis.

7 Bibliography

Abel, A. M., A. A. Tiwari, Z. J. Gerbec, J. R. Siebert, C. Yang, N. J. Schloemer, K. J. Dixon, M. S. Thakar, and S. Malarkannan. 2018. 'IQ Domain-Containing GTPase-Activating Protein 1 Regulates Cytoskeletal Reorganization and Facilitates NKG2D-Mediated Mechanistic Target of Rapamycin Complex 1 Activation and Cytokine Gene Translation in Natural Killer Cells', *Front Immunol*, 9: 1168.

Adams, C. M., J. Reitz, J. K. De Brabander, J. D. Feramisco, L. Li, M. S. Brown, and J. L. Goldstein. 2004. 'Cholesterol and 25-hydroxycholesterol inhibit activation of SREBPs by different mechanisms, both involving SCAP and Insigs', *J Biol Chem*, 279: 52772-80.

Amemiya-Kudo, M., H. Shimano, A. H. Hasty, N. Yahagi, T. Yoshikawa, T. Matsuzaka, H. Okazaki, Y. Tamura, Y. Iizuka, K. Ohashi, J. Osuga, K. Harada, T. Gotoda, R. Sato, S. Kimura, S. Ishibashi, and N. Yamada. 2002. 'Transcriptional activities of nuclear SREBP-1a, -1c, and -2 to different target promoters of lipogenic and cholesterogenic genes', *J Lipid Res*, 43: 1220-35.

Assmann, N., K. L. O'Brien, R. P. Donnelly, L. Dyck, V. Zaiatz-Bittencourt, R. M. Loftus, P. Heinrich, P. J. Oefner, L. Lynch, C. M. Gardiner, K. Dettmer, and D. K. Finlay. 2017. 'Srebp-controlled glucose metabolism is essential for NK cell functional responses', *Nat Immunol*, 18: 1197-206.

Aversa, F., A. Terenzi, A. Tabilio, F. Falzetti, A. Carotti, S. Ballanti, R. Felicini, F. Falcinelli, A. Velardi, L. Ruggeri, T. Aloisi, J. P. Saab, A. Santucci, K. Perruccio, M. P. Martelli, C. Mecucci, Y. Reisner, and M. F. Martelli. 2005. 'Full haplotype-mismatched hematopoietic stem-cell transplantation: a phase II study in patients with acute leukemia at high risk of relapse', *J Clin Oncol*, 23: 3447-54.

Avni, O., D. Lee, F. Macian, S. J. Szabo, L. H. Glimcher, and A. Rao. 2002. 'T(H) cell differentiation is accompanied by dynamic changes in histone acetylation of cytokine genes', *Nat Immunol*, 3: 643-51.

Bakan, I., and M. Laplante. 2012. 'Connecting mTORC1 signaling to SREBP-1 activation', *Curr Opin Lipidol*, 23: 226-34.

Balmer, M. L., E. H. Ma, G. R. Bantug, J. Grahlert, S. Pfister, T. Glatter, A. Jauch, S. Dimeloe, E. Slack, P. Dehio, M. A. Krzyzaniak, C. G. King, A. V. Burgener, M. Fischer, L. Develioglu, R. Belle, M. Recher, W. V. Bonilla, A. J. Macpherson, S. Hapfelmeier, R. G. Jones, and C. Hess. 2016. 'Memory CD8(+) T Cells Require Increased Concentrations of Acetate Induced by Stress for Optimal Function', *Immunity*, 44: 1312-24.

Bauman, D. R., A. D. Bitmansour, J. G. McDonald, B. M. Thompson, G. Liang, and D. W. Russell. 2009. '25-Hydroxycholesterol secreted by macrophages in response to Toll-like receptor activation suppresses immunoglobulin A production', *Proc Natl Acad Sci U S A*, 106: 16764-9.

Bello-Fernandez, C., G. Packham, and J. L. Cleveland. 1993. 'The ornithine decarboxylase gene is a transcriptional target of c-Myc', *Proc Natl Acad Sci U S A*, 90: 7804-8.

Bensinger, S. J., M. N. Bradley, S. B. Joseph, N. Zelcer, E. M. Janssen, M. A. Hausner, R. Shih, J. S. Parks, P. A. Edwards, B. D. Jamieson, and P. Tontonoz. 2008.

'LXR signaling couples sterol metabolism to proliferation in the acquired immune response', *Cell*, 134: 97-111.

Berod, L., C. Friedrich, A. Nandan, J. Freitag, S. Hagemann, K. Harmrolfs, A. Sandouk, C. Hesse, C. N. Castro, H. Bahre, S. K. Tschirner, N. Gorinski, M. Gohmert, C. T. Mayer, J. Huehn, E. Ponimaskin, W. R. Abraham, R. Muller, M. Lochner, and T. Sparwasser. 2014. 'De novo fatty acid synthesis controls the fate between regulatory T and T helper 17 cells', *Nat Med*, 20: 1327-33.

Bersell, K., S. Choudhury, M. Mollova, B. D. Polizzotti, B. Ganapathy, S. Walsh, B. Wadugu, S. Arab, and B. Kuhn. 2013. 'Moderate and high amounts of tamoxifen in alphaMHC-MerCreMer mice induce a DNA damage response, leading to heart failure and death', *Dis Model Mech*, 6: 1459-69.

Bevec, D., H. Klier, W. Holter, E. Tschachler, P. Valent, F. Lottspeich, T. Baumruker, and J. Hauber. 1994. 'Induced gene expression of the hypusine-containing protein eukaryotic initiation factor 5A in activated human T lymphocytes', *Proc Natl Acad Sci U S A*, 91: 10829-33.

Bezman, N. A., C. C. Kim, J. C. Sun, G. Min-Oo, D. W. Hendricks, Y. Kamimura, J. A. Best, A. W. Goldrath, and L. L. Lanier. 2012. 'Molecular definition of the identity and activation of natural killer cells', *Nat Immunol*, 13: 1000-9.

Bhat, R., and C. Watzl. 2007. 'Serial killing of tumor cells by human natural killer cells--enhancement by therapeutic antibodies', *PLoS One*, 2: e326.

Bihl, F., J. Pecheur, B. Breart, G. Poupon, J. Cazareth, V. Julia, N. Glaichenhaus, and V. M. Braud. 2010. 'Primed antigen-specific CD4+ T cells are required for NK cell activation in vivo upon Leishmania major infection', *J Immunol*, 185: 2174-81.

Biron, C. A., K. S. Byron, and J. L. Sullivan. 1989. 'Severe herpesvirus infections in an adolescent without natural killer cells', *N Engl J Med*, 320: 1731-5.

Bluman, E. M., K. J. Bartynski, B. R. Avalos, and M. A. Caligiuri. 1996. 'Human natural killer cells produce abundant macrophage inflammatory protein-1 alpha in response to monocyte-derived cytokines', *J Clin Invest*, 97: 2722-7.

Boden, G., and G. I. Shulman. 2002. 'Free fatty acids in obesity and type 2 diabetes: defining their role in the development of insulin resistance and beta-cell dysfunction', *Eur J Clin Invest*, 32 Suppl 3: 14-23.

Borgquist, S., A. Giobbie-Hurder, T. P. Ahern, J. E. Garber, M. Colleoni, I. Lang, M. Debled, B. Ejlertsen, R. von Moos, I. Smith, A. S. Coates, A. Goldhirsch, M. Rabaglio, K. N. Price, R. D. Gelber, M. M. Regan, and B. Thurlimann. 2017. 'Cholesterol, Cholesterol-Lowering Medication Use, and Breast Cancer Outcome in the BIG 1-98 Study', *J Clin Oncol*, 35: 1179-88.

Bottos, A., D. Gotthardt, J. W. Gill, A. Gattelli, A. Frei, A. Tzankov, V. Sexl, A. Wodnar-Filipowicz, and N. E. Hynes. 2016. 'Decreased NK-cell tumour immunosurveillance consequent to JAK inhibition enhances metastasis in breast cancer models', *Nat Commun*, 7: 12258.

Bowlin, T. L., B. J. McKown, G. F. Babcock, and P. S. Sunkara. 1987. 'Intracellular polyamine biosynthesis is required for interleukin 2 responsiveness during lymphocyte mitogenesis', *Cell Immunol*, 106: 420-7.

Boyd, N. F., and V. McGuire. 1990. 'Evidence of association between plasma high-density lipoprotein cholesterol and risk factors for breast cancer', *J Natl Cancer Inst*, 82: 460-8.

Boyman, O., and J. Sprent. 2012. 'The role of interleukin-2 during homeostasis and activation of the immune system', *Nat Rev Immunol*, 12: 180-90.

Brown, M. S., and J. L. Goldstein. 1974. 'Suppression of 3-hydroxy-3-methylglutaryl coenzyme A reductase activity and inhibition of growth of human fibroblasts by 7-ketocholesterol', *J Biol Chem*, 249: 7306-14.

Brown, M.S. 2009. 'Cholesterol feedback: from Schoenheimer's bottle to Scap's MELADL', *J Lipid Res*, 50 Suppl: S15-27.

Browne, K. A., E. Blink, V. R. Sutton, C. J. Froelich, D. A. Jans, and J. A. Trapani. 1999. 'Cytosolic delivery of granzyme B by bacterial toxins: evidence that endosomal disruption, in addition to transmembrane pore formation, is an important function of perforin', *Mol Cell Biol*, 19: 8604-15.

Bryceson, Y. T., M. E. March, H. G. Ljunggren, and E. O. Long. 2006. 'Synergy among receptors on resting NK cells for the activation of natural cytotoxicity and cytokine secretion', *Blood*, 107: 159-66.

Calle, E. E., and R. Kaaks. 2004. 'Overweight, obesity and cancer: epidemiological evidence and proposed mechanisms', *Nat Rev Cancer*, 4: 579-91.

Campbell, K. S., and J. Hasegawa. 2013. 'Natural killer cell biology: an update and future directions', *J Allergy Clin Immunol*, 132: 536-44.

Caras, I., A. Grigorescu, C. Stavaru, D. L. Radu, I. Mogos, G. Szegli, and A. Salageanu. 2004. 'Evidence for immune defects in breast and lung cancer patients', *Cancer Immunol Immunother*, 53: 1146-52.

Castro, W., S. T. Chelbi, C. Niogret, C. Ramon-Barros, S. P. M. Welten, K. Osterheld, H. Wang, G. Rota, L. Morgado, E. Vivier, M. E. Raeber, O. Boyman, M. Delorenzi, D. Barras, P. C. Ho, A. Oxenius, and G. Guarda. 2018. 'The transcription factor Rfx7 limits metabolism of NK cells and promotes their maintenance and immunity', *Nat Immunol*, 19: 809-20.

Cerwenka, A., and L. L. Lanier. 2016. 'Natural killer cell memory in infection, inflammation and cancer', *Nat Rev Immunol*, 16: 112-23.

Chan, C. J., M. J. Smyth, and L. Martinet. 2014. 'Molecular mechanisms of natural killer cell activation in response to cellular stress', *Cell Death Differ*, 21: 5-14.

Chang, C. H., J. D. Curtis, L. B. Maggi, Jr., B. Faubert, A. V. Villarino, D. O'Sullivan, S. C. Huang, G. J. van der Windt, J. Blagih, J. Qiu, J. D. Weber, E. J. Pearce, R. G. Jones, and E. L. Pearce. 2013. 'Posttranscriptional control of T cell effector function by aerobic glycolysis', *Cell*, 153: 1239-51.

Chang, C. H., J. Qiu, D. O'Sullivan, M. D. Buck, T. Noguchi, J. D. Curtis, Q. Chen, M. Gindin, M. M. Gubin, G. J. van der Windt, E. Tonc, R. D. Schreiber, E. J. Pearce, and E. L. Pearce. 2015. 'Metabolic Competition in the Tumor Microenvironment Is a Driver of Cancer Progression', *Cell*, 162: 1229-41.

Chang, S., and T. M. Aune. 2005. 'Histone hyperacetylated domains across the Ifng gene region in natural killer cells and T cells', *Proc Natl Acad Sci U S A*, 102: 17095-100.

Chen, G., G. Liang, J. Ou, J. L. Goldstein, and M. S. Brown. 2004. 'Central role for liver X receptor in insulin-mediated activation of Srebp-1c transcription

and stimulation of fatty acid synthesis in liver', *Proc Natl Acad Sci U S A*, 101: 11245-50.

Chen, H. W., H. J. Heiniger, and A. A. Kandutsch. 1975. 'Relationship between sterol synthesis and DNA synthesis in phytohemagglutinin-stimulated mouse lymphocytes', *Proc Natl Acad Sci U S A*, 72: 1950-4.

Chiossone, L., J. Chaix, N. Fuseri, C. Roth, E. Vivier, and T. Walzer. 2009. 'Maturation of mouse NK cells is a 4-stage developmental program', *Blood*, 113: 5488-96.

Chisholm, S. E., and H. T. Reyburn. 2006. 'Recognition of vaccinia virus-infected cells by human natural killer cells depends on natural cytotoxicity receptors', *J Virol*, 80: 2225-33.

Choi, P. J., and T. J. Mitchison. 2013. 'Imaging burst kinetics and spatial coordination during serial killing by single natural killer cells', *Proc Natl Acad Sci U S A*, 110: 6488-93.

Clement, P. M., H. M. Hanauske-Abel, E. C. Wolff, H. K. Kleinman, and M. H. Park. 2002. 'The antifungal drug ciclopirox inhibits deoxyhypusine and proline hydroxylation, endothelial cell growth and angiogenesis in vitro', *Int J Cancer*, 100: 491-8.

Coca, S., J. Perez-Piqueras, D. Martinez, A. Colmenarejo, M. A. Saez, C. Vallejo, J. A. Martos, and M. Moreno. 1997. 'The prognostic significance of intratumoral natural killer cells in patients with colorectal carcinoma', *Cancer*, 79: 2320-8.

Colgan, S. M., D. Tang, G. H. Werstuck, and R. C. Austin. 2007. 'Endoplasmic reticulum stress causes the activation of sterol regulatory element binding protein-2', *Int J Biochem Cell Biol*, 39: 1843-51.

Collins, J. L., A. M. Fivush, M. A. Watson, C. M. Galardi, M. C. Lewis, L. B. Moore, D. J. Parks, J. G. Wilson, T. K. Tippin, J. G. Binz, K. D. Plunket, D. G. Morgan, E. J. Beaudet, K. D. Whitney, S. A. Kliewer, and T. M. Willson. 2002. 'Identification of a nonsteroidal liver X receptor agonist through parallel array synthesis of tertiary amines', *J Med Chem*, 45: 1963-6.

Colvin, S. C., B. Maier, D. L. Morris, S. A. Tersey, and R. G. Mirmira. 2013. 'Deoxyhypusine synthase promotes differentiation and proliferation of T helper type 1 (Th1) cells in autoimmune diabetes', *J Biol Chem*, 288: 36226-35.

Cong, J., X. Wang, X. Zheng, D. Wang, B. Fu, R. Sun, Z. Tian, and H. Wei. 2018. 'Dysfunction of Natural Killer Cells by FBP1-Induced Inhibition of Glycolysis during Lung Cancer Progression', *Cell Metab*, 28: 243-55.e5.

Conlon, K. C., E. Lugli, H. C. Welles, S. A. Rosenberg, A. T. Fojo, J. C. Morris, T. A. Fleisher, S. P. Dubois, L. P. Perera, D. M. Stewart, C. K. Goldman, B. R. Bryant, J. M. Decker, J. Chen, T. A. Worthy, W. D. Figg, Sr., C. J. Peer, M. C. Sneller, H. C. Lane, J. L. Yovandich, S. P. Creekmore, M. Roederer, and T. A. Waldmann. 2015. 'Redistribution, hyperproliferation, activation of natural killer cells and CD8 T cells, and cytokine production during first-in-human clinical trial of recombinant human interleukin-15 in patients with cancer', *J Clin Oncol*, 33: 74-82.

Cooper, M. A., J. E. Bush, T. A. Fehniger, J. B. VanDeusen, R. E. Waite, Y. Liu, H. L. Aguila, and M. A. Caligiuri. 2002. 'In vivo evidence for a dependence on interleukin 15 for survival of natural killer cells', *Blood*, 100: 3633-8.

Cooper, M. A., J. M. Elliott, P. A. Keyel, L. Yang, J. A. Carrero, and W. M. Yokoyama. 2009. 'Cytokine-induced memory-like natural killer cells', *Proc Natl Acad Sci U S A*, 106: 1915-9.

Crick, P. J., W. J. Griffiths, J. Zhang, M. Beibel, J. Abdel-Khalik, J. Kuhle, A. W. Sailer, and Y. Wang. 2017. 'Reduced Plasma Levels of 25-Hydroxycholesterol and Increased Cerebrospinal Fluid Levels of Bile Acid Precursors in Multiple Sclerosis Patients', *Mol Neurobiol*, 54: 8009-20.

Cui, G., X. Qin, L. Wu, Y. Zhang, X. Sheng, Q. Yu, H. Sheng, B. Xi, J. Z. Zhang, and Y. Q. Zang. 2011. 'Liver X receptor (LXR) mediates negative regulation of mouse and human Th17 differentiation', *J Clin Invest*, 121: 658-70.

Dennis, E. A., R. A. Deems, R. Harkewicz, O. Quehenberger, H. A. Brown, S. B. Milne, D. S. Myers, C. K. Glass, G. Hardiman, D. Reichart, A. H. Merrill, Jr., M. C. Sullards, E. Wang, R. C. Murphy, C. R. Raetz, T. A. Garrett, Z. Guan, A. C. Ryan, D. W. Russell, J. G. McDonald, B. M. Thompson, W. A. Shaw, M. Sud, Y. Zhao, S. Gupta, M. R. Maurya, E. Fahy, and S. Subramaniam. 2010. 'A mouse macrophage lipidome', *J Biol Chem*, 285: 39976-85.

Diczfalusy, U., K. E. Olofsson, A. M. Carlsson, M. Gong, D. T. Golenbock, O. Rooyackers, U. Flaring, and H. Bjorkbacka. 2009. 'Marked upregulation of cholesterol 25-hydroxylase expression by lipopolysaccharide', *J Lipid Res*, 50: 2258-64.

Dong, H., N. M. Adams, Y. Xu, J. Cao, D. S. J. Allan, J. R. Carlyle, X. Chen, J. C. Sun, and L. H. Glimcher. 2019. 'The IRE1 endoplasmic reticulum stress sensor activates natural killer cell immunity in part by regulating c-Myc', *Nat Immunol*, 20: 865-78.

Donnelly, R. P., and D. K. Finlay. 2015. 'Glucose, glycolysis and lymphocyte responses', *Mol Immunol*, 68: 513-9.

Donnelly, R. P., R. M. Loftus, S. E. Keating, K. T. Liou, C. A. Biron, C. M. Gardiner, and D. K. Finlay. 2014. 'mTORC1-dependent metabolic reprogramming is a prerequisite for NK cell effector function', *J Immunol*, 193: 4477-84.

Duvel, K., J. L. Yecies, S. Menon, P. Raman, A. I. Lipovsky, A. L. Souza, E. Triantafellow, Q. Ma, R. Gorski, S. Cleaver, M. G. Vander Heiden, J. P. MacKeigan, P. M. Finan, C. B. Clish, L. O. Murphy, and B. D. Manning. 2010. 'Activation of a metabolic gene regulatory network downstream of mTOR complex 1', *Mol Cell*, 39: 171-83.

Eibinger, G., G. Fauler, E. Bernhart, S. Frank, A. Hammer, A. Wintersperger, H. Eder, A. Heinemann, P. S. Mischel, E. Malle, and W. Sattler. 2013. 'On the role of 25-hydroxycholesterol synthesis by glioblastoma cell lines. Implications for chemotactic monocyte recruitment', *Exp Cell Res*, 319: 1828-38.

Eisenberg, T., H. Knauer, A. Schauer, S. Buttner, C. Ruckenstuhl, D. Carmona-Gutierrez, J. Ring, S. Schroeder, C. Magnes, L. Antonacci, H. Fussi, L. Deszcz, R. Hartl, E. Schraml, A. Criollo, E. Megalou, D. Weiskopf, P. Laun, G. Heeren, M. Breitenbach, B. Grubeck-Loebenstein, E. Herker, B. Fahrenkrog, K. U. Frohlich, F. Sinner, N. Tavernarakis, N. Minois, G. Kroemer, and F. Madeo.

2009. 'Induction of autophagy by spermidine promotes longevity', *Nat Cell Biol*, 11: 1305-14.

Epis, M. R., K. M. Giles, F. C. Kalinowski, A. Barker, R. J. Cohen, and P. J. Leedman. 2012. 'Regulation of expression of deoxyhypusine hydroxylase (DOHH), the enzyme that catalyzes the activation of eIF5A, by miR-331-3p and miR-642-5p in prostate cancer cells', *J Biol Chem*, 287: 35251-9.

Eriksson, M., G. Leitz, E. Fallman, O. Axner, J. C. Ryan, M. C. Nakamura, and C. L. Sentman. 1999. 'Inhibitory receptors alter natural killer cell interactions with target cells yet allow simultaneous killing of susceptible targets', *J Exp Med*, 190: 1005-12.

Fauriat, C., E. O. Long, H. G. Ljunggren, and Y. T. Bryceson. 2010. 'Regulation of human NK-cell cytokine and chemokine production by target cell recognition', *Blood*, 115: 2167-76.

Fehniger, T. A., S. F. Cai, X. Cao, A. J. Bredemeyer, R. M. Presti, A. R. French, and T. J. Ley. 2007. 'Acquisition of murine NK cell cytotoxicity requires the translation of a pre-existing pool of granzyme B and perforin mRNAs', *Immunity*, 26: 798-811.

Feldman, M. E., and K. M. Shokat. 2010. 'New inhibitors of the PI3K-Akt-mTOR pathway: insights into mTOR signaling from a new generation of Tor Kinase Domain Inhibitors (TORKinibs)', *Curr Top Microbiol Immunol*, 347: 241-62.

Felices, M., A. J. Lenvik, R. McElmurry, S. Chu, P. Hinderlie, L. Bendzick, M. A. Geller, J. Tolar, B. R. Blazar, and J. S. Miller. 2018. 'Continuous treatment with IL-15 exhausts human NK cells via a metabolic defect', *JCI Insight*, 3.

Feng, T. H., K. H. Tsui, and H. H. Juang. 2005. 'Cholesterol modulation of the expression of mitochondrial aconitase in human prostatic carcinoma cells', *Chin J Physiol*, 48: 93-100.

Fernandez-Sanchez, A., A. Baragano Raneros, R. Carvajal Palao, A. B. Sanz, A. Ortiz, F. Ortega, B. Suarez-Alvarez, and C. Lopez-Larrea. 2013. 'DNA demethylation and histone H3K9 acetylation determine the active transcription of the NKG2D gene in human CD8+ T and NK cells', *Epigenetics*, 8: 66-78.

Fields, P. E., S. T. Kim, and R. A. Flavell. 2002. 'Cutting edge: changes in histone acetylation at the IL-4 and IFN-gamma loci accompany Th1/Th2 differentiation', *J Immunol*, 169: 647-50.

Finlay, D. K., E. Rosenzweig, L. V. Sinclair, C. Feijoo-Carnero, J. L. Hukelmann, J. Rolf, A. A. Panteleyev, K. Okkenhaug, and D. A. Cantrell. 2012a. 'PDK1 regulation of mTOR and hypoxia-inducible factor 1 integrate metabolism and migration of CD8+ T cells', *J Exp Med*, 209: 2441-53.

Fogel-Petrovic, M., D. L. Kramer, S. Vujcic, J. Miller, J. S. McManis, R. J. Bergeron, and C. W. Porter. 1997. 'Structural basis for differential induction of spermidine/spermine N1-acetyltransferase activity by novel spermine analogs', *Mol Pharmacol*, 52: 69-74.

Frey, P. A. 1996. 'The Leloir pathway: a mechanistic imperative for three enzymes to change the stereochemical configuration of a single carbon in galactose', *Faseb j*, 10: 461-70.

Garg, A., P. F. Barnes, A. Porgador, S. Roy, S. Wu, J. S. Nanda, D. E. Griffith, W. M. Girard, N. Rawal, S. Shetty, and R. Vankayalapati. 2006. 'Vimentin

expressed on Mycobacterium tuberculosis-infected human monocytes is involved in binding to the NKp46 receptor', *J Immunol*, 177: 6192-8.

Gerosa, F., B. Baldani-Guerra, C. Nisii, V. Marchesini, G. Carra, and G. Trinchieri. 2002. 'Reciprocal activating interaction between natural killer cells and dendritic cells', *J Exp Med*, 195: 327-33.

Gobert, A. P., Y. Cheng, J. Y. Wang, J. L. Boucher, R. K. Iyer, S. D. Cederbaum, R. A. Casero, Jr., J. C. Newton, and K. T. Wilson. 2002. 'Helicobacter pylori induces macrophage apoptosis by activation of arginase II', *J Immunol*, 168: 4692-700.

Gorelik, E., R. H. Wiltrout, K. Okumura, S. Habu, and R. B. Herberman. 1982. 'Role of NK cells in the control of metastatic spread and growth of tumor cells in mice', *Int J Cancer*, 30: 107-12.

Gosmain, Y., E. Lefai, S. Ryser, M. Roques, and H. Vidal. 2004. 'Sterol regulatory element-binding protein-1 mediates the effect of insulin on hexokinase II gene expression in human muscle cells', *Diabetes*, 53: 321-9.

Gostynski, M., F. Gutzwiller, K. Kuulasmaa, A. Doring, M. Ferrario, D. Grafnetter, and A. Pajak. 2004. 'Analysis of the relationship between total cholesterol, age, body mass index among males and females in the WHO MONICA Project', *Int J Obes Relat Metab Disord*, 28: 1082-90.

Grupp, S. A., M. Kalos, D. Barrett, R. Aplenc, D. L. Porter, S. R. Rheingold, D. T. Teachey, A. Chew, B. Hauck, J. F. Wright, M. C. Milone, B. L. Levine, and C. H. June. 2013. 'Chimeric antigen receptor-modified T cells for acute lymphoid leukemia', *N Engl J Med*, 368: 1509-18.

Guan, K. L., and Y. Xiong. 2011. 'Regulation of intermediary metabolism by protein acetylation', *Trends Biochem Sci*, 36: 108-16.

Guillerey, C., N. D. Huntington, and M. J. Smyth. 2016. 'Targeting natural killer cells in cancer immunotherapy', *Nat Immunol*, 17: 1025-36.

Gutierrez, E., B. S. Shin, C. J. Woolstenhulme, J. R. Kim, P. Saini, A. R. Buskirk, and T. E. Dever. 2013. 'eIF5A promotes translation of polyproline motifs', *Mol Cell*, 51: 35-45.

Hameyer, D., A. Loonstra, L. Eshkind, S. Schmitt, C. Antunes, A. Groen, E. Bindels, J. Jonkers, P. Krimpenfort, R. Meuwissen, L. Rijswijk, A. Bex, A. Berns, and E. Bockamp. 2007. 'Toxicity of ligand-dependent Cre recombinases and generation of a conditional Cre deleter mouse allowing mosaic recombination in peripheral tissues', *Physiol Genomics*, 31: 32-41.

Hanahan, D., and R. A. Weinberg. 2011. 'Hallmarks of cancer: the next generation', *Cell*, 144: 646-74.

Harmon, C., M. W. Robinson, F. Hand, D. Almuaili, K. Mentor, D. D. Houlihan, E. Hoti, L. Lynch, J. Geoghegan, and C. O'Farrelly. 2019. 'Lactate-Mediated Acidification of Tumor Microenvironment Induces Apoptosis of Liver-Resident NK Cells in Colorectal Liver Metastasis', *Cancer Immunol Res*, 7: 335-46.

Hawkins, J. L., M. D. Robbins, L. C. Warren, D. Xia, S. F. Petras, J. J. Valentine, A. H. Varghese, I. K. Wang, T. A. Subashi, L. D. Shelly, B. A. Hay, K. T. Landschulz, K. F. Geoghegan, and H. J. Harwood, Jr. 2008. 'Pharmacologic inhibition of site 1 protease activity inhibits sterol regulatory element-binding protein processing and reduces lipogenic enzyme gene expression and lipid

synthesis in cultured cells and experimental animals', *J Pharmacol Exp Ther*, 326: 801-8.

Heiberg, I. L., L. J. Pallett, T. N. Winther, B. Hogh, M. K. Maini, and D. Peppa. 2015. 'Defective natural killer cell anti-viral capacity in paediatric HBV infection', *Clin Exp Immunol*, 179: 466-76.

Heng, T. S., and M. W. Painter. 2008. 'The Immunological Genome Project: networks of gene expression in immune cells', *Nat Immunol*, 9: 1091-4.

Herberman, R. B., M. E. Nunn, H. T. Holden, and D. H. Lavrin. 1975. 'Natural cytotoxic reactivity of mouse lymphoid cells against syngeneic and allogeneic tumors. II. Characterization of effector cells', *Int J Cancer*, 16: 230-9.

Horowitz, A., K. A. Stegmann, and E. M. Riley. 2011. 'Activation of natural killer cells during microbial infections', *Front Immunol*, 2: 88.

Horton, J. D., J. L. Goldstein, and M. S. Brown. 2002. 'SREBPs: activators of the complete program of cholesterol and fatty acid synthesis in the liver', *J Clin Invest*, 109: 1125-31.

Horton, J. D., N. A. Shah, J. A. Warrington, N. N. Anderson, S. W. Park, M. S. Brown, and J. L. Goldstein. 2003. 'Combined analysis of oligonucleotide microarray data from transgenic and knockout mice identifies direct SREBP target genes', *Proc Natl Acad Sci U S A*, 100: 12027-32.

Horton, J. D., I. Shimomura, M. S. Brown, R. E. Hammer, J. L. Goldstein, and H. Shimano. 1998. 'Activation of cholesterol synthesis in preference to fatty acid synthesis in liver and adipose tissue of transgenic mice overproducing sterol regulatory element-binding protein-2', *J Clin Invest*, 101: 2331-39.

Hua, X., C. Yokoyama, J. Wu, M. R. Briggs, M. S. Brown, J. L. Goldstein, and X. Wang. 1993. 'SREBP-2, a second basic-helix-loop-helix-leucine zipper protein that stimulates transcription by binding to a sterol regulatory element', *Proc Natl Acad Sci U S A*, 90: 11603-7.

Huang, S. C., B. Everts, Y. Ivanova, D. O'Sullivan, M. Nascimento, A. M. Smith, W. Beatty, L. Love-Gregory, W. Y. Lam, C. M. O'Neill, C. Yan, H. Du, N. A. Abumrad, J. F. Urban, Jr., M. N. Artyomov, E. L. Pearce, and E. J. Pearce. 2014. 'Cell-intrinsic lysosomal lipolysis is essential for alternative activation of macrophages', *Nat Immunol*, 15: 846-55.

Hukelmann, J. L., K. E. Anderson, L. V. Sinclair, K. M. Grzes, A. B. Murillo, P. T. Hawkins, L. R. Stephens, A. I. Lamond, and D. A. Cantrell. 2016. 'The cytotoxic T cell proteome and its shaping by the kinase mTOR', *Nat Immunol*, 17: 104-12.

Hume, D. A., J. L. Radik, E. Ferber, and M. J. Weidemann. 1978. 'Aerobic glycolysis and lymphocyte transformation', *Biochem J*, 174: 703-9.

Ikeda, H., L. J. Old, and R. D. Schreiber. 2002. 'The roles of IFN gamma in protection against tumor development and cancer immunoediting', *Cytokine Growth Factor Rev*, 13: 95-109.

Im, S. S., L. Yousef, C. Blaschitz, J. Z. Liu, R. A. Edwards, S. G. Young, M. Raffatellu, and T. F. Osborne. 2011. 'Linking lipid metabolism to the innate immune response in macrophages through sterol regulatory element binding protein-1a', *Cell Metab*, 13: 540-9.

Imai, K., S. Matsuyama, S. Miyake, K. Suga, and K. Nakachi. 2000. 'Natural cytotoxic activity of peripheral-blood lymphocytes and cancer incidence: an 11-year follow-up study of a general population', *Lancet*, 356: 1795-9.

Ishigami, S., S. Natsugoe, K. Tokuda, A. Nakajo, X. Che, H. Iwashige, K. Aridome, S. Hokita, and T. Aikou. 2000. 'Prognostic value of intratumoral natural killer cells in gastric carcinoma', *Cancer*, 88: 577-83.

Jackowski, S., J. Wang, and I. Baburina. 2000. 'Activity of the phosphatidylcholine biosynthetic pathway modulates the distribution of fatty acids into glycerolipids in proliferating cells', *Biochim Biophys Acta*, 1483: 301-15.

Janowski, B. A., P. J. Willy, T. R. Devi, J. R. Falck, and D. J. Mangelsdorf. 1996. 'An oxysterol signalling pathway mediated by the nuclear receptor LXR alpha', *Nature*, 383: 728-31.

Jensen, H., M. Potempa, D. Gotthardt, and L. L. Lanier. 2017. 'Cutting Edge: IL-2-Induced Expression of the Amino Acid Transporters SLC1A5 and CD98 Is a Prerequisite for NKG2D-Mediated Activation of Human NK Cells', *J Immunol*, 199: 1967-72.

Kagi, D., B. Ledermann, K. Burki, P. Seiler, B. Odermatt, K. J. Olsen, E. R. Podack, R. M. Zinkernagel, and H. Hengartner. 1994. 'Cytotoxicity mediated by T cells and natural killer cells is greatly impaired in perforin-deficient mice', *Nature*, 369: 31-7.

Kammoun, H. L., H. Chabanon, I. Hainault, S. Luquet, C. Magnan, T. Koike, P. Ferre, and F. Foufelle. 2009. 'GRP78 expression inhibits insulin and ER stress-induced SREBP-1c activation and reduces hepatic steatosis in mice', *J Clin Invest*, 119: 1201-15.

Kandutsch, A. A., and H. W. Chen. 1974. 'Inhibition of sterol synthesis in cultured mouse cells by cholesterol derivatives oxygenated in the side chain', *J Biol Chem*, 249: 6057-61.

Kandutsch, A. A. 1975. 'Regulation of sterol synthesis in cultured cells by oxygenated derivatives of cholesterol', *J Cell Physiol*, 85: 415-24.

Kang, H. A., and J. W. Hershey. 1994. 'Effect of initiation factor eIF-5A depletion on protein synthesis and proliferation of Saccharomyces cerevisiae', *J Biol Chem*, 269: 3934-40.

Karre, K., H. G. Ljunggren, G. Piontek, and R. Kiessling. 1986. 'Selective rejection of H-2-deficient lymphoma variants suggests alternative immune defence strategy', *Nature*, 319: 675-8.

Keating, S. E., V. Zaiatz-Bittencourt, R. M. Loftus, C. Keane, K. Brennan, D. K. Finlay, and C. M. Gardiner. 2016. 'Metabolic Reprogramming Supports IFN-gamma Production by CD56bright NK Cells', *J Immunol*, 196: 2552-60.

Kedia-Mehta, N., and D. K. Finlay. 2019. 'Competition for nutrients and its role in controlling immune responses', *Nat Commun*, 10: 2123.

Kedia-Mehta, Nidhi, Chloe Choi, Aisling McCrudden, Elisabeth Littwitz-Salomon, Proinnsias G. Fox, Clair M. Gardiner, and David K. Finlay. 2019. 'Natural Killer Cells Integrate Signals Received from Tumour Interactions and IL2 to Induce Robust and Prolonged Anti-Tumour Metabolic Responses', *Immunometabolism*, 1: e190014.

Kennedy, M. K., M. Glaccum, S. N. Brown, E. A. Butz, J. L. Viney, M. Embers, N. Matsuki, K. Charrier, L. Sedger, C. R. Willis, K. Brasel, P. J. Morrissey, K.

Stocking, J. C. Schuh, S. Joyce, and J. J. Peschon. 2000. 'Reversible defects in natural killer and memory CD8 T cell lineages in interleukin 15-deficient mice', *J Exp Med*, 191: 771-80.

Keppel, M. P., N. Saucier, A. Y. Mah, T. P. Vogel, and M. A. Cooper. 2015. 'Activation-specific metabolic requirements for NK Cell IFN-gamma production', *J Immunol*, 194: 1954-62.

Keppel, M. P., L. Yang, and M. A. Cooper. 2013. 'Murine NK cell intrinsic cytokine-induced memory-like responses are maintained following homeostatic proliferation', *J Immunol*, 190: 4754-62.

Kidani, Y., H. Elsaesser, M. B. Hock, L. Vergnes, K. J. Williams, J. P. Argus, B. N. Marbois, E. Komisopoulou, E. B. Wilson, T. F. Osborne, T. G. Graeber, K. Reue, D. G. Brooks, and S. J. Bensinger. 2013. 'Sterol regulatory element-binding proteins are essential for the metabolic programming of effector T cells and adaptive immunity', *Nat Immunol*, 14: 489-99.

Kim, S. C., R. Sprung, Y. Chen, Y. Xu, H. Ball, J. Pei, T. Cheng, Y. Kho, H. Xiao, L. Xiao, N. V. Grishin, M. White, X. J. Yang, and Y. Zhao. 2006. 'Substrate and functional diversity of lysine acetylation revealed by a proteomics survey', *Mol Cell*, 23: 607-18.

Koka, R., P. R. Burkett, M. Chien, S. Chai, F. Chan, J. P. Lodolce, D. L. Boone, and A. Ma. 2003. 'Interleukin (IL)-15R[alpha]-deficient natural killer cells survive in normal but not IL-15R[alpha]-deficient mice', *J Exp Med*, 197: 977-84.

Kolehmainen, M., H. Vidal, E. Alhava, and M. I. Uusitupa. 2001. 'Sterol regulatory element binding protein 1c (SREBP-1c) expression in human obesity', *Obes Res*, 9: 706-12.

Koppenol, W. H., P. L. Bounds, and C. V. Dang. 2011. 'Otto Warburg's contributions to current concepts of cancer metabolism', *Nat Rev Cancer*, 11: 325-37.

Kruse, M., O. Rosorius, F. Kratzer, D. Bevec, C. Kuhnt, A. Steinkasserer, G. Schuler, and J. Hauber. 2000. 'Inhibition of CD83 cell surface expression during dendritic cell maturation by interference with nuclear export of CD83 mRNA', *J Exp Med*, 191: 1581-90.

Lanier, L. L. 2005. 'NK cell recognition', *Annu Rev Immunol*, 23: 225-74.

Laplante, M., and D. M. Sabatini. 2013. 'Regulation of mTORC1 and its impact on gene expression at a glance', *J Cell Sci*, 126: 1713-9.

Lappano, R., A. G. Recchia, E. M. De Francesco, T. Angelone, M. C. Cerra, D. Picard, and M. Maggiolini. 2011. 'The cholesterol metabolite 25-hydroxycholesterol activates estrogen receptor alpha-mediated signaling in cancer cells and in cardiomyocytes', *PLoS One*, 6: e16631.

Lebeau, P., J. H. Byun, T. Yousof, and R. C. Austin. 2018. 'Pharmacologic inhibition of S1P attenuates ATF6 expression, causes ER stress and contributes to apoptotic cell death', *Toxicol Appl Pharmacol*, 349: 1-7.

Lee, J. N., and J. Ye. 2004. 'Proteolytic activation of sterol regulatory element-binding protein induced by cellular stress through depletion of Insig-1', *J Biol Chem*, 279: 45257-65.

Lee, J., M. C. Walsh, K. L. Hoehn, D. E. James, E. J. Wherry, and Y. Choi. 2014. 'Regulator of fatty acid metabolism, acetyl coenzyme a carboxylase 1, controls T cell immunity', *J Immunol*, 192: 3190-9.

Lee, J., T. Zhang, I. Hwang, A. Kim, L. Nitschke, M. Kim, J. M. Scott, Y. Kamimura, L. L. Lanier, and S. Kim. 2015. 'Epigenetic modification and antibody-dependent expansion of memory-like NK cells in human cytomegalovirus-infected individuals', *Immunity*, 42: 431-42.

Lee, S. H., M. F. Fragoso, and C. A. Biron. 2012. 'Cutting edge: a novel mechanism bridging innate and adaptive immunity: IL-12 induction of CD25 to form high-affinity IL-2 receptors on NK cells', *J Immunol*, 189: 2712-6.

Leong, J. W., J. M. Chase, R. Romee, S. E. Schneider, R. P. Sullivan, M. A. Cooper, and T. A. Fehniger. 2014. 'Preactivation with IL-12, IL-15, and IL-18 induces CD25 and a functional high-affinity IL-2 receptor on human cytokine-induced memory-like natural killer cells', *Biol Blood Marrow Transplant*, 20: 463-73.

Levin, V. A., M. D. Prados, W. K. Yung, M. J. Gleason, S. Ictech, and M. Malec. 1992. 'Treatment of recurrent gliomas with eflornithine', *J Natl Cancer Inst*, 84: 1432-7.

Li, C., Y. Q. Deng, S. Wang, F. Ma, R. Aliyari, X. Y. Huang, N. N. Zhang, M. Watanabe, H. L. Dong, P. Liu, X. F. Li, Q. Ye, M. Tian, S. Hong, J. Fan, H. Zhao, L. Li, N. Vishlaghi, J. E. Buth, C. Au, Y. Liu, N. Lu, P. Du, F. X. Qin, B. Zhang, D. Gong, X. Dai, R. Sun, B. G. Novitch, Z. Xu, C. F. Qin, and G. Cheng. 2017. '25-Hydroxycholesterol Protects Host against Zika Virus Infection and Its Associated Microcephaly in a Mouse Model', *Immunity*, 46: 446-56.

Li, D., W. Long, R. Huang, Y. Chen, and M. Xia. 2018. '27-Hydroxycholesterol Inhibits Sterol Regulatory Element-Binding Protein 1 Activation and Hepatic Lipid Accumulation in Mice', *Obesity (Silver Spring)*, 26: 713-22.

Li, S., M. S. Brown, and J. L. Goldstein. 2010. 'Bifurcation of insulin signaling pathway in rat liver: mTORC1 required for stimulation of lipogenesis, but not inhibition of gluconeogenesis', *Proc Natl Acad Sci U S A*, 107: 3441-6.

Li, S., W. Ogawa, A. Emi, K. Hayashi, Y. Senga, K. Nomura, K. Hara, D. Yu, and M. Kasuga. 2011. 'Role of S6K1 in regulation of SREBP1c expression in the liver', *Biochem Biophys Res Commun*, 412: 197-202.

Li, T., M. Liu, X. Feng, Z. Wang, I. Das, Y. Xu, X. Zhou, Y. Sun, K. L. Guan, Y. Xiong, and Q. Y. Lei. 2014. 'Glyceraldehyde-3-phosphate dehydrogenase is activated by lysine 254 acetylation in response to glucose signal', *J Biol Chem*, 289: 3775-85.

Li, X., J. B. Wu, Q. Li, K. Shigemura, L. W. Chung, and W. C. Huang. 2016. 'SREBP-2 promotes stem cell-like properties and metastasis by transcriptional activation of c-Myc in prostate cancer', *Oncotarget*, 7: 12869-84.

Li, Y., D. L. Hermanson, B. S. Moriarity, and D. S. Kaufman. 2018. 'Human iPSC-Derived Natural Killer Cells Engineered with Chimeric Antigen Receptors Enhance Anti-tumor Activity', *Cell Stem Cell*, 23: 181-92.e5.

Liesche, C., P. Sauer, I. Prager, D. Urlaub, M. Claus, R. Eils, J. Beaudouin, and C. Watzl. 2018. 'Single-Fluorescent Protein Reporters Allow Parallel Quantification of Natural Killer Cell-Mediated Granzyme and Caspase Activities in Single Target Cells', *Front Immunol*, 9: 1840.

Liu, C. C., B. Perussia, Z. A. Cohn, and J. D. Young. 1986. 'Identification and characterization of a pore-forming protein of human peripheral blood natural killer cells', *J Exp Med*, 164: 2061-76.

Liu, S. Y., R. Aliyari, K. Chikere, G. Li, M. D. Marsden, J. K. Smith, O. Pernet, H. Guo, R. Nusbaum, J. A. Zack, A. N. Freiberg, L. Su, B. Lee, and G. Cheng. 2013. 'Interferon-inducible cholesterol-25-hydroxylase broadly inhibits viral entry by production of 25-hydroxycholesterol', *Immunity*, 38: 92-105.

Loftus, R. M., N. Assmann, N. Kedia-Mehta, K. L. O'Brien, A. Garcia, C. Gillespie, J. L. Hukelmann, P. J. Oefner, A. I. Lamond, C. M. Gardiner, K. Dettmer, D. A. Cantrell, L. V. Sinclair, and D. K. Finlay. 2018. 'Amino acid-dependent cMyc expression is essential for NK cell metabolic and functional responses in mice', *Nat Commun*, 9: 2341.

Loftus, R. M., and D. K. Finlay. 2016. 'Immunometabolism: Cellular Metabolism Turns Immune Regulator', *J Biol Chem*, 291: 1-10.

LoGiudice, N., L. Le, I. Abuan, Y. Leizorek, and S. C. Roberts. 2018. 'Alpha-Difluoromethylornithine, an Irreversible Inhibitor of Polyamine Biosynthesis, as a Therapeutic Strategy against Hyperproliferative and Infectious Diseases', *Med Sci (Basel)*, 6.

Long, E. O. 2007. 'Ready for prime time: NK cell priming by dendritic cells', *Immunity*, 26: 385-7.

Loonstra, A., M. Vooijs, H. B. Beverloo, B. A. Allak, E. van Drunen, R. Kanaar, A. Berns, and J. Jonkers. 2001. 'Growth inhibition and DNA damage induced by Cre recombinase in mammalian cells', *Proc Natl Acad Sci U S A*, 98: 9209-14.

Lopez-Soto, A., S. Gonzalez, M. J. Smyth, and L. Galluzzi. 2017. 'Control of Metastasis by NK Cells', *Cancer Cell*, 32: 135-54.

Lozier, A. M., M. E. Rich, A. P. Grawe, A. S. Peck, P. Zhao, A. T. Chang, J. P. Bond, and G. S. Sholler. 2015. 'Targeting ornithine decarboxylase reverses the LIN28/Let-7 axis and inhibits glycolytic metabolism in neuroblastoma', *Oncotarget*, 6: 196-206.

Lu, Y., B. Hong, H. Li, Y. Zheng, M. Zhang, S. Wang, J. Qian, and Q. Yi. 2014. 'Tumor-specific IL-9-producing CD8+ Tc9 cells are superior effector than type-I cytotoxic Tc1 cells for adoptive immunotherapy of cancers', *Proc Natl Acad Sci U S A*, 111: 2265-70.

Lucas, M., W. Schachterle, K. Oberle, P. Aichele, and A. Diefenbach. 2007. 'Dendritic cells prime natural killer cells by trans-presenting interleukin 15', *Immunity*, 26: 503-17.

Luengo, A., D. Y. Gui, and M. G. Vander Heiden. 2017. 'Targeting Metabolism for Cancer Therapy', *Cell Chem Biol*, 24: 1161-80.

Lunt, S. Y., and M. G. Vander Heiden. 2011. 'Aerobic glycolysis: meeting the metabolic requirements of cell proliferation', *Annu Rev Cell Dev Biol*, 27: 441-64.

Lynch, L. A., J. M. O'Connell, A. K. Kwasnik, T. J. Cawood, C. O'Farrelly, and D. B. O'Shea. 2009. 'Are natural killer cells protecting the metabolically healthy obese patient?', *Obesity (Silver Spring)*, 17: 601-5.

Ma, X., E. Bi, Y. Lu, P. Su, C. Huang, L. Liu, Q. Wang, M. Yang, M. F. Kalady, J. Qian, A. Zhang, A. A. Gupte, D. J. Hamilton, C. Zheng, and Q. Yi. 2019. 'Cholesterol Induces CD8(+) T Cell Exhaustion in the Tumor Microenvironment', *Cell Metab*, 30: 143-56.e5.

Ma, Xingzhe, Enguang Bi, Chunjian Huang, Yong Lu, Gang Xue, Xing Guo, Aibo Wang, Maojie Yang, Jianfei Qian, Chen Dong, and Qing Yi. 2018. 'Cholesterol negatively regulates IL-9–producing CD8⁺ T cell differentiation and antitumor activity', *J Exp Med*, 215: 1555-69.

Mah, A. Y., A. Rashidi, M. P. Keppel, N. Saucier, E. K. Moore, J. B. Alinger, S. K. Tripathy, S. K. Agarwal, E. K. Jeng, H. C. Wong, J. S. Miller, T. A. Fehniger, E. M. Mace, A. R. French, and M. A. Cooper. 2017. 'Glycolytic requirement for NK cell cytotoxicity and cytomegalovirus control', *JCI Insight*, 2.

Mamont, P. S., M. C. Duchesne, J. Grove, and P. Bey. 1978. 'Anti-proliferative properties of DL-alpha-difluoromethyl ornithine in cultured cells. A consequence of the irreversible inhibition of ornithine decarboxylase', *Biochem Biophys Res Commun*, 81: 58-66.

Mandelboim, O., N. Lieberman, M. Lev, L. Paul, T. I. Arnon, Y. Bushkin, D. M. Davis, J. L. Strominger, J. W. Yewdell, and A. Porgador. 2001. 'Recognition of haemagglutinins on virus-infected cells by NKp46 activates lysis by human NK cells', *Nature*, 409: 1055-60.

Marcais, A., J. Cherfils-Vicini, C. Viant, S. Degouve, S. Viel, A. Fenis, J. Rabilloud, K. Mayol, A. Tavares, J. Bienvenu, Y. G. Gangloff, E. Gilson, E. Vivier, and T. Walzer. 2014. 'The metabolic checkpoint kinase mTOR is essential for IL-15 signaling during the development and activation of NK cells', *Nat Immunol*, 15: 749-57.

Marcais, A., S. Viel, M. Grau, T. Henry, J. Marvel, and T. Walzer. 2013. 'Regulation of mouse NK cell development and function by cytokines', *Front Immunol*, 4: 450.

Martin-Fontecha, A., L. L. Thomsen, S. Brett, C. Gerard, M. Lipp, A. Lanzavecchia, and F. Sallusto. 2004. 'Induced recruitment of NK cells to lymph nodes provides IFN-gamma for T(H)1 priming', *Nat Immunol*, 5: 1260-5.

Matsuda, M., B. S. Korn, R. E. Hammer, Y. A. Moon, R. Komuro, J. D. Horton, J. L. Goldstein, M. S. Brown, and I. Shimomura. 2001. 'SREBP cleavage-activating protein (SCAP) is required for increased lipid synthesis in liver induced by cholesterol deprivation and insulin elevation', *Genes Dev*, 15: 1206-16.

Maude, S. L., N. Frey, P. A. Shaw, R. Aplenc, D. M. Barrett, N. J. Bunin, A. Chew, V. E. Gonzalez, Z. Zheng, S. F. Lacey, Y. D. Mahnke, J. J. Melenhorst, S. R. Rheingold, A. Shen, D. T. Teachey, B. L. Levine, C. H. June, D. L. Porter, and S. A. Grupp. 2014. 'Chimeric antigen receptor T cells for sustained remissions in leukemia', *N Engl J Med*, 371: 1507-17.

Michelet, X., L. Dyck, A. Hogan, R. M. Loftus, D. Duquette, K. Wei, S. Beyaz, A. Tavakkoli, C. Foley, R. Donnelly, C. O'Farrelly, M. Raverdeau, A. Vernon, W. Pettee, D. O'Shea, B. S. Nikolajczyk, K. H. G. Mills, M. B. Brenner, D. Finlay, and L. Lynch. 2018. 'Metabolic reprogramming of natural killer cells in obesity limits antitumor responses', *Nat Immunol*, 19: 1330-40.

Miller, J. S., C. Morishima, D. G. McNeel, M. R. Patel, H. E. K. Kohrt, J. A. Thompson, P. M. Sondel, H. A. Wakelee, M. L. Disis, J. C. Kaiser, M. A. Cheever, H. Streicher, S. P. Creekmore, T. A. Waldmann, and K. C. Conlon. 2018. 'A First-in-Human Phase I Study of Subcutaneous Outpatient Recombinant Human

IL15 (rhIL15) in Adults with Advanced Solid Tumors', *Clin Cancer Res*, 24: 1525-35.

Miller, Jeffrey S., and Lewis L. Lanier. 2019. 'Natural Killer Cells in Cancer Immunotherapy', *Annual Review of Cancer Biology*, 3: 77-103.

Moon, Y. A., G. Liang, X. Xie, M. Frank-Kamenetsky, K. Fitzgerald, V. Koteliansky, M. S. Brown, J. L. Goldstein, and J. D. Horton. 2012. 'The Scap/SREBP pathway is essential for developing diabetic fatty liver and carbohydrate-induced hypertriglyceridemia in animals', *Cell Metab*, 15: 240-6.

Moore, C. C., E. N. Martin, G. Lee, C. Taylor, R. Dondero, L. L. Reznikov, C. Dinarello, J. Thompson, and W. M. Scheld. 2008. 'Eukaryotic translation initiation factor 5A small interference RNA-liposome complexes reduce inflammation and increase survival in murine models of severe sepsis and acute lung injury', *J Infect Dis*, 198: 1407-14.

Morvan, M. G., and L. L. Lanier. 2016. 'NK cells and cancer: you can teach innate cells new tricks', *Nat Rev Cancer*, 16: 7-19.

Mounce, B. C., M. E. Olsen, M. Vignuzzi, and J. H. Connor. 2017. 'Polyamines and Their Role in Virus Infection', *Microbiol Mol Biol Rev*, 81.

Mullarky, E., N. C. Lucki, R. Beheshti Zavareh, J. L. Anglin, A. P. Gomes, B. N. Nicolay, J. C. Wong, S. Christen, H. Takahashi, P. K. Singh, J. Blenis, J. D. Warren, S. M. Fendt, J. M. Asara, G. M. DeNicola, C. A. Lyssiotis, L. L. Lairson, and L. C. Cantley. 2016. 'Identification of a small molecule inhibitor of 3-phosphoglycerate dehydrogenase to target serine biosynthesis in cancers', *Proc Natl Acad Sci U S A*, 113: 1778-83.

Must, A., J. Spadano, E. H. Coakley, A. E. Field, G. Colditz, and W. H. Dietz. 1999. 'The disease burden associated with overweight and obesity', *Jama*, 282: 1523-9.

Nakanishi, S., and J. L. Cleveland. 2016. 'Targeting the polyamine-hypusine circuit for the prevention and treatment of cancer', *Amino Acids*, 48: 2353-62.

Nandagopal, N., A. K. Ali, A. K. Komal, and S. H. Lee. 2014. 'The Critical Role of IL-15-PI3K-mTOR Pathway in Natural Killer Cell Effector Functions', *Front Immunol*, 5: 187.

Nelson, E. R., S. E. Wardell, J. S. Jasper, S. Park, S. Suchindran, M. K. Howe, N. J. Carver, R. V. Pillai, P. M. Sullivan, V. Sondhi, M. Umetani, J. Geradts, and D. P. McDonnell. 2013. '27-Hydroxycholesterol links hypercholesterolemia and breast cancer pathophysiology', *Science*, 342: 1094-8.

Newman, K. C., and E. M. Riley. 2007. 'Whatever turns you on: accessory-cell-dependent activation of NK cells by pathogens', *Nat Rev Immunol*, 7: 279-91.

Ni, J., M. Miller, A. Stojanovic, N. Garbi, and A. Cerwenka. 2012. 'Sustained effector function of IL-12/15/18-preactivated NK cells against established tumors', *J Exp Med*, 209: 2351-65.

O'Brien, K. L., and D. K. Finlay. 2019. 'Immunometabolism and natural killer cell responses', *Nat Rev Immunol*, 19: 282-90.

O'Connor, R. S., L. Guo, S. Ghassemi, N. W. Snyder, A. J. Worth, L. Weng, Y. Kam, B. Philipson, S. Trefely, S. Nunez-Cruz, I. A. Blair, C. H. June, and M. C. Milone. 2018. 'The CPT1a inhibitor, etomoxir induces severe oxidative stress at commonly used concentrations', *Sci Rep*, 8: 6289.

O'Donnell, K. A., D. Yu, K. I. Zeller, J. W. Kim, F. Racke, A. Thomas-Tikhonenko, and C. V. Dang. 2006. 'Activation of transferrin receptor 1 by c-Myc enhances cellular proliferation and tumorigenesis', *Mol Cell Biol*, 26: 2373-86.

O'Neill, L. A., R. J. Kishton, and J. Rathmell. 2016. 'A guide to immunometabolism for immunologists', *Nat Rev Immunol*, 16: 553-65.

O'Shea, D., T. J. Cawood, C. O'Farrelly, and L. Lynch. 2010. 'Natural killer cells in obesity: impaired function and increased susceptibility to the effects of cigarette smoke', *PLoS One*, 5: e8660.

O'Sullivan, D., G. J. van der Windt, S. C. Huang, J. D. Curtis, C. H. Chang, M. D. Buck, J. Qiu, A. M. Smith, W. Y. Lam, L. M. DiPlato, F. F. Hsu, M. J. Birnbaum, E. J. Pearce, and E. L. Pearce. 2014. 'Memory CD8(+) T cells use cell-intrinsic lipolysis to support the metabolic programming necessary for development', *Immunity*, 41: 75-88.

O'Sullivan, T. E., L. R. Johnson, H. H. Kang, and J. C. Sun. 2015. 'BNIP3- and BNIP3L-Mediated Mitophagy Promotes the Generation of Natural Killer Cell Memory', *Immunity*, 43: 331-42.

Olenchock, B. A., J. C. Rathmell, and M. G. Vander Heiden. 2017. 'Biochemical Underpinnings of Immune Cell Metabolic Phenotypes', *Immunity*, 46: 703-13.

Orange, J. S. 2008. 'Formation and function of the lytic NK-cell immunological synapse', *Nat Rev Immunol*, 8: 713-25.

Orange, J.S. 2013. 'Natural killer cell deficiency', *J Allergy Clin Immunol*, 132: 515-25.

Ortiz, A., J. Gui, F. Zahedi, P. Yu, C. Cho, S. Bhattacharya, C. J. Carbone, Q. Yu, K. V. Katlinski, Y. V. Katlinskaya, S. Handa, V. Haas, S. W. Volk, A. K. Brice, K. Wals, N. J. Matheson, R. Antrobus, S. Ludwig, T. L. Whiteside, C. Sander, A. A. Tarhini, J. M. Kirkwood, P. J. Lehner, W. Guo, H. Rui, A. J. Minn, C. Koumenis, J. A. Diehl, and S. Y. Fuchs. 2019. 'An Interferon-Driven Oxysterol-Based Defense against Tumor-Derived Extracellular Vesicles', *Cancer Cell*, 35: 33-45.e6.

Osinska, I., K. Popko, and U. Demkow. 2014. 'Perforin: an important player in immune response', *Cent Eur J Immunol*, 39: 109-15.

Ozcan, U., L. Ozcan, E. Yilmaz, K. Duvel, M. Sahin, B. D. Manning, and G. S. Hotamisligil. 2008. 'Loss of the tuberous sclerosis complex tumor suppressors triggers the unfolded protein response to regulate insulin signaling and apoptosis', *Mol Cell*, 29: 541-51.

Park, K., and A. L. Scott. 2010. 'Cholesterol 25-hydroxylase production by dendritic cells and macrophages is regulated by type I interferons', *J Leukoc Biol*, 88: 1081-7.

Park, M. H., H. L. Cooper, and J. E. Folk. 1981. 'Identification of hypusine, an unusual amino acid, in a protein from human lymphocytes and of spermidine as its biosynthetic precursor', *Proc Natl Acad Sci U S A*, 78: 2869-73.

Park, M. H., K. Nishimura, C. F. Zanelli, and S. R. Valentini. 2010. 'Functional significance of eIF5A and its hypusine modification in eukaryotes', *Amino Acids*, 38: 491-500.

Pearce, E. L., and E. J. Pearce. 2013. 'Metabolic pathways in immune cell activation and quiescence', *Immunity*, 38: 633-43.

Pearce, E. L., M. C. Poffenberger, C. H. Chang, and R. G. Jones. 2013. 'Fueling immunity: insights into metabolism and lymphocyte function', *Science*, 342: 1242454.

Pegg, A. E. 2016. 'Functions of Polyamines in Mammals', *J Biol Chem*, 291: 14904-12.

Peng, M., N. Yin, S. Chhangawala, K. Xu, C. S. Leslie, and M. O. Li. 2016. 'Aerobic glycolysis promotes T helper 1 cell differentiation through an epigenetic mechanism', *Science*, 354: 481-84.

Peng, T., T. R. Golub, and D. M. Sabatini. 2002. 'The immunosuppressant rapamycin mimics a starvation-like signal distinct from amino acid and glucose deprivation', *Mol Cell Biol*, 22: 5575-84.

Peterson, T. R., S. S. Sengupta, T. E. Harris, A. E. Carmack, S. A. Kang, E. Balderas, D. A. Guertin, K. L. Madden, A. E. Carpenter, B. N. Finck, and D. M. Sabatini. 2011. 'mTOR complex 1 regulates lipin 1 localization to control the SREBP pathway', *Cell*, 146: 408-20.

Piccioli, D., S. Sbrana, E. Melandri, and N. M. Valiante. 2002. 'Contact-dependent stimulation and inhibition of dendritic cells by natural killer cells', *J Exp Med*, 195: 335-41.

Piersma, S. J., M. A. Pak-Wittel, A. Lin, B. Plougastel-Douglas, and W. M. Yokoyama. 2019. 'Activation Receptor-Dependent IFN-gamma Production by NK Cells Is Controlled by Transcription, Translation, and the Proteasome', *J Immunol*, 203: 1981-88.

Pietra, G., C. Manzini, M. Vitale, M. Balsamo, E. Ognio, M. Boitano, P. Queirolo, L. Moretta, and M. C. Mingari. 2009. 'Natural killer cells kill human melanoma cells with characteristics of cancer stem cells', *Int Immunol*, 21: 793-801.

Pollizzi, K. N., and J. D. Powell. 2014. 'Integrating canonical and metabolic signalling programmes in the regulation of T cell responses', *Nat Rev Immunol*, 14: 435-46.

Porstmann, T., C. R. Santos, B. Griffiths, M. Cully, M. Wu, S. Leevers, J. R. Griffiths, Y. L. Chung, and A. Schulze. 2008. 'SREBP activity is regulated by mTORC1 and contributes to Akt-dependent cell growth', *Cell Metab*, 8: 224-36.

Poso, H., and A. E. Pegg. 1982. 'Effect of alpha-difluoromethylornithine on polyamine and DNA synthesis in regenerating rat liver: reversal of inhibition of DNA synthesis by putrescine', *Biochim Biophys Acta*, 696: 179-86.

Poulin, R., L. Lu, B. Ackermann, P. Bey, and A. E. Pegg. 1992. 'Mechanism of the irreversible inactivation of mouse ornithine decarboxylase by alpha-difluoromethylornithine. Characterization of sequences at the inhibitor and coenzyme binding sites', *J Biol Chem*, 267: 150-8.

Prager, I., and C. Watzl. 2019. 'Mechanisms of natural killer cell-mediated cellular cytotoxicity', *J Leukoc Biol*, 105: 1319-29.

Preston, G. C., L. V. Sinclair, A. Kaskar, J. L. Hukelmann, M. N. Navarro, I. Ferrero, H. R. MacDonald, V. H. Cowling, and D. A. Cantrell. 2015. 'Single cell tuning of Myc expression by antigen receptor signal strength and interleukin-2 in T lymphocytes', *Embo j*, 34: 2008-24.

Preukschas, M., C. Hagel, A. Schulte, K. Weber, K. Lamszus, H. Sievert, N. Pallmann, C. Bokemeyer, J. Hauber, M. Braig, and S. Balabanov. 2012. 'Expression of eukaryotic initiation factor 5A and hypusine forming enzymes in glioblastoma patient samples: implications for new targeted therapies', *PLoS One*, 7: e43468.

Puleston, D. J., M. D. Buck, R. I. Klein Geltink, R. L. Kyle, G. Caputa, D. O'Sullivan, A. M. Cameron, A. Castoldi, Y. Musa, A. M. Kabat, Y. Zhang, L. J. Flachsmann, C. S. Field, A. E. Patterson, S. Scherer, F. Alfei, F. Baixauli, S. K. Austin, B. Kelly, M. Matsushita, J. D. Curtis, K. M. Grzes, M. Villa, M. Corrado, D. E. Sanin, J. Qiu, N. Pallman, K. Paz, M. E. Maccari, B. R. Blazar, G. Mittler, J. M. Buescher, D. Zehn, S. Rospert, E. J. Pearce, S. Balabanov, and E. L. Pearce. 2019. 'Polyamines and eIF5A Hypusination Modulate Mitochondrial Respiration and Macrophage Activation', *Cell Metab*, 30: 352-63.e8.

Puleston, D. J., M. Villa, and E. L. Pearce. 2017. 'Ancillary Activity: Beyond Core Metabolism in Immune Cells', *Cell Metab*, 26: 131-41.

Puleston, D. J., H. Zhang, T. J. Powell, E. Lipina, S. Sims, I. Panse, A. S. Watson, V. Cerundolo, A. R. Townsend, P. Klenerman, and A. K. Simon. 2014. 'Autophagy is a critical regulator of memory CD8(+) T cell formation', *Elife*, 3.

Raccosta, L., R. Fontana, D. Maggioni, C. Lanterna, E. J. Villablanca, A. Paniccia, A. Musumeci, E. Chiricozzi, M. L. Trincavelli, S. Daniele, C. Martini, J. A. Gustafsson, C. Doglioni, S. G. Feo, A. Leiva, M. G. Ciampa, L. Mauri, C. Sensi, A. Prinetti, I. Eberini, J. R. Mora, C. Bordignon, K. R. Steffensen, S. Sonnino, S. Sozzani, C. Traversari, and V. Russo. 2013. 'The oxysterol-CXCR2 axis plays a key role in the recruitment of tumor-promoting neutrophils', *J Exp Med*, 210: 1711-28.

Radhakrishnan, A., J. L. Goldstein, J. G. McDonald, and M. S. Brown. 2008. 'Switch-like control of SREBP-2 transport triggered by small changes in ER cholesterol: a delicate balance', *Cell Metab*, 8: 512-21.

Radhakrishnan, A., Y. Ikeda, H. J. Kwon, M. S. Brown, and J. L. Goldstein. 2007a. 'Sterol-regulated transport of SREBPs from endoplasmic reticulum to Golgi: oxysterols block transport by binding to Insig', *Proc Natl Acad Sci U S A*, 104: 6511-8.

Radhakrishnan, Arun, Yukio Ikeda, Hyock Joo Kwon, Michael S. Brown, and Joseph L. Goldstein. 2007b. 'Sterol-regulated transport of SREBPs from endoplasmic reticulum to Golgi: Oxysterols block transport by binding to Insig', *Proceedings of the National Academy of Sciences*, 104: 6511-18.

Raud, B., D. G. Roy, A. S. Divakaruni, T. N. Tarasenko, R. Franke, E. H. Ma, B. Samborska, W. Y. Hsieh, A. H. Wong, P. Stuve, C. Arnold-Schrauf, M. Guderian, M. Lochner, S. Rampertaap, K. Romito, J. Monsale, M. Bronstrup, S. J. Bensinger, A. N. Murphy, P. J. McGuire, R. G. Jones, T. Sparwasser, and L. Berod. 2018. 'Etomoxir Actions on Regulatory and Memory T Cells Are Independent of Cpt1a-Mediated Fatty Acid Oxidation', *Cell Metab*, 28: 504-15.e7.

Reboldi, A., E. V. Dang, J. G. McDonald, G. Liang, D. W. Russell, and J. G. Cyster. 2014. 'Inflammation. 25-Hydroxycholesterol suppresses interleukin-1-

driven inflammation downstream of type I interferon', *Science*, 345: 679-84.

Reed, B. D., A. E. Charos, A. M. Szekely, S. M. Weissman, and M. Snyder. 2008. 'Genome-wide occupancy of SREBP1 and its partners NFY and SP1 reveals novel functional roles and combinatorial regulation of distinct classes of genes', *PLoS Genet*, 4: e1000133.

Repa, J. J., G. Liang, J. Ou, Y. Bashmakov, J. M. Lobaccaro, I. Shimomura, B. Shan, M. S. Brown, J. L. Goldstein, and D. J. Mangelsdorf. 2000. 'Regulation of mouse sterol regulatory element-binding protein-1c gene (SREBP-1c) by oxysterol receptors, LXRalpha and LXRbeta', *Genes Dev*, 14: 2819-30.

Rezvani, K., R. Rouce, E. Liu, and E. Shpall. 2017. 'Engineering Natural Killer Cells for Cancer Immunotherapy', *Mol Ther*, 25: 1769-81.

Romee, R., S. E. Schneider, J. W. Leong, J. M. Chase, C. R. Keppel, R. P. Sullivan, M. A. Cooper, and T. A. Fehniger. 2012. 'Cytokine activation induces human memory-like NK cells', *Blood*, 120: 4751-60.

Samant, S. A., H. J. Zhang, Z. Hong, V. B. Pillai, N. R. Sundaresan, D. Wolfgeher, S. L. Archer, D. C. Chan, and M. P. Gupta. 2014. 'SIRT3 deacetylates and activates OPA1 to regulate mitochondrial dynamics during stress', *Mol Cell Biol*, 34: 807-19.

Schall, R. P., J. Sekar, P. M. Tandon, and B. M. Susskind. 1991. 'Difluoromethylornithine (DFMO) arrests murine CTL development in the late, pre-effector stage', *Immunopharmacology*, 21: 129-43.

Schuller, A. P., C. C. Wu, T. E. Dever, A. R. Buskirk, and R. Green. 2017. 'eIF5A Functions Globally in Translation Elongation and Termination', *Mol Cell*, 66: 194-205.e5.

Schurich, A., L. J. Pallett, D. Jajbhay, J. Wijngaarden, I. Otano, U. S. Gill, N. Hansi, P. T. Kennedy, E. Nastouli, R. Gilson, C. Frezza, S. M. Henson, and M. K. Maini. 2016. 'Distinct Metabolic Requirements of Exhausted and Functional Virus-Specific CD8 T Cells in the Same Host', *Cell Rep*, 16: 1243-52.

Screpanti, V., R. P. Wallin, A. Grandien, and H. G. Ljunggren. 2005. 'Impact of FASL-induced apoptosis in the elimination of tumor cells by NK cells', *Mol Immunol*, 42: 495-9.

Screpanti, V., R. P. Wallin, H. G. Ljunggren, and A. Grandien. 2001. 'A central role for death receptor-mediated apoptosis in the rejection of tumors by NK cells', *J Immunol*, 167: 2068-73.

Seidel, U. J., P. Schlegel, and P. Lang. 2013. 'Natural killer cell mediated antibody-dependent cellular cytotoxicity in tumor immunotherapy with therapeutic antibodies', *Front Immunol*, 4: 76.

Shi, F. D., H. G. Ljunggren, A. La Cava, and L. Van Kaer. 2011. 'Organ-specific features of natural killer cells', *Nat Rev Immunol*, 11: 658-71.

Shi, L. Z., R. Wang, G. Huang, P. Vogel, G. Neale, D. R. Green, and H. Chi. 2011. 'HIF1alpha-dependent glycolytic pathway orchestrates a metabolic checkpoint for the differentiation of TH17 and Treg cells', *J Exp Med*, 208: 1367-76.

Shimano, H. 2001. 'Sterol regulatory element-binding proteins (SREBPs): transcriptional regulators of lipid synthetic genes', *Prog Lipid Res*, 40: 439-52.

Shimano, H., J. D. Horton, I. Shimomura, R. E. Hammer, M. S. Brown, and J. L. Goldstein. 1997. 'Isoform 1c of sterol regulatory element binding protein is less active than isoform 1a in livers of transgenic mice and in cultured cells', *J Clin Invest*, 99: 846-54.

Shimomura, I., H. Shimano, J. D. Horton, J. L. Goldstein, and M. S. Brown. 1997. 'Differential expression of exons 1a and 1c in mRNAs for sterol regulatory element binding protein-1 in human and mouse organs and cultured cells', *J Clin Invest*, 99: 838-45.

Sinclair, L. V., J. Rolf, E. Emslie, Y. B. Shi, P. M. Taylor, and D. A. Cantrell. 2013. 'Control of amino-acid transport by antigen receptors coordinates the metabolic reprogramming essential for T cell differentiation', *Nat Immunol*, 14: 500-8.

Slattery, Karen, Vanessa Zaiatz-Bittencourt, Elena Woods, Kiva Brennan, Sam Marks, Sonya Chew, Michael Conroy, Caitriona Goggin, John Kennedy, David K. Finlay, and Clair M. Gardiner. 2019. 'TGFβ drives mitochondrial dysfunction in peripheral blood NK cells during metastatic breast cancer', *bioRxiv*: 648501.

Smith, A. G., P. A. Sheridan, J. B. Harp, and M. A. Beck. 2007. 'Diet-induced obese mice have increased mortality and altered immune responses when infected with influenza virus', *J Nutr*, 137: 1236-43.

Smith, J. R., T. F. Osborne, J. L. Goldstein, and M. S. Brown. 1990. 'Identification of nucleotides responsible for enhancer activity of sterol regulatory element in low density lipoprotein receptor gene', *J Biol Chem*, 265: 2306-10.

Smyth, M. J., E. Cretney, J. M. Kelly, J. A. Westwood, S. E. Street, H. Yagita, K. Takeda, S. L. van Dommelen, M. A. Degli-Esposti, and Y. Hayakawa. 2005. 'Activation of NK cell cytotoxicity', *Mol Immunol*, 42: 501-10.

Smyth, M. J., C. O. Zachariae, Y. Norihisa, J. R. Ortaldo, A. Hishinuma, and K. Matsushima. 1991. 'IL-8 gene expression and production in human peripheral blood lymphocyte subsets', *J Immunol*, 146: 3815-23.

Song, M., T. A. Sandoval, C. S. Chae, S. Chopra, C. Tan, M. R. Rutkowski, M. Raundhal, R. A. Chaurio, K. K. Payne, C. Konrad, S. E. Bettigole, H. R. Shin, M. J. P. Crowley, J. P. Cerliani, A. V. Kossenkov, I. Motorykin, S. Zhang, G. Manfredi, D. Zamarin, K. Holcomb, P. C. Rodriguez, G. A. Rabinovich, J. R. Conejo-Garcia, L. H. Glimcher, and J. R. Cubillos-Ruiz. 2018. 'IRE1alpha-XBP1 controls T cell function in ovarian cancer by regulating mitochondrial activity', *Nature*, 562: 423-28.

Spits, Hergen, David Artis, Marco Colonna, Andreas Diefenbach, James P. Di Santo, Gerard Eberl, Shigeo Koyasu, Richard M. Locksley, Andrew N. J. McKenzie, Reina E. Mebius, Fiona Powrie, and Eric Vivier. 2013. 'Innate lymphoid cells [mdash] a proposal for uniform nomenclature', *Nat Rev Immunol*, 13: 145-49.

Stanic, I., A. Facchini, R. M. Borzi, C. Stefanelli, and F. Flamigni. 2009. 'The polyamine analogue N1,N11-diethylnorspermine can induce chondrocyte apoptosis independently of its ability to alter metabolism and levels of natural polyamines', *J Cell Physiol*, 219: 109-16.

Stetson, D. B., M. Mohrs, R. L. Reinhardt, J. L. Baron, Z. E. Wang, L. Gapin, M. Kronenberg, and R. M. Locksley. 2003. 'Constitutive cytokine mRNAs mark

natural killer (NK) and NK T cells poised for rapid effector function', *J Exp Med*, 198: 1069-76.

Stevens, A. P., K. Dettmer, G. Kirovski, K. Samejima, C. Hellerbrand, A. K. Bosserhoff, and P. J. Oefner. 2010. 'Quantification of intermediates of the methionine and polyamine metabolism by liquid chromatography-tandem mass spectrometry in cultured tumor cells and liver biopsies', *J Chromatogr A*, 1217: 3282-8.

Suck, G., M. Odendahl, P. Nowakowska, C. Seidl, W. S. Wels, H. G. Klingemann, and T. Tonn. 2016. 'NK-92: an 'off-the-shelf therapeutic' for adoptive natural killer cell-based cancer immunotherapy', *Cancer Immunol Immunother*, 65: 485-92.

Sukumar, M., J. Liu, Y. Ji, M. Subramanian, J. G. Crompton, Z. Yu, R. Roychoudhuri, D. C. Palmer, P. Muranski, E. D. Karoly, R. P. Mohney, C. A. Klebanoff, A. Lal, T. Finkel, N. P. Restifo, and L. Gattinoni. 2013. 'Inhibiting glycolytic metabolism enhances CD8+ T cell memory and antitumor function', *J Clin Invest*, 123: 4479-88.

Sun, J. C., J. N. Beilke, and L. L. Lanier. 2009. 'Adaptive immune features of natural killer cells', *Nature*, 457: 557-61.

Sun, J. C., and L. L. Lanier. 2011. 'NK cell development, homeostasis and function: parallels with CD8(+) T cells', *Nat Rev Immunol*, 11: 645-57.

Sun, L. P., J. Seemann, J. L. Goldstein, and M. S. Brown. 2007. 'Sterol-regulated transport of SREBPs from endoplasmic reticulum to Golgi: Insig renders sorting signal in Scap inaccessible to COPII proteins', *Proc Natl Acad Sci U S A*, 104: 6519-26.

Swamy, M., S. Pathak, K. M. Grzes, S. Damerow, L. V. Sinclair, D. M. van Aalten, and D. A. Cantrell. 2016. 'Glucose and glutamine fuel protein O-GlcNAcylation to control T cell self-renewal and malignancy', *Nat Immunol*, 17: 712-20.

Tabula Muris Consortium. 2018. 'Single-cell transcriptomics of 20 mouse organs creates a Tabula Muris', *Nature*, 562: 367-72.

Talmadge, J. E., K. M. Meyers, D. J. Prieur, and J. R. Starkey. 1980. 'Role of natural killer cells in tumor growth and metastasis: C57BL/6 normal and beige mice', *J Natl Cancer Inst*, 65: 929-35.

Thiery, J., D. Keefe, S. Boulant, E. Boucrot, M. Walch, D. Martinvalet, I. S. Goping, R. C. Bleackley, T. Kirchhausen, and J. Lieberman. 2011. 'Perforin pores in the endosomal membrane trigger the release of endocytosed granzyme B into the cytosol of target cells', *Nat Immunol*, 12: 770-7.

Tobin, L. M., M. Mavinkurve, E. Carolan, D. Kinlen, E. C. O'Brien, M. A. Little, D. K. Finlay, D. Cody, A. E. Hogan, and D. O'Shea. 2017. 'NK cells in childhood obesity are activated, metabolically stressed, and functionally deficient', *JCI Insight*, 2.

Tremblay-Franco, M., C. Zerbinati, A. Pacelli, G. Palmaccio, C. Lubrano, S. Ducheix, H. Guillou, and L. Iuliano. 2015. 'Effect of obesity and metabolic syndrome on plasma oxysterols and fatty acids in human', *Steroids*, 99: 287-92.

Van den Bossche, J., J. Baardman, N. A. Otto, S. van der Velden, A. E. Neele, S. M. van den Berg, R. Luque-Martin, H. J. Chen, M. C. Boshuizen, M. Ahmed, M. A. Hoeksema, A. F. de Vos, and M. P. de Winther. 2016. 'Mitochondrial

Dysfunction Prevents Repolarization of Inflammatory Macrophages', *Cell Rep*, 17: 684-96.

van der Windt, G. J., B. Everts, C. H. Chang, J. D. Curtis, T. C. Freitas, E. Amiel, E. J. Pearce, and E. L. Pearce. 2012. 'Mitochondrial respiratory capacity is a critical regulator of CD8+ T cell memory development', *Immunity*, 36: 68-78.

Vander Heiden, M. G., L. C. Cantley, and C. B. Thompson. 2009. 'Understanding the Warburg effect: the metabolic requirements of cell proliferation', *Science*, 324: 1029-33.

Vankayalapati, R., A. Garg, A. Porgador, D. E. Griffith, P. Klucar, H. Safi, W. M. Girard, D. Cosman, T. Spies, and P. F. Barnes. 2005. 'Role of NK cell-activating receptors and their ligands in the lysis of mononuclear phagocytes infected with an intracellular bacterium', *J Immunol*, 175: 4611-7.

Varghese, J. F., R. Patel, and U. C. S. Yadav. 2019. 'Sterol regulatory element binding protein (SREBP) -1 mediates oxidized low-density lipoprotein (oxLDL) induced macrophage foam cell formation through NLRP3 inflammasome activation', *Cell Signal*, 53: 316-26.

Viel, S., A. Marcais, F. S. Guimaraes, R. Loftus, J. Rabilloud, M. Grau, S. Degouve, S. Djebali, A. Sanlaville, E. Charrier, J. Bienvenu, J. C. Marie, C. Caux, J. Marvel, L. Town, N. D. Huntington, L. Bartholin, D. Finlay, M. J. Smyth, and T. Walzer. 2016. 'TGF-beta inhibits the activation and functions of NK cells by repressing the mTOR pathway', *Sci Signal*, 9: ra19.

Villablanca, E. J., L. Raccosta, D. Zhou, R. Fontana, D. Maggioni, A. Negro, F. Sanvito, M. Ponzoni, B. Valentinis, M. Bregni, A. Prinetti, K. R. Steffensen, S. Sonnino, J. A. Gustafsson, C. Doglioni, C. Bordignon, C. Traversari, and V. Russo. 2010. 'Tumor-mediated liver X receptor-alpha activation inhibits CC chemokine receptor-7 expression on dendritic cells and dampens antitumor responses', *Nat Med*, 16: 98-105.

Vivier, E., D. Artis, M. Colonna, A. Diefenbach, J. P. Di Santo, G. Eberl, S. Koyasu, R. M. Locksley, A. N. J. McKenzie, R. E. Mebius, F. Powrie, and H. Spits. 2018. 'Innate Lymphoid Cells: 10 Years On', *Cell*, 174: 1054-66.

Vivier, E., S. Ugolini, D. Blaise, C. Chabannon, and L. Brossay. 2012. 'Targeting natural killer cells and natural killer T cells in cancer', *Nat Rev Immunol*, 12: 239-52.

Vosshenrich, C. A., T. Ranson, S. I. Samson, E. Corcuff, F. Colucci, E. E. Rosmaraki, and J. P. Di Santo. 2005. 'Roles for common cytokine receptor gamma-chain-dependent cytokines in the generation, differentiation, and maturation of NK cell precursors and peripheral NK cells in vivo', *J Immunol*, 174: 1213-21.

Waggoner, S. N., M. Cornberg, L. K. Selin, and R. M. Welsh. 2011. 'Natural killer cells act as rheostats modulating antiviral T cells', *Nature*, 481: 394-8.

Waggoner, S. N., S. D. Reighard, I. E. Gyurova, S. A. Cranert, S. E. Mahl, E. P. Karmele, J. P. McNally, M. T. Moran, T. R. Brooks, F. Yaqoob, and C. E. Rydyznski. 2016. 'Roles of natural killer cells in antiviral immunity', *Curr Opin Virol*, 16: 15-23.

Wagner, A. J., C. Meyers, L. A. Laimins, and N. Hay. 1993. 'c-Myc induces the expression and activity of ornithine decarboxylase', *Cell Growth Differ*, 4: 879-83.

Walzer, T., M. Blery, J. Chaix, N. Fuseri, L. Chasson, S. H. Robbins, S. Jaeger, P. Andre, L. Gauthier, L. Daniel, K. Chemin, Y. Morel, M. Dalod, J. Imbert, M. Pierres, A. Moretta, F. Romagne, and E. Vivier. 2007. 'Identification, activation, and selective in vivo ablation of mouse NK cells via NKp46', *Proc Natl Acad Sci U S A*, 104: 3384-9.

Walzer, T., S. Jaeger, J. Chaix, and E. Vivier. 2007. 'Natural killer cells: from CD3(-)NKp46(+) to post-genomics meta-analyses', *Curr Opin Immunol*, 19: 365-72.

Wang, R., C. P. Dillon, L. Z. Shi, S. Milasta, R. Carter, D. Finkelstein, L. L. McCormick, P. Fitzgerald, H. Chi, J. Munger, and D. R. Green. 2011. 'The transcription factor Myc controls metabolic reprogramming upon T lymphocyte activation', *Immunity*, 35: 871-82.

Webster, B. R., I. Scott, K. Han, J. H. Li, Z. Lu, M. V. Stevens, D. Malide, Y. Chen, L. Samsel, P. S. Connelly, M. P. Daniels, J. P. McCoy, Jr., C. A. Combs, M. Gucek, and M. N. Sack. 2013. 'Restricted mitochondrial protein acetylation initiates mitochondrial autophagy', *J Cell Sci*, 126: 4843-9.

Webster, B. R., I. Scott, J. Traba, K. Han, and M. N. Sack. 2014. 'Regulation of autophagy and mitophagy by nutrient availability and acetylation', *Biochim Biophys Acta*, 1841: 525-34.

Wellen, K. E., G. Hatzivassiliou, U. M. Sachdeva, T. V. Bui, J. R. Cross, and C. B. Thompson. 2009. 'ATP-citrate lyase links cellular metabolism to histone acetylation', *Science*, 324: 1076-80.

Werstuck, G. H., S. R. Lentz, S. Dayal, G. S. Hossain, S. K. Sood, Y. Y. Shi, J. Zhou, N. Maeda, S. K. Krisans, M. R. Malinow, and R. C. Austin. 2001. 'Homocysteine-induced endoplasmic reticulum stress causes dysregulation of the cholesterol and triglyceride biosynthetic pathways', *J Clin Invest*, 107: 1263-73.

Wu, Q., T. Ishikawa, R. Sirianni, H. Tang, J. G. McDonald, I. S. Yuhanna, B. Thompson, L. Girard, C. Mineo, R. A. Brekken, M. Umetani, D. M. Euhus, Y. Xie, and P. W. Shaul. 2013. '27-Hydroxycholesterol promotes cell-autonomous, ER-positive breast cancer growth', *Cell Rep*, 5: 637-45.

Wulfing, C., B. Purtic, J. Klem, and J. D. Schatzle. 2003. 'Stepwise cytoskeletal polarization as a series of checkpoints in innate but not adaptive cytolytic killing', *Proc Natl Acad Sci U S A*, 100: 7767-72.

Yang, K., S. Shrestha, H. Zeng, P. W. Karmaus, G. Neale, P. Vogel, D. A. Guertin, R. F. Lamb, and H. Chi. 2013. 'T cell exit from quiescence and differentiation into Th2 cells depend on Raptor-mTORC1-mediated metabolic reprogramming', *Immunity*, 39: 1043-56.

Yang, M., S. Chen, J. Du, J. He, Y. Wang, Z. Li, G. Liu, W. Peng, X. Zeng, D. Li, P. Xu, W. Guo, Z. Chang, S. Wang, Z. Tian, and Z. Dong. 2016. 'NK cell development requires Tsc1-dependent negative regulation of IL-15-triggered mTORC1 activation', *Nat Commun*, 7: 12730.

Yang, W., Y. Bai, Y. Xiong, J. Zhang, S. Chen, X. Zheng, X. Meng, L. Li, J. Wang, C. Xu, C. Yan, L. Wang, C. C. Chang, T. Y. Chang, T. Zhang, P. Zhou, B. L. Song, W.

Liu, S. C. Sun, X. Liu, B. L. Li, and C. Xu. 2016. 'Potentiating the antitumour response of CD8(+) T cells by modulating cholesterol metabolism', *Nature*, 531: 651-5.

Yao, Cong-Hui, Gao-Yuan Liu, Rencheng Wang, Sung Ho Moon, Richard W. Gross, and Gary J. Patti. 2018. 'Identifying off-target effects of etomoxir reveals that carnitine palmitoyltransferase I is essential for cancer cell proliferation independent of β-oxidation', *PLoS biology*, 16: e2003782-e82.

Yokoyama, C., X. Wang, M. R. Briggs, A. Admon, J. Wu, X. Hua, J. L. Goldstein, and M. S. Brown. 1993. 'SREBP-1, a basic-helix-loop-helix-leucine zipper protein that controls transcription of the low density lipoprotein receptor gene', *Cell*, 75: 187-97.

York, A. G., K. J. Williams, J. P. Argus, Q. D. Zhou, G. Brar, L. Vergnes, E. E. Gray, A. Zhen, N. C. Wu, D. H. Yamada, C. R. Cunningham, E. J. Tarling, M. Q. Wilks, D. Casero, D. H. Gray, A. K. Yu, E. S. Wang, D. G. Brooks, R. Sun, S. G. Kitchen, T. T. Wu, K. Reue, D. B. Stetson, and S. J. Bensinger. 2015. 'Limiting Cholesterol Biosynthetic Flux Spontaneously Engages Type I IFN Signaling', *Cell*, 163: 1716-29.

Zaiatz-Bittencourt, V., D. K. Finlay, and C. M. Gardiner. 2018. 'Canonical TGF-beta Signaling Pathway Represses Human NK Cell Metabolism', *J Immunol*, 200: 3934-41.

Zhao, Y. M., and A. R. French. 2012. 'Two-compartment model of NK cell proliferation: insights from population response to IL-15 stimulation', *J Immunol*, 188: 2981-90.

Zou, T., O. Garifulin, R. Berland, and V. L. Boyartchuk. 2011. 'Listeria monocytogenes infection induces prosurvival metabolic signaling in macrophages', *Infect Immun*, 79: 1526-35.